NOTICE

The quality of this microform is heavily dependent upon the quality of the original thesis submitted for microfilming. Every effort has been made to ensure the highest quality of reproduction possible.

If pages are missing, contact the university which granted the degree.

Some pages may have indistinct print especially if the original pages were typed with a poor typewriter ribbon or if the university sent us an inferior photocopy.

Previously copyrighted materials (journal articles, published tests, etc.) are not filmed.

Reproduction in full or in part of this microform is governed by the Canadian Copyright Act, R.S.C. 1970, c. C-30.

AVIS

La qualité de cette microforme dépend grandement de la qualité de la thèse soumise au microfilmage. Nous avons tout fait pour assurer une qualité supérieure de reproduction.

S'il manque des pages, veuillez communiquer avec l'université qui a conféré le grade.

La qualité d'impression de certaines pages peut laisser à désirer, surtout si les pages originales ont été dactylographiées à l'aide d'un ruban usé ou si l'université nous a fait parvenir une photocopie de qualité inférieure.

Les documents qui font déjà l'objet d'un droit d'auteur (articles de revue, tests publiés, etc.) ne sont pas microfilmés.

La reproduction, même partielle, de cette microforme est soumise à la Loi canadienne sur le droit d'auteur, SRC 1970, c. C-30.

Canada

THE UNIVERSITY OF ALBERTA

Mass Transfer with Chemical Reaction in Alkanolamine Treating Units

by

© Raymond A. Tomcej

A THESIS

SUBMITTED TO THE FACULTY OF GRADUATE STUDIES AND RESEARCH

IN PARTIAL FULFILMENT OF THE REQUIREMENTS FOR THE DEGREE

OF DOCTOR OF PHILOSOPHY

IN

CHEMICAL ENGINEERING

EDMONTON, ALBERTA

FALL 1987

ISBN 0-315-41002-7

THE UNIVERSITY OF ALBERTA

RELEASE FORM

NAME OF AUTHOR : Raymond A. Tomcej

TITLE OF THESIS : Mass Transfer with Chemical Reaction in Alkanolamine Treating Units

DEGREE FOR WHICH THESIS WAS PRESENTED: DOCTOR OF PHILOSOPHY

YEAR THIS DEGREE GRANTED : FALL 1987

Permission is hereby granted to THE UNIVERSITY OF ALBERTA LIBRARY to reproduce single copies of this thesis and to lend or sell such copies for private, scholarly or scientific research purposes only.

The author reserves other publication rights, and neither the thesis nor extensive extracts from it may be printed or otherwise reproduced without the author's written permission.

(SIGNED) Raymond Tomcej

PERMANENT ADDRESS:

13915 Valleyview Drive

EDMONTON, Alberta

T5R 5T9

DATED SEPT. 10 19 87

THE UNIVERSITY OF ALBERTA

FACULTY OF GRADUATE STUDIES AND RESEARCH

The undersigned certify that they have read, and recommend to the Faculty of Graduate Studies and Research, for acceptance, a thesis entitled "Mass Transfer with Chemical Reaction in Alkanolamine Treating Units" submitted by Raymond A. Tomcej in partial fulfilment of the requirements for the degree of Doctor of Philosophy in Chemical Engineering.

Supervisor

External Examiner

Date Sept. 10 1987

ABSTRACT

A single sphere absorber was used to determine the diffusion coefficient of nitrous oxide (N_2O) in aqueous solutions of methyldiethanolamine (MDEA). Measurements were made over a temperature range of 25°C to 75°C and for solution strengths of 20 wt % and 40 wt % MDEA. The diffusion coefficients were found to lie in the range of 0.6×10^{-9} to 2.9×10^{-9} m^2/s. The accuracy of the diffusion data is estimated to be within ±5 %.

The single sphere absorber was used to determine the rate constant for the aqueous phase reaction between carbon dioxide (CO_2) and MDEA. Measurements were taken over a temperature range of 25°C to 75°C and for solution strengths of 20 wt % and 40 wt % MDEA. The sphere absorber operated in the fast reaction regime and under pseudo-first order conditions. The second-order rate constants were found to lie in the range of 5 to 65 $m^3/kmol \cdot s$. The activation energy of the reaction was estimated to be 42.7 kJ/mol MDEA. The accuracy of the rate constants is estimated to be within ±10 %.

The rate of absorption of CO_2 in 40 wt % MDEA solution containing from 0 $kmol/m^3$ to 0.4 $kmol/m^3$ piperazine was measured at a temperature of 40°C. The absorption rate was found to increase with piperazine concentration.

A nonequilibrium stage model based on the tray efficiency concept was developed to simulate the absorption of H_2S and CO_2 on a tray in an industrial contactor. The model incorporates the experimental rate constants and other fundamental mass transfer parameters to predict the stage efficiency of H_2S and CO_2 on each tray in a multistage model. Equilibrium and kinetic data for monoethanolamine, diethanolamine, methyldiethanolamine and triethanolamine have been included. The Ishii-Otto approach was used in the development of a new algorithm to solve the rigorous model when the tray efficiency is included in the stage equations.

A steady-state process simulation package was developed to model amine treating facilities for process design purposes. The multistage nonequilibrium model was used to simulate the performance of contactors and regenerators. Other process unit modules such as heat exchangers and flash tanks are available in the simulator. A direct substitution method was used in the sequential-modular solution procedure to obtain an overall flowsheet material and energy balance.

ACKNOWLEDGEMENTS

The author wishes to express his sincere appreciation to Dr. F.D. Otto for his guidance, encouragement and patience throughout the course of this investigation.

The author gratefully acknowledges the contribution of Mr. D. Lal for his valuable assistance in operating the sphere absorber equipment.

Dr. F.-Y. Jou provided advice on laboratory procedures and measured the equilibrium solubility of nitrous oxide in the test solutions. Dr. H.A. Rangwala also offered his assistance in the analysis of the experimental data obtained from the sphere absorber.

The technical advice and skills of Mr. K. Faulder, Mr. J. Van Doorn, Mr. R. Van den Heuvel, and Mr. R. Scott made it possible to construct and maintain the equipment.

Mr. D. Sutherland and his staff provided the expertise required to install and maintain the instrumentation on the equipment.

The financial assistance of the University of Alberta and the Natural Sciences and Engineering Research Council of Canada are gratefully acknowledged.

Special thanks are due to my parents, my sister, and my wife Dr. Roberta Grynoch for their loving support.

TABLE OF CONTENTS

LIST OF TABLES

LIST OF FIGURES

NOMENCLATURE

A	cross-sectional area of column, (m^2)
A_a	actual interfacial surface area of sphere, (m^2)
A_j	interfacial surface area of laminar jet, (m^2)
A_s	surface area of a dry sphere, (m^2)
$\underline{a}$	interfacial area per unit volume of dispersion, (m^2/m^3)
a'	interfacial area per unit tray area, (m^2/m^2)
a_o	surface area of dry packing, (m^2)
C	concentration of solute gas, ($kmol/m^3$)
C	component material imbalance function defined by Equation (122), (kmol)
C_d	discharge coefficient, dimensionless
C_{eq}	concentration of solute gas in the bulk liquid at equilibrium, ($kmol/m^3$)
C_o	concentration of solute gas in the bulk liquid, ($kmol/m^3$)
D	molecular diffusion coefficient, (m^2/s)
$D°$	molecular diffusion coefficient of the dissolved solute gas in water, (m^2/s)
D_g	molecular diffusion coefficient of the solute gas in the gas phase, (m^2/s)
D_p	nominal packing size, (m)
D_o	diameter of sieve tray holes, (m)
d	diameter of gas bubble, (m)
d_j	diameter of the jet, (m)
E	energy imbalance function defined by Equation (123), (kJ)
E	Murphree vapor-stage efficiency, dimensionless
e	vaporization efficiency, dimensionless

F	molar feed rate, (kmol/s)
f	fugacity, (kPa)
f	general nonlinear equation used in Equation (127)
f^{o}_{L}	fugacity of pure liquid, (kPa)
G	rate of absorption of the solute gas in the liquid, (kmol/s)
G	superficial gas mass velocity, (kg/m^2·s)
G_j	rate of absorption of solute gas in the liquid jet, (kmol/s)
G_s	rate of absorption of solute gas in the liquid over the sphere, (kmol/s)
g	acceleration due to gravity, 9.80665 (m/s^2)
H	Henry's law coefficient, (kPa·m^3/kmol)
H	Henry's law coefficient, (kPa/mole fraction)
H	enthalpy of vapor, (kJ/kmol)
$H°$	Henry's Law coefficient of the dissolved solute gas in water, (kPa·m^3/kmol)
H_F	enthalpy of feed, (kJ/kmol)
ΔH_{soln}	heat of solution, (kJ/kmol)
ΔH_v	latent heat of vaporization, (kJ/kmol)
h	enthalpy of liquid, (kJ/kmol)
h	salting-out parameter in Equation (211), (m^3/kmol)
h_j	height or length of jet, (m)
h_{TO}	take-off height, (m)
I	enhancement factor, dimensionless
J	ionic strength of liquid solution, (kg-ion/m^3)
K	equilibrium ratio, $K \equiv Y/X$
K_L	overall liquid-phase mass-transfer coefficient, (m/s)

K_{og}	overall gas-phase mass-transfer coefficient, (kmol/s·m²·kPa)
K_p	amine protonation constant, (kmol/m³)
K_w	water dissociation constant, (kmol²/m⁶)
K_1 ~ K_7	equilibrium constants defined by Equations (172) to (178)
k	Boltzmann's constant, 1.3805×10^{-28} (kJ/K)
k	iteration number
k_2	second order rate constant, (m³/kmol·s)
k_3	rate constant for the forward reaction given by Equation (203), (m³/kmol·s)
k_{-3}	rate constant for the reverse reaction given by Equation (203), (s^{-1})
k_b	rate constant for the reaction given by Equation (204), (m³/kmol·s)
k_g	gas-phase mass-transfer coefficient, (kmol/m²·s·kPa)
k_{H_2O}	pseudo-first order rate constant for CO_2 hydrolysis, (s^{-1})
k_L	liquid-phase mass-transfer coefficient, (m/s)
k°_L	liquid-phase mass-transfer coefficient without chemical reaction, (m/s)
k_{OH^-}	second order rate constant for reaction of CO_2 with OH^-, (m³/kmol·s)
k_{ov}	pseudo-first order overall rate constant, (s^{-1})
L	volumetric liquid flow rate, (m³/s)
L	molar liquid flow rate, (kmol/s)
L	superficial liquid mass velocity, (kg/m²·s)
M	overall material imbalance function defined by Equation (121), (kmol)
M	molecular weight, (kg/kmol)
m	concentration of alkanolamine in liquid, (kmol/m³)

NC	number of components
N_o	number of holes on sieve tray
N_{og}	number of overall gas-phase transfer units
NSTG	number of stages
P	stage efficiency imbalance function defined by Equation (124), (kmol)
P	total pressure, (kPa)
p	partial pressure, (kPa)
Q'	volumetric flow rate of liquid, (m^3/s)
Q	heat duty, (kW)
R	radius of sphere, (m)
R^*	ideal gas constant, 8.31434 ($kPa \cdot m^3/kmol \cdot K$)
Re_l	Reynolds number of liquid phase, dimensionless
Re_g	Reynolds number of gas phase, dimensionless
r	rate of reaction of solute gas, ($kmol/m^3 \cdot s$)
S	summation imbalance function defined by Equation (125), dimensionless
S	length of bubble travel on a tray, (m)
Sc_g	Schmidt number of gas phase, dimensionless
Sh_g	Sherwood number of gas phase, dimensionless
SL	molar flow rate of side liquid, (kmol/s)
SV	molar flow rate of side vapor, (kmol/s)
T	temperature, (K)
t	time, (s)
t	weighting factor in multistage solution procedure
t_D	diffusion time available for mass transfer, (s)
t_g	gas-liquid contact time, (s)
V	molar vapor flow rate, (kmol/s)

V_o	velocity of liquid free surface, (m/s)
v	superficial velocity through tray, (m/s)
v_g	superficial velocity of gas phase in the absorption chamber, (m/s)
v_t	terminal rise velocity of bubble, (m/s)
v_ψ	velocity along streamline ψ, (m/s)
W	length of outlet weir, (m)
X	mole fraction in the liquid
x	depth into liquid measured from the free surface, (m)
Y	mole fraction in the vapor
y	depth of penetration, dimensionless
Z	height above tray deck, (m)
Z	mole fraction in feed
Z_i	electrical charge of ion i

Greek Symbols

α	parameter defined by Equation (51)
α	bulk phase CO_2 loading, (mol CO_2/mol MDEA)
α	mole ratio in liquid, (mol acid gas/mol amine)
α	matrix defined by Equation (141)
β	coefficient used in Equation (50)
β	matrix defined by Equation (141)
Γ	Gamma function
γ	coefficient used in Equation (50)
γ	matrix defined by Equation (141)
γ	liquid phase activity coefficient, dimensionless

Δ	thickness of the liquid film around the sphere, (m)
Δ	numerical difference (i.e. new minus old)
Δ_o	thickness of the liquid film at the equator of the sphere, (m)
δ	vector defined by Equation (141)
ϵ	characteristic Lennard-Jones energy used in Equations (79) and (83), (K)
ϵ	convergence tolerance
ζ	parameter defined by Equation (43)
ζ_o	parameter defined by Equation (49)
ζ_1	parameter defined by Equation (88)
ζ_2	parameter defined by Equation (89)
η	stage efficiency defined by Equation (105), dimensionless
η_g	absolute viscosity of gas phase, (kg/m·s)
Θ	matrix defined by Equation (140)
θ	angle between the vertical axis of sphere and a radial line, (radians)
κ_1-κ_8	parameters used in Equations (74), (75) and (77), and listed in Table 3
Λ	matrix defined by Equation (139)
λ	generalized independent variable
λ_1-λ_8	parameters used in Equation (82), and listed in Table 3
μ	absolute viscosity of liquid phase, (kg/m·s)
ν	kinematic viscosity, (m^2/s)
Ξ	matrix defined by Equation (140)
ξ	matrix defined by Equation (148)
Π	matrix defined by Equation (139)
ρ	density, (kg/m^3)

σ	characteristic length used in Equations (74) and (81), (Å)
σ	surface tension of liquid, (dyne/cm)
σ_c	critical liquid surface tension for packing material, (dyne/cm)
τ	reduced temperature given by Equations (78) and (83), dimensionless
ϕ	longitudinal angle, (radians)
ϕ	matrix defined by Equation (141)
ϕ	vapor phase fugacity coefficient, dimensionless
ϕ	relative dispersion density, dimensionless
ϕ_{ij}	Wilke parameter for gas mixture viscosity, dimensionless
Ψ	matrix defined by Equation (139)
ψ	matrix defined by Equation (149)
ψ	functionality of flowsheet equations
ψ	stream function, (m^3/s)
Ω_D	diffusion collision integral defined by Equation (77), dimensionless
Ω_V	viscosity collision integral defined by Equation (82), dimensionless
Ω	matrix defined by Equation (145)
ω	matrix defined by Equation (147)
ω	parameter defined by Equation (60)
∇^2	$\frac{1}{r^2}\frac{\partial(r^2(\partial/\partial r))}{\partial r} + \frac{1}{r^2\sin\theta}\frac{\partial(\sin\theta(\partial/\partial\theta))}{\partial\theta} + \frac{1}{r^2(\sin\theta)^2}\frac{\partial^2}{\partial\phi^2}$
$\underline{v}\cdot\nabla$	$v_r\frac{\partial}{\partial r} + v_\theta\frac{1}{r}\frac{\partial}{\partial\theta} + v_\phi\frac{1}{r\sin\theta}\frac{\partial}{\partial\phi}$
[ ]	concentration in liquid phase, ($kmol/m^3$)
$\|\|X\|\|$	Euclidean norm of matrix X

Subscripts

CL	clear liquid
F	feed.
g	gas phase
i	component number
i	gas-liquid interface
j	stage number
L	liquid phase
T	total

1. INTRODUCTION

The removal of acid gases such as hydrogen sulphide (H_2S), carbon dioxide (CO_2) and trace sulphur compounds such as carbonyl sulphide (COS), carbon disulphide (CS_2) and alkyl mercaptans (RSH) from gas streams is often required in natural gas plants and in oil refineries. There are many treating processes available; however, no single process is ideal for all applications. The initial selection of a particular process may be based on feed parameters such as composition, pressure, temperature and the nature of the impurities, as well as product specifications. These considerations are described by Tennyson and Schaaf (1977). Final selection is ultimately based on process economics, reliability, versatility and environmental constraints. Clearly the selection procedure is not a trivial matter and any tool which provides a reliable mechanism for process design is highly desirable.

Chludzinski (1986) considered the processes available to remove acid gas impurities and categorized them as: absorption, physical separation, regenerable direct conversion, nonregenerable direct conversion, and dry bed processes. Absorption processes can be further subdivided according to the nature of the solvent as either chemical, physical, or mixed solvent types. Table 1 lists some of the commercially available processes in each category. In this work, attention is focused only on the chemical absorption

category.

The list of processes employing chemical absorption technology is dominated by the alkanolamine-based process. Conventional alkanolamines include: monoethanolamine (MEA), diethanolamine (DEA), β,β'-hydroxy-aminoethylether (DGA), diisopropanolamine (DIPA), methyldiethanolamine (MDEA) and triethanolamine (TEA). Kohl and Riesenfeld (1985) and Stenson (1985) present excellent reviews of the history of the alkanolamine treating process. While the chemical absorption processes in Table 1 vary in the formulation of the chemical solvent used, the same basic process flowsheet is used. The conventional alkanolamine treating process consists of an absorption step taking place at relatively high pressure and low temperature, followed by a solvent regeneration step at relatively low pressure and high temperature.

Figure 1 shows the conventional process configuration for a gas treating system using aqueous alkanolamine solution. The sour gas feed is contacted with amine solution countercurrently in a trayed or packed absorber. Acid gases are absorbed into the solvent which is then heated and fed to the top of the regeneration column. Stripping steam produced by the reboiler causes the acid gases to desorb from the amine solution as it passes down the column. A condenser provides reflux and the acid gases are recovered overhead as a vapor product. Lean amine

Table 1.

Processes Available for Acid Gas Removal

- Chemical Absorption

MEA	Potassium carbonate
DEA	ADIP
DGA	Amine Guard
DIPA	Beavon sulphur removal/MDEA
MDEA	Econamine
TEA	Catacarb
Activated MDEA	SNPA (P)-MDEA
FLEXSORB SE	SNPA (P)-DEA
FLEXSORB HP	SCOT
Merox	Gas/Spec FT
UCARSOL HS	UCARSOL CR
Benfield	

- Physical Absorption

Methanol	Sulfolane
Selexol	Sepasolv
Propylene carbonate	Rectisol
N-methyl-2-pyrrolidone	Purisol

- Mixed Solvents

Amisol	Sulfinol
Sulfinol M	FLEXSORB PS
UCARSOL LE	Optisol
Selefining	

- Physical Separation

Ryan-Holmes	Membranes

- Regenerable Direct Conversion

Stretford	Catasulf
LO CAT	

- Nonregenerable Direct Conversion

Zinc oxide	Chemsweet
Slurrisweet	Iron Sponge
Caustic	

- Dry Bed

Molecular sieve	SULFREEN

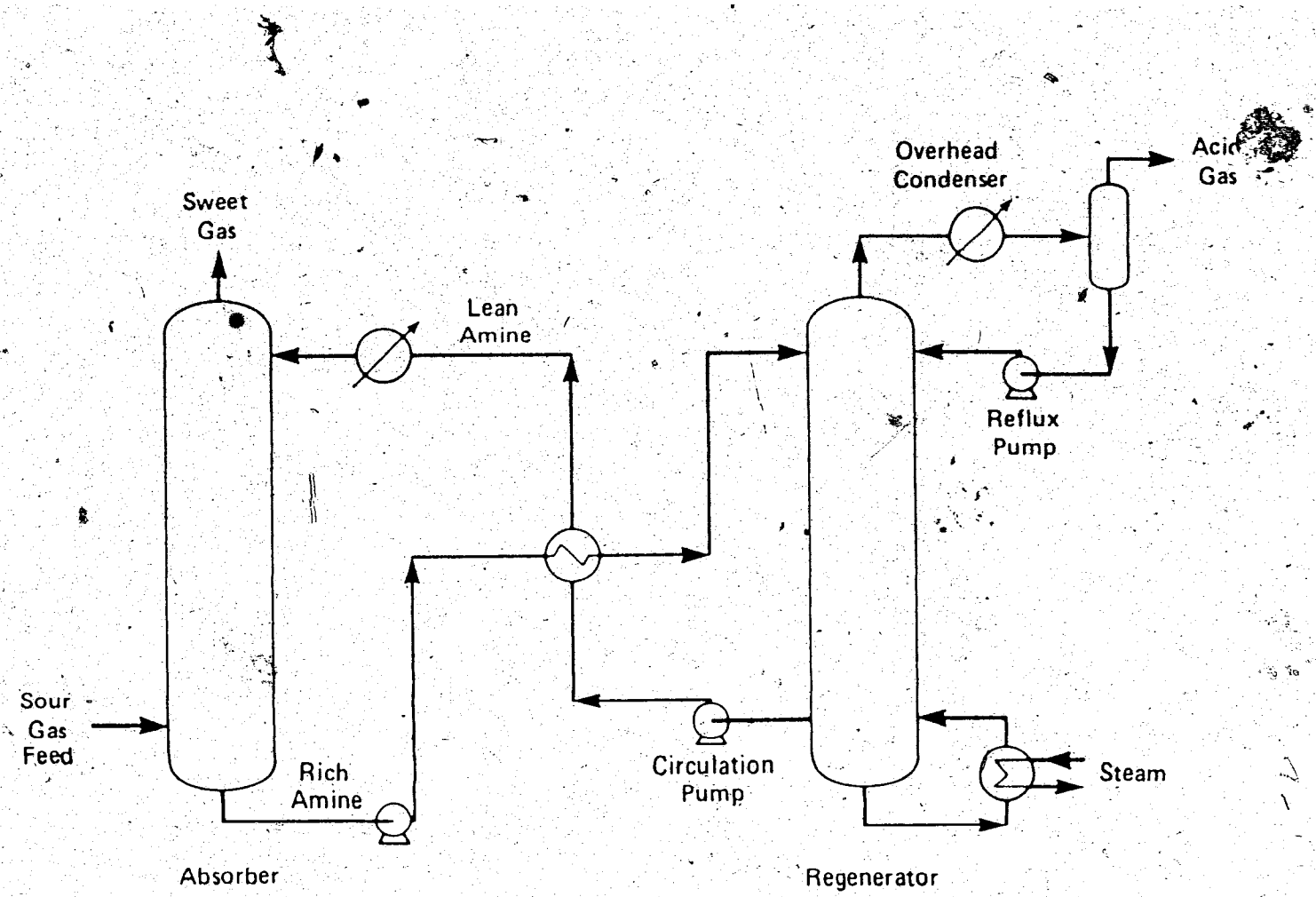

Figure 1.

Conventional Alkanolamine Treating Process

solution is cooled and recycled to the absorber. A partially-stripped semi-lean amine stream may be withdrawn from the regenerator and fed to the absorber in the split-flow modification to the conventional plant flowsheet. A three-phase separator or flash tank may be installed at the outlet of the absorber to allow for the recovery of dissolved and entrained hydrocarbons in the rich amine and to reduce the hydrocarbon content of the acid gas product.

In the past, amine treating units have been designed to remove essentially all of the H_2S and CO_2 in the feed gas. Recent industrial interest has led to the development of gas absorption processes for the selective removal of H_2S from gases containing substantial amounts of CO_2. Goar (1980) presents a few gas processing schemes which employ selective absorption technology and describes several advantages of using aqueous solutions of tertiary alkanolamines such as methyldiethanolamine (MDEA) over other alkanolamine solvents. Tertiary amines such as MDEA may be used to process gas mixtures with very low H_2S/CO_2 mole ratios ($<1:10$). In some cases, it is possible to remove essentially all of the H_2S from the feed gas yet allow 90 % or more of the CO_2 to pass through the contactor without being absorbed.

The alkanolamine treating process is also used to remove bulk quantities of CO_2 from gas streams as an alternative to cryogenic fractionation or membrane

separation technology. Primary and secondary amines are capable of removing CO_2 to very low (ppm) levels, but their use results in excessive energy requirements for solution regeneration. Tertiary amines such as MDEA are capable of removing bulk quantities of CO_2 to moderately low levels (<1 mol %) with reduced energy costs owing to their lower heats of solution. However, the rate of absorption of CO_2 in tertiary amine solutions is much lower than in primary and secondary amine solutions of comparable molarity. Consequently, process developers have investigated the use of mass-transfer promoting additives.

Astarita et al.(1981) and Astarita et al.(1982) discuss the use of arsenite as a promoter in the hot potassium carbonate process to enhance the CO_2 absorption rate. Similarly, Appl et al.(1982) propose the addition of small quantities of monomethylethanolamine (MMEA) or piperazine to MDEA solutions to accelerate the rate of absorption of CO_2. This increased absorption rate permits lower solution circulation rates and reduces the capital and operating costs of the plant.

The design of amine treating units involves the selection of: the process configuration, the amine type and concentration, the solution circulation rate, the reboiler heat requirements, and the operating pressures and temperatures. The mechanical tray design and the number of stages in the contactor are known to affect the process

performance and are particularly important in selective absorption applications.

Amine treating units have been designed in the past using hand calculations and operating experience. Design conditions were typically chosen within a conservative range in order to cover the deficiencies in the data used in the hand calculations. Goel et al.(1982) discuss the importance of accurate data in gas treating design. Computer modelling of amine treating units has become a popular means of obtaining a suitable process design.

In order to successfully model and predict the H_2S selectivity in industrial contactors that use MDEA, Blauwhoff et al.(1983) indicate that three factors must be considered: 1) there must be an understanding of the kinetics of the chemical reactions between H_2S/CO_2 and MDEA solutions, 2) the mechanical design of mass transfer equipment affects the selectivity, and 3) the equilibrium conditions of the system must be known. Furthermore, the absorption of pure H_2S or pure CO_2 by MDEA solutions must be fully understood before the problem of simultaneous absorption can be considered. In Chapters 6 to 10, a nonequilibrium stage model which addresses each of these considerations is presented. The focus of research in Chapters 2 to 5 is on the experimental measurement of CO_2 absorption kinetics.

The absorption of CO_2 in aqueous MDEA solutions is a mass transfer process accompanied by chemical reaction in the liquid phase. In aqueous alkanolamine systems, the liquid-phase mass-transfer coefficient for CO_2 transfer is a function of temperature, the diffusion coefficient of CO_2 in the solvent, the reaction rate constant, the reacting species concentrations, and the physical properties of the solution. For process design calculations, this transfer coefficient must be estimated; however, experimental data for diffusion coefficients and the reaction rate constant in MDEA solutions are limited.

In this investigation, experimental measurements of the rate of absorption of CO_2 into aqueous solutions of MDEA were taken. Temperatures and MDEA concentration studied were in a range of industrial interest. A laboratory absorber was used such that fundamental mass transfer parameters were obtained from the absorption measurements. These fundamental parameters can be used in a nonequilibrium stage model to predict the performance of industrial contactors using MDEA as the chemical solvent. The enhancing effect of piperazine on the CO_2 absorption rate was also studied.

Background material on the chemical reactions which occur between acid gases and alkanolamines is contained in Chapter 2, along with a review of previous work in this area. Chapter 2 also covers the theoretical expressions

that were used to obtain the fundamental mass transfer parameters from raw absorption rate data taken using the single sphere absorber. Chapter 3 presents a description of the experimental apparatus and procedures used to obtain the raw data. Experimental results are presented in Chapter 4 and discussed in Chapter 5.

Ford (1979) describes the value and use of process simulation for engineering design. In the research and development stage, simulation of a process using a minimum of input data can provide a means of checking the economic feasibility of a process. In the critical examination stage, once a financially-attractive process has been identified, different flowsheet configurations and operating conditions can be tested to determine optimum values. For example, the program could be used to establish the sensitivity of plant operation to changes in reboiler heat duty or amine circulation rate. Use of the simulator in the pilot plant stage may help obtain estimates for the operating conditions of the full-scale plant. Simulation of the full-scale plant would provide the process data required for the detailed design of mechanical equipment. These include the temperature profile within each column and the vapor and liquid loadings on each tray. Finally, the simulation of an existing plant may be useful if there is a need to change the operating conditions. In this stage, simulation is an ideal way of searching for bottlenecks or for adapting existing equipment to new feedstocks or product

specifications.

A theoretical model has been developed to simulate the performance of the alkanolamine treating process. Chapter 6 contains a review of the previous modelling work documented in the open literature. The nonequilibrium stage concept, upon which the simulator is based, is described in Chapter 7 along with the generalized multicomponent multistage rigorous separation model. Chapter 7 also covers the numerical technique used to solve the nonlinear multistage model equations and the calculation of the acid gas stage efficiency. Finally, Chapter 7 closes with a discussion of the individual thermodynamic and physico-chemical models used to generate equilibrium ratios, phase enthalpies, reaction rates and fluid properties.

In Chapter 8, the individual process unit-modules developed in Chapter 7 are combined to assemble a process flowsheet simulator suitable for engineering design calculations. The approach to simulation, the recycle convergence technique and the capabilities of the model are described. Chapter 9 contains an extensive evaluation of the proposed model. Examples of single- and multi-column process configurations using primary, secondary and tertiary alkanolamine solvents are presented. A discussion of the model follows in Chapter 10.

Finally, the conclusions that can be drawn from the experimental and modelling studies in this work are

summarized in Chapter 11.

2. BACKGROUND MATERIAL FOR EXPERIMENTAL STUDY

2.1 Amine Chemistry

Amines are generally grouped according to the nature and extent of substitution of the amino group and are either primary, secondary, or tertiary. Figure 2 gives the molecular structure of several amines used in gas and liquid treating applications. The structural differences of these amines plays a major role in governing their reactivities with H_2S and CO_2. Sartori and Savage (1983) have defined sterically hindered amines as those for which either a primary amino group is attached to a tertiary carbon atom or a secondary amino group is attached to a secondary or tertiary carbon atom. AMP and PE are examples of sterically hindered amines.

The absorption and desorption of H_2S and CO_2 in aqueous amine solutions is a complex phenomenon involving mass transfer with chemical reaction in the liquid phase. Detailed analyses of the reactions of H_2S and CO_2 with primary, secondary, and tertiary amines may be found in Astarita (1967), Danckwerts (1970), Astarita et al.(1983) and Kohl and Riesenfeld (1985). These acid gases react with amines according to the following scheme

Figure 2. Selected Amino Compounds

Primary

Ammonia

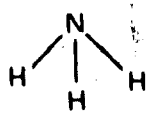

Monoethanolamine (MEA)

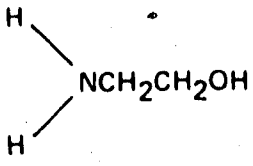

2–Amino–2–methyl–1–propanol (AMP)

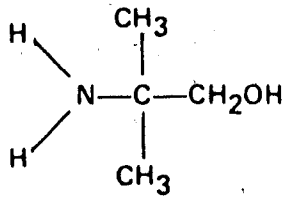

Secondary

Diethanolamine (DEA)

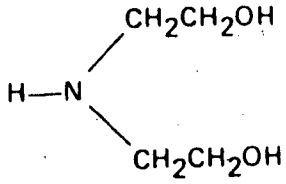

2–Piperidineethanol (PE)

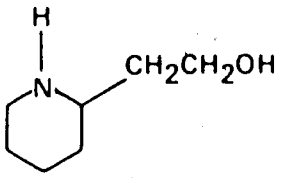

Piperazine

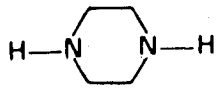

Tertiary

Methyldiethanolamine (MDEA)

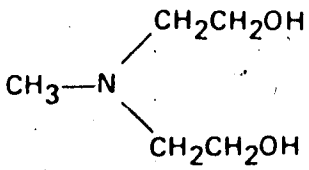

Triethanolamine (TEA)

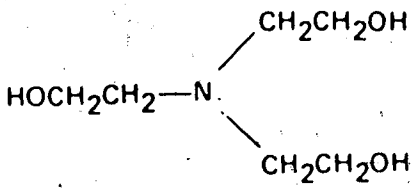

Primary and Secondary Amines

$$R_1R_2NH + H_2S \rightleftharpoons R_1R_2NH_2^+ + HS^- \quad (1)$$

$$R_1R_2NH + CO_2 \rightleftharpoons R_1R_2NCOO^- + H^+ \quad (2)$$

$$R_1R_2NCOO^- + H_2O \rightleftharpoons R_1R_2NH + HCO_3^- \quad (3)$$

Tertiary Amines

$$R_1R_2R_3N + H_2S \rightleftharpoons R_1R_2R_3NH^+ + HS^- \quad (4)$$

$$R_1R_2R_3N + CO_2 \longrightarrow \text{No carbamate formed} \quad (5)$$

$$R_1R_2R_3N + CO_2 + H_2O \rightleftharpoons R_1R_2R_3NH^+ + HCO_3^- \quad (6)$$

where R_1, R_2, and R_3 represent the substituted groups and R_2 is a proton in the case of primary amine.

Dissolved H_2S reacts directly with free amine as shown in Equations (1) and (4) by exchanging a proton. This reaction can occur with primary, secondary, and tertiary amines and proceeds at a rate which is virtually instantaneous.

Primary and secondary amines react directly with CO_2 to form a carbamate ion ($R_1R_2NCOO^-$) as given by Equation (2). Carbamate can be further hydrolyzed to bicarbonate. This slow hydrolysis reaction, shown by Equation (3), occurs in the bulk liquid and regenerates free amine. The reactions given by Equations (2) and (3) proceed in parallel. The carbamate reversion reaction generally becomes significant at high CO_2 loadings when the concentration of carbamate ion in the liquid is substantial.

Tertiary amines cannot react directly with CO_2 to form carbamate. The overall reaction between CO_2 and tertiary amines is given in Equation (6). Herein lies the reason why tertiary amines are used in applications which call for selective H_2S removal. While primary and secondary amines exhibit some kinetic selectivity for H_2S at low pressures, they generally coabsorb the acid gases at comparable rates. Because there is no direct reaction with CO_2, tertiary amines absorb the gas at a much slower rate. The desired extent of CO_2 removal can be achieved with careful design of the mass transfer equipment and selection of operating variables such as gas-liquid contact time.

When H_2S and CO_2 are absorbed simultaneously, there is an interaction between the two absorption rates because both gases compete for the free amine reactant. Although Goettler (1967) emphasizes the need to study the kinetics of simultaneous absorption of H_2S and CO_2 in these types of systems, there is still some uncertainty of the role that MDEA plays in the CO_2 absorption process. Experimental study of the single-gas system can answer some of these questions and provides a basis to develop future experiments involving the simultaneous absorption of both H_2S and CO_2.

Carbon dioxide undergoes the following two reactions in aqueous solutions

$$CO_2 + H_2O \underset{}{\overset{k_{H_2O}}{\rightleftharpoons}} HCO_3^- + H^+ \qquad (7)$$

$$CO_2 + OH^- \underset{}{\overset{k_{OH^-}}{\rightleftharpoons}} HCO_3^- \qquad (8)$$

Measured rates of CO_2 absorption in aqueous tertiary amine solutions are well in excess of the rate predicted by theory assuming that the two parallel reactions (7) and (8) occur as indicated. It is generally accepted that MDEA acts as a catalyst for the CO_2 hydrolysis reaction (7); however, there is no general agreement on the catalytic mechanism.

Astarita et al.(1981) and Savage et al.(1984) suggest that chemical species with a pyramidal structure and a lone pair of electrons on the nitrogen atom may act as homogeneous catalysts for CO_2 hydrolysis. For example, sulphite, arsenite and selenite are recognized rate promoters for CO_2 absorption in potassium carbonate solutions. A reaction mechanism postulated by Donaldson and Nguyen (1980) suggests that the tertiary amine MDEA acts as a base catalyst for the CO_2 hydrolysis reaction. Hydrogen bonding between amine and water weakens the H-O bond and increases the nucleophilic reactivity of the water with CO_2. This mechanism is in accordance with the findings of Blauwhoff et al.(1983), Barth et al.(1984) and Versteeg et al.(1986).

Recently, Kim and Savage (1986) have proposed another viable reaction mechanism by drawing an analogy with the known chemistry of aminothiols. In the new mechanism, tertiary amines which contain the N-C-C-OH structural group,

form a highly-polarized internal-salt-like intermediate and provide nucleophilic assistance to the subsequent CO_2 reaction through the polarized hydroxyl group.

Barth et al.(1981) and Yu et al.(1985) speculate that MDEA may alternatively form a zwitterionic intermediate with CO_2. This unstable intermediate would then react with water to regenerate free amine and form bicarbonate ion.

The rate of absorption of CO_2 in aqueous MDEA solutions may be expressed as the sum of three terms

$$r_{CO_2} = (k_{H_2O} + k_{OH^-}\ [OH^-] + k_2[MDEA])[CO_2] \qquad (9)$$

where k_2 is the second-order rate constant for the increase in the CO_2 absorption rate which is a result of MDEA base catalysis. This rate expression is seen to depend on [MDEA], the concentration of free amine in the liquid. When measured using a laboratory absorber, an overall reaction rate constant, k_{ov}, is obtained from the raw absorption data such that

$$r_{CO_2} = k_{ov}\ [CO_2] \qquad (10)$$

Pinsent et al.(1956) present a correlation for the pseudo-first order rate constant for reaction (7)

$$\log_{10} k_{H_2O} = 329.80 - 110.54 \log_{10} T - \frac{17265}{T} \qquad (11)$$

The second-order rate constant for reaction (8) at infinite

dilution is given by

$$\log_{10} k_{OH^-} = 13.635 - \frac{2895}{T} \qquad (12)$$

The hydroxyl ion concentration may be estimated by the model of Astarita et al.(1983)

$$[OH^-] = (K_w / K_p) \frac{1 - \alpha}{\alpha} \qquad (13)$$

where α is the bulk phase CO_2 loading in mol CO_2 per mol MDEA. Sweeton et al.(1974) give an expression for the water dissociation constant

$$\log_{10} K_w = \frac{31286}{T} + 94.9734 \ln T - 0.097611\, T - \frac{2170870}{T^2} - 606.522 \qquad (14)$$

Barth et al.(1984) present a correlation for the protonation constant of MDEA

$$\log_{10} K_p = -14.01 + 0.0184\, T \qquad (15)$$

The alcoholic group of an alkanolamine may participate directly in an aqueous reaction with CO_2 under certain conditions. The formation of monoalkylcarbonate from CO_2 and triethanolamine (TEA) is described by Jørgensen and Faurholt (1954). Reaction (16) reportedly occurs only at pH values above 10

$$CO_2 + R_1R_2NR_3OH + OH^- \rightleftharpoons R_1R_2NR_3CO_3^- + H_2O \qquad (16)$$

At lower pH values, the contribution of this reaction to the

overall rate of absorption of CO_2 may be assumed to be negligible. This assumption is in accordance with the conclusions of Blauwhoff et al.(1983), Yu et al.(1985), and Versteeg et al.(1986).

2.2 Literature Review

2.2.1 Previous Studies of Alkanolamine Reaction Kinetics

The technical literature on CO_2-alkanolamine reaction kinetics is dominated by studies of systems containing monoethanolamine (MEA) and diethanolamine (DEA). For MEA systems, some examples are those by Shneerson and Leibush (1946), Clarke (1964), Thomas (1966), Sada et al.(1976a), Sada et al.(1976), Hikita et al.(1977), Hikita et al.(1979), Laddha and Danckwerts (1981), Alvarez-Fuster et al.(1981), Penny and Ritter (1983), and Sada et al.(1985). For DEA systems, the studies of Sada et al.(1976b), Hikita et al.(1977), Danckwerts (1979), Giavarini et al.(1980), Alvarez-Fuster et al.(1980), Alvarez-Fuster et al.(1981), Laddha and Danckwerts (1981), Blanc and Demarais (1981), Laddha and Danckwerts (1982), Barth et.al.(1983), Blauwhoff et al.(1983), Barth et al.(1984), Sada et al.(1985), Savage and Kim (1985) and Sada et al.(1986) are well known.

These investigations generally involved the use of a laminar jet absorber, a wetted wall column, or a quiescent

surface stirred-cell reactor to measure the rate of absorption of pure CO_2 into alkanolamine solutions. Sada et al.(1976) studied the simultaneous absorption of H_2S and CO_2 into MEA solutions. Alvarez-Fuster et al.(1981), Sada et al.(1985) and Sada et al.(1986) measured the rate of absorption of CO_2 into mixed solvents containing alcohols and either MEA or DEA. Savage and Kim (1985) used a single sphere absorber to determine the absorption kinetics of CO_2 with DEA and diisopropanolamine (DIPA) solutions.

Other studies have been performed to evaluate potential new gas treating solvents. Weiland and Trass (1971) used a laminar jet to measure the absorption kinetics of CO_2 in ethylenediamine (EDA) solutions. Giavarini and Moresi (1982a) used a stirred-cell reactor to measure the absorption kinetics of CO_2 in neopentanolamine (NPA) solutions. Giavarini and Moresi (1982b) then studied modified tetraethylenepentamine (TEPA) solutions. Chakraborty et al.(1986) measured the rate of absorption of CO_2 into aqueous solutions of sterically-hindered AMP. Zioudas and Dadach (1986) measured the simultaneous absorption of H_2S and CO_2 into aqueous solutions of AMP.

Experimental studies of CO_2 absorption kinetics in aqueous MDEA solutions have become available only recently. Frazier and Kohl (1950) and Miller and Kohl (1953) present pilot-scale operating data for a MDEA contactor. The data illustrate the selectivity of MDEA for H_2S in the presence

of CO_2. MDEA fell out of favor due to its cost until 1977 when Vidaurri and Kahre (1977) published new laboratory data and proposed its commercial use.

Barth et al.(1981) performed experiments using a stopped-flow method to measure the rate of absorption of CO_2 in dilute MDEA solutions. Their study covered a range of MDEA concentrations from 0.02 kmol/m³ to 0.2 kmol/m³ and a range of temperatures from 20° to 40°C. Blauwhoff et al.(1983) used a stirred-cell reactor to measure the absorption rate of CO_2 in MDEA solutions. Their investigation was performed at 25°C and covered a range of MDEA concentrations from 0.45 kmol/m³ to 1.63 kmol/m³. Barth et al.(1984) reexamined their earlier data in view of the paper of Blauwhoff et al.(1983) and concluded that their new data were consistent with a reaction mechanism that included the base-catalyzed hydrolysis reaction.

Haimour and Sandall (1984) measured the rate of absorption of CO_2 in MDEA solutions using a laminar jet absorber. Their study covered a range of MDEA concentrations from 0.855 kmol/m³ to 1.71 kmol/m³ MDEA and a range of temperatures from 15° to 35°C. They found that the 12 ms contact time of the laminar jet was insufficient to allow any reaction to occur between CO_2 and MDEA.

Yu et al.(1985) measured the rate of absorption of CO_2 in MDEA solutions using a stirred-cell reactor. Their investigation covered a range of MDEA concentrations from

0.25 kmol/m³ to 2.5 kmol/m³ and temperatures ranging from 40° to 60°C.

Versteeg (1986) extended the measurements of Blauwhoff et al.(1983) for MDEA solutions using a stirred-cell reactor. New data are presented for MDEA concentrations ranging from 0.2 kmol/m³ to 3.0 kmol/m³ and temperatures ranging from 20° to 60°C.

Brabson and Bullin (1986) constructed a single-stage contactor to measure the rate of absorption of CO_2 in 0.85 kmol/m³ MDEA. Difficulties in operating the equipment were experienced and the results agree poorly with other studies. Critchfield and Rochelle (1987) used a stirred-cell reactor to measure rates of absorption of CO_2 into 2.0 molal MDEA solutions at temperatures ranging from 9.5° to 62°C.

Khalil (1984) used a stirred-cell reactor to measure the simultaneous rates of absorption of H_2S and CO_2 into MDEA solutions. Bidarian and Sandall (1986) studied the simultaneous absorption phenomenon using a packed column.

2.2.2 Previous Experience with the Sphere Absorber

A single sphere absorber may be used to measure the rate of absorption of sparingly-soluble gases into liquids. In operation, degassed liquid flows over a solid sphere enclosed in an absorption chamber filled with solute gas.

The rate of absorption of gas into the laminar film is determined by measuring the rate at which gas is added to the absorption chamber to maintain a constant pressure in the chamber. The absorption chamber may be enclosed in a controlled environment to enable measurements to be taken at different temperatures. When the system under study involves only physical absorption, the molecular diffusion coefficient can be calculated from the measured rate of absorption of gas into the liquid film on the sphere. When a first-order chemical reaction occurs in the liquid phase, the reaction rate constant can be calculated from the measured rate of absorption. General comparisons between laboratory absorbers such as the laminar jet, the wetted wall column and the single sphere absorber are presented in Astarita (1967), Charpentier (1982) and Astarita et al.(1983).

The single sphere absorber may be selected over other laboratory absorbers for the following reasons:

1) The diffusion or contact time can be in the order of 0.1 to 1 s. This is desirable for operation in the fast reaction regime.

2) The hydrodynamics are known to the extent that rigorous calculations of the diffusion time and surface area can be made.

3) The high surface area per unit volume of flowing

liquid makes it suitable for studies involving slightly soluble gases.

4) The entrance and exit effects are much less than those of other laboratory absorbers such as the wetted wall column.

5) Relatively high liquid flow rates are possible with the absence of surface rippling.

Several experimental studies involving the use of the single sphere absorber have been reported in the literature. Lynn et al.(1955c) used a single sphere absorber to measure the absorption rate of sulphur dioxide (SO_2) into water. Davidson and Cullen (1957) measured the diffusion coefficients of CO_2, nitrous oxide (N_2O), oxygen, hydrogen, chlorine and SO_2 in water at various temperatures. Ratcliff and Holdcroft (1961) used the sphere absorber to determine the first-order rate constant for the reaction between CO_2 and sodium carbonate-bicarbonate solution, and the rate constant for the reaction between 1,1-dimethoxyethane and aqueous hydrochloric acid. Goettler and Pigford (1968) studied the simultaneous absorption of CO_2 and SO_2 into aqueous solutions of sodium hydroxide. Wild and Potter (1968) measured the rate of absorption of CO_2 into potassium carbonate-bicarbonate solution. Olbrich and Wild (1969) present experimental results for the absorption of nitrogen in cyclohexane. Wild and Potter (1972) measured the rate of

absorption of CO_2 in water. Kalra et al.(1972) determined the diffusion coefficient of hydrogen in liquid aminomethane. Kalra and Otto (1974) measured the pseudo-first order rate constant for the exchange of deuterium between hydrogen and aminomethane catalyzed by potassium methylamide. Malcolm (1977) extended the range of data for the deuterium exchange reaction using potassium and lithium methylamide catalysts. Savage et al.(1980) and Joshi (1980) used a sphere absorber to measure the absorption and desorption rate of CO_2 from hot carbonate solutions. Sartori and Savage (1983) measured CO_2 absorption rate data for several sterically hindered amines. Tseng et al.(1986) measured the rate of absorption of CO_2 into promoted carbonate solutions. Kim and Savage (1986) used the absorber to determine the absorption kinetics of CO_2 in diethylaminoethanol (DEAE).

Moore (1971) and Kalra (1973) present detailed discussions of the important factors to consider in the operation of sphere absorbers.

2.2.3 End Effects and Surface Instability

In laboratory absorbers which are based on a moving gas-liquid interface, end effects, surface instability and wetting problems must be controlled. End effects involve the distortion of the velocity profile in the vicinity of the gas-liquid interface. This distortion may affect the

mass transfer process in a way which is usually not provided for in the theoretical analysis of experimental data. End effects (entrance and exit) must therefore be minimized. As mentioned in the previous section, some laboratory absorbers are prone to more severe end effects than other absorbers. For example, wetted-wall columns are generally affected by end effects more than sphere absorbers.

The severity of entrance effects depends on the nature of the device used to admit liquid onto the sphere. Liquid on the top hemisphere is relatively fresh, and for physical absorption studies, most of the absorption takes place in this region. Liquid should be admitted to the sphere in such a way that a stable, ripple-free spherical film is quickly established. Kalra (1973) reports that the stability of the spherical film is affected by the stability of the liquid feed system. Goettler (1967) notes that the presence of small gas bubbles in the liquid feed can disrupt the formation of a stable film.

Several designs exist for feeding liquid to a sphere absorber. These include: 1) wetted support rod, 2) internal flow types, and 3) a laminar jet. Davidson and Cullen (1957) used a 3 mm support rod to feed liquid to a 38 mm table tennis ball. Joshi (1980) fed liquid internally, up through the base of a 50 mm sphere and out a hole at the top of the sphere. Goettler (1967), Moore (1971) and Kalra (1973) used a laminar jet to feed liquid to a sphere

absorber.

With a laminar jet feed system, the stability of the jet is determined at low flow rates by the break-up of the jet and at high flow rates by turbulence. Goettler (1967) established by experimental observation, a general criterion for the upper stability limit based on a jet Reynolds number

$$Re_j = \frac{4L}{\pi d_j \nu} \simeq 3500 \qquad (17)$$

Another consideration is the length of the laminar jet. When the jet is too long, turbulence can occur. If the jet is too short, the liquid may spray or form a cone between the nozzle and the sphere. Goettler (1967) used jet lengths between 3.5 to 6.0 mm while Moore (1971) and Kalra (1973) recommend a jet length of 2.0 mm.

Other investigators using sphere absorbers, including Davidson and Cullen (1957), Goettler (1967), Moore (1971) and Kalra (1973) have noted an exit effect which is a function of the exposed length of support rod, referred to as the take-off length effect. The exit effect has been described as a stagnant monolayer of liquid which develops on the surface of the liquid on the support rod down to the take-off liquid level. This stagnant layer eventually saturates with solute gas which in turn reduces the rate of absorption of gas over that surface area. When the stagnant layer reaches the junction between the sphere and the support rod, the gas-liquid interfacial area on the support

rod is essentially inactive to mass transfer. If the stagnant layer is forced up on the surface of the sphere, and if the diameter of the sphere is much greater than the support rod, a dramatic decrease in the observed rate of absorption will result. If the stagnant layer is maintained at the junction of the sphere and the support rod, the rate of gas absorption on the support rod can be neglected. The take-off length at this point is referred to as the optimum take-off length.

Davidson and Cullen (1957) found no effect of liquid receiver geometry on the optimum take-off length. For the 38 mm sphere, they used a 15 mm take-off length. Goettler (1967), Moore (1971) and Kalra (1973) each used a take-off length of 20 mm in their work. Goettler (1967) observed no effect of liquid flow rate on the optimum take-off length.

The theoretical analysis of absorption rate data from a sphere absorber is based on the assumption of fully-developed laminar flow. Surface instability can result in waves or ripples forming in the liquid which disturb the laminar flow velocity profiles. This instability is a complex function of system properties, flow conditions, film thickness and the peculiarities of a particular apparatus. Vibration of the apparatus and convection currents formed due to density differences in the liquid may also contribute to ripple formation.

Goettler (1967) reports that surface waves can increase the interfacial surface area by 2.5 %, thereby affecting the mass transfer coefficient calculated from experimental data. More important than increased surface area is the potential for localized mixing of the liquid. This may result in 50 % to 100 % increases in the observed absorption rate. Goettler (1967) and Kalra (1973) report the Reynolds number criterion for the onset of surface rippling. The Reynolds number of the sphere is given by

$$Re_s = \frac{2L}{\pi R \nu} \tag{18}$$

Based on experimental observation, their results suggest that Re_s should be less than 37 and 50 respectively. Moore (1971) presents a comprehensive review of several authors' experience with incipient wavy flow.

Surfactants may be used to dampen out surface rippling and to avoid spurious results. Opponents claim that surface active agents introduce interfacial resistance to mass transfer and impede the gas absorption process. In addition, surfactants may affect the mixing mechanism at the jet-sphere junction and the sphere-support rod junction. Many studies have been performed in which surfactants have been successfully used to reduce surface rippling and to promote wetting of a solid surface. In special cases, mass transfer experiments can be performed using liquids with and without surfactant to obtain a direct comparison of gas

absorption rates.

Lynn et al.(1955a, 1955b, 1955c) used 0.05 wt % Teepol™ in water to study the absorption of SO_2 using a single sphere absorber, a wetted-wall column, and a string of spheres absorber. Cullen and Davidson (1956) used 0.2 wt % Teepol™ in a laminar jet absorber to demonstrate the stagnant layer effect using the CO_2-water system. Davidson et al.(1959) used 1.0 vol % Lissapol™ in water to study the absorption of CO_2 using a string of spheres absorber. Nysing and Kramers (1958) used a "small amount" of Lubrol-W™ in a wetted-wall column to study the absorption of CO_2 in carbonate-bicarbonate solutions. They reported no decrease in the rate of absorption of CO_2 with the addition of Lubrol-W™. Roberts and Danckwerts (1962) also used Lubrol-W™ to study the absorption of CO_2 in alkaline solutions and reported no surface resistance to mass transfer as a result of the surfactant. Hikita et al.(1979) used 0.01 vol % to 0.05 vol % Scourol-100™ in the CO_2-MEA system to supress rippling and interfacial turbulence due to the Marangoni effect. Khalil (1984) used 0.1 wt % Tween-80™ in water to measure the rate of absorption of H_2S and CO_2 in a laminar jet absorber with no reported interfacial resistance.

2.3 Theoretical Analysis

2.3.1 Hydrodynamics of a Spherical Liquid Film

The hydrodynamic behavior of the spherical liquid film flowing over the sphere absorber has been analyzed by Lynn et al.(1955c). They assumed that the film thickness of the liquid flowing at any latitude on the sphere is the same as it would be for the same flow rate per unit length on an inclined plane making the same angle with the vertical. This assumption was later verified and used by Davidson and Cullen (1957), Ratcliff and Holdcroft (1961), Goettler (1967), Wild and P[illegible]ter (1968), Moore (1971), Kalra (1973) and Malcolm (197[illegible]yure and Krantz (1983) analyzed the hydrodynamics of [illegible]minar spherical film using a perturbation method and obtained expressions for the film thickness at any radial position.

Figure 3 shows the geometry of the flow system. The liquid film thickness Δ at any angle θ is given by

$$\Delta = \left[\frac{3\nu L}{2\pi Rg} \right]^{1/3} / (\sin \theta)^{2/3} \qquad (19)$$

The velocity distribution along a streamline ψ in the film is given by

$$v_{\psi} = V_o \left[1 - (x/\Delta)^2 \right] \qquad (20)$$

where V_o is the velocity of the free surface and is given by

Figure 3.

Co-ordinate Representation of Flow Over a Sphere Absorber

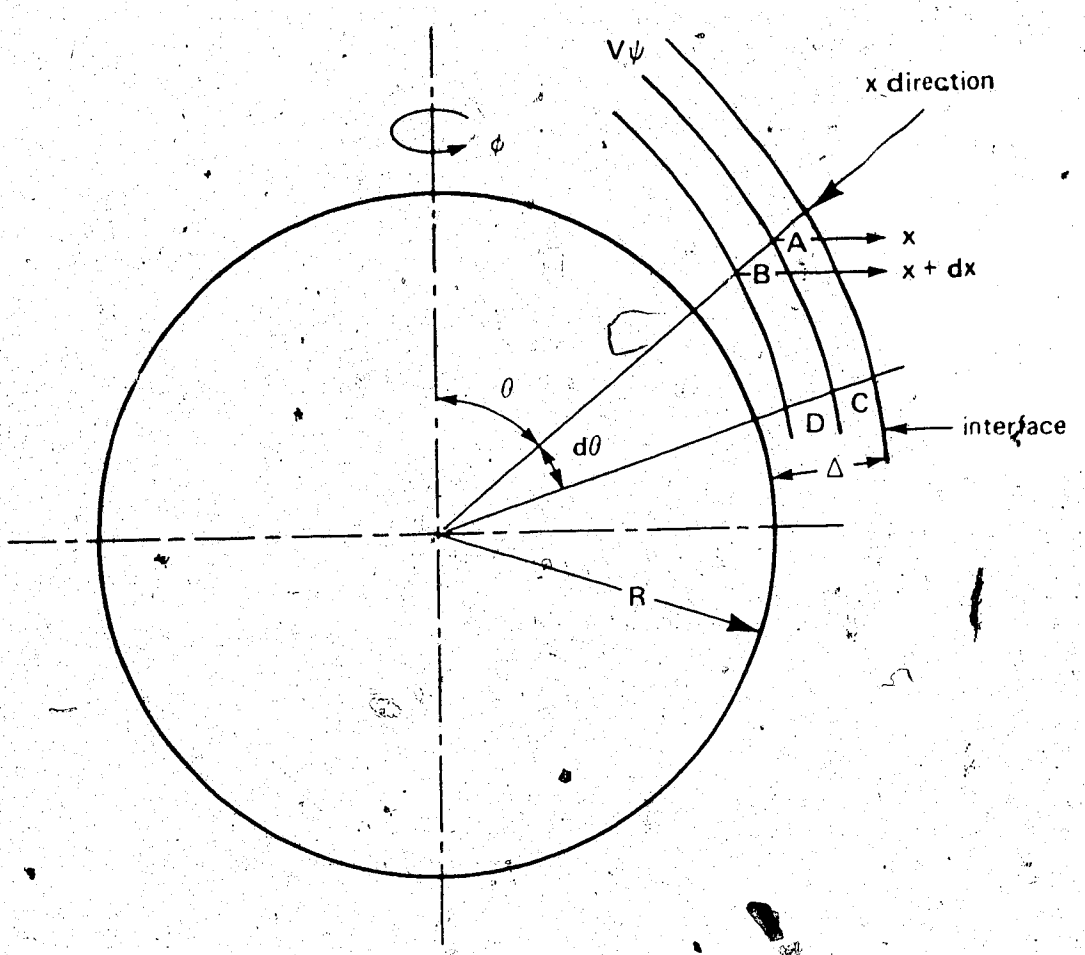

$$V_o = \left[\frac{3L}{4\pi R\Delta_o} \right] / (\sin\theta)^{1/3} \qquad (21)$$

Δ_o is the film thickness at the equator of the sphere and is given by

$$\Delta_o = \left[\frac{3\nu L}{2\pi Rg} \right]^{1/3} \qquad (22)$$

The diffusion time t_D available for mass transfer to a surface element of liquid flowing over the sphere is given by

$$t_D = \int_o^\pi \frac{R\, d\theta}{V_o}$$
$$= \frac{4\pi R^2}{3} \left[\frac{3\nu}{2\pi Rg} \right]^{1/3} L^{-2/3} \int_o^\pi (\sin\theta)^{1/3}\, d\theta \qquad (23)$$

where

$$\int_o^\pi (\sin\theta)^{1/3}\, d\theta = \frac{\Gamma(2/3)\Gamma(1/2)}{\Gamma(7/6)} = 2.58712 \qquad (24)$$

Note that although the values of Δ and V_o become undefined at $\theta = 0$ and $\theta = \pi$, the resulting integral is a closed function. Wild and Potter (1968) used Equation (21) in a numerical study of flow over a sphere. Their recommendation was to consider only the domain from $\theta = 4°$ to $\theta = 176°$ in the analysis to avoid indefinite values of V_o.

2.3.2 Physical Absorption of a Single Gas in a Spherical Liquid Film

The continuity equation for the solute gas may be written as

$$\frac{\partial C}{\partial t} + \underline{v} \cdot \nabla C = D\nabla^2 C \tag{25}$$

where the terms represent accumulation, convective transfer, and molecular diffusion respectively. In the spherical co-ordinate system, Equation (25) may be expanded to give

$$\frac{\partial C}{\partial t} + v_r \frac{\partial C}{\partial r} + v_\theta \frac{1}{r} \frac{\partial C}{\partial \theta} + v_\phi \frac{1}{r \sin\theta} \frac{\partial C}{\partial \phi}$$
$$= D\{ \frac{1}{r^2} \frac{\partial(r^2(\partial C/\partial r))}{\partial r} + \frac{1}{r^2 \sin\theta} \frac{\partial(\sin\theta(\partial C/\partial \theta))}{\partial \theta}$$
$$+ \frac{1}{r^2(\sin\theta)^2} \frac{\partial^2 C}{\partial \phi^2} \} \tag{26}$$

where v_r, v_θ and v_ϕ represent the components of velocity in the r, θ and ϕ directions respectively.

Assume that the flow field is streaming such that θ lies along a streamline. Hence

$$v_\theta \equiv v_\psi \tag{27}$$

$$v_r \equiv 0 \tag{28}$$

Assume that the flow field is uniform in the ϕ direction.

$$v_\phi = 0 \tag{29}$$

Hence due to symmetry, bulk transfer and diffusion in the ϕ direction are identically zero.

Assume that mass transfer in the direction of flow is dominated by bulk convection so that diffusion in the θ direction is negligible. Assuming that the density of the solution and the molecular diffusion coefficient D are constant over the flow field, the steady-state equation of continuity may be written as

$$v_\psi \frac{1}{r} \frac{\partial C}{\partial \theta} = D\{ \frac{1}{r^2} \frac{\partial (r^2 \partial C/\partial r)}{\partial r} \} \tag{30}$$

Expanding further gives

$$v_\psi \frac{1}{r} \frac{\partial C}{\partial \theta} = D\{ \frac{1}{r^2} [2r \frac{\partial C}{\partial r} + r^2 \frac{\partial^2 C}{\partial r^2}]\} \tag{31}$$

Changing the co-ordinate system using

$$\frac{\partial}{\partial x} = - \frac{\partial}{\partial r} \tag{32}$$

and assuming that $r \simeq R$ results in

$$DR[\frac{\partial^2 C}{\partial x^2}]_\theta - 2D[\frac{\partial C}{\partial x}]_\theta = v_\psi [\frac{\partial C}{\partial \theta}]_\psi \tag{33}$$

Furthermore, if the liquid film thickness Δ is assumed to be small relative to the sphere radius R, then Equation (33) reduces to

$$DR[\frac{\partial^2 C}{\partial x^2}]_\theta = v_\psi [\frac{\partial C}{\partial \theta}]_\psi \tag{34}$$

with the following boundary conditions.

$$\theta = 0 \qquad x > 0 \qquad C = C_o \tag{35}$$

$$\theta > 0 \qquad x = 0 \qquad C = C_i \tag{36}$$

$$\theta > 0 \qquad x = \Delta \qquad \frac{\partial C}{\partial x} = 0 \tag{37}$$

Equations (34) to (37) describe the steady-state physical absorption of a solute gas in the spherical liquid film. Equation (34) has been solved by several authors including Lynn et al.(1955c), Davidson and Cullen (1957) and Olbrich and Wild (1969). The formulation of Olbrich and Wild (1969) is an extension to the solution by Davidson and Cullen (1957). Moore (1971) and Kalra (1973) present comprehensive reviews of the solution to Equation (34) as documented by various authors.

Davidson and Cullen (1957) define a dimensionless depth of penetration $y = x/\Delta$ and introduce it into Equation (34)

$$DR\left[\frac{\partial^2 C}{\partial y^2}\right]_\theta = \Delta^2 v_\psi \left[\frac{\partial C}{\partial \theta}\right]_\psi \tag{38}$$

Substituting Equation (20) for v_ψ and rearranging gives

$$\left[\frac{\partial^2 C}{\partial y^2}\right]_\theta = \frac{V_o \Delta^2 (1-y^2)}{DR}\left[\frac{\partial C}{\partial \theta}\right]_\psi \tag{39}$$

Davidson and Cullen (1957) define a stream function ψ

$$\psi(y) = \int_o^x v_\psi \, 2\pi(R+\Delta-x') \sin\theta \, dx' \tag{40}$$

By substituting Equation (20) for v_ψ and neglecting Δ and x' in comparison to R, Equation (40) becomes

$$\psi(y) = \frac{3}{2} L \left(y - \frac{y^3}{3} \right) \tag{41}$$

Since ψ is a function of y only

$$\left[\frac{\partial C}{\partial \theta} \right]_{\psi} = \left[\frac{\partial C}{\partial \theta} \right]_{y} \tag{42}$$

Defining ζ such that

$$\left[\frac{\partial \zeta}{\partial \theta} \right]_{y} = \frac{R}{V_o \Delta^2} \tag{43}$$

one obtains

$$\left[\frac{\partial^2 C}{\partial y^2} \right]_{\zeta} = \frac{(1-y^2)}{D} \left[\frac{\partial C}{\partial \zeta} \right]_{y} \tag{44}$$

with the following boundary conditions

$$\zeta = 0 \quad y > 0 \quad C = C_o \tag{45}$$

$$\zeta > 0 \quad y = 0 \quad C = C_i \tag{46}$$

$$\zeta > 0 \quad y = 1 \quad \frac{\partial C}{\partial y} = 0 \tag{47}$$

The overall absorption rate of solute gas in the spherical liquid film, G_s , is obtained by integrating the interfacial concentration gradient over the surface of the sphere.

$$G_s = \frac{3LD}{2} \int_o^{\zeta_o} -\left[\frac{\partial C}{\partial y} \right]_{y=0} d\zeta \tag{48}$$

For a sphere

$$\zeta_o = 1.12175\pi \left[\frac{2\pi g}{3\nu} \right]^{1/3} R^{7/3} L^{-4/3} \tag{49}$$

Equation (48) is presented by Davidson and Cullen (1957) in the form of a finite series expansion

$$G_s = L(C_i - C_o)\left[1 - \sum_i \beta_i e^{-\gamma_i \alpha}\right] \quad (50)$$

where

$$\alpha = 3D\zeta_o = 3.3653\pi\left\{\frac{2\pi g}{3\nu}\right\}^{1/3} D R^{7/3} L^{-4/3} \quad (51)$$

Olbrich and Wild (1969) extended the solution of Davidson and Cullen (1957) by adding more terms in Equation (50). The coefficients β_i and γ_i are listed in Table 2.

Equation (50) considers the gas-liquid interfacial surface area to be equal to that of a dry sphere of radius R. Goettler (1967) indicates that the actual interfacial surface area is larger than the area of a dry sphere due to the thickness of the liquid film and suggests the use of the following average correction

$$A_a / A_s = 1 + 2.58712\Delta_o/R \quad (52)$$

The rate of absorption of solute gas in a laminar jet, G_j, may be calculated from the rate predicted by the penetration theory

$$G_j = 4\sqrt{h_j LD}\,(C_i - C_o) \quad (53)$$

Table 2.

Coefficients Used in the Physical Absorption Series Solution

i	β_i	γ_i
1	0.7897026	3.414446
2	0.09725511	26.440559
3	0.03609362	70.832821
4	0.01868637	136.57071
5	0.011401760	223.64880
6	0.007675970	332.06472
7	0.005517943	421.81720
8	0.004157034	612.90545
9	0.003243974	785.32896
10	0.002601795	979.08735

2.3.3 Absorption with Chemical Reaction of a Single Gas in a Spherical Liquid Film

The occurrence of a chemical reaction between the solute gas and a component in the liquid affects the rate of absorption by decreasing the concentration of the dissolved solute gas in the bulk phase. This increases the concentration gradient at the gas-liquid interface for systems in which the liquid phase is the controlling resistance to mass transfer. The continuity equation for the solute gas is similar to Equation (25), but includes an additional term which represents the rate of reaction of the solute gas

$$\frac{\partial C}{\partial t} + \underline{v}\cdot\nabla C = D\nabla^2 C - r \qquad (54)$$

Using the same assumptions as in the previous section, the analog to equation (33) becomes

$$DR\left\{\frac{\partial^2 C}{\partial x^2}\right\}_\theta - 2D\left\{\frac{\partial C}{\partial x}\right\}_\theta = v_\psi \left\{\frac{\partial C}{\partial \theta}\right\}_\psi + Rr \qquad (55)$$

Assuming that the reaction occurs under first order or pseudo-first order reaction conditions, Equation (55) may be written as

$$DR\left\{\frac{\partial^2 C}{\partial x^2}\right\}_\theta - 2D\left\{\frac{\partial C}{\partial x}\right\}_\theta = v_\psi \left\{\frac{\partial C}{\partial \theta}\right\}_\psi + Rk_{ov}(C - C_o) \qquad (56)$$

with the following boundary conditions

$$\theta = 0 \qquad x > 0 \qquad C = C_o \tag{57}$$

$$\theta > 0 \qquad x = 0 \qquad C = C_i \tag{58}$$

$$\theta > 0 \qquad x = \Delta \qquad \frac{\partial C}{\partial x} = 0 \tag{59}$$

Solutions to Equation (56) have been presented by Ratcliff and Holdcroft (1961), Astarita (1967) and Wild and Potter (1968). Kalra (1973) presents a review of these three solutions and compares the assumptions that went into each solution.

Wild and Potter (1968) define a parameter ω such that

$$d\omega = \left[\frac{RD}{V_o \Delta^2} \right] d\theta = \left[\frac{4\pi R^2 D}{3L\Delta_o} \right] (\sin \theta)^{5/3} \, d\theta \tag{60}$$

where V_o, Δ and Δ_o are given by Equations (21), (19) and (22) respectively. Integrating gives

$$\omega = \int_o^{\omega} d\omega = \frac{4\pi R^2 D}{3L} \left[\frac{2\pi Rg}{3\nu L} \right]^{1/3} \int_o^{\pi} (\sin \theta)^{5/3} \, d\theta \tag{61}$$

where

$$\int_o^{\pi} (\sin \theta)^{5/3} \, d\theta = \frac{\Gamma(1/2)\Gamma(4/3)}{\Gamma(11/6)} = 1.62863 \tag{62}$$

The solutions obtained by Wild and Potter (1968) are given by

1) $k_{ov} \, t_D = 0$

$$G_s = L (C_i - C_o) \sqrt{\omega} \sqrt{9/\pi} \tag{63}$$

2) $k_{ov}\ t_D < 1.0$

$$G_s = L\ (C_i - C_{eq})\sqrt{\omega}\ \{0.455\ k_{ov}\ t_D + 1.693\} \qquad (64)$$

3) $1.0 < k_{ov}\ t_D < 5.0$

$$G_s = L\ (C_i - C_{eq})\sqrt{\omega}\ \{1.428\sqrt{k_{ov}\ t_D} + \frac{0.689}{\sqrt{k_{ov}\ t_D}} \qquad (65)$$

4) $5.0 < k_{ov}\ t_D < 25.0$

$$G_s = L\ (C_i - C_{eq})\sqrt{\omega}\ \{1.428\sqrt{k_{ov}\ t_D} + \frac{0.54}{\sqrt{k_{ov}\ t_D}}\} \qquad (66)$$

5) $k_{ov}\ t_D > 25.0$

$$G_s = L\ (C_i - C_{eq})\sqrt{\omega}\ \{1.428\sqrt{k_{ov}\ t_D}\} \qquad (67)$$

Note that in Equations (64) to (67) the bulk liquid concentration C_o has been replaced by C_{eq}, the chemical equilibrium value. By substituting Equation (23) for t_D and Equation (61) for ω, Equation (67) can be rewritten as

$$G_s = 4\pi R^2\sqrt{k_{ov}\ D}\ (C_i - C_{eq}) \qquad (68)$$

which is the more familiar form. As in the case of physical absorption, Equation (52) may be used to make the minor correction to the interfacial surface area to account for the thickness of the liquid film.

2.4 Gas Phase Resistance

For gas absorption accompanied by chemical reaction in the liquid phase, the liquid mass-transfer coefficient, k_L, increases as the rate of reaction increases. Gas phase resistance to mass transfer must be considered when determining the value of k_L from absorption measurements taken using a laboratory absorber. Gas phase resistance has the effect of altering the interfacial concentration of solute gas, C_i. This concentration is required when determining reaction rate constants from chemical absorption studies. A similar but much smaller correction may be applied in the analysis of experimental data when only physical absorption occurs. Goettler (1967) determined the gas-phase mass-transfer coefficient experimentally for a 38 mm sphere at 25°C to be in the order of 5×10^{-6} kmol/m² · s · kPa.

Based on the two-film theory of mass transfer, the overall liquid-phase resistance may be expressed as a sum of the two individual film resistances

$$\frac{1}{K_L} = \frac{1}{k_L} + \frac{1}{H\, k_g} \qquad (69)$$

In this model the interfacial resistance to mass transfer is assumed to be negligible.

Kalra (1973) and Malcolm (1977) used the equation developed by Froessling (1938) to estimate the mass transfer

coefficient k_g for forced convection mass transfer from gases to spheres

$$Sh_g = 2.0 + 0.556\ Re_g^{1/2}\ Sc_g^{1/3} \tag{70}$$

where

$$Sh_g = 2k_g\ R^*\ TR/D_g \tag{71}$$

$$Re_g = 2\rho_g\ v_g\ R/\eta_g \tag{72}$$

$$Sc_g = \nu_g\ /D_g \tag{73}$$

The diffusion coefficient of the solute gas in the gas phase may be estimated using the Wilke-Lee modification to the Chapman-Enskog equation for binary gas systems at low pressures. This correlation is presented in Reid et al.(1977).

$$D_g = 10^{-4}\ \kappa_1 T^{3/2}\ \frac{[(M_1+M_2)/M_1M_2]^{1/2}}{P_T\ \sigma_{12}\Omega_D} \tag{74}$$

where

$$\kappa_1 = 0.00217 - 0.00050\ [(M_1+M_2)/M_1M_2]^{1/2} \tag{75}$$

$$\sigma_{12} = \frac{\sigma_1 + \sigma_2}{2} \tag{76}$$

$$\Omega_D = \kappa_2/\tau^{\kappa_3} + \kappa_4/\exp(\kappa_5\tau) + \kappa_6/\exp(\kappa_7\tau) + \kappa_8/\exp(\kappa_9\tau) \tag{77}$$

$$\tau = kT/\epsilon_{12} \tag{78}$$

$$\epsilon_{12} = \sqrt{(\epsilon_1/k)(\epsilon_2/k)} \tag{79}$$

The viscosity of the gas phase may be estimated using Wilke's method for low pressure gas mixtures. The pure gas

viscosity may be estimated using the Chapman-Enskog equation. These correlations are also presented in Reid et al.(1977).

$$\eta_g = \frac{Y_1\eta_1}{Y_1 + Y_2\phi_{12}} + \frac{Y_2\eta_2}{Y_2 + Y_1\phi_{21}} \qquad (80)$$

where

$$\eta = 26.69\times10^{-7}\ \frac{[M\ T]^{1/2}}{\sigma^2\Omega_V} \qquad (81)$$

$$\Omega_V = \lambda_1/\tau^{\lambda_2} + \lambda_3/\exp(\lambda_4\tau) + \lambda_5/\exp(\lambda_6\tau) \qquad (82)$$

$$\tau = kT/\epsilon \qquad (83)$$

$$\phi_{12} = \frac{[1 + (\eta_1/\eta_2)^{1/2}\ (M_2/M_1)^{1/4}\ ]^2}{\sqrt{[8(1 + M_1/M_2)]}} \qquad (84)$$

$$\phi_{21} = \frac{\eta_2 M_1}{\eta_1 M_2}\ \phi_{12} \qquad (85)$$

Table 3 contains the values for the parameters used in the above equations.

The superficial gas velocity used in Equation (72) may be estimated by considering the geometry of the system and the flowing conditions. A suitable equation of state may be used to determine the density of the gas phase.

2.5 Nitrous Oxide Analogy

The determination of the reaction rate constant k_{ov} from experimental chemical absorption studies requires an accurate knowledge of the molecular diffusion coefficient and the physical solubility of the reacting gas in the liquid. However, these cannot be measured directly because

Table 3.

Parameter Values Used to Estimate Gas Phase Properties

Parameter	CO_2	N_2O	H_2O
ϵ/k (K)	195.2	232.4	809.1
σ (Å)	3.941	3.828	2.641
M (kg/kmol)	44.010	44.013	18.018

Parameter	Value	Parameter	Value
		λ_1	1.16145
κ_2	1.06036	λ_2	0.14874
κ_3	0.15610	λ_3	0.52487
κ_4	0.19300	λ_4	0.77320
κ_5	0.47635	λ_5	2.16178
κ_6	1.03587	λ_6	2.43787
κ_7	1.52996		
κ_8	1.76474		
κ_9	3.89411		

of the chemical reaction that takes place. The similarity between the critical properties and molecular weights of nitrous oxide (N_2O) and CO_2 has led several authors to use the "N_2O Analogy" to infer the effect of amine concentration on the molecular diffusion coefficient and the physical solubility of CO_2 from corresponding measurements taken with N_2O. Table 4 shows the critical properties of CO_2 and N_2O. A partial list of authors that have used the N_2O analogy in their analysis include: Clarke (1964), Hikita et al.(1977), Sada et al.(1976, 1985, 1986), Laddha et al.(1981), Blanc and Demarais (1981), Blauwhoff et al.(1983), Haimour and Sandall (1984), Bidarian and Sandall (1986) and Versteeg et al.(1986).

Following this approach, the Henry's constant for CO_2 in MDEA solutions, H_{CO_2}, may be assumed to be given by

$$H_{CO_2} = H_{N_2O} \left[H^{\circ}_{CO_2} / H^{\circ}_{N_2O} \right] \qquad (86)$$

The values of H_{N_2O} and $H^{\circ}_{N_2O}$ must be determined by experimental measurement. The Henry's constant for CO_2 in water, $H^{\circ}_{CO_2}$, can be estimated from the equation of Mason and Kao (1980)

$$H^{\circ}_{CO_2} = 101.325\ \rho\ 10^{\zeta} \qquad (87)$$

where

Table 4.

Critical Properties of Gases

Property	CO_2	N_2O
Critical Pressure P_c (kPa)	7380	7240
Critical Temperature T_c (K)	304.2	309.6
Acentric Factor	0.225	0.160

$$\zeta_1 = 3.822 - 7.8665\times10^{-4} \exp(\zeta_2) - 0.04145\ \zeta_2^2 - \frac{17.457}{\zeta_2^2} \quad (88)$$

$$\zeta_2 = T/100 \quad (89)$$

This equation predicts the CO_2 solubility within 5 % of the equation given by Edwards et al.(1978).

The diffusivity of CO_2 in MDEA solutions, D_{CO_2}, may be assumed to be given by

$$D_{CO_2} = D_{N_2O} \left[D^\circ_{CO_2} / D^\circ_{N_2O} \right] \quad (90)$$

The value of D_{N_2O} must be determined by experimental measurement. The diffusivities of N_2O and CO_2 in water have been reported by Davidson and Cullen (1957), Thomas and Adams (1965), and Haimour and Sandall (1984).

3. DESIGN OF EXPERIMENT

3.1 Scope

The objective of this study was to measure the rate of absorption of CO_2 into aqueous solutions of MDEA in order to determine the rate constant for the liquid phase reaction. A single sphere absorber was designed and constructed for this purpose. A detailed description of the sphere absorber follows in this chapter.

Upon assembly, the equipment was initially used to measure the rate of absorption of CO_2 into pure water at 25°C. The CO_2-water system was chosen as a standard to verify the operating procedure and to determine the sensitivity of the measured absorption rate and the calculated diffusion coefficient to equipment operating variables.

The absorber was used to measure the rate of physical absorption of N_2O into 1.71 kmol/m³ (20 wt %) and 3.42 kmol/m³ (40 wt %) MDEA solutions at 25°, 50° and 75°C. Identical measurements were then taken of the rate of chemical absorption of CO_2 into the same solutions at the same temperatures.

The 40 wt % MDEA solution was used to study the effect of piperazine on the CO_2 absorption kinetics. Rate measurements were taken at 40°C with piperazine

concentrations of 0.0, 0.05, 0.10, 0.15, 0.20 and 0.40 kmol/m^3.

Interpretation of absorption rate data obtained using a single sphere absorber requires an accurate knowledge of several system properties. These properties include: the physical solubility of the solute gas at the gas-liquid interface, the kinematic viscosity and the density of the liquid solution. Experimental measurements were taken of the equilibrium physical solubility of N_2O and the kinematic viscosity of MDEA solutions.

The physical solubility of N_2O in pure water, 20 wt % and 40 wt % MDEA solutions was determined by Dr. F.-Y. Jou at 25°, 50°, 75°, 100° and 125°C using an equilibrium cell apparatus as described by Jou et al.(1982). The kinematic viscosity of aqueous MDEA solutions was measured over a range of concentrations from 10 wt % to 50 wt % MDEA and over a range of temperatures from 25° to 75°C. A Cannon-Fenske Routine viscometer was used for this purpose. Additional detail of the equilibrium solubility and viscosity experiments may be found in Appendix 4. The viscosity of water was obtained from Perry and Chilton (1973) and Bird et al.(1960). Published data were used to estimate the density of the liquid.

3.2 Description of Equipment

The design of the basic sphere absorber was fashioned after those used by Goettler (1967), Moore (1971), Kalra (1973) and Malcolm (1977). Some of the original equipment of Moore (1971) was salvaged and modified for re-use in this study. A simplified schematic diagram of the equipment is given in Figure 4. All parts of the equipment in contact with the amine solutions were made of 316 stainless steel, Teflon® or Pyrex® glass unless otherwise noted. Tubing was generally 6 mm (1/4 inch) nominal diameter and liquid lines were insulated with 10 mm Armaflex insulation wherever possible. General purpose valves were specified as Whitey® SS-1VS4 and minor control valves were specified as Whitey® SS-1RS4 forged body regulating valves. The equipment consisted of six major systems

1) Absorption Chamber
2) Gas Feed System
3) Liquid Feed System
4) Liquid Circulation System
5) Temperature Control System
6) Amine Regeneration System

Each of these individual systems will be discussed in this section.

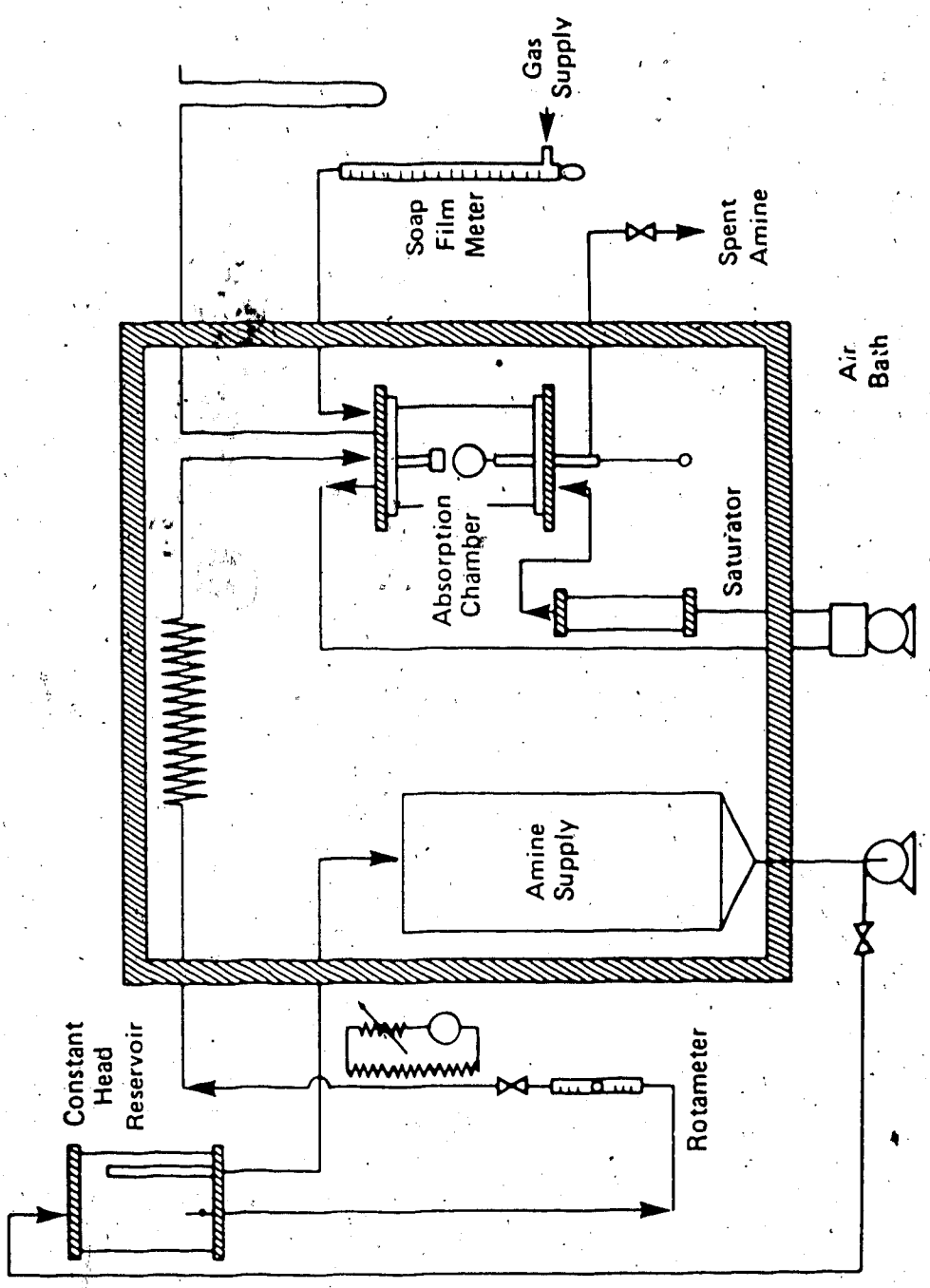

Figure 4. Schematic Diagram of the Single Sphere Absorber

3.2.1 Absorption Chamber

The design of the single sphere absorption chamber was similar in concept to the absorber of Goettler (1967). A schematic diagram of the absorption chamber is given in Figure 5. A 165 mm thick-walled glass pipe section with an inside diameter of 127 mm was used for the chamber wall and the steel end flanges of Moore (1971) were used to provide the necessary inlet and outlet ports. Steel adapter flanges and neoprene gaskets were used to mate the glass section with the end flanges. The cross-sectional area of the chamber was 127 cm^2. This minimized the volume of the chamber but provided sufficient clearance between the chamber wall and the sphere to avoid any mechanical disturbance of the liquid film due to gas circulation. Goettler (1967) noticed this effect in his original chamber design.

A laminar jet was used to introduce the amine solution onto the sphere. The laminar jet as described by Moore (1971) was designed in a similar manner to that of Goettler (1967). The jet nozzle consisted of a precision-bored ruby watch jewel which was press fitted into the nozzle cap. Nozzle sizes ranging from 0.45 mm to 1.16 mm were tested. For the range of liquid flow rates encountered in this study, the 0.60 mm nozzle provided the best performance. The laminar jet was aligned accurately with the north pole

Figure 5.

Schematic Diagram of the Absorption Chamber

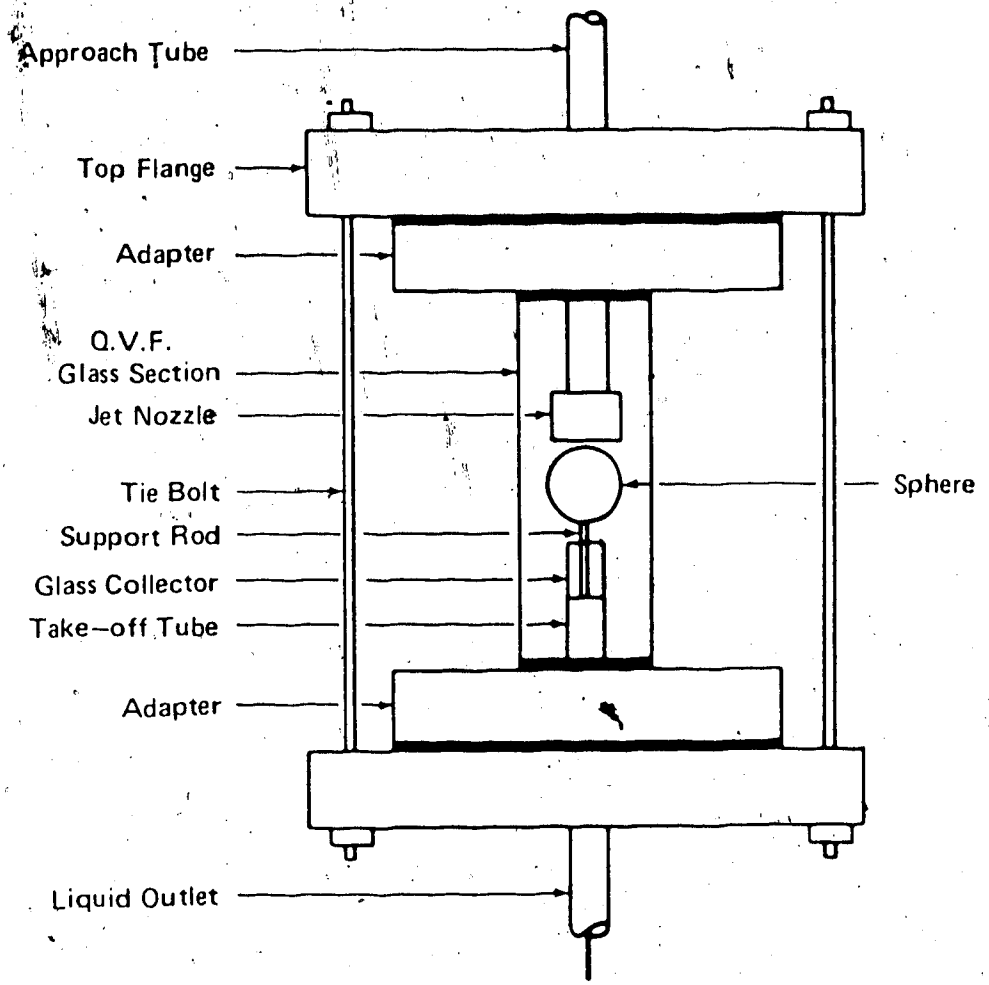

of the sphere using an eccentric mechanism that was mounted in the top flange of the absorption chamber. Alignment was done visually.

Spheres made from ceramic, polypropylene, glass and Teflon® were investigated as candidates, but steel was considered the most appropriate material to withstand the temperature and corrosive conditions in this study, as well as being the most convenient material to mount on the support rod. A 50.8 mm sphere was machined from 316 stainless steel stock to a sphericity of 0.15 mm and was polished until it was shiny. The tolerance on sphericity was deemed acceptable. A hole was drilled in the sphere to enable mounting on a 300 mm support rod with a diameter of 3.2 mm. The rod was machined from mild spring steel, which provided sufficient strength and rigidity to support the sphere. The rod was machined to a diameter of 1.6 mm over a length of 25 mm extending below the south pole of the sphere and the entire length was chrome plated. The support rod passed through the centre of the take-off tube and through the flow diverter elbow. A Teflon® bushing was used to maintain the liquid seal in the flow diverter. A knurled knob was attached to the end of the support rod. By turning the support rod, the entire surface of the sphere could by viewed, and the sphere elevation relative to the floor of the absorption chamber could be adjusted by up to 10 mm.

Liquid flowing over the sphere and the support rod passed through a glass collector cap mounted on a 12 mm diameter take-off tube. This connection was fabricated from a Kovar® joint. The take-off tube passed through an O-ring seal in the bottom flange of the absorber and was connected to the flow diverter. The support rod was centered in the take-off tube by two perforated Teflon® inserts. Liquid level in the take-off tube was controlled by a Whitey® SS-31RS4 union bonnet metering valve on the outlet liquid flow line.

A 25 mm diameter side port equipped with a stainless steel slide valve assembly was added to the absorption chamber wall to provide direct access to the sphere. This port was temporarily opened during start-up to allow the operator to wet the entire surface of the sphere. The slide valve was sealed with neoprene O-rings. Adequate purging time was provided following the wetting process to vent any contamination by air.

Details of the top flange housing the eccentric mechanism and the bottom base flange may be obtained in the thesis of Moore (1971).

The absorption chamber was mounted on a steel cage frame which rested on rubber vibration arrestors. The entire apparatus sat on a bench made from iron beams. The sheer weight of the supporting equipment provided a relatively vibration-free environment.

3.2.2 Gas Feed System

Solute gas was reduced from cylinder pressure to absorber pressure in three stages. A high pressure regulator connected to the cylinder delivered gas at approximately 350 kPa absolute to a Matheson Model 71 Low Pressure Line regulator. This second regulator further reduced the gas pressure to approximately 125 kPa absolute. Final pressure reduction was achieved with a bleed regulator used to control air pressure in industrial pneumatic control systems. The bleed regulator provided precise control over a range of pressures from 2 to 6 kPa above ambient. With this arrangement gas was delivered to the absorption chamber at approximately 96 kPa absolute. Chamber pressure was measured directly with a Meriam Instrument Co. Model 10AA25WM 30" Range U-tube manometer using water as the indicating fluid. The maximum flow rate of gas that could be delivered to the absorption chamber was 150 mL/s at this pressure. This was well above the maximum absorption rate of 2.5 mL/s that was encountered in this study.

The gas flow rate was measured with a soap film meter which was enclosed in a 50 mm nominal diameter Lucite tube packed with glass wool to isolate it from environmental temperature variations. Three soap film meter sizes were available for use. The choice between the 10 mL, 25 mL and 100 mL sizes was made so that the time required to sweep a

soap bubble through the meter was in the order of 1 minute. Each was graduated with 0.1 mL divisions. The calibration of the soap film meters is contained in Appendix 3. Soap traps were installed at both ends of the soap film meter to prevent contamination of the absorption chamber and bleed regulator.

Gas from the soap film meter was fed directly into the absorption chamber. The gas temperature was measured at the soap film meter with thermocouple 3 and at the inlet port of the absorption chamber with thermocouple 4. Sufficient residence time was available in the hot tubing and top adapter flange of the absorption chamber to heat the feed gas to the system temperature.

A gas circulation loop was installed to saturate the absorption chamber vapor space with liquid and to ensure gas phase homogeneity. Gas was withdrawn from an outlet port on the absorption chamber top flange and fed to the inlet of a Robbins & Myers Model MB-158 1/10 hp metal bellows pump. A bypass circuit was included to control the circulation rate. Pump output was directed to a 203 mm Q.V.F. PS 1/8 glass pipe section with an inside diameter of 25 mm. Steel end flanges were held in place by tie bolts. The saturator was packed with 20 mm lengths of 6 mm steel tubing and filled half full with distilled water. The packing served to reduce the surging and entrainment of liquid caused by the bellows pump.

Gas leaving the saturator was metered by a Brooks Full View 150 mm rotameter and passed through a 150 mL gas sampling bomb which served as a liquid knockout vessel. Liquid-free saturated gas exited the bomb through a side arm and was fed to an inlet port on the absorption chamber bottom flange. Thermocouple 5 was used to measure the temperature of the saturated gas as it entered the absorption chamber and thermocouple 6 measured the gas temperature leaving the absorber.

In operation, the absorption chamber was initially purged with solute gas to expel any inert gases which may have accumulated in the chamber or the gas feed system.

3.2 Liquid Feed System

A 200 mm thick-walled glass pipe section with an inside diameter of 150 mm was used as a constant head reservoir for liquid feed. A schematic diagram of the reservoir is given in Figure A2.1 of Appendix 2. Steel end flanges were held in place by tie bolts. The reservoir was wrapped with 25 mm Babcock and Wilcox Kaowool ceramic fiber insulation to reduce the heat loss from the hot liquid. The reservoir was mounted approximately 2 m above the absorption chamber and provided pulsation-free liquid feed flow to the sphere.

Liquid was drawn from the reservoir at a rate ranging from 0.4 mL/s to 2.0 mL/s. Flow rate was regulated with a

metering valve and measured by a Matheson 150 mm rotameter tube #603 equipped with glass and stainless steel floats. All measurements were taken with the steel float. The flow meter was insulated with 10 mm Armaflex insulation and was calibrated directly for each fluid at each temperature. Details of the rotameter calibration may be found in Appendix 3. The liquid temperature at the rotameter was measured with thermocouple 7.

Liquid leaving the rotameter passed through a section of tubing which was wrapped with 2 m of electrical heating tape. This heater was regulated manually with a Superior Electric Powerstat® variable autotransformer (variac) and compensated for the heat loss incurred from circulating the liquid outside the air bath. A 6.1 m length of tubing coiled in a diameter of 90 mm was installed in the air bath and provided sufficient residence time for the liquid feed to attain the temperature of the system. Thermocouple 1 was used to measure the temperature of the liquid feed as it entered the approach tube to the laminar jet.

Liquid leaving the absorption chamber was regulated with a precision needle valve as discussed earlier. Thermocouple 2 was used to record the temperature of the liquid leaving the absorber. Spent solution was collected in a stainless steel receiving tank which was 310 mm in diameter and 673 mm in height (approximately 51 L). The spent solution was blanketed with helium (He). A pressure

equalizing vent line was connected to the He purge system. Liquid sampling facilities were installed in the liquid lines entering the rotameter and leaving the absorption chamber. Liquid was occasionally sampled at the rotameter and analyzed for CO_2 content and solution normality.

3.2.4 Liquid Circulation System

A liquid circulation system was required to maintain the liquid level in the constant head reservoir. Fresh degassed liquid feed was preheated to the system temperature in a 51 L stainless steel feed tank situated inside the air bath. The feed tank had the identical dimensions of the spent solution receiving tank. The feed tank was blanketed with He and the internal pressure was balanced by a vent line connected to the He purge system. A vacuum line connected to a Central Scientific Co. Cenco Hyvac 2 vacuum pump was installed on the top of the feed tank to enable the transfer of regenerated amine from the reboiler to the feed tank. The vacuum transfer also served to further degas the lean solution.

Liquid was drawn from the bottom of the feed tank and fed to a 208 W Little Giant® Model 5-MD-SC centrifugal pump. Pump output was regulated by a Whitey® SS-1RS4 needle valve and sent to an inlet port on the top flange of the constant head reservoir. The tubing section from the pump to the

reservoir contained a Cajon® 60 μm stainless steel sintered metal filter and a glass wool filter to remove any particulate matter in the liquid. A 2 m length of tubing was wrapped with 3 m of electrical heating tape which was regulated by a second variac. The temperature of the liquid entering the reservoir was monitored by a Thermo Electric digital temperature indicator.

Liquid filled the constant head reservoir to a depth of approximately 165 mm. Liquid overflow was returned directly to the feed tank through a 12 mm diameter overflow line. A sight glass was installed on the constant head reservoir to visually indicate the liquid level. The vapor space above the liquid was purged with He on start-up and a pressure equalization vent was connected to the He purge system. A line was included to allow the reservoir to drain completely on shut-down.

3.2.5 Temperature Control System

The absorption chamber, supporting frame and the liquid feed tank were housed in a 1.06 m^3 air bath with inside dimensions of 1.4 m x 1.2 m x 0.6 m. The bath temperature was maintained at ± 0.5°C of the setpoint by a Hallikainen Instruments Thermotrol® temperature controller. The air bath walls were insulated with 40 mm fiber insulation made by Forty Eight Insulation Inc. and were lined with stainless

steel sheeting. Seven 250 W Chromalox electrical strip heaters provided sufficient capacity to maintain the bath at temperatures ranging from 25° to 100°C. Two of the finned heaters were under manual control and were only used to bring the bath up to temperature initially. The air bath heating system also included a Chromalox Type ARC-260 High Temperature Limit Control.

At least 12 h were required to allow the large volume of liquid in the feed tank to equilibrate when setpoint changes were made in the air bath temperature. A copper pipe cooling system provided excess heat loss and stabilized the air bath temperature when absorption measurements were taken at temperatures below 40°C. A 250 mm diameter 4-blade fan driven by a 1/4 hp electric motor at 1725 RPM continuously mixed the air within the bath.

The temperatures of the flowing liquid and gas phases were measured with iron-constantan Type J thermocouples. The thermocouples were calibrated against a Leeds and Northrup platinum resistance thermometer in the temperature range of interest. A Leeds and Northrup Millivolt potentiometer was used to measure each thermocouple potential relative to a cold junction maintained at 0°C. A Thermo Electric 12-point low-resistance silver conductor switch mounted on the sphere absorber main control panel was used to select the thermocouple to be measured.

3.2.6 Amine Regeneration System

A regeneration system was used to strip the soluble gas from the amine solution so that it could be reused. A schematic diagram of the regenerator is given in Figure A2.2 of Appendix 2. The regenerator consisted of a Q.V.F. VS 20/PL 20 L spherical glass vessel for a reboiler, a Q.V.F. PS 3/18 glass pipe section and a Q.V.F. HE3 glass condenser. The reboiler was fitted with two 38 mm access ports, a 25-mm access port, one 13 mm access port on the top hemisphere, and one external 38 mm port on the bottom. The 38 mm ports were each capped with stainless steel flanges to allow the use of Swagelok® tubing connectors.

The kettle rested in a Glas-Col Apparatus Model TM-118S heating mantle equipped with two 770 W heaters and was supported by a steel frame. Solvent vapors passed through the intermediate pipe section and entered the overhead condenser. Water flowing through the condenser was cold enough to provide total reflux. A vent line was attached to the top of the condenser to equalize the internal and external pressures, and exhausted to a fume hood. Nitrogen was purged through the regenerator during liquid transfer to prevent atmospheric oxygen from entering the reboiler and reacting with the hot amine solution.

Details of the operating procedure may be found in Appendix 2. Trial regeneration runs were performed using 20 wt % MDEA solutions saturated with CO_2 at atmospheric pressure. Measurement of the CO_2 content of the amine solution after regeneration showed that the device was capable of stripping the solution to a loading of approximately 0.03 mol CO_2 per mol MDEA.

3.3 Operation of Equipment

The sphere absorber apparatus was operated continuously and consequently a condition of steady state was required before any measurements could be taken. A detailed desciption of the procedure used to bring the absorber to a steady state can be found in Appendix 2. The equipment can be run by one experienced operator, however it is advised that a second operator be present on occasion throughout the run. A typical set of data may be collected in five to six hours.

Special attention was given to the assumption of laminar flow over the surface of the sphere. Initial attempts to achieve flow rates of liquid similar to those reported by Goettler (1967), Savage and Kim (1985) and Kim and Savage (1986) resulted in liquid films with visible rippling. To avoid surface rippling, liquid flow rates were restricted to less than 2.0 mL/s. In operation, the laminar

jet length and liquid take-off length were maintained at 2.0 mm and 25 mm respectively.

The surface wetting characteristics of the solutions in this work were found to deteriorate with increased temperature and increased water content. All attempts possible were made to eliminate any contamination of the liquid feed system by oils and greases. The sphere was thoroughly cleaned with low-pressure steam and only handled with optical lens cleaning paper. The spherical film was easily ruptured at temperatures above 40°C when the liquid did not contain any surfactant. At 75°C, it was not possible to wet the sphere during start-up. A decision was made to investigate the use of a surface active agent to improve the ability of the liquid to wet the solid surface of the sphere.

Sodium lauryl sulphate (Teepol™) was used as the surface active agent in this study. Teepol™ was added to the 20 wt % amine solution to maintain a stable film at 75°C. The minimum amount required was found to be 0.01 wt %. This concentration was used for all runs with the 20 wt % solution. A surfactant content of 0.0075 wt % was used for the 40 wt % MDEA solution. A surfactant concentration of 0.1 wt % was needed to maintain a stable film of water at 25°C. Experimental measurements of the rate of absorption of N_2O in 20 wt % MDEA solution were taken at 25°C before and after the addition of surfactant. The absorption rates

were identical and the effect of Teepol™ was assumed to be negligible.

3.4 Chemicals and Gases

The aqueous MDEA solutions were prepared from distilled water and N-methyldiethanolamine supplied by Aldrich Chemical Co. The MDEA had a minimum purity of 99 % and was used without further purification. Chakma and Meisen (1985) analyzed the MDEA supplied by Aldrich by gas chromatography and confirmed the 99 % purity specification. Samples of the MDEA stock were analyzed by gas chromatography using columns packed with Chromosorb W and Poropak Q. The 0.4 % impurity was found to be water.

Amine solutions were prepared by weight in 45 kg batches in a polypropylene carboy. The water in the MDEA stock was not accounted for in the solution preparation. Special care was taken to reduce the time that the solution was exposed to atmospheric oxygen and CO_2 while being prepared. The sodium lauryl sulphate (Teepol™) was supplied by Fisher Scientific Co. in powdered form. The piperazine was supplied by Aldrich Chemical Co. and had a minimum purity of 99 %.

The He and nitrogen gases used in the experiment were supplied by Linde and had minimum purities of 99.996 % and 99.93 % respectively. The CO_2 and N_2O were also supplied by

Linde and had minimum purities of 99.9 % and 98.5 % respectively. The N_2O was analyzed by gas chromatography and found to have a purity of 99.4 %.

3.5 Measurement of Data

The sphere absorber variables which were recorded during an experimental run are shown below. Estimates of the experimental precision in measuring each variable are also included.

- Barometric pressure (±0.1 mm Hg)
- Room temperature (±0.5°C)
- Absorber pressure (±5 mm H_2O)
- Jet length (±0.02 mm)
- Liquid take-off length (±0.02 mm)
- Liquid rotameter reading (±0.5 mm)
- Standard gas volume in soap film meter (±0.05 mL)
- Time required to sweep a soap bubble through the gas volume (±0.1 s)
- Seven process temperatures (±1 μV)
- Variac and Thermotrol settings

Once a steady state condition was achieved, the data were recorded. Other variables which were recorded included: MDEA concentration, the solute gas type, piperazine concentration, Teepol™ concentration, the jet nozzle diameter, and the elapsed time. Approximately ten

absorption rates were recorded at each liquid flow rate studied. Three liquid flow rates were generally tested each day in operation.

The seven process temperatures measured were:

T_1	Amine to Absorption Chamber
T_2	Amine from Absorption Chamber
T_3	Gas at Soap Film Meter
T_4	Gas at Absorption Chamber
T_5	Gas from Circulation Pump
T_6	Gas to Circulation Pump
T_7	Amine at Liquid Rotameter

Process temperatures were recorded at the start and end of each liquid flow rate.

3.6 Analysis of Data

The physical absorption process on the sphere was assumed to be described by Equation (50), the extended series solution of Olbrich and Wild (1969). The physical absorption on the jet was assumed to be described by Equation (53) given by the penetration theory. Any errors incurred by neglecting the entrance region effects in the laminar jet itself were considered to be small. This was justified by the relatively small active surface area of the jet in comparison to the surface area of the sphere.

Nevertheless, the presence of the laminar jet was still considered in the analysis of the raw data.

The measured overall absorption rate of solute gas is a combination of absorption by the laminar jet, G_j , and absorption by liquid on the sphere, G_s .

$$G = G_j + G_s \tag{91}$$

Absorption of gas into the liquid on the support rod was assumed to be negligible. This was later verified when measurements were taken at different liquid take-off lengths. The fraction of the total absorption rate that occurred on the laminar jet was later determined to be 0.02 or less.

Both G_j and G_s are nonlinear functions of the molecular diffusion coefficient D. Hence the value of D was determined numerically using an iterative procedure.

Correlations of the physical solubility of N_2O in MDEA solutions, the kinematic viscosity and the density of MDEA solutions as described in Appendix 4, were used in the analysis. Gas density was estimated using the ideal gas law. The average of T_1 and T_2 was used to evaluate the physical properties of the system. It was assumed that there was no increase in the interfacial temperature due to heat of solution, and interfacial turbulence was assumed to be negligible.

The interfacial area of the laminar jet was calculated from the nozzle diameter and the measured jet length

$$A_j = \pi d_j h_j \qquad (92)$$

The interfacial area of the spherical film was estim[illegible] Equation (52).

The value of K_L was calculated from the measu[illegible]olute gas absorption rate by using the following expression

$$(G_s + G_j) = (A_a + A_j) K_L \left[\frac{p}{H} - C_o\right] \qquad (93)$$

Equations (70) to (85) were then used to estimate the value of k_g. The value of k_L was calculated using Equation (69). By equating the mass transfer rates in both films

$$k_g (A_a + A_j)[P_T - p_{H_2O} - H C_i] = k_L (A_a + A_j)[C_i - C_o] \qquad (94)$$

Rearranging gives

$$C_i = [k_g (P_T - p_{H_2O}) + k_L C_o]/[k_L + k_g H] \qquad (95)$$

This value of C_i was used in all subsequent calculations. The bulk phase gas concentration in the liquid entering the absorption chamber was assumed to be zero. Complete mixing was assumed to occur at the jet-sphere junction, such that the concentration of solute gas in the bulk liquid entering the spherical film was

$$C_o = G_j / L \qquad (96)$$

The overall gas absorption rate was calculated from the soap film meter volume and the soap bubble sweep time, and was converted to kmol/s using the ideal gas law. The average value of all the measurements of G for a single liquid flow rate was used in the calculation.

The amount of solute gas absorbed by the laminar jet was estimated by first guessing the value of the diffusion coefficient and then using Equation (53) to calculate G_j. The value of G_s was determined from Equation (91) and was scaled to the diameter of the dry sphere using the area correction, A_a / A_s. Equation (50) was solved for the value of D which caused the predicted absorption rate on the sphere to equal the measured experimental value. This calculated value of D was then used to revise the estimate of the amount of solute gas absorbed by the laminar jet. The calculation procedure was continued until the value of D did not change by more than 0.01 %.

The solution procedure, similar to that used by Moore (1971), involved a bisection method search routine. A computer program was developed to carry out these calculations and is listed in Appendix 6.

The chemical absorption process on the sphere was assumed to be described by Equations (63) to (67), the model

of Wild and Potter (1968). The absorption on the laminar jet was assumed to be described by the model of Danckwerts (1970)

$$G_j = 4\sqrt{h_j\, LD}\,(C_i - C_o)\,(1 + k_{ov}\, t/3) \qquad (97)$$

where t is the gas-liquid contact time of the laminar jet.

The nitrous oxide analogy was used to estimate the molecular diffusion coefficient and the physical solubility of CO_2 in MDEA solutions. The physical property correlations, gas phase resistance correlation, and interfacial area corrections described above were also used in the analysis of CO_2 absorption rate data. In general, the logic required to determine the value of k_{ov} from the raw absorption rate data is analogous to the procedure used to calculate the molecular diffusion coefficient from N_2O absorption rate data. Once the value of k_{ov} was determined, the product $k_{ov}\, t_D$ was calculated to check whether the proper Equation (63) to (67) was used in the analysis.

The contribution of uncatalyzed CO_2 hydrolysis, k_{H_2O}, given by Equation (11), was assumed to be negligible relative to the magnitude of k_{ov}. Since the solution pH was usually below 9, no formation of alkylcarbonates was assumed to occur in the liquid. The rate of reaction of CO_2 with OH^- ion was assumed to be given by Equation (12). The effect of the ionic strength of the solution on the value of k_{OH^-} was assumed to be small. The concentration of OH^- was

estimated with Equations (13) to (15).

The inlet CO_2 loading was determined to be 0.03 mol CO_2 per mol MDEA by experimental measurement as described in Chapter 3.2.6. The average CO_2 loading in the spherical film was used in Equation (13). The equilibrium concentration of free CO_2 in the liquid, C_{eq}, was assumed to be zero. Since the CO_2 loading was small, the concentration of free amine was assumed to be given by

$$[MDEA] = [MDEA]_0 \ (\ 1 - \alpha \ ) \qquad (98)$$

Appendix 7 contains a sample calculation which provides additional detail of the data reduction procedure. A computer program was developed to carry out these calculations and is listed in Appendix 6.

4. EXPERIMENTAL RESULTS

The sphere absorber was initially used to measure the rate of physical absorption of CO_2 into water. To determine whether there was an effect of liquid take-off length on the observed absorption rate, measurements were taken at take-off lengths ranging from 7 to 28 mm. Figure 6a illustrates the effect of the liquid take-off length on the observed absorption rate of CO_2. The experimental data were collected on 85/11/22 at a constant temperature of 24°C and a constant liquid flow rate of 0.77 mL/s, using a jet length of 1.7 mm. Raw data for all runs using the sphere absorber are contained in Appendix 1 and may be consulted for additional detail about the experimental conditions.

The data suggest that there is a definite effect of take-off length. At take-off lengths larger than 20 mm, the absorption rate remains relatively unchanged. When the liquid level rises above the 20 mm mark, the stagnant monolayer is forced onto the surface of the sphere and the absorption rate is decreased. The rate was reduced by 11 % when the take-off length was changed from 20 mm to 8 mm.

A similar study was performed at a later date as a check, using 20 wt % MDEA and N_2O as the solute gas. Similar behavior was revealed and is shown in Figure 6b. The data collected on 86/05/06 were at a temperature of 75°C, using a liquid flow rate of 0.82 mL/s and a jet length of 2.05 mm. In view of these results, the optimum take-off

length was assumed to be 20 mm and all experiments were conducted using this length.

Once the optimum take-off length had been established, the operating procedure was verified by calculating the molecular diffusion coefficient of CO_2 in water and comparing the value to those found in the literature. Using the sphere absorber, the diffusion coefficient at 25°C was determined to be 1.97×10^{-9} m^2/s. The gas phase resistance to mass transfer was estimated to be 2.2 % of the total resistance. Table 5 contains a comparison of experimental values of $D^\circ_{CO_2}$ at 25°C as reported by several authors. The results of this work compared favorably, and the equipment was considered to be operational.

Following the CO_2-water study, the absorption apparatus was used to measure the rate of absorption of N_2O into MDEA solutions. The raw data, contained in Appendix 1, were processed using the methods described in Chapter 3.6. Table 6 contains a summary of the pertinent results obtained in the data reduction procedure. Results are presented for each of the two amine solutions at three temperatures. The calculated values of the N_2O diffusion coefficient are listed in the fifth column of the table and are believed to be known to an accuracy of ±5 %.

The physical solubility of N_2O in MDEA solutions and the kinematic viscosity of MDEA solutions were measured experimentally. Details are described in Appendix 4.

Figure 6.

Effect of Take-off Length on Gas Absorption Rate

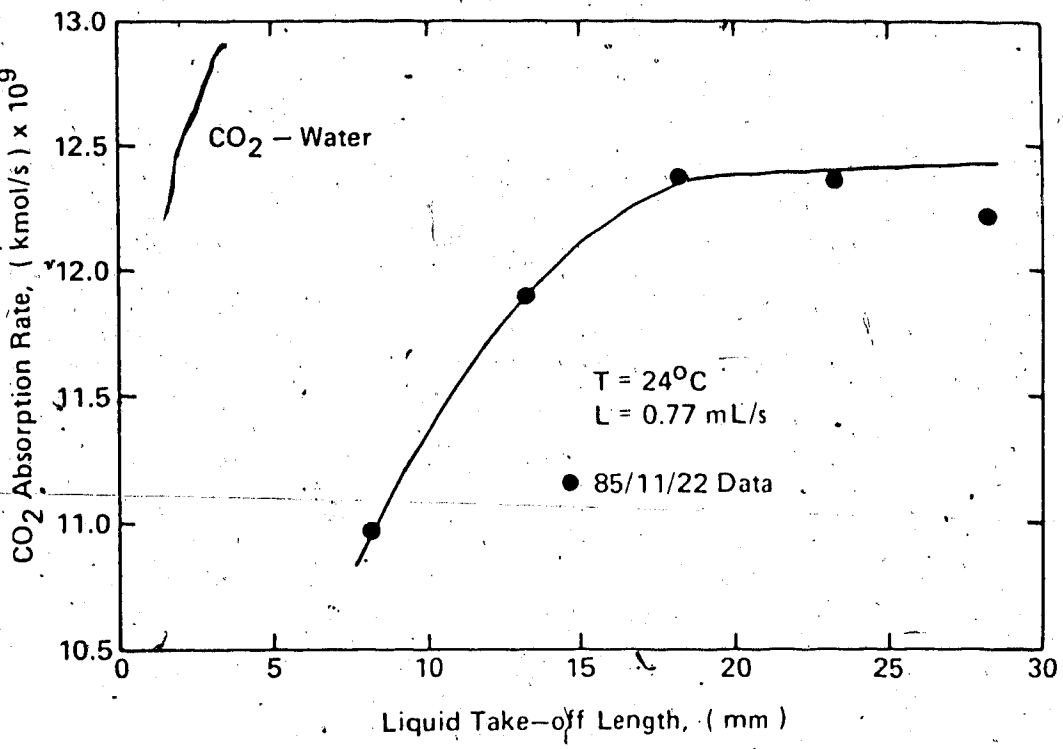

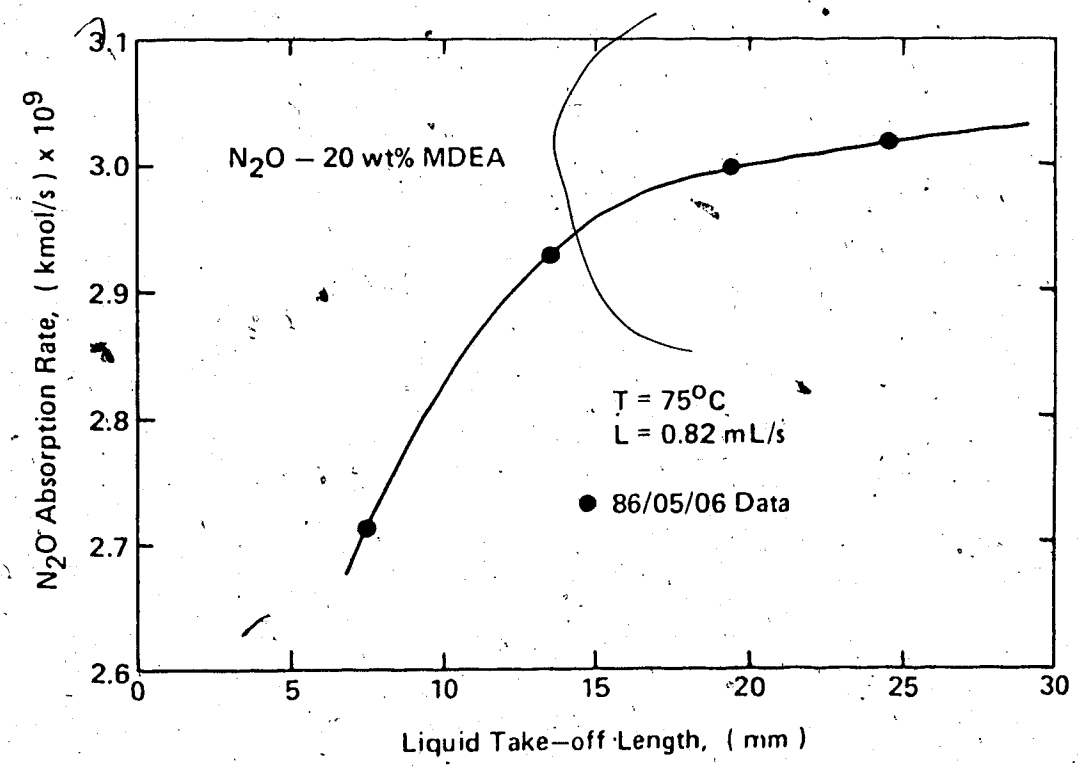

Table 5.

Diffusion Coefficient for CO_2 in Water at 25°C

D x 10^9 (m^2/s)	Reference
1.92	Davidson and Cullen (1957)
1.92	Ratcliff and Holdcroft (1963)
2.00	Vivian and King (1964)
1.95	Thomas and Adams (1965)
1.93	Khalil (1984)
1.97	This work

Table 6.

Diffusion Coefficient for N_2O in MDEA Solutions

wt % MDEA	T (°C)	$\mu \times 10^3$ (kg/m·s)	Gas Phase Resistance (%)	$D \times 10^9$ (m^2/s)
20	25.0	1.94	0.94	0.934
20	49.6	1.02	0.89	1.87
20	74.7	0.642	0.83	2.82
40	25.0	5.31	0.55	0.629
40	49.6	2.30	0.70	1.40
40	74.8	1.23	0.77	2.28

Correlations of the physical N_2O solubility, the kinematic viscosity and the solution density were used in the analysis of the absorption rate data. The third column of Table 6 contains the predicted value of the absolute viscosity of the amine solution at experimental conditions. The gas phase resistance in the fourth column was estimated using the techniques described in Chapters 2.4 and 3.6. The circulation of gas through the saturated absorption chamber was maintained at 110 mL/s. This corresponded to effective superficial gas phase velocity of 0.87 cm/s in the absorption chamber.

The raw experimental measurements for the CO_2 absorption studies are contained in Appendix 1 and were processed using the techniques presented in Chapter 3.6. Table 7 contains a summary of the results of the data reduction procedure. Results are presented for each of the two amine solutions at four temperatures.

The free amine concentration was estimated using Equation (98) and the gas phase resistance in the third column was estimated using the same approach as for the N_2O studies. The fourth column contains the overall observed rate constant that is calculated from the experimental data. The fifth column gives the pseudo-first order rate constant for the base catalysis contribution and the sixth column lists the second-order rate constant. The second-order rate constants are believed to be known to an accuracy of ±10 %.

Reviewing Equations (9) and (10) may provide some clarification of the various rate constants. Recall that the value of k_{H_2O} was assumed to be negligible.

The sphere absorber was then used to determine the effect of piperazine on the CO_2 absorption rate when used as an additive to MDEA solutions. The 40 wt % MDEA solution was maintained at 40°C and measurements were taken of the rate of absorption of CO_2 at a constant liquid flow rate. The results of the experiments are listed in Table 8. The ideal gas law was used to convert the soap film meter volumetric flow rate to molar absorption rate.

Table 7.

Reaction Rate Constant for CO_2 Absorption in MDEA Solutions

20 wt % MDEA Solution

T (°C)	[MDEA] (kmol/m³)	Gas Resist (%)	k_{ov} (s^{-1})	k_2[MDEA] (s^{-1})	k_2 (m³/kmol·s)
25.1	1.64	4.1	9.7	9.0	5.5
49.7	1.61	7.2	44.9	39.0	24.2
59.9	1.59	8.2	65.4	53.8	33.7
74.8	1.58	10.7	130.3	99.1	62.8

40 wt % MDEA Solution

25.3	3.35	4.1	19.3	18.5	5.5
40.2	3.32	6.0	43.5	40.2	12.1
49.9	3.30	7.6	71.4	64.1	19.4
74.9	3.23	13.4	246.7	207.2	64.1

Table 8.

Effect of Piperazine Concentration on CO_2 Absorption Rate in 40 wt % MDEA at 40°C

Liquid Flow Rate = 0.58 mL/s

[Piperazine] (kmol/m³)	G x 10^8 (kmol/s)
0.00	3.13
0.05	3.66
0.10	4.36
0.15	5.08
0.20	6.03
0.40	9.18

5. DISCUSSION OF EXPERIMENTAL RESULTS

5.1 Physical Absorption Studies

The results of the analysis of the N_2O absorption studies may be conveniently represented in graphical form as shown in Figure 7. This plot illustrates the combined influence of temperature and liquid viscosity on the N_2O diffusion coefficient. The experimental data from this work are plotted along with data from other sources. The data of Thomas and Adams (1965) are for N_2O absorption in water-glycerol solutions at 20°C. The data of Haimour and Sandall (1984) are for N_2O absorption in water and 20 wt % MDEA solutions at temperatures ranging from 15° to 35°C. All the experimental data points display the same general trends. Diffusivity is seen to increase with temperature and to decrease with increasing liquid viscosity.

The theory of liquids has not yet progressed to the level where theoretical predictions of the molecular diffusion coefficient may be made with confidence. The existing methods for predicting diffusion coefficients are based on empirical correlations of experimental data. Reid et al.(1977) have reviewed several correlations such as the Wilke-Chang method. Most models have the following form

$$\frac{D\mu^{\widetilde{C}_1}}{T} = C_2 \qquad (99)$$

where C_1 and C_2 are functions of solute and solvent

Figure 7.

Stokes-Einstein Relationship for N_2O Diffusivity Results

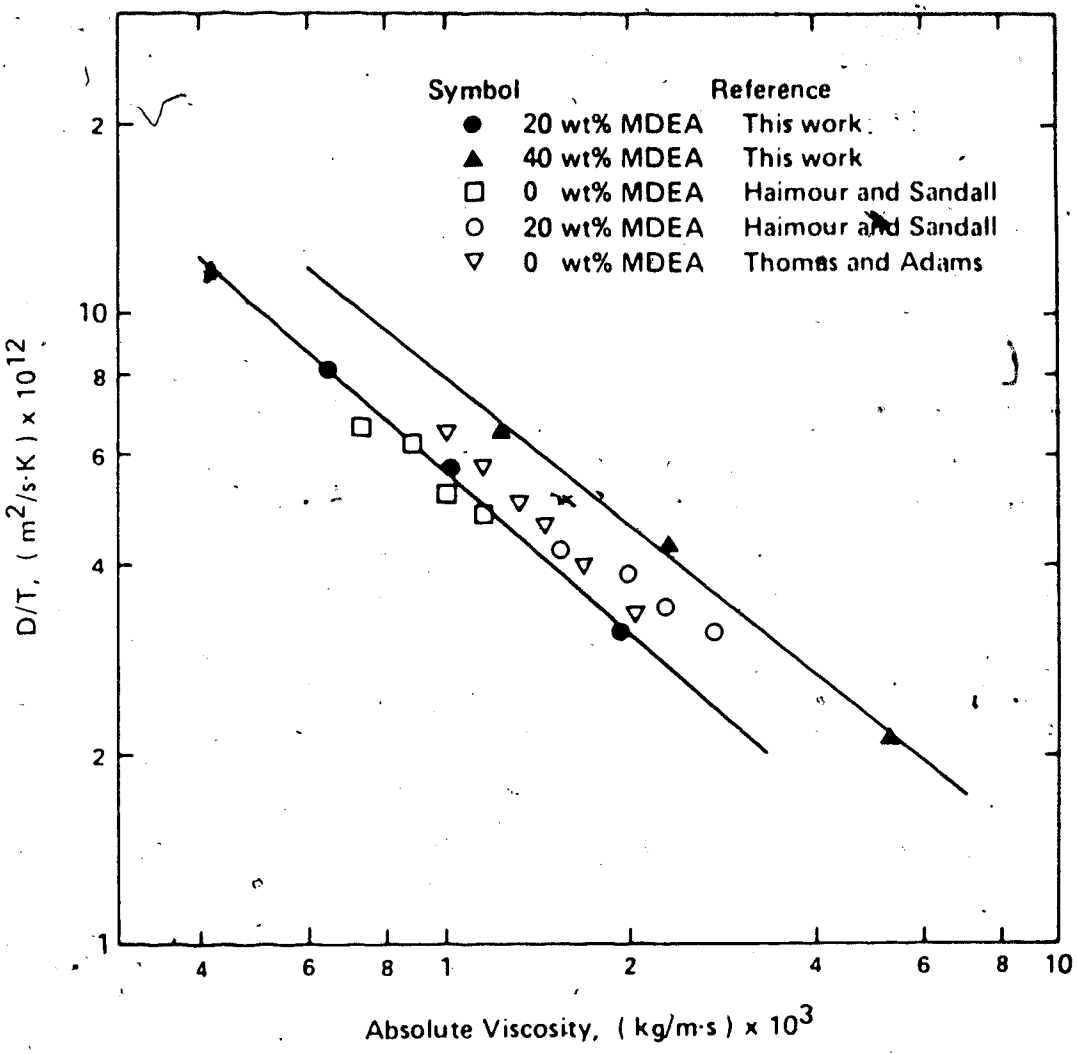

properties. Using this approach, the data for the 20 wt % and 40 wt % solutions were correlated with the following expressions

20 wt % MDEA

$$\ln D_{N_2O} /T = -31.8133 - 0.8558 \ln \mu \qquad (100)$$

40 wt % MDEA

$$\ln D_{N_2O} /T = -30.9420 - 0.7785 \ln \mu \qquad (101)$$

These correlations were required to interpret the results from the chemical absorption studies using CO_2 and are shown as the solid lines in Figure 7.

The data from this work show a similar effect of solution viscosity as the data of Thomas and Adams (1965) but differ from the results of Haimour and Sandall (1984). Their data were correlated with a slope of -0.63 while the results of this work suggest a value of about -0.8. The difference is believed to be caused by the values of solution viscosity and density used in their data analysis.

It was of interest to determine whether or not the experimental data followed the same trends in liquid flow rate as the theoretical expressions predict. Equation (100) was used in conjunction with Equations (50) to (53) to estimate the overall rate of absorption of N_2O in a

jet-sphere system. Figure 8 shows the simulated overall N_2O absorption rate as a function of liquid flow rate for 20 wt % MDEA at 50°C using an absorber pressure of 96 kPa and a diffusion coefficient of 1.85×10^{-9} m^2/s. The jet dimensions of 2.1 mm by 0.60 mm used in the simulation were the same as those in the experimental data set collected on 86/05/05. The experimental data are plotted in the figure as well. Although the experimental data were used to generate the correlation in Equation (100), the data clearly display a general relationship where G is proportional to $L^{1/3}$.

The sphere absorber apparatus proved to be an effective device for determining the molecular diffusion coefficient for sparingly soluble gases such as N_2O in aqueous solutions. The apparatus is a steady-state device and provides sufficient interfacial surface area to obtain measurable absorption rates. At the higher temperatures where gas solubilities are low, other laboratory absorbers such as the laminar jet would be unable to obtain measurable absorption rates.

There is scope for improvement in the theoretical models, considered in Chapter 2, which describe the hydrodynamics of the spherical film and the gas absorption process. Surface tension plays a role in the force balance used to establish the boundary condition at the free surface. Temperature- or composition - dependent liquid density will have an effect on the concentration of

Figure 8.

Rate of Absorption of N_2O into 20 wt % MDEA at 50°C

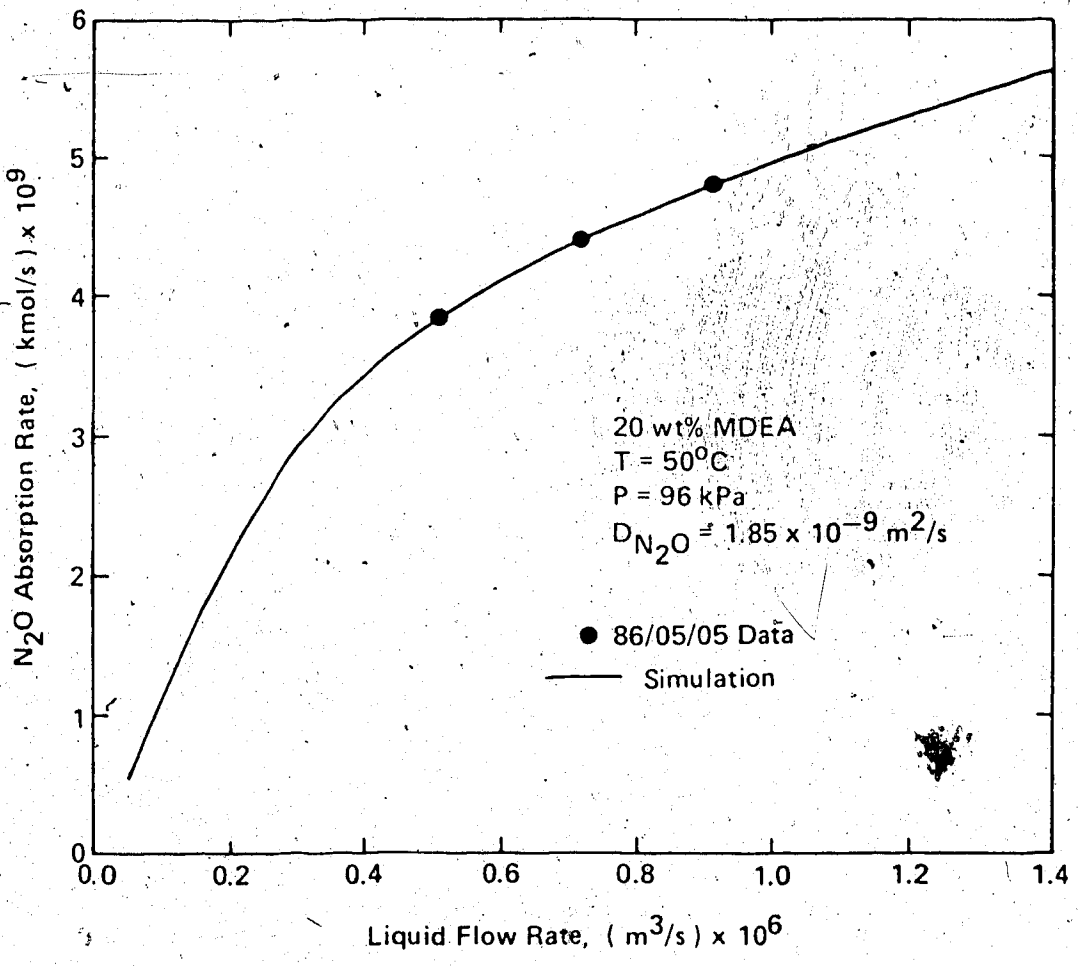

molecular species in the liquid phase. Temperature- or composition - dependent liquid viscosity will have an effect on the shear forces along a streamline. These effects will alter the shape of the free surface which will alter the velocity profile within the spherical film. The mass transfer rate of absorbing gas will be affected in turn because the material balance expression in Equation (26) is coupled to the hydrodynamics of the system through the velocity profile in the bulk convection term. A more accurate understanding of the hydrodynamics of the film would provide a basis to improve the mass transfer model which describes the concentration profile of the solute gas within the liquid film. These nontrivial modifications to the models were beyond the scope of this study.

5.2 Chemical Absorption Studies

The results of the analysis of the CO_2 absorption studies are summarized in Table 7. Most points were found to lie in the fast reaction regime, however, the measurements for both solutions at 25°C fell into the transition zone from the fast to slow reaction regimes. This in no way affected the results at 25°C. When calculating the value of k_{ov}, Equation (66) was used rather than Equation (67). The overall reaction rate constant is seen to range from 9 to 250 s^{-1} and to increase with temperature and free amine concentration.

In order to quantify the catalytic effect of MDEA, the contribution of hydroxyl ion was eliminated using the methods described in Chapter 2.1. The pseudo-first order reaction rate constant for the CO_2 hydrolysis reaction, $k_2[MDEA]$, is plotted in Figure 9 as a function of reciprocal temperature and amine concentration. The data of Yu (1985) for 30 wt % MDEA (2.5 kmol/m^3) are included for comparison. The results compare favorably with the data of Yu (1985).

To confirm the dependence of the pseudo-first order rate constant on the free amine concentration, the data from Table 7 were plotted in Figure 10 against free amine concentration. On a log-log scale, a slope of one indicates a direct dependence of the rate constant on free amine concentration. To a good approximation, the experimental data indicate that the dependence is linear. Therefore, it can be assumed that the base-catalyzed hydrolysis reaction proceeds at a rate which is proportional to the free amine concentration.

The data of Yu (1985) and the correlation developed by Versteeg et al.(1986) are plotted on Figure 10 for comparison. The correlation of Versteeg et al.(1986) is approximately 19 % lower than the results of this work. In view of the fact that these results were obtained by a completely different experimental technique, this difference may be explained by three possible causes. Assuming that in both methods, the measured absorption rate was the same, a

Figure 9.

Effect of Temperature on the Pseudo-First Order Rate Constant.

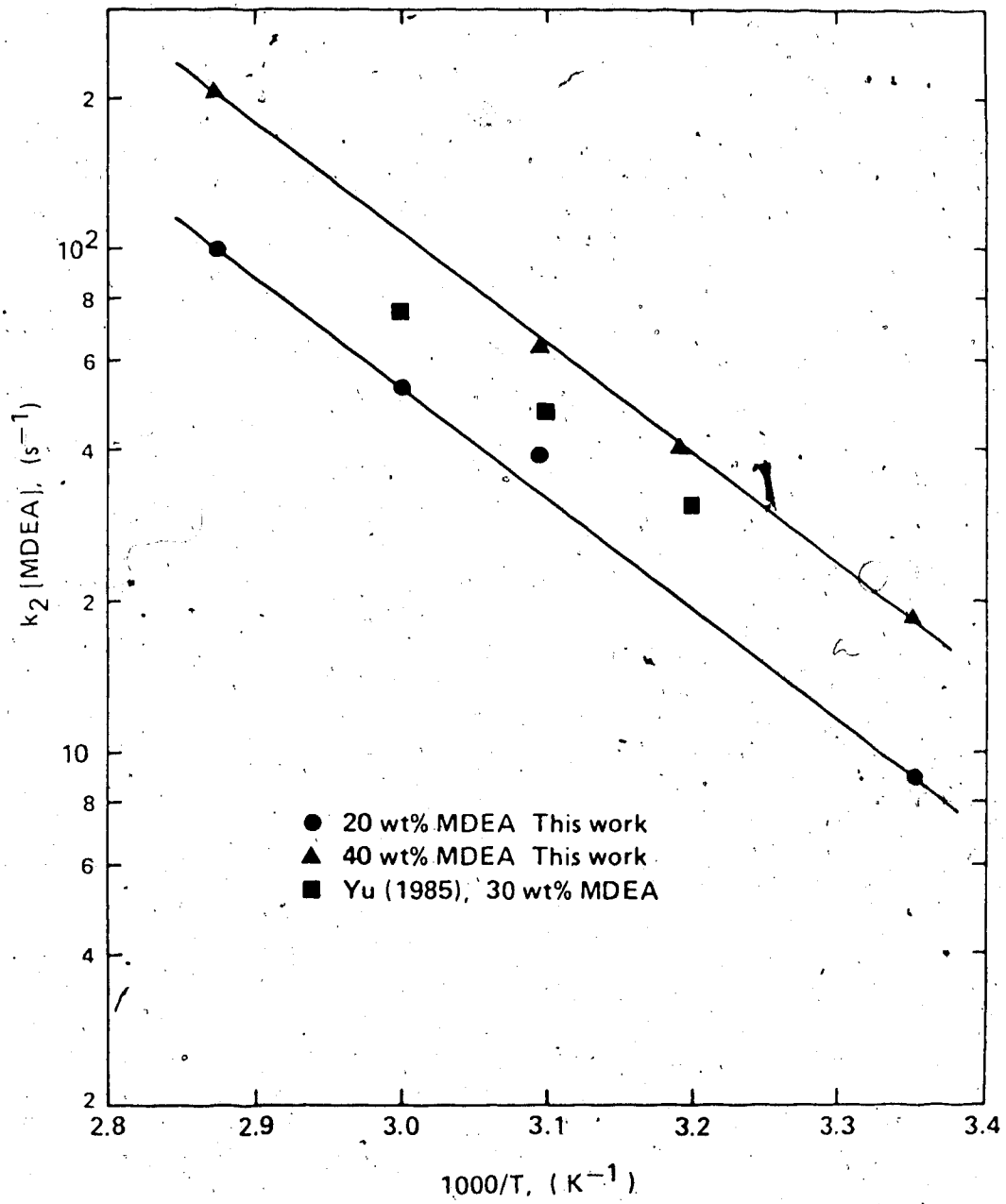

Figure 10.

Effect of MDEA Concentration on the Pseudo-First Order Rate Constant

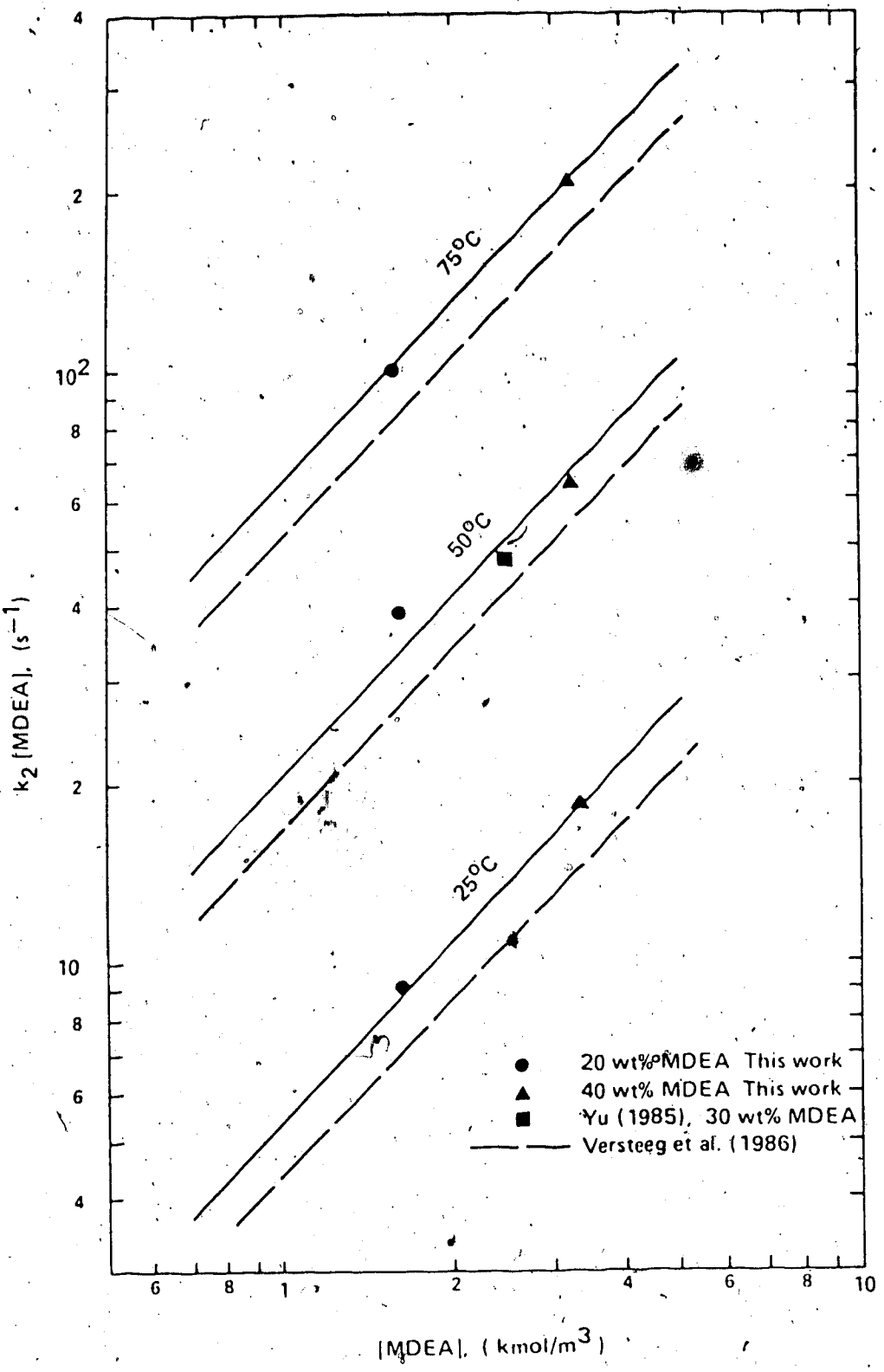

10 % difference in the correlations used to estimate the physical solubility of CO_2 in the solution would cause this discrepancy. In a similar manner, a 19 % difference in the correlations used to estimate the molecular diffusion coefficient of CO_2 in the solution would cause this discrepancy. Versteeg et al.(1986) did not consider gas phase resistance to mass transfer in their analysis of data. Table 7 shows that in this work, the gas phase resistance for chemical absorption studies was estimated to be an order of magnitude greater than for the case of pure physical absorption. For CO_2 absorption, the gas phase resistance was estimated to be approximately 5 to 10 %. Therefore, by Equation (69), if the resistance was ignored, the value of k_L would decrease by about the same amount. This would have the same effect as differences in the estimates of physical solubility.

The pseudo-first order reaction rate constants in Table 7 were divided by the free amine concentration to calculate the second order rate constant k_2, which is independent of concentration. The values of k_2 derived from the experimental data are plotted in Figure 11 as a function of reciprocal temperature. The values reported by Yu (1985), Versteeg et al.(1986), and Bidarian and Sandall (1986) are included for comparison. The experimental data for k_2 were correlated with the following expression

$$k_2 = 1.615 \times 10^8 \exp\left(\frac{-5134}{T}\right) \qquad (102)$$

Figure 11.

Effect of Temperature on the Second Order Rate Constant

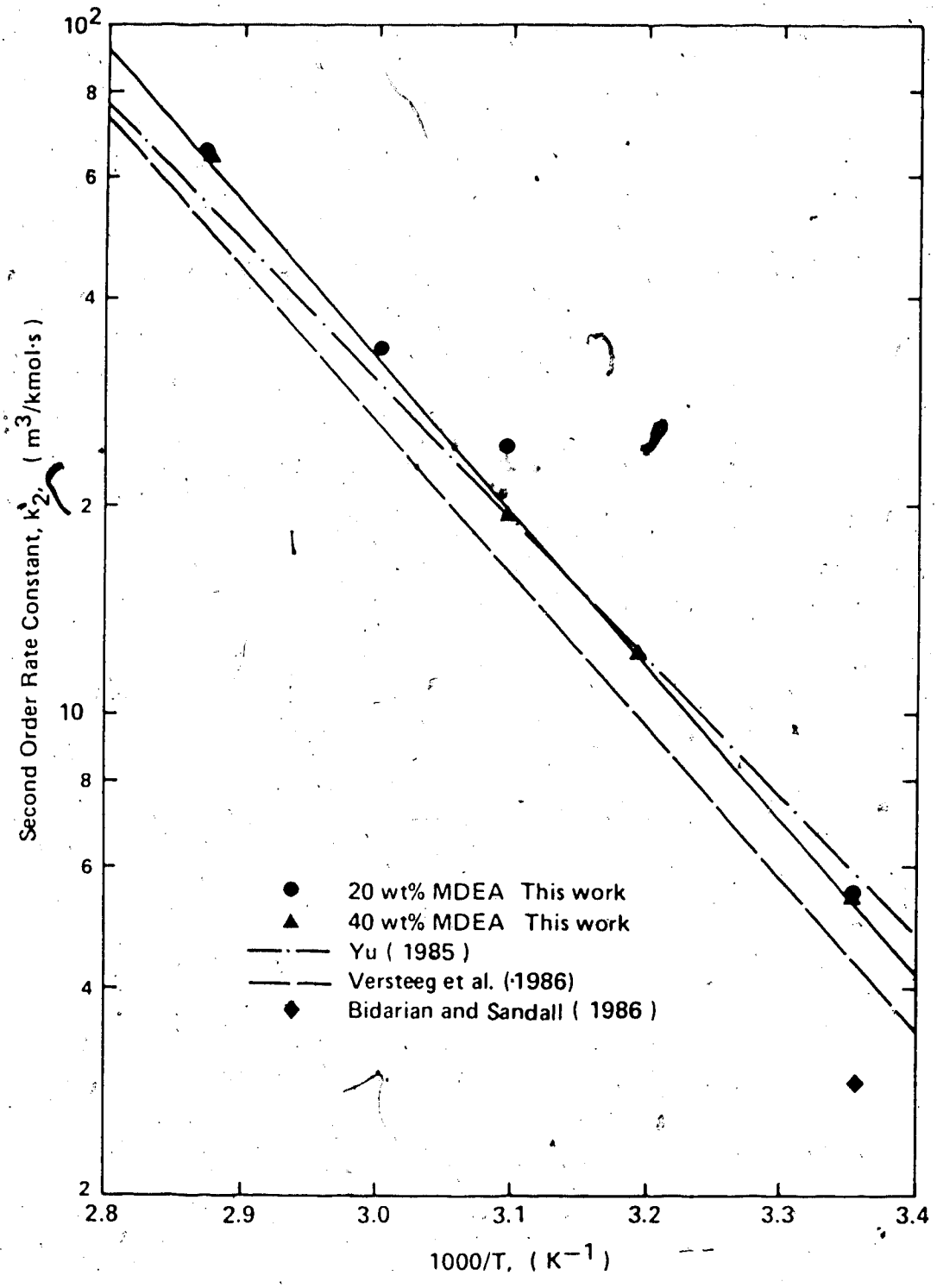

The activation energy was calculated to be 42.7 kJ/mol (10.2 kcal/mol). This compares with the values of 38.5 kJ/mol and 42.4 kJ/mol as determined by Yu (1985) and Versteeg et al.(1986) respectively.

As in the case of physical absorption studies, the use of the sphere absorber to determine reaction rate constants proved to be successful. The advantage of the sphere absorber over a stirred-cell reactor is that it is a steady-state device. The gas phase "sees" a liquid with a constant composition; therefore the device can be operated with a fresh amine solution such that effects due to reversible reactions or CO_2 backpressure can be virtually eliminated.

5.3 Absorption Rate Promotion

It is known that trace amounts of certain additives can have a dramatic effect on the rate of absorption of CO_2 into alkaline solutions. An additional objective in this experimental study was to quantify the effect of a rate promoter on the absorption rate of CO_2 in MDEA solutions. Appl et al.(1982) developed a bulk removal process which uses the diamine piperazine to increase the rate of absorption of CO_2 in MDEA solutions. This process is covered in US Patent #4,336,233.

The patent calls for the use of 1.5 kmol/m³ to 4.[redacted] kmol/m³ MDEA with 0.05 kmol/m³ to 0.8 kmol/m³ piperazine as an absorption accelerator. The scrubbing temperature should be approximately 40°C. Piperazine may be used by itself in amounts from 0.81 kmol/m³ to 1.3 kmol/m³ but is not of interest for industrial applications since these low concentrations do not provide sufficient cyclic capacity for treating units. At high CO_2 partial pressures, the carbamate of piperazine precipitates as a solid. Furthermore, the solubility of piperazine in water at 20°C is only 1.5 kmol/m³.

Figure 12 contains a plot of the experimental absorption rate data from Table 8. The CO_2 absorption rate can be seen to increase with piperazine concentration. Using 0.40 kmol/m³ (≃3.5 wt %) piperazine in the 40 wt % MDEA solution, the CO_2 absorption rate was increased by a factor of three over the rate into MDEA with no promoter.

The patent briefly describes laboratory experiments that were conducted to demonstrate the superiority of piperazine as an absorption accelerator. Using a laminar jet absorber, CO_2 absorption rate measurements were taken at "standard conditions" for a solution containing 3.5 kmol/m³ MDEA and 5 mol % piperazine. This corresponds to approximately 14 wt % piperazine. The patent data suggest that the rate is increased by a factor of 8.1 over the case where the solution contains no piperazine. From an

Figure 12.

Effect of Piperazine Concentration on Absorption Rate of CO_2 into 40 wt % MDEA at 40°C

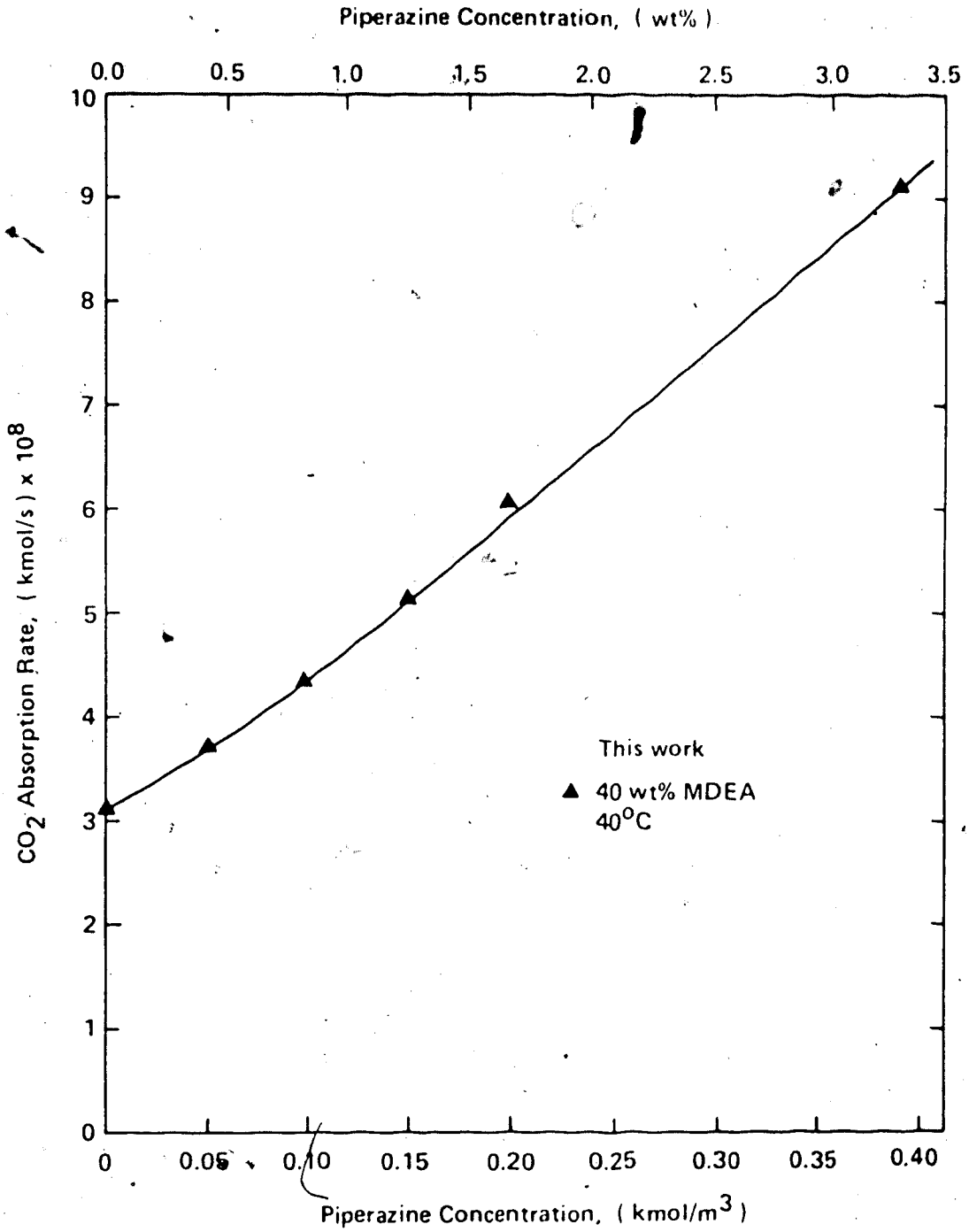

industrial application standpoint, these data suggest that a substantial reduction in solution circulation rate can be realized in bulk CO_2 removal schemes using MDEA solutions with piperazine as an additive.

A rigorous analysis of the absorption rate data calls for a mass transfer model which accounts for the parallel reactions of CO_2 with both MDEA and piperazine in the liquid film. The scenario is further complicated since piperazine is a secondary amine and reacts directly with CO_2 to form a carbamate salt as well as participating in the hydrolysis reaction. The theoretical work of Chakravarty et al.(1985) and Critchfield and Rochelle (1987) may be used to develop such a model, but this was beyond the scope of the present study.

The studies of Astarita et al.(1981, 1982), Mahajani and Danckwerts (1983), and Yih and Sun (1987) have dealt with the promotion of CO_2 absorption in carbonate - bicarbonate solutions. On a purely speculative basis, the promotion in the piperazine-MDEA system may be described by the "shuttle" mechanism. At the gas-liquid interface, CO_2 is dissolved in the liquid and reacts directly with the piperazine to form the carbamate ion. This reaction increases the CO_2 concentration gradient at the interface and results in enhancement of the mass-transfer rate over the case where only MDEA is present. The reversion of the carbamate to bicarbonate is a slow reaction which takes

place in the bulk liquid after the carbamate ion has diffused from the interface. The reversion regenerates piperazine which then diffuses back to the interface where it can further react with CO_2. This "shuttle" behavior proceeds in parallel with the base catalysis effect of the MDEA on the CO_2 hydrolysis reaction.

6. BACKGROUND MATERIAL FOR MODELLING STUDY

6.1 Nature of the Alkanolamine Treating Process

Alkanolamine treating units, or amine plants, have been used for decades to purify sour gas streams. The chemistry, engineering and operational aspects of conventional amine technology are described in detail by Butwell et al.(1982), Astarita et al.(1983) and Kohl and Riesenfeld (1985). In recent years, specialized applications of amine treating technology have been investigated. These applications include bulk CO_2 removal and selective absorption of H_2S from gases containing substantial amounts of CO_2.

Schendel (1983) describes a process using the formulated UCARSOL HS solvent and Petty and Ho (1984) present pilot plant data for a TEA plant which is used to recover bulk quantities of CO_2 from produced gases associated with CO_2-miscible flooding for the enhanced recovery of oil (EOR). Meissner and Wagner (1982), Meissner (1983) and Ripperger and Stover (1986) promote the use of activated-MDEA in similar applications. Goddin (1982) shows TEA-based bulk CO_2 recovery to be competitive with cryogenic methods when the CO_2 content of the feed gas is greater than 40 mole %.

The concept of selective absorption using aqueous amines has been around for some time. It is generally accepted that MDEA is the preferred alkanolamine for

selective absorption applications. Frazier and Kohl (1950), and Miller and Kohl (1953) presented pilot plant data for amine treating units using MDEA. At that time, the cost advantage of selective gas treating was insufficient to justify the use of the more expensive MDEA over a cheaper MEA solvent.

In the late 1970's and early 1980's, the increased cost of energy brought selective absorption technology back into the industrial scene. Vidaurri and Kahre (1977) presented pilot plant data which illustrated the relative rates of absorption of H_2S and CO_2 between different alkanolamines and showed MDEA as the most suitable amine. Pearce (1978) discussed Dow Chemical's experience with MDEA. Goar (1980) described the use of MDEA to enrich the feed streams to Claus Sulphur Recovery Units (SRU) and presented a scheme where an amine plant used a common regenerator with a Tail Gas Clean-Up (TGCU) process. Since then, research on topics relating to amine treating have been confined to experimental studies of gas absorption kinetics in various solvents, the development of specialized solvents for selective H_2S removal, and the development of improved process configurations and mechanical tray designs.

The literature review presented in Chapter 2.2 summarized the recent experimental studies of acid gas absorption kinetics in various alkanolamine solvents. Most studies involved measurement of the rate of absorption of

CO_2 in aqueous solutions of alkanolamines. A few investigations dealt with simultaneous absorption of H_2S and CO_2 but few fundamental data are available for the absorption kinetics of acid gases in the proprietary formulated solvents or in amine blends.

Some of the specialty solvents are most likely blends of tertiary amines, generally MDEA, and physical solvents such as Sulfolane, or blends of MDEA and other lower order amines and rate promoters. Sulfinol M, as described by Flynn et al.(1978), is a mixed solvent consisting of MDEA, Sulfolane and water and complements Shell's conventional Sulfinol solvent. The Exxon Research and Engineering solvents consisting of FLEXSORB SE, FLEXSORB HP, and FLEXSORB PS as described by Goldstein (1983), Chludzinski (1985, 1986), and Weichert et al.(1986) are proprietary blends of tertiary and/or hindered amines and organic physical solvents. Similarly, Union Carbide Corporation has developed a competitive suite of proprietary solvents including UCARSOL HS, UCARSOL CR and UCARSOL LE. These are briefly described by Thomas (1985). As with the FLEXSORB solvents, each has a specific application, either for high H_2S selectivity, bulk CO_2 removal, or mixed solvent applications. Other more exotic tertiary amine solvents such as tropine and diethylmonoethanolamine (DEAE) have been proposed and studied by Stogryn et al.(1983).

For modifications to the conventional process configuration, several examples include: Union Carbide's HS process for selective H_2S removal as discussed by Sigmund et al.(1981), the BASF Activated MDEA process for bulk CO_2 removal as presented by Meissner (1983), and the Selefining process for mixed solvent selective absorption as described by Snamprogetti's Gazzi et al.(1986).

Novel contactor designs include the structured packing products of Koch Engineering Co. and Sulzer Brothers Ltd. A recent contactor design described by Schendel (1986) and Bucklin and Won (1987) consists of a rotating packed bed. The HIGEE Liquid Vapor Contactor is claimed to provide advantageous conditions for selective H_2S absorption.

At this point, one can recognize the plight of a design engineer faced with selecting and designing a gas treating installation. In order to justify the selection of a particular process, adequate comparisons must be made with one or more process alternatives. Simulation tools which can be used for the rational design of amine treating facilities assist the engineer at this stage and provide new opportunities to select optimum values for process operating parameters.

Traditional procedures for amine plant design relied heavily on rules-of-thumb derived from operating experience. Goar (1975) discusses some of these rules-of-thumb by developing a hypothetical MEA plant design. The contactor

and regenerator were typically designed to use 20 stages, regardless of the minimum number required. The reboiler was designed to operate with a heat duty ranging from 925 to 1200 BTU per gallon of circulating amine solution (260 to 335 kJ/L). Amine circulation rates were usually based on a net amine loading of 3.0 SCF acid gas per gallon circulating solution (0.0224 m^3/L) or on a maximum rich amine loading. A 15 wt % MEA solution was a common solution strength. Similar guidelines exist for DEA systems.

More recently, the design of contacting devices in an amine treating unit has been based on the steady-state solution of the equations describing an equilibrium stage model. It was usually assumed that 4 or 5 ideal stages could be used to simulate the performance of amine absorbers and regenerators. An overall column efficiency of ≈25 % was then applied to account for deficiencies in the data used for design, to account for inadequate mixing on a stage, or to account for gas phase resistance to mass transfer. In any event, the design was usually padded with contingency factors. This approach was very successful for high pressure MEA and DEA systems. However, H_2S selectivity has been observed in a low-pressure DEA contactor (Donnelly and Henderson, 1974). In addition, the use of an overall column efficiency implied that the individual component stage efficiencies were equal.

Experimental and operating data presented by Vidaurri and Kahre (1977), Pearce (1978), Ammons and Sitton (1981), Blanc et al.(1981), Daviet et al.(1984) and Harbison and Handwerk (1987) show substantial evidence that the performance of a contactor using MDEA solution is affected by the relative rates of absorption of H_2S and CO_2 under different operating conditions. These data suggest that the absorption of acid gases into amine solutions must be considered as a rate process.

6.2 Simulation of Amine Treating Units

Technology to rigorously simulate absorption and distillation unit operations has been available for many decades, but has only recently been applied to simulate amine treating facilities. Reliable and accurate simulation of the amine treating process can only be achieved with a combination of a realistic and fundamentally-based generalized stage model, a robust and efficient numerical procedure to obtain a convergent solution, and an established thermodynamic and physico-chemical properties data base. In the model, an appropriate approach to account for the complex mass transfer and rate phenomena on a stage is to use the concept of a stage efficiency.

Perhaps the most widely used efficiency is the Murphree vapor stage efficiency. Rowland and Grens (1971) used a

stage-to-stage method which included Murphree vapor efficiencies to model the performance of MEA and DEA contactors. The Murphree vapor stage efficiency, $E_{i,j}$, is given by

$$E_{i,j} = (Y_{i,j} - Y_{i,j+1})/(K_{i,j} X_{i,j} - Y_{i,j+1}) \qquad (103)$$

where $Y_{i,j}$ and $Y_{i,j+1}$ represent the average compositions of the vapor leaving stages j and j+1 respectively. The quantity $K_{i,j} X_{i,j}$ represents the equilibrium vapor composition above liquid of composition $X_{i,j}$.

In their work, values of E were calculated for each component on each stage as functions of composition and temperature using an expression similar to Equation (119) described later in Chapter 7.1. The dependence of Murphree vapor stage efficiencies on composition and temperature was represented in terms of individual-phase mass-transfer coefficients. The mass-transfer coefficients were assumed to be constant on all stages and the calculated efficiencies were assumed to be equal for all components on a stage, but the efficiencies were allowed to vary through the column. The analysis of Rowland and Grens (1971) demonstrated the importance of considering the tray efficiencies in the stage model. In their MEA contactor example, E for CO_2 ranged from 0.0442 to 0.667. An equilibrium or ideal stage is represented by E = 1.0.

Browne (1976) combined the rigorous multistage multicomponent separation model of Ishii and Otto (1973) with the vaporization efficiency described by Holland (1981) and presented simulation results for MEA and DEA contactors and regenerators. The vaporization efficiency, $e_{i,j}$, is given by

$$Y_{i,j} = e_{i,j} K_{i,j} X_{i,j} \qquad (104)$$

Values of e range from 1.0 to ∞ for contactors and from 0.0 to 1.0 for regenerators. Browne (1976) used fundamental mass-transfer parameters to estimate the values of $e_{i,j}$ for H_2S and CO_2 in a MEA absorber and calculated the corresponding Murphree stage efficiencies. These were found to lie in the range 0.8 to 1.0 for H_2S and from 0.26 to 1.0 for CO_2 transfer in his example.

Browne (1976) was able to demonstrate the utility of an amine unit simulator by evaluating the processing benefits of the split-flow configuration and by performing several sensitivity studies on process variables to determine the effect on the predicted treated gas composition. Browne (1976) concluded that the program predictions were highly dependent on the acid-gas equilibrium solubility model used and that stage efficiencies are important and must be considered for accurate process design. The need for reliable fundamental absorption rate data required to estimate stage efficiencies was also identified.

Bullin et al.(1981) developed a process simulation program which models the performance of amine treating facilities. Little technical information about the program has been released, although the multistage model is claimed to use the approach of Ishii and Otto (1973), combined with a kinetic model that accounts for the chemical reaction rates and diffusional mass transfer rates. No reference has been made to any particular equilibrium solubility model or any mass-transfer coefficients and kinetic rate constants used in the model. Applications of the program have been presented by Bullin and Polasek (1982), Daviet et al.(1984), Holmes et al.(1984), and MacKenzie et al.(1986).

Krishnamurthy and Taylor (1984, 1985a, 1985b, 1985c, 1986) developed a nonequilibrium stage model in which each stage is characterized by a set of component mass-transfer rate expressions, an overall material balance, a heat-transfer rate between the vapor and liquid phase, and by thermodynamic equilibrium in the bulk liquid phase. Published correlations for mass and heat transfer coefficients, interfacial surface area and reaction rate constants are used. When several stages are combined to represent an absorber or regenerator, the large set of resulting equations must be solved simultaneously. The numerical complexity of the resulting system of equations has restricted the use of this model to computers where sophisticated algorithms for solving large systems of nonlinear equations are available. Despite the numerical

difficulties in this approach, several examples presented by Sivasubramanian et al.(1985), Sardar et al.(1985), Katti and Langfitt (1986), and Katti and McDougal (1986) have shown that the model is capable of simulating existing columns and may be used to design new facilities.

Other studies of the rigorous simulation of multistage devices, in which mass transfer involving H_2S, CO_2 and aqueous alkanolamine solutions is accompanied by chemical reaction in the liquid phase, include those of: Bourne et al.(1974), Ouwerkerk (1977), Vaz et al.(1981), Majeed et al.(1982), Suenson et al.(1985), Marini et al.(1985), Blauwhoff et al.(1985), De Leye and Froment (1986b) and Thompson (1986). The rigorous simulation of packed columns in amine treating units has been investigated by Trass and Weiland (1971), Krishnamurthy and Taylor (1985d), De Leye and Froment (1986a) and Yu and Astarita (1987a, 1987b).

7. MODELLING ABSORPTION AND REGENERATION COLUMNS

7.1 Nonequilibrium Stage Model

In order to simulate the operation of a stage which is under pseudo-steady-state mass-transfer conditions, a nonequilibrium stage model is proposed. The nomenclature and configuration for stage j in a column are shown in Figure 13. The model is based on the component stage efficiency concept. The stage efficiencies may be different for different components and the values may vary from stage to stage. This represents an improvement over equilibrium stage models where an overall stage efficiency is used. This model can be expanded to the multistage case and be used to represent many common column configurations.

The stage operates at a pressure P_j and at a temperature T_j. Vapor of composition $Y_{i,j+1}$ and with enthalpy H_{j+1} enters stage j from the stage below (j+1) at a molar flow rate of V_{j+1}. Similarly, liquid of composition $X_{i,j-1}$ and with enthalpy h_{j-1} enters from the stage above (j-1) at a molar flow rate of L_{j-1}. Feed of composition $Z_{i,j}$ and with enthalpy $H_{F,j}$ is admitted at a molar feed rate of F_j. Energy is added or removed from stage j at a rate of Q_j. Vapor of composition $Y_{i,j}$ leaves stage j at a molar flow rate of $(V_j + SV_j)$ and with an enthalpy of H_j. Liquid of composition $X_{i,j}$ leaves at a molar flow rate of $(L_j + SL_j)$ and with an enthalpy of h_{j-1}. Vapor or liquid

Figure 13.

Generalized Stage Model

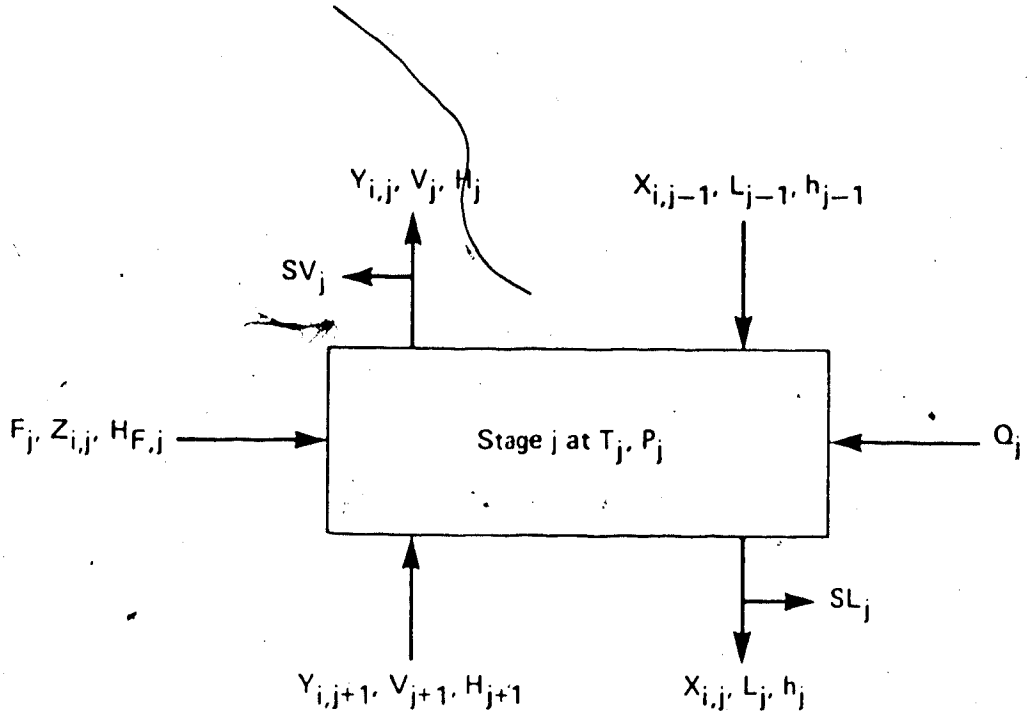

side product streams may be removed from the device at molar draw rates of SV_j and SL_j respectively.

It is assumed that the product streams leave the tray with an approach to equilibrium that is characterized by a modified Murphree vapor efficiency. The efficiency, $\eta_{i,j}$, for any component i is given by

$$\eta_{i,j} = \frac{(V_j + SV_j)Y_{i,j} - V_{j+1} Y_{i,j+1}}{(V_j + SV_j)K_{i,j} X_{i,j} - V_{j+1} Y_{i,j+1}} \qquad (105)$$

The value of $\eta_{i,j}$ relates the moles of component i leaving stage j in the vapor phase to the number of moles that would leave if it were an equilibrium stage.

By including the molar flow rates in the definition, the material balance problems that arise when using the Murphree efficiency in cases where there is a substantial difference between V_j and V_{j+1} can be avoided. It is assumed that the vapor and liquid phases leave in thermal equilibrium, that there is complete mixing of liquid on the tray, and that the vapor phase is completely mixed between stages but unmixed in passing through the liquid dispersion. When $\eta_{i,j} = 1.0$ the model reduces to the equilibrium stage case where $Y_{i,j} = K_{i,j} X_{i,j}$. When $V_{j+1} \simeq (V_j + SV_j)$ the definition of $\eta_{i,j}$ reduces to $E_{i,j}$, the Murphree vapor efficiency.

The value of $\eta_{i,j}$ is a function of pressure, temperature, phase compositions, flow rates, physical properties, mechanical tray design and dimensions, as well as kinetic and mass-transfer parameters. Furthermore, $\eta_{i,j}$ may be different on each stage in a column.

Consider the flow of liquid and gas on a tray with an effective cross-sectional area of A, as shown in Figure 14. In a real tray, the active tray area is essentially the entire tower cross-sectional area less the area taken up by the presence of the liquid downcomer baffles. Assume that the gas stream bubbles uniformly through this liquid and that the tray is maintained at a total pressure P. Let Z_T denote the average total height of liquid dispersion on the tray and $\underline{a}$ denote the interfacial surface area available for mass transfer per unit volume of dispersion. Let Y represent the actual mole fraction of the vapor phase at any point and KX represent the vapor phase composition that would be in equilibrium with a liquid of composition X. Let V denote the molar flow rate of vapor at any point.

Consider a differential section of dispersion with thickness ΔZ. As gas passes through the liquid, material is absorbed into the liquid according to

$$VY|_{Z=Z} = VY|_{Z=Z+\Delta Z} + K_{og}(\underline{a}AP)(Y - KX)\Delta Z \qquad (106)$$

where K_{og} is the overall gas-phase mass-transfer coefficient. Rearranging gives

Figure 14.

Mass Transfer Model

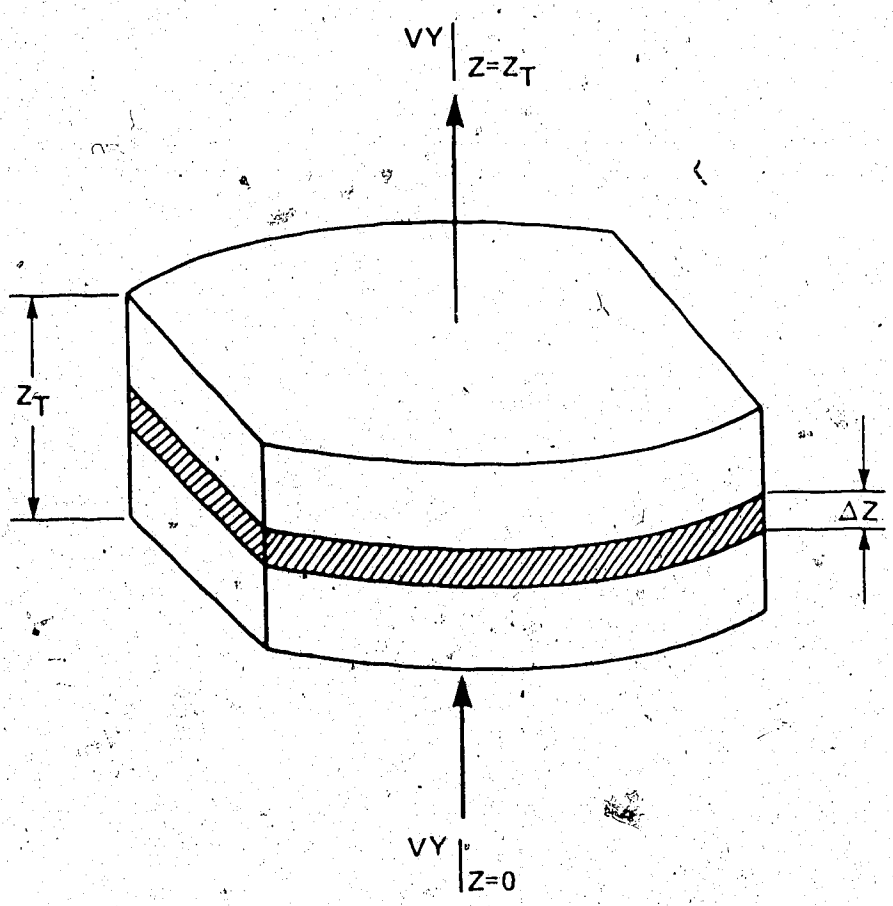

$$(VY|_{Z=Z+\Delta Z} - VY|_{Z=Z})/\Delta Z = K_{og}\,(\underline{a}AP)(KX - Y) \qquad (107)$$

When ΔZ approaches zero, the limit becomes

$$\frac{d\,VY}{dZ} = K_{og}\,(\underline{a}AP)(KX - Y) \qquad (108)$$

Differentiating the product gives

$$V\,\frac{dY}{dZ} + Y\,\frac{dV}{dZ} = K_{og}\,(\underline{a}AP)(KX - Y) \qquad (109)$$

where

$$V = V_{j+1} \qquad \text{at } Z = 0 \qquad (110)$$

$$V = V_j + SV_j \qquad \text{at } Z = Z_T \qquad (111)$$

The vapor flow rate derivative in Equation (109) may be approximated by

$$\frac{dV}{dZ} \simeq (V_j + SV_j - V_{j+1})/Z_T \qquad (112)$$

Equation (109) can then be expressed as

$$\left[\, V_{j+1} + Z\,\frac{dV}{dZ} \,\right]\frac{dY}{dZ} + Y\,\frac{dV}{dZ} = K_{og}\,(\underline{a}AP)(KX - Y) \qquad (113)$$

Rearranging gives

$$\frac{dY}{dZ} = \left[\, K_{og}\,(\underline{a}AP)(KX - \quad - Y\,\frac{dV}{dZ} \,\right]/\left[\, V_{j+1} + Z\,\frac{dV}{dZ} \,\right] \qquad (114)$$

where

$$Y = Y_{i,j+1} \qquad \text{at } Z = 0 \qquad (115)$$

Equation (114) may be used in the case of gas absorption or gas desorption. In the limit, if $V_{j+1} \simeq (V_j + SV_j) = V$, then $\frac{dV}{dZ} = 0$ and Equation (114) can be simplified to

$$\frac{dY}{dZ} = K_{og} \underline{a} \frac{AP}{V} (KX - Y) \qquad (116)$$

which can be rearranged to give

$$\frac{dY}{KX - Y} = K_{og} \underline{a} \frac{AP}{V} dZ \qquad (117)$$

Integrating the left hand side from $Y_{i,j+1}$ to $Y_{i,j}$ and the right hand side from zero to Z_T gives

$$\ln(1 - E_{i,j}) = -K_{og} \underline{a} \frac{AP}{V} Z_T = -N_{og} \qquad (118)$$

or

$$E_{i,j} = 1 - e^{-N_{og}} \qquad (119)$$

where N_{og} is the number of overall gas phase transfer units. The Murphree vapor efficiency can be calculated analytically with Equation (119) if the value of N_{og} is known. The more complex form of $\eta_{i,j}$ does not permit the separation of variables as in Equation (117), therefore the efficiency cannot be calculated analytically. Equation (114) must be integrated using the initial condition in Equation (115), and the calculated value of $Y_{i,j}$ at $Z = Z_T$ is then used in Equation (105) to calculate the value of $\eta_{i,j}$.

The overall gas-phase mass-transfer coefficient K_{og} may be estimated from the sum of the two individual film resistances

$$\frac{1}{K_{og}} = \frac{1}{k_g} + \frac{H}{I\ k^\circ_L} \qquad (120)$$

where I is the enhancement factor that accounts for chemical reaction in the liquid phase. In this model the interfacial resistance to mass transfer is assumed to be negligible. Values of I may be estimated from fundamental principles if the nature of the reacting system is understood. For example, it must be determined whether the reaction takes place in the fast or instantaneous reaction regimes. Values of $\underline{a}$, k_g and k°_L usually are obtained from empirical correlations. Physico-chemical properties of the solute gases in the amine solvent including: the physical solubility, or Henry's constant H, and molecular diffusivity D, are required in the calculation of the enhancement factor. The Henry's constant and the molecular diffusion coefficient can only be obtained reliably by experimental measurement. Solvent density and viscosity, as shown in Chapters 4 and 5, also influence the mass transfer rate of the absorbing solute gas.

7.2 Multistage Multicomponent Separation Model

Using the nonequilibrium stage model as a basis, consider the generalized multistage model shown in Figure 15. The model provides for a feed stream to any stage, side coolers or heaters on any stage and side product streams. These may be either vapor (SV) or liquid (SL) side streams. With these options, the model may be used to represent a wide variety of separation devices including amine contactors and regenerators.

The imbalance functions M_j , $C_{i,j}$, E_j , $P_{i,j}$ and S_j can be defined to represent the overall, component material, and energy balances, the stage efficiency relationship and the mole fraction summation respectively. These nonlinear algebraic imbalance functions are listed below

Overall Material Balances

$$F_j + L_{j-1} + V_{j+1} - (L_j + SL_j) - (V_j + SV_j) \equiv M_j = 0 \qquad (121)$$

$$1 \leq j \leq NSTG$$

Component Material Balances

$$F_j Z_{i,j} + L_{j-1} X_{i,j-1} + V_{j+1} Y_{i,j+1} - (L_j + SL_j) X_{i,j} - (V_j + SV_j) Y_{i,j} \equiv C_{i,j} = 0 \qquad (122)$$

$$1 \leq i \leq NC$$

$$1 \leq j \leq NSTG$$

Figure 15.

Generalized Multistage Model

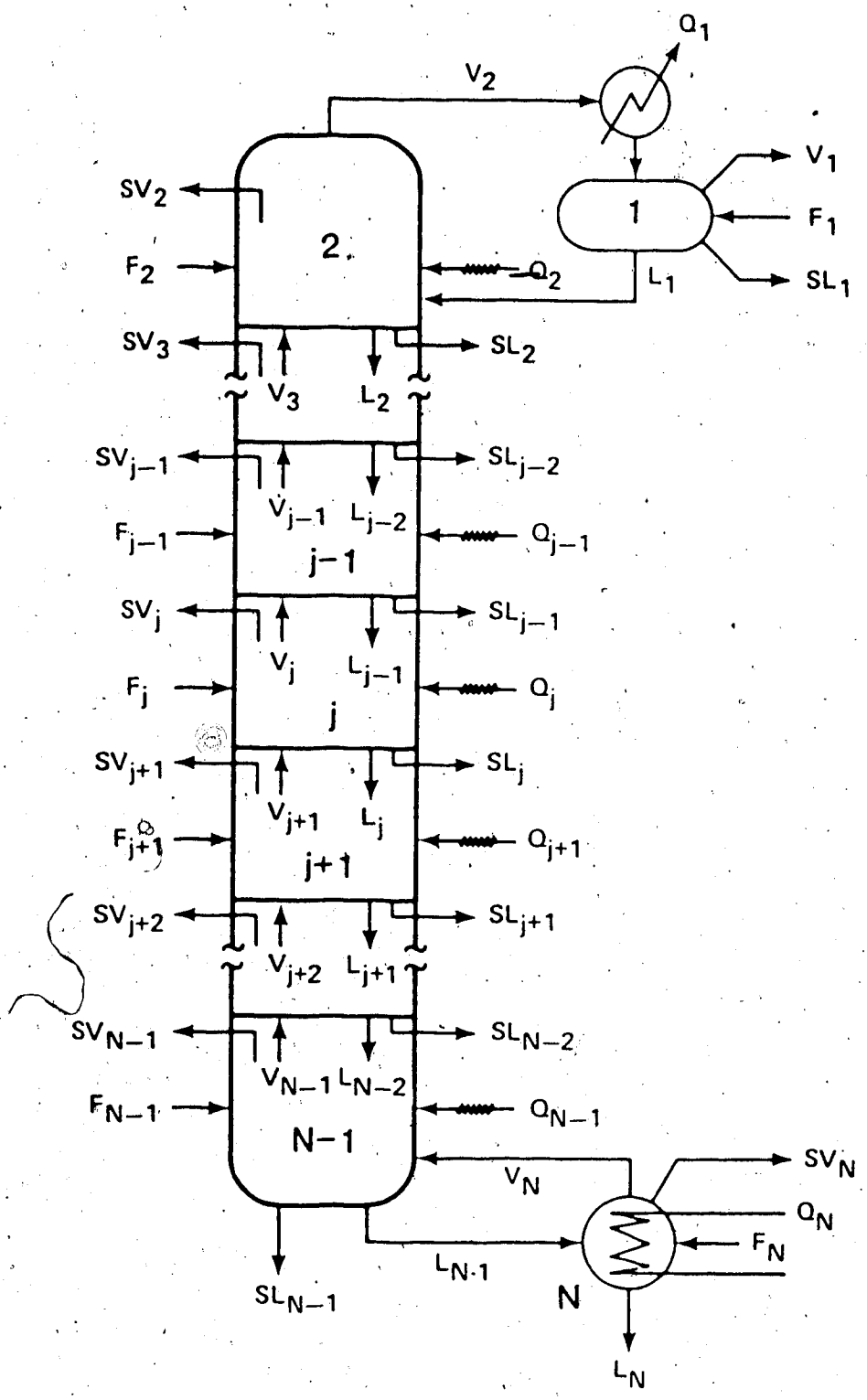

Energy Balances

$$F_j H_{F,j} + Q_j + L_{j-1} h_{j-1} + V_{j+1} H_{j+1} - (L_j + SL_j) h_j - (V_j + SV_j) H_j \equiv E_j = 0 \qquad (123)$$

$$1 \le j \le NSTG$$

Stage Efficiency Relationships

$$\eta_{i,j} K_{i,j} X_{i,j} (V_j + SV_j) - (V_j + SV_j) Y_{i,j} + (1 - \eta_{i,j}) V_{j+1} Y_{i,j+1} \equiv P_{i,j} = 0 \qquad (124)$$

$$1 \le i \le NC$$

$$1 \le j \le NSTG$$

Summation Equations

$$\sum_i Y_{i,j} - 1.0 \equiv S_j = 0 \qquad (125)$$

$$\sum_i X_{i,j} - 1.0 \equiv S_j = 0 \qquad (126)$$

$$1 \le j \le NSTG$$

Note that when $\eta_{i,j} = 1.0$ the model reduces to the equilibrium stage case where $Y_{i,j} = K_{i,j} X_{i,j}$. In this work, the liquid phase composition, $X_{i,j}$, is always renormalized to satisfy Equation (126).

The dependent variables on each stage include: component mole fractions in both the vapor ($Y_{i,j}$) and liquid ($X_{i,j}$) phases, the overall phase rates of vapor (V_j) and liquid (L_j), and the stage temperature (T_j). Therefore, there are NSTG(2NC+1) unknowns in a column with

NSTG stages and NC components. The object of the design calculation is to find a set of vapor and liquid flow rates, vapor and liquid mole fractions, and temperatures which satisfy all the equations of the model and force the imbalance functions to zero. Alternatively, it is desired to determine the values of the variables which remain after an appropriate number of independent variables have been specified.

Smith (1963) presents an excellent discussion of the degrees of freedom in multistage multicomponent separation processes and describes common sets of system specifications. For a simple absorption unit with one liquid and one vapor feed, there are 2NSTG+2NC+5 degrees of freedom. The pressure, temperature, molar flow rate and composition of each feed stream is specified; NC+2 items per feed are fixed. The number of stages NSTG are specified as well as the pressure and heat leak Q_j on each stage. For a stripper with a partial condenser and a single feed, there are 2NSTG+NC+4 degrees of freedom. In addition to feed specification, pressure and heat leak on each tray, four other variables are fixed. These may include the total number of stages NSTG, the feed stage location, the condenser temperature and the reboiler heat duty. Using this set, the condenser heat duty replaces the condenser temperature as an unknown. Other combinations of specifications are possible.

7.3 Multistage Model Solution Procedure

In general, the nonequilibrium multistage model equations form a complex system of nonlinear equations, and therefore, numerical techniques are required to obtain a solution. A general nonlinear equation $f(\underline{\lambda})=0$ may be expanded using a Taylor series.

$$f(\underline{\lambda} + \underline{\Delta\lambda}) \simeq f(\underline{\lambda}) + f'(\underline{\lambda})\underline{\Delta\lambda} + \ldots \qquad (127)$$

Assuming that $f(\underline{\lambda} + \underline{\Delta\lambda}) = 0$ and that the higher order derivatives may be neglected in comparison to the first order terms, the series can be truncated after the linear term to give

$$\sum_i \left(\frac{\partial f}{\partial \lambda_i} \right) \Delta\lambda_i = - f(\underline{\lambda}) \qquad (128)$$

In this example, f may be referred to as an imbalance function. In the Newton-Raphson method, values of $\Delta\lambda_i$ are determined by solving Equation (128) iteratively until $f(\underline{\lambda})$ approaches zero. In the nonequilibrium stage model, the imbalance functions are M_j , $C_{i,j}$, E_j , $P_{i,j}$ and S_j .

The model equations may be linearized using the approach described by Ishii (1973). The equilibrium ratios, the vapor and liquid phase enthalpies and the component stage efficiencies are complex functions of pressure, temperature, composition. These quantities are calculated as such at each iteration in the solution procedure.

However, for purposes of linearization only, the following functional forms are assumed

$$K_{i,j} \simeq K_{i,j}(P_j, T_j, X_{i,j}) \quad (129)$$

$$H_j \simeq H_j(P_j, T_j) \quad (130)$$

$$h_j \simeq h_j(P_j, T_j) \quad (131)$$

$$\eta_{i,j} \simeq \text{Constant} \quad (132)$$

Since the stage efficiencies are assumed constant in the linearization, an outer convergence loop is required in the solution procedure to obtain a converged set of efficiencies. In the general multistage algorithm, the following partial derivatives are required

$$\frac{\partial K}{\partial T}, \quad \frac{\partial K}{\partial X}, \quad \frac{\partial H}{\partial T} \quad \text{and} \quad \frac{\partial h}{\partial T}$$

for all stages j and components i. In this work, the K-value derivatives were determined numerically at each iteration, and the heat capacities were determined analytically. Using the recommendations of Ishii and Otto (1973), the Jacobian matrix is reduced to include only the partial derivatives which have a dominant influence on the solution. This simplification in no way affects the rigor of the solution. The values of F_j, SL_j, SV_j, Q_j and $H_{F,j}$ are specified quantities and therefore do not appear as variables in the linearized model. The linearized model equations are

Overall Material Balances

$$\Delta L_{j-1} + \Delta V_{j+1} - \Delta L_j - \Delta V_j = -M_j \tag{133}$$

in general

$$\Delta L_j = \sum_k M_k + \Delta V_{j+1} - \Delta V_1 \tag{134}$$
$$1 \le k \le j$$

Component Material Balances

$$\begin{aligned} &\Delta L_{j-1}\, X_{i,j-1} + L_{j-1}\, \Delta X_{i,j-1} + \Delta V_{j+1}\, Y_{i,j+1} \\ &\quad + V_{j+1}\, \Delta Y_{i,j+1} - \Delta L_j\, X_{i,j} - (L_j + SL_j)\Delta X_{i,j} \\ &\quad - \Delta V_j\, Y_{i,j} - (V_j + SV_j)\Delta Y_{i,j} \\ &\quad = -C_{i,j} \end{aligned} \tag{135}$$

Energy Balances

$$\begin{aligned} &\Delta L_{j-1}\, h_{j-1} + L_{j-1}\, (\partial h_{j-1}/\partial T_{j-1})\Delta T_{j-1} + \Delta V_{j+1}\, H_{j+1} \\ &\quad + V_{j+1}\, (\partial H_{j+1}/\partial T_{j+1})\Delta T_{j+1} - \Delta L_j\, h_j - \Delta V_j\, H_j \\ &\quad - [(L_j + SL_j)\partial h_j/\partial T_j + (V_j + SV_j)\partial H_j/\partial T_j]\Delta T_j \\ &\quad = E_j \end{aligned} \tag{136}$$

Stage Efficiency Relationships

$$\begin{aligned} &[\eta_{i,j}\, X_{i,j}\, V_j\, (\partial K_{i,j}/\partial X_{i,j}) + \eta_{i,j}\, K_{i,j}\, V_j]\Delta X_{i,j} \\ &\quad + [-V_j]\Delta Y_{i,j} + [(1 - \eta_{i,j})V_{j+1}]\Delta Y_{i,j+1} \\ &\quad + [\eta_{i,j}\, X_{i,j}\, V_j\, (\partial K_{i,j}/\partial T_j)]\Delta T_j \\ &\quad + [\eta_{i,j}\, K_{i,j}\, X_{i,j} - Y_{i,j}]\Delta V_j \\ &\quad + [(1 - \eta_{i,j})Y_{i,j+1}]\Delta V_{j+1} = -P_{i,j} \end{aligned} \tag{137}$$

Summation Equations

$$\sum_i \Delta Y_{i,j} = -S_j \qquad (138)$$

The linearized overall material balance may be substituted into the component material and energy balance equations to eliminate all terms involving ΔL_j . The resulting equations may be written in a simpler form using matrix notation where the underscore denotes a dimension of NSTG

Component Material Balances

$$\underline{\Psi}_i \, \Delta\underline{X}_i + \underline{\Lambda}_i \, \Delta\underline{Y}_i + \underline{\Pi}_i \, \Delta\underline{V} = \underline{C}_i \qquad (139)$$

$$1 \le i \le NC$$

Energy Balances

$$\underline{\Theta} \, \Delta\underline{T} + \underline{\Xi} \, \Delta\underline{V} = \underline{E} \qquad (140)$$

Stage Efficiency Relationships

$$\underline{\alpha}_i \, \Delta\underline{X}_i + \underline{\beta}_i \, \Delta\underline{Y}_i + \underline{\gamma}_i \, \Delta\underline{T} + \underline{\phi}_i \, \Delta\underline{V} = \underline{\delta}_i \qquad (141)$$

$$1 \le i \le NC$$

Summation Equations

$$\sum_i \Delta\underline{Y}_i = -\underline{S} \qquad (142)$$

$$1 \le i \le NC$$

The tridiagonal matrix $\underline{\alpha}_i$ may be inverted using the procedure described by Ishii and Otto (1973). Rearranging Equation (141) gives

$$\Delta\underline{X}_i = -(\underline{\alpha}_i^{-1}\,\underline{\beta}_i)\Delta\underline{Y}_i - (\underline{\alpha}_i^{-1}\,\underline{\gamma}_i)\Delta\underline{T} - (\underline{\alpha}_i^{-1}\,\underline{\phi}_i)\Delta\underline{V} + \underline{\alpha}_i^{-1}\,\underline{\delta}_i \tag{143}$$

Substituting Equation (143) into Equation (139) and rearranging gives

$$\Delta\underline{Y}_i = \underline{\Omega}_i\,[\underline{\Psi}_i\,(\underline{\alpha}_i^{-1}\,\underline{\gamma}_i)]\Delta\underline{T} + \underline{\Omega}_i\,[\underline{\Psi}_i\,(\underline{\alpha}_i^{-1}\,\underline{\phi}_i) - \underline{\Pi}_i]\Delta\underline{V} + \underline{\Omega}_i\,[\underline{C}_i - \underline{\Psi}_i\,(\underline{\alpha}_i^{-1}\,\underline{\delta}_i)] \tag{144}$$

where

$$\underline{\Omega}_i = [\underline{\Lambda}_i - \underline{\Psi}_i\,(\underline{\alpha}_i^{-1}\,\underline{\beta}_i)]^{-1} \tag{145}$$

Summing Equation (144) for all components and substituting Equation (142) gives

$$\sum_i \Delta\underline{Y}_i = \underline{\omega}\Delta\underline{T} + \underline{\xi}\Delta\underline{V} + \underline{\psi} = -\underline{S} \tag{146}$$

where

$$\underline{\omega} = \sum_i \underline{\Omega}_i\,[\underline{\Psi}_i\,(\underline{\alpha}_i^{-1}\,\underline{\gamma}_i)] \tag{147}$$

$$\underline{\xi} = \sum_i \underline{\Omega}_i\,[\underline{\Psi}_i\,(\underline{\alpha}_i^{-1}\,\underline{\phi}_i) - \underline{\Pi}_i] \tag{148}$$

$$\underline{\psi} = \sum_i \underline{\Omega}_i\,[\underline{C}_i - \underline{\Psi}_i\,(\underline{\alpha}_i^{-1}\,\underline{\delta}_i)] \tag{149}$$

$\underline{\Theta}$ is also a tridiagonal matrix and may easily be inverted. From Equation (140)

$$\Delta\underline{T} = (\underline{\Theta}^{-1}\,\underline{E}) - (\underline{\Theta}^{-1}\,\underline{\Xi})\Delta\underline{V} \tag{150}$$

Substituting (150) into (146) gives

$$[\underline{\xi} - \underline{\omega}(\underline{\theta}^{-1}\,\underline{\Xi})]\Delta\underline{V} = -(\underline{S} + \underline{\psi}) - \underline{\omega}(\underline{\theta}^{-1}\,\underline{E}) \qquad (151)$$

which is a system of linear equations with dimension, NSTGxNSTG. The system may be solved by Gaussian elimination.

Method of Solution

A suitable iterative procedure to obtain a convergent solution is as follows :

1) Assume initial values for $X_{i,j}$, $Y_{i,j}$, V_j , T_j and $\eta_{i,j}$
2) Calculate H_j , h_j , $\frac{\partial K}{\partial \overline{T}}$, $\frac{\partial K}{\partial \overline{X}}$, $\frac{\partial H}{\partial \overline{T}}$ and $\frac{\partial h}{\partial \overline{T}}$ using the current stage variables
3) Evaluate the coefficient matrix and right hand side vector in Equation (151) and solve for ΔV_j using Gaussian elimination
4) Using the new ΔV_j , solve Equation (150) for ΔT_j
5) Using the new ΔV_j and the new ΔT_j , solve Equation (144) for each value of $\Delta Y_{i,j}$
6) Using the new ΔV_j , the new ΔT_j and the new $\Delta Y_{i,j}$, solve Equation (143) for each value of $\Delta X_{i,j}$
7) Check the convergence criterion and go to Step 12) if converged
8) Update the independent variables using

$$\lambda_i^{k+1} = \lambda_i^{k} + t\Delta\lambda_i \qquad (152)$$

where λ_i is either V_j , T_j , $Y_{i,j}$ or $X_{i,j}$

9) Calculate new L_j using Equation (121) with $M_j = 0$

10) Renormalize $X_{i,j}$ to avoid truncation errors

11) Go to Step 2)

12) Calculate new $\eta_{i,j}$ using Equations (114) and (115) with the new column profile data

13) Check the convergence of η-values and stop if converged

14) Update the values of $\eta_{i,j}$ using direct substitution

15) Go to Step 2)

As recommended by Holland (1981), constraints were placed on the individual values of ΔV_j and ΔT_j to dampen severe corrections. The value of ΔV_j was constrained so as to prevent V_j from being increased or reduced by more than a factor of 2.0. The value of ΔT_j was constrained to within ±30.0 K. The value of t may be chosen by an appropriate single-variable search technique such that the following is satisfied

$$\epsilon^{k+1} \leq \epsilon^{k} \tag{153}$$

where k denotes the iteration number. Values of t range from $0.0 < t \leq 1.0$. The convergence criterion, ϵ, is given by

$$\epsilon = \sum_j \left[S_j^2 + \left(\sum_i P_{i,j}\right)^2 + \left(E_j / (F_j H_{F,j} + Q_j + L_{j-1} h_{j-1} + V_{j+1} H_{j+1})\right)^2 \right] \quad (154)$$

Calculations are completed when ϵ is reduced to a value less than NSTG x 10^{-7} .

With a knowledge of $\underline{a}$, K_{og} , and Z_T , Equation (114) can be integrated over the depth of the liquid dispersion on stage j. The resulting vapor flow and composition profiles can be used in Equation (105) to determine a revised estimate of the efficiency $\eta_{i,j}$ on each stage in the column. The new values of $\eta_{i,j}$ are then used in the multistage model to determine new values of V_j , T_j , $Y_{i,j}$ and $X_{i,j}$. This iteration is continued until convergence of $\eta_{i,j}$ is achieved. In this work, the procedure was continued until successive iterations did not result in the values of $\eta_{i,j}$ being changed by more than NSTG x 10^{-5} .

Equations (133) to (151) have been developed for the case when all the stages in the column operate with a fixed heat duty (e.g. adiabatic operation). It is often desirable to interchange some of the specified variables with the unknown variables. For distillation problems, it is usual to specify the amount of top product and the external reflux ratio, and to treat the reboiler and condenser heat duties as unknowns. Similarly, in the case of a reboiled absorber, the vapor flow rate leaving the top of the column, V_1, is

usually specified and the reboiler heat duty is treated as an unknown.

In order to impose other types of column specifications on the stage model, it is necessary to modify the form of the linearized model equations on those stages of interest. If the top product rate is specified in a reboiled absorber, then the dependent variable V_1 is a constant. Consequently, the value of ΔV_1 is always zero. In order to meet the vapor rate specification in this case, the reboiler heat duty is allowed to vary. This introduces a quantity ΔQ_{NSTG} into the linearized energy balance on the bottom stage. All the coefficients for ΔV_1 are set to zero and the quantity ΔQ_{NSTG} is used to replace the vapor correction ΔV_1. For example, the linearized energy balance on the bottom stage would be

$$\begin{aligned} &\Delta Q_{NSTG} + [L_{NSTG-1}\ \partial h_{NSTG-1}/\partial T_{NSTG-1}]\Delta T_{NSTG-1} \\ &\quad - [L_{NSTG}\ \partial h_{NSTG}/\partial T_{NSTG} \\ &\quad + (V_{NSTG} + SV_{NSTG})\partial H_{NSTG}/\partial T_{NSTG}]\Delta T_{NSTG} \\ &\quad + [h_{NSTG-1} - H_{NSTG}]\Delta V_{NSTG} \\ &\quad = -E_{NSTG} - (\sum_j M)h_{NSTG-1} + (\sum_j M)h_{NSTG} \end{aligned} \qquad (155)$$

Similar expressions can be developed for other column configurations. Table 9 contains the replacement Newton corrections which may be incorporated into the solution procedure for these cases. For an an amine regenerator, the configuration studied in this work was a distillation column with specified condenser temperature and reboiler heat duty.

Table 9.

Replacement Newton Corrections for the New Algorithm

Specification	Original Correction	Replacement Correction
Bottom Product Rate	ΔV_1	ΔQ_{NSTG}
Reflux Ratio	ΔV_2	ΔQ_{NSTG}
Bottom Product Rate	ΔV_1	ΔQ_1
Condenser Temperature	ΔT_1	ΔQ_1
Reboiler Temperature	ΔT_{NSTG}	ΔQ_{NSTG}

7.4 Initial Assumptions

The iterative solution procedure requires initial values for V_j , L_j , T_j , $X_{i,j}$, and $Y_{i,j}$. The convergence characteristics of a particular multistage solution procedure often depends on the initial column profiles provided to the method. Although the present multistage solution procedure is robust, a knowledge of the operating characteristics of alkanolamine treating units can add insight to the prudent selection of initial column profiles.

Vapor Flow Rate, V_j

Contactor

Hydrocarbon and associated nonhydrocarbon components can be assumed to pass through the contactor unabsorbed. The amount of acid gas absorbed may be estimated by the initial stage efficiency. For example, if the stage efficiency for CO_2 transfer is initialized at 0.25, then 0.75 of the CO_2 may be assumed to pass through the contactor. Using these guidelines, an initial vapor profile in the contactor can be generated.

Regenerator

After estimating the amount of acid gas that will be absorbed in each contactor serviced by the regenerator, the regenerator top product rate, V_1, may be initialized to this value. Using a starting reflux ratio of 2.0 permits the

value of V_2 to be determined. The remaining vapor rates in the column may be assumed to equal V_2.

Liquid Flow Rate, L_j

Once the value of V_j has been determined in each column, the values of L_j can be obtained from Equation (121) with $M_j = 0$.

Temperature, T_j

Contactor

A linear interpolation between the top and bottom stage temperatures is generally sufficient. The temperature of the top stage may be set to equal the lean amine feed temperature. After estimating the amount of H_2S and CO_2 that will be absorbed in the contactor, approximate heats of solution can be used to determine the amount of energy that will be released in the liquid when the gases are absorbed. Using the flow rate of amine solution and an average liquid heat capacity, the bottom stage temperature can be estimated.

Regenerator

In the regenerator, the condenser temperature is a specified quantity. Using the specified values of P_j on each stage, and assuming that the liquid is pure water, a correlation of saturated steam temperatures can be used to determine the temperature on each of the remaining stages.

Liquid Phase Composition, $X_{i,j}$

Contactor

The liquid composition on all stages can be initialized to the composition of the lean amine. Using the assumed stage efficiency for H_2S and CO_2 absorption, the acid gas compositions on the bottom few stages can be corrected to account for the estimated moles of gas that will be absorbed. It can be assumed that amine and water are involatile and that hydrocarbons and associated nonhydrocarbon gases remain in the vapor phase.

Regenerator

The liquid composition in the overhead condenser can be estimated to be 1 mol % amine and 99 mol % water. Using the number of moles of dissolved gases in the rich amine feed, the condenser pressure and the Henry's constant for each gas, the solubilities in water may be used as a starting composition. This composition may be carried down the column until the feed stage, where the composition of the rich amine feed is used. The remaining stage compositions can be initialized using a linear interpolation from the rich amine feed acid gas content, to zero acid gas content in the lean amine.

Vapor Phase Composition, $Y_{i,j}$

Once the liquid phase compositions have been estimated and normalized, K-values can be determined for all stages in each column. The values of $Y_{i,j}$ can be estimated by assuming a stage efficiency of 1.0.

7.5 Thermodynamic and Physico-chemical Models

7.5.1 Gas Solubility

Equilibrium ratios, or K-values, for H_2S and CO_2 above amine solutions are required in rigorous multistage separation algorithms used to simulate absorption and regeneration columns. An equilibrium ratio represents the distribution of a component between two phases and is given by

$$K_i \equiv Y_i / X_i = \gamma_i f^{\circ}_L / \phi_i P \qquad (156)$$

where γ_i is the liquid phase activity coefficient, f°_L is the fugacity of the pure liquid, and ϕ_i is the vapor phase fugacity coefficient. If the liquid phase activity coefficient and the vapor phase fugacity coefficient are assumed to equal unity, and if the pure liquid fugacity is approximated by the vapor pressure, K-values may be determined from

$$K_i \simeq p_i'/(P X_i) \qquad (157)$$

where p_i is the partial pressure, P is the total pressure and X_i is the mole fraction in the liquid phase. When calculating the equilibrium ratios of H_2S and CO_2 in contact with aqueous solutions of alkanolamines, it is therefore necessary to predict the equilibrium vapor pressure of the acid gas above the liquid solution at a constant temperature.

The Kent and Eisenberg (1976) model was chosen as a basis for this study. For the H_2S-CO_2-water-alkanolamine system, the following chemical reactions were assumed to take place in the liquid phase under equilibrium conditions

Primary and Secondary Amines

$$R_1R_2NH + H_2O \rightleftharpoons R_1R_2NH_2^+ + OH^- \quad (158)$$

$$2\ R_1R_2NH + CO_2 \rightleftharpoons R_1R_2NCOO^- + R_1R_2NH_2^+ \quad (159)$$

Tertiary Amines

$$R_1R_2R_3N + H_2O \rightleftharpoons R_1R_2R_3NH^+ + OH^- \quad (160)$$

Aqueous Solutions

$$H_2O \rightleftharpoons H^+ + OH^- \quad (161)$$

$$H_2S \rightleftharpoons H^+ + HS^- \quad (162)$$

$$CO_2 + H_2O \rightleftharpoons H^+ + HCO_3^- \quad (163)$$

$$HS^- \rightleftharpoons H^+ + S^= \quad (164)$$

$$HCO_3^- \rightleftharpoons H^+ + CO_3^= \quad (165)$$

$$H_2S_{(g)} \rightleftharpoons H_2S_{(L)} \quad (166)$$

$$CO_{2(g)} \rightleftharpoons CO_{2(L)} \quad (167)$$

where R denotes a substituted group on the amino nitrogen atom. For example, for DEA, R_1 and R_2 represent the $-CH_2-CH_2OH$ group.

In addition to the above chemical reactions, three material balance expressions and an electroneutrality expression can be written

Amine Material Balance

$$m = [R_1R_2R_3N] + [R_1R_2NCOO^-] + [R_1R_2R_3NH^+] \quad (168)$$

Sulphur Material Balance

$$m\,\alpha_{H_2S} = [H_2S] + [HS^-] + [S^=] \quad (169)$$

Carbon Material Balance

$$m\,\alpha_{CO_2} = [CO_2] + [HCO_3^-] + [CO_3^=] + [R_1R_2NCOO^-] \quad (170)$$

Electroneutrality Expression

$$[R_1R_2R_3NH^+] + [H^+] - [HCO_3^-] - [R_1R_2NCOO^-] - 2\,[CO_3^=] - [HS^-] - 2\,[S^=] - [OH^-] = 0 \quad (171)$$

In the case of tertiary amines, the concentration of the carbamate ion, $R_1R_2NCOO^-$, is identically zero. Corresponding equilibrium constant expressions may be written for each of the reactions identified above

$$K_1 = \frac{[H^+][R_1R_2R_3N]}{[R_1R_2R_3NH^+]} \quad (172)$$

$$K_2 = \frac{[HCO_3^-][R_1R_2NH]}{[R_1R_2NCOO^-]} \quad (173)$$

$$K_3 = \frac{[H^+][HCO_3^-]}{[CO_2]} \quad (174)$$

$$K_4 = [H^+][OH^-] \quad (175)$$

$$K_5 = \frac{[H^+][CO_3^{=}]}{[HCO_3^-]} \quad (176)$$

$$K_6 = \frac{[H^+][HS^-]}{[H_2S]} \quad (177)$$

$$K_7 = \frac{[H^+][S^{=}]}{[HS^-]} \quad (178)$$

The physical equilibrium of acid gases may be expressed as

$$p_{H_2S} = H_{H_2S}\,[H_2S] \quad (179)$$

$$p_{CO_2} = H_{CO_2}\,[CO_2] \quad (180)$$

where H_{H_2S} and H_{CO_2} are the Henry's constants for H_2S and CO_2 respectively.

The equilibrium and Henry's constants in the model are strong functions of temperature, solution composition and ionic strength. However, the literature values for these quantities can usually only be applied at infinite dilution, and sufficient information to provide quantitative extension to higher ionic strength is not yet available. If the literature values for all equilibrium and Henry's constants are used in the model, the partial pressure predictions are in poor agreement with experimental data.

Using published values for all Henry's constants and ionization constants except the two constants that describe the amine equilibria, all the nonidealities of the system

may be combined into the parameters K_1 and K_2. Vapor phase fugacity coefficient and the liquid phase activity coefficient were assumed to be unity. The values of K_1 and K_2 were backed out of the model by using available experimental acid gas equilibrium data for each of the amine systems. The constant K_1 was determined from data on the system H_2S-$R_1R_2R_3N$-H_2O and then the constant K_2 was determined from data on the system CO_2-$R_1R_2R_3N$-H_2O using the value of K_1 determined in the first step. These parameters were determined to be functions of temperature, amine type and concentration, and acid gas loading. For tertiary amine systems, where no carbamate is formed, two values of K_1 were obtained from H_2S and CO_2 data.

The values of K_3 to K_7, H_{H_2S} and H_{CO_2} were estimated using the functions presented by Kent and Eisenberg (1976). Two minor corrections were made to the constants presented in their paper: for K_4, E = +1.4292; for K_6, C = -6.31007. Parameters K_1 and K_2 for MEA, DEA, TEA, MDEA and DGA were obtained from the experimental data sets of: Atwood et al.(1957), Murzin and Leites (1971), Murzin et al.(1971), Lee et al.(1972, 1973a, 1973b, 1974a, 1974b, 1975, 1976a, 1976b, 1976c), Lawson and Garst (1976), Nasir and Mather (1977), Martin et al.(1978), Isaacs et al.(1980), Lal et al.(1980), Jou et al.(1982), Dingman et al.(1983) and Jou et al.(1984, 1986). In general, the model is able to reproduce the available partial pressure data at fixed loading to within an average absolute relative deviation of 15 %. Data

have been correlated over a loading range of 0.001 to 1.0 mol acid gas per mol amine, for temperatures ranging from 25° to 125°C and for solution strengths from about 1.0 kmol/m³ to 4.0 kmol/m³.

The partial pressure, p_i, for use in Equation (157) was calculated from either Equation (179) or (180). Hence, in order to calculate a single K-value for H_2S and CO_2, the values of $[H_2S]$ and $[CO_2]$ must be determined. By specifying the system temperature, m, α_{H_2S} and α_{CO_2}, the values of $[H_2S]$ and $[CO_2]$ can be calculated by solving Equations (168) to (178) simultaneously.

The solubility of light hydrocarbons and associated nonhydrocarbons in the aqueous liquid phase was estimated using a Henry's constant approach

$$K_i \simeq H_i / P \qquad (181)$$

and assuming that the solubility in amine solutions is similar to that in water at the same temperature. The experimental data presented by Kobayashi and Katz (1953), Azarnoosh and McKetta (1958), Katz et al.(1959), Perry and Chilton (1973), Lawson and Garst (1976) and Otto et al.(1984) were used to establish the Henry's constants. The solubility of H_2S in the overhead condenser reflux liquid was calculated using the expression for water given by Lee and Mather (1977), and the correlation of Mason and Kao (1980) was used for CO_2.

7.5.2 Mass Transfer and Kinetic Parameters

The use of Equation (114) to calculate the amount of H_2S and CO_2 that is removed from the gas phase when a bubble passes through the liquid dispersion on a tray requires estimates of the values of $\underline{a}$ and K_{og}.

Interfacial Surface Area in Liquid Dispersions

Estimates for the interfacial surface area available for mass transfer usually are obtained from correlations based on operating data. For trayed towers, the value of $\underline{a}$ depends on the depth of liquid on the tray, the superficial velocity of gas bubbling through the dispersion, the surface tension of the liquid, the densities of the liquid and vapor phases and the mechanical design of the tray. Experimental and theoretical studies to determine the effective interfacial area available for mass transfer in gas-liquid contactors include those of: Calderbank (1959), Onda et al.(1968), Onda et al.(1968), Sharma et al.(1969), McNeil (1970), Sridharan and Sharma (1976), Landau et al.(1977), Fukushima et al.(1978) and Sedelies et al.(1987).

Calderbank (1959) presented an equation for $\underline{a}$ on sieve trays

$$\underline{a} = 0.38 \left(v_g / v_t\right)^{0.775} \left(v_g \rho_L / \frac{N_o}{A} D_o \mu_L\right)^{0.125} \cdot \left(\rho_L g/(1000\, D_o \sigma)\right)^{1/3} \qquad (182)$$

where v_g is the superficial velocity of the gas through the active tray area, v_t is the terminal rise velocity of the gas bubble, N_o is the number of holes on the sieve tray, A is the cross-sectional area of the sieve tray, D_o is the diameter of the sieve holes and σ is the interfacial surface tension between the gas and liquid in dynes/cm.

Onda et al.(1968) developed a correlation for the wetted surface area in packed columns

$$\underline{a}/a_o = 1 - \exp\left(-1.45\,(\sigma_c/\sigma)^{0.75}\left(\frac{L}{a_o\mu_L}\right)^{0.1}\right.$$

$$\left.\left(\frac{L^2 a_o}{\rho_L^2 g}\right)^{-0.05}\left(\frac{L^2}{1000\sigma a_o \rho_L}\right)^{0.2}\right. \qquad (183)$$

where a_o is the surface area of dry packing, σ_c is the critical surface tension and L is the superficial mass velocity of the liquid.

Sharma et al.(1969) used the theory of gas absorption accompanied by fast pseudo-first order reaction in the liquid phase to determine the effective interfacial area on a bubble cap tray under various hydrodynamic conditions. Based on the results of CO_2 absorption into a number of chemical solvents, they developed the following correlation

$$\underline{a} = 324.9\, v_g^{1/2} S^{-1/6} \qquad (184)$$

where S is the length of travel of a bubble in the dispersion. Blauwhoff et al.(1985) used the correlation of

Nonhebel (1972)

$$a' = \underline{a}Z_T = 30\ (\rho_g v_g)^{0.5} \rho_g^{-0.25} \qquad (185)$$

Scheffe and Weiland (1987) performed experiments using Glitsch V-1 valve trays and recommended the use of

$$a' = \underline{a}Z_T = 0.270 \left(\frac{Gd}{\mu_g}\right)^{0.375} \left(\frac{Ld}{\mu_L}\right)^{0.247} (Z_{weir}/d)^{0.515} \qquad (186)$$

where G and L are the superficial gas and liquid mass velocities and d is a characteristic length (d = 1 m).

Values of $\underline{a}$ typically lie between 100 and 600 m^2/m^3. Predicted areas using Equations (182) to (186) vary somewhat depending on the correlation used.

Liquid Dispersion Height

The dispersion height in industrial contactors is a complex function of system properties, gas velocity and tray design. Blauwhoff et al.(1985) used a dispersion height of 0.30 m to simulate the relative performance of a contactor using MDEA and DIPA solutions. McNeil (1970) measured a dispersion height of 200 mm in a 152 mm diameter bubble cap column with a superficial gas velocity of 0.385 m/s and a liquid flow rate of 5.66 mL/s. To determine the height of clear liquid on a tray, the equations developed by Gerhart

and Gross (1985) for flow over a full-span-sharp-crested weir may be used. The geometry of the physical system is illustrated in Figure 16. The volumetric flow rate of liquid leaving the stage, Q', may be calculated by

$$Q' = L_j \frac{M}{\rho} \tag{187}$$

where M is the molecular weight of the liquid and ρ is the density of the liquid. The additional height of liquid, ΔZ, flowing over the outlet weir of length W and height Z_{weir} can be calculated using

$$Q' = C_d \frac{2\sqrt{2g}}{3} W \Delta Z^{3/2} \tag{188}$$

$$C_d = 0.611 + 0.075 \frac{\Delta Z}{Z_{weir}} \tag{189}$$

where the height of clear liquid on the tray, Z_{CL}, is given by

$$Z_{CL} = Z_{weir} + \Delta Z \tag{190}$$

For fixed values of Q', W and Z_{weir}, Equations (188) and (189) can be solved simultaneously for ΔZ, and Equation (190) can be used to determine the total clear liquid height Z_{CL}. The height of liquid dispersion may be estimated by the use of a relative dispersion density, ϕ

$$\phi = Z_{CL} / Z_T \tag{191}$$

Values of relative dispersion density generally lie within the range 1.0 to 0.2.

Figure 16.

Hydrodynamics of Flow Over a Weir

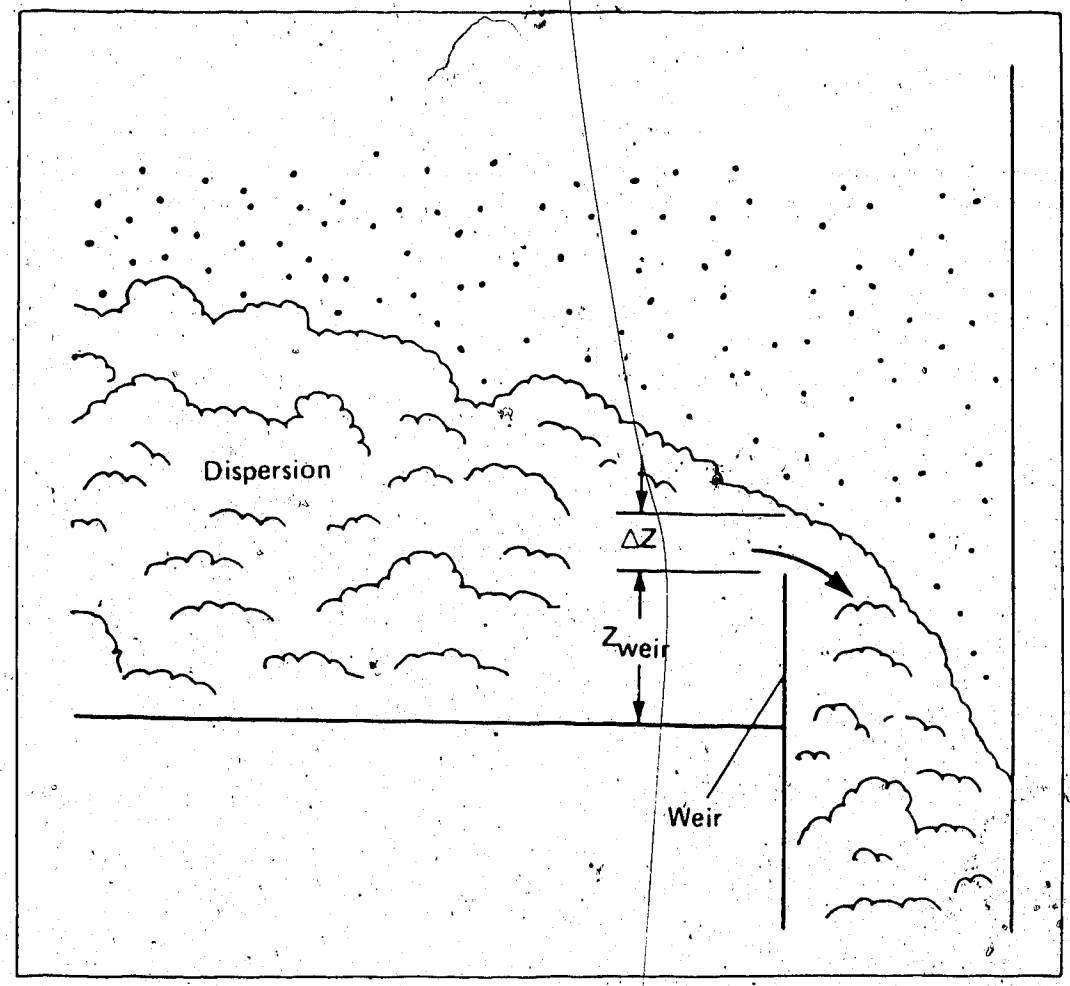

Gas-Phase Mass-Transfer Coefficient

Experimental and theoretical studies to determine the gas-phase mass-transfer coefficient in gas-liquid contactors include those of: Vidwans and Sharma (1967), Onda et al.(1968), Onda et al.(1968), Sharma et al.(1969) and Sridharan and Sharma (1976). Onda et al.(1968) correlated gas-side transfer coefficients with

$$k_g = 5.23\ (a_o D_g / R^* T)\ (G/a_o \mu_g)^{0.7}\ (\mu_g / \rho_g D_g)^{1/3} \cdot (a_o D_p)^{-2.0} \qquad (192)$$

where D_g is the molecular diffusion coefficient of the solute gas in the gas phase and D_p is the nominal packing size.

Sharma et al.(1969) performed experiments to measure the gas-phase resistance to mass transfer in bubble cap trays. They developed an expression for k_g based on the results of ammonia, sulphur dioxide and chlorine absorption into a number of chemical solvents.

$$k_g = 2.214\ R^* T v_g^{1/4} (D_g / S)^{1/2} \qquad (193)$$

Mashelkar (1970) discussed an approximate gas-phase mass transfer coefficient given by

$$k_g = \{-d/6R^* T t_g\} \left[1 - \frac{6}{\pi^2} \exp(-D_g \pi^2 t_g / (d/2)^2\right] \qquad (194)$$

where d is the bubble diameter and t_g is the gas-liquid contact time. Blauwhoff et al.(1985) used the following correlation for sieve trays at high pressure

$$\underline{a}k_g = 0.10\ R^*\ T\ (v_L\ \rho_L)^{0.6}\ v_g\ /H_{CO_2} \qquad (195)$$

where v_L is the superficial velocity of the liquid phase and H_{CO_2} is the Henry's constant for CO_2 in the solvent.

Scheffe and Weiland (1987) measured gas-phase transfer coefficients in a Glitsch V-1 valve tray and correlated the data with

$$a'k_g\ Pd/\rho_g\ D_g = 9.93\ \left(\frac{Gd}{\mu_g}\right)^{0.865}\left(\frac{Ld}{\mu_L}\right)^{0.130} \cdot (Z_{weir}/d)^{0.389}\ (\mu_g/\rho_g\ D_g)^{0.5} \qquad (196)$$

where d is a characteristic length (d = 1 m).

Values of k_g for trayed towers are typically in the order of 3×10^{-6} kmol/m²·s·kPa. Depending on the correlation, values predicted by Equations (192) to (196) vary somewhat about this guideline.

Liquid-Phase Mass-Transfer Coefficient

The experimental and theoretical studies of: Sharma et al.(1969), Akita and Yoshida (1973), Sridharan and Sharma (1976), Fukushima et al.(1978) and Sedelies et al.(1987) were designed to determine the liquid-phase mass-transfer

coefficient in gas-liquid contactors of various types. The liquid-phase mass-transfer coefficient in the absence of chemical reaction, k°_L, may, for example, be estimated for bubble-cap trays using the expression of Sharma et al.(1969)

$$k^\circ_L = 3.478\ v_g^{1/4}\ (D_L/S)^{1/2} \qquad (197)$$

where D_L is the molecular diffusion coefficient of the solute gas in the liquid phase. Onda et al.(1968) correlated k°_L data for packed columns with

$$k^\circ_L = 0.0051\ (\mu_L\, g/\rho_L)^{1/3}\ (L/\underline{a}\mu_L)^{2/3}\ (\mu_L/\rho_L D_L)^{-1/2}\ (a_o D_p)^{0.4} \qquad (198)$$

Blauwhoff et al.(1985) used the following expression to estimate the liquid-phase mass-transfer coefficient for sieve trays at high pressure

$$\underline{a}k^\circ_L = 4.9\times10^{-7}\ (v_L\,\rho_L)^{0.6}\ v_g^{1.2} \qquad (199)$$

Scheffe and Weiland (1987) measured liquid-phase transfer coefficients in a Glitsch V-1 valve tray and correlated the data with

$$a'k^\circ_L\, pd/H\rho_L D_L = 125\ \left(\frac{Gd}{\mu_g}\right)^{0.684}\ \left(\frac{Ld}{\mu_L}\right)^{0.087}\ (z_{weir}/d)^{0.051}\ (\mu_L/\rho_L D_L)^{0.5} \qquad (200)$$

Values of k°_L for packed towers are typically in the order of 3×10^{-4} m/s. Depending on the correlation, values predicted using Equations (197) to (200) vary somewhat about this guideline.

Enhancement Factor

The enhancement factor, I, is a measure of how much the rate of mass transfer across the gas-liquid interface is increased by the presence of chemical reaction, and it can be expressed as a function of the reaction rate for a given reaction regime:

$$I = k_L / k^{\circ}_L \qquad (201)$$

To calculate the local enhancement factors for H_2S and CO_2, a suitable kinetic model was required to account for the molecular diffusion and the chemical reactions that occur in the liquid phase. A model for the H_2S-CO_2-DIPA-H_2O system is described by Blauwhoff and Van Swaaij (1985). The details of their model are beyond the scope of this study, but the concepts may be used as a basis in the future to upgrade the model developed in this work.

In order to determine the reaction rate and the reaction regime, the nature of the chemical reactions that take place must be understood. Briefly, the major chemical reactions that must be accounted for in the rate expressions are:

Primary and Secondary Amines

$$H_2S + R_1R_2NH \rightleftharpoons R_1R_2NH_2^+ + HS^- \quad (202)$$

$$CO_2 + R_1R_2NH \underset{k_{-3}}{\overset{k_3}{\rightleftharpoons}} R_1R_2NH^+COO^- \quad (203)$$

$$R_1R_2NH^+COO^- + R_1R_2NH \xrightarrow{k_b} R_1R_2NCOO^- + R_1R_2NH_2^+ \quad (204)$$

$$CO_2 + OH^- \underset{}{\overset{k_{OH^-}}{\rightleftharpoons}} HCO_3^- \quad (205)$$

Tertiary Amines

$$H_2S + R_1R_2R_3N \rightleftharpoons R_1R_2R_3NH^+ + HS^- \quad (206)$$

$$CO_2 + R_1R_2R_3N + H_2O \underset{}{\overset{k_2}{\rightleftharpoons}} R_1R_2R_3NH^+ + HCO_3^- \quad (207)$$

$$CO_2 + OH^- \underset{}{\overset{k_{OH^-}}{\rightleftharpoons}} HCO_3^- \quad (208)$$

where k_2, k_3, k_{-3}, k_b and k_{OH^-} are the rate constants for the appropriate reactions.

As discussed in Chapter 2.1, the H_2S reactions involve a simple proton transfer and may be regarded as instantaneous for all amines of interest. For the case of simultaneous absorption of H_2S and CO_2, the H_2S enhancement factor is given by Danckwerts and Sharma (1966) as

$$I_{H_2S} = \frac{\{1 + \frac{[R_1R_2R_3N]}{\beta[H_2S]_i}\,(D_{R_1R_2R_3N}/D_{H_2S})\}}{\sqrt{D_{H_2S}/D_{R_1R_2R_3N}}}$$

(209)

where

$$\beta = 1 + q[CO_2]_i D_{CO_2} / [H_2S]_i D_{H_2S} \quad (210)$$

The concentration of free amine, $[R_1R_2R_3N]$, must be estimated by a suitable thermodynamic/mass transfer model. The value of q is the number of moles of amine that react with dissolved CO_2 in the liquid phase. For primary and secondary amines, q = 2; for tertiary amines, q = 1. The concentration of H_2S and CO_2 at the gas-liquid interface may be estimated by Equations (179) and (180) respectively. The Henry's constant for H_2S may be obtained by correcting the value in water, $H^\circ_{H_2S}$, for ionic strength effects. Danckwerts (1970) gives the following expression

$$\log_{10} (H_{H_2S} / H^\circ_{H_2S}) = h J \quad (211)$$

where J is the ionic strength of the solution and h is a constant salting-out parameter comprised of a sum of contributions of different ionic species in the solution.

$$h = h_+ + h_- + h_g \quad (212)$$

When H_2S is absorbed into amine solution, the liquid in the vicinity of the interface is concentrated in $R_1R_2R_3NH^+$ and HS^- ions. The salting-out parameter for the cation is not known but may be assumed to be zero. This was used by

Hikita et al.(1977) in their analysis of CO_2 absorption into DEA solutions. The value for the HS^- anion can be assumed to be similar to that of OH^- which has $h_- = 0.066$ m³/kg-ion. Danckwerts (1970) also gives the salting-out parameter for H_2S gas as $h_g = -0.033$ m³/kmol.

The ionic strength of the amine solution is given by

$$J = \frac{1}{2} \sum_i [\text{ion } i] Z_i^2 \qquad (213)$$

where Z_i is the electrical charge of the ion.

The molecular diffusion coefficient for H_2S may be obtained by correcting the value in water for solution viscosity effects using the Stokes-Einstein relationship presented by Haimour and Sandall (1984)

$$D_{H_2S} \mu^{0.74} / T = 3.476 \times 10^{-14} \qquad (214)$$

The molecular diffusivity of amines in aqueous solutions were measured by Hikita et al.(1980) and were correlated with

$$D = D^\circ \left(\frac{\mu}{\mu^\circ} \right)^{-2/3} \qquad (215)$$

where D° is the diffusivity at infinite dilution and μ and μ° are the absolute viscosities of amine solution and water respectively. The infinite dilution diffusivity was assumed to obey the Stokes-Einstein relationship. The Henry's constant and diffusivity of CO_2 in amine solutions may be

estimated using the nitrous oxide analogy as described in Chapter 2.5.

There are no explicit expressions for I_{CO_2} that apply for the general case of simultaneous absorption of H_2S and CO_2 and are valid for all amine types over the entire range of concentrations encountered in industrial solutions. As a first approximation, the simultaneous absorption of H_2S and CO_2 may be assumed to proceed independently with no direct interaction other than through the concentration of free amine in the liquid film. Yu and Astarita (1987a) suggest that the rapid absorption of H_2S into lean amines at the top of industrial contactors results in an acidic liquid film which tends to reduce the simultaneous rate of CO_2 absorption. Hence a more rigorous simultaneous absorption rate model must consider these effects.

The concentration of CO_2 at the gas-liquid interface is approximately the same as in the bulk liquid if the following condition is satisfied

$$\sqrt{D_{CO_2}\, k_{ov}} < k^{\circ}_L \left(1 + \frac{[R_1R_2R_3N]}{q[CO_2]_i}\right) \qquad (216)$$

where k_{ov} represents the overall pseudo-first order reaction rate constant. If this holds true, and if

$$\sqrt{D_{CO_2}\, k_{ov}} \geq k^{\circ}_L \qquad (217)$$

then CO_2 undergoes a pseudo-first order reaction and the enhancement factor may be approximated by

$$I_{CO_2} = \sqrt{(k^\circ_L{}^2 + D_{CO_2}\, k_{ov})}/k^\circ_L \qquad (218)$$

The value of k_{ov} may be determined for all alkanolamines using

$$k_{ov} = k_1 + k_{OH^-}\,[OH^-] \qquad (219)$$

where the second term accounts for the parallel reaction of CO_2 with hydroxyl ion. Additional detail on methods that can be used to estimate the contribution of hydroxyl ion to the overall CO_2 reaction rate are described in Chapter 2.1.

For primary and secondary amines, an apparent first-order rate constant may be defined for the reactions of CO_2 with amine as

$$k_1 = k_3[R_1R_2NH]/\{1 + \frac{k_{-3}}{k_b\,[R_1R_2NH]}\} \qquad (220)$$

For tertiary amines, the analogous rate constant is given by

$$k_1 = k_2[R_1R_2R_3N] \qquad (221)$$

Table 10 contains a list of the reaction rate constants that were used in the model.

Table 10.

Rate Constants for the Aqueous Reaction Between CO_2 and Alkanolamines

Amine	Rate Constant Expression
MEA	$\log_{10} k_3 = 10.99 - 2152/T$
DEA	$\log_{10} k_3 = 10.4493 - 2274.5/T$
MDEA	$\ln k_2 = 18.9001 - 5134.07/T$

References:

MEA - Hikita et al.(1977)

DEA - Blanc and Demarais (1981)

MDEA - This work

7.5.3 Phase Enthalpies

The simulation of a multistage separation device usually includes the consideration of the overall energy balance. For the special case of alkanolamine treating units, the absorption/desorption of acid gases into the amine solution is accompanied by substantial heat effects. The predicted temperature profile in the contactor is strongly dependent on the acid gas heat of solution that is used in the model. Similarly, the energy supplied to the regenerator is used to reverse the chemical reactions that bind acid gas in solution, therefore, the degree of stripping also depends on the heat of solution used in the model.

Heats of solution of H_2S and CO_2 in amine solutions have been published by Dow (1964), Union Carbide (1969), Murzin and Leites (1971), Ouwerkerk (1976), Kahrim and Mather (1976), Pearce (1978), Blanc et al.(1981), and Kohl and Riesenfeld (1985). They may also be determined by making use of the experimental equilibrium solubility data and the following thermodynamic relationship

$$\Delta H_{soln,d} = \left[\frac{\partial \ln f_1}{\partial (1/T)} \right]_{X_1} \qquad (222)$$

where the subscript 1 refers to the acid gas and X is the mole fraction of the acid gas in the liquid. Jou et al.(1982) used this method in their analysis of the MDEA

system and were able to demonstrate the effect of temperature and solution loading on $\Delta H_{soln,d}$.

The molar enthalpy of a pure component in the vapor phase, H_i, was assumed to be equal to the ideal gas enthalpy. Enthalpy departure was assumed to be negligible. The tabulated ideal gas enthalpy coefficients available in the API Technical Data Book (1970) were used in the following polynomial expression

$$H_i = a_0 + a_1 T + a_2 T^2 + a_3 T^3 + a_4/T \qquad (223)$$

Ideal gas enthalpy coefficients for components not in the API Technical Data Book (1970) were obtained by integrating liquid heat capacities over a range of temperature to derive liquid enthalpies, and adding on the latent heat of vaporization. These vapor enthalpy values were then correlated according to Equation (223).

The molar enthalpy of a gas mixture was calculated using

$$H_j = \sum_i Y_{i,j} H_i \qquad (224)$$

assuming that the heat of mixing was negligible.

The latent heat of vaporization, ΔH_v, for condensible components such as water and alkanolamine, was calculated using the Clausius-Clapeyron equation and experimental vapor pressure data

$$\frac{dP}{P} = (\Delta H_v / R^*) \frac{dT}{T^2} \qquad (225)$$

The latent heat was then correlated as a function of temperature using

$$\Delta H_v = b_0 + b_1 T + b_2 T^2 \qquad (226)$$

The molar enthalpy of a pure component in the liquid phase, h_i, was assumed to be given by

$$h_i = H_i - \Delta H_{v,i} - \Delta H_{soln,i} \qquad (227)$$

The values of $\Delta H_{v,i}$ and $\Delta H_{soln,i}$ were equal to zero for noncondensible and nonreacting components respectively. The molar enthalpy of a liquid mixture was calculated using

$$h_j = \sum_i X_{i,j} h_i \qquad (228)$$

When calculating the enthalpy of the liquid phase, it is important to use the integral heat of solution, $\Delta H_{soln,i}$, and not the differential heat of solution, $\Delta H_{soln,d}$. Appendix 8 contains a theoretical analysis of the integral heat of solution in the case of alkanolamine systems. A comparison between the differential and integral heat of solution for MDEA is shown in Figure 17. The data of Jou et al.(1982) were used to determine ΔH_i. The integral heat of solution is higher than the differential heat of solution at the same acid gas loading.

Figure 17.

Comparison of Integral and Differential Heats of Solution for H_2S and CO_2 in MDEA Solutions

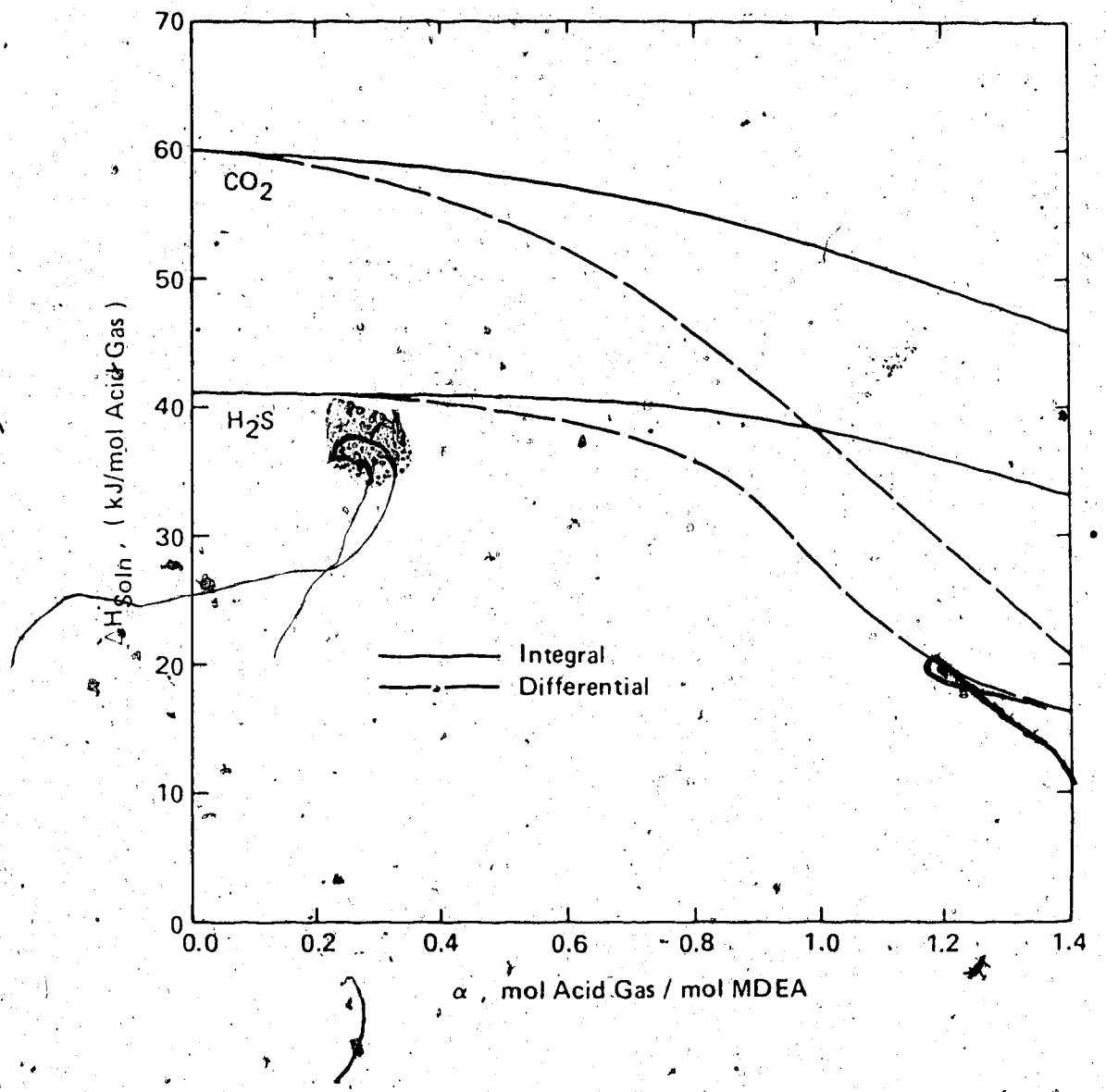

7.5.4 Fluid Properties

The density of pure saturated liquid water was correlated with the following polynomial expression

$$\rho^{\circ} = \kappa_5/(\kappa_0 + \kappa_1 T + \kappa_2 T^2 + \kappa_3 T^3 + \kappa_4 T^4) \qquad (229)$$

where

$\kappa_0 = 0.037648$

$\kappa_1 = -2.2948 \times 10^{-4}$

$\kappa_2 = 8.9732 \times 10^{-7}$

$\kappa_3 = -1.5347 \times 10^{-9}$

$\kappa_4 = 1.0484 \times 10^{-12}$

$\kappa_5 = 16.0185$

The data presented by Dow (1964), Union Carbide (1969) and Pennwalt (1980) were used to generate correlations for amine solution densities with the following form

$$\rho = \rho^{\circ} + wt\ \% \ (\beta_0 + \beta_1 T) \qquad (230)$$

where wt % represents the weight percent amine in the liquid and β_0 and β_1 are constants:

Liquid phase kinematic viscosities were correlated using an equation of the following form

$$\ln \nu = \zeta_0 + \frac{\zeta_1}{T} + \frac{\zeta_2}{T^2} \qquad (231)$$

where ζ_0, ζ_1 and ζ_2 are parameters that were determined to

be functions of amine weight percent.

Dingman (1963) presented data which illustrated the effect of temperature and solution loading on the physical properties of MEA solutions. The solution viscosity and density are shown to be affected by the presence of dissolved H_2S and CO_2.

Gas phase density was estimated using the ideal gas law. Gas phase viscosity and diffus[illegible] estimated using the techniques described in Ch[illegible]

8. DEVELOPMENT OF AMINE TREATING PROCESS SIMULATOR

Process simulation is the representation of a chemical process by a mathematical model which is then solved to obtain information about the performance of the chemical process. The mathematical model is usually a computer program and is generally known as a process simulation program or a flowsheeting program. Motard et al.(1975) present an excellent review of methods available for steady-state chemical process simulation.

Process simulation has been used by chemical engineers since the 1950's; however, advances in simulation capability have been restricted by computer technology and by limitations in the available theoretical models. Recent developments in computer hardware have removed the restrictions on program size and rigor. With theoretical models such as those developed in Chapter 7, it is possible to assemble a simulation model for amine treating process analysis and design.

Early simulators were developed with such a complex structure, that the program authors were the only ones who could effectively use the program. Present day simulators are developed with much more emphasis on the user interface and the modularity of the program. Indeed software engineering has become a thriving field of study, largely as a result of an increased industrial demand for simulation software for process design and control. Myers (1978) and

Fairley (1985) discuss the important concepts that need to be considered when designing and managing a large-scale computer program such as a process simulator.

8.1 Approach to Process Simulation

The first fundamental decision to be addressed in the design of a process simulator is whether the program will operate in the simulation mode or in the design mode. In the simulation mode, all system inputs and design parameters are specified and the information flow is in the same direction as energy and material flow in the plant. In this mode, feed streams must be specified. For example, amine circulation rate and reboiler heat duty must be fixed, and plant outputs such as temperatures and compositions are calculated by the program. In the design mode, information flows in the opposite direction; system inputs and design parameters are calculated from specified outputs. In this case, amine circulation rate and reboiler heat duty are calculated by the program to meet specifications such as treated gas residual H_2S content or net rich amine loading. Both modes of simulation are required by industry. A third mode involving optimization of a cost function combines both simulation and design. Variables associated with feed streams and design variables may be left unspecified and the program will determine their values according to specified equality and inequality constraints.

A simulator can realistically only be written to operate in one of these modes. Furthermore, the simulation mode is generally more stable numerically. For this reason, nearly all commercial programs perform design calculations using iterative simulation in which external calculation loops are used to force design constraints on the simulation results. A discussion of the process simulation and optimization problem is presented by Kisala et al.(1986) in which the successive quadratic programming method was used to force equality and inequality design constraints on the results calculated by a process simulator. The simulation mode is sometimes referred to as the performance rating mode.

The second fundamental decision to be addressed is the approach to simulation. In the flexible flowsheet approach, a simulator is designed to model any combination of process unit modules. On the other extreme, the program may be set up to simulate a particular process with a fixed plant flowsheet. Process unit modules are independent mathematical models that represent specific unit operations such as isothermal flash, heat exchanger or absorber calculations.

The flexible flowsheet approach has been used by most commercial flowsheet simulation programs such as Simulation Sciences Inc. PROCESS™, Aspen Technology Inc. ASPEN PLUS™, Monsanto Co. FLOWTRAN™, Badger America Inc. GMB™ and

ChemShare DESIGN II™, because of the general nature of their application. Russell (1980) reports that these programs are all similar in function and that the differences lie in the areas of program structure, style of input, physical property facilities and features which provide convenience and flexibility. The unit modules within the program are connected according to the user's specification of the flowsheet configuration and an executive program supervises the flow of data and organizes the calculation sequence to obtain a convergent solution to the problem. Although the flexible flowsheet approach provides unlimited simulation capability, the disadvantages include: the need for additional logic to keep track of individual unit module stream connections, efficient equation-tearing methods required to solve recycle calculations, and a tendency for users to "over-simulate" a process and to lose sight of the important unit operations.

The classical fixed flowsheet approach to simulation is merely an extended mathematical problem in which all equations and constraints are defined. In this method, the program already knows which unit modules are required and the interlinking stream connections. An executive program is not needed since the software designer has already "hard-coded" the flowsheet configuration into the simulator. Although the classical fixed flowsheet approach provides no freedom to change the flowsheet configuration, it is computationally more efficient than the flexible flowsheet

approach because of the reduced housekeeping overhead.

In view of the objectives in this study, it was considered unnecessary to develop a generalized chemical process simulation program. However, it was of interest to be able to compare several modifications to the conventional amine treating process illustrated in Figure 1, and to evaluate the sensitivity of plant operation to certain process variables. Therefore, the program was set up to operate in the simulation mode and a hybrid approach was developed to combine the advantages of the flexible and classical fixed flowsheet approaches to process simulation.

8.2 Flowsheet Solution Techniques

For simple processes involving no material or energy recycle, solution of the flowsheet is obtained by simple propagation of information from upstream to downstream unit modules. Starting with the feed streams, outputs from the first unit are calculated and directed to the next module. This continues until the outputs for the last unit are calculated.

Industrial processes frequently have recycle streams, such as in the amine treating process. In these cases, simple propagation of information will not be sufficient to obtain a solution since at some point, the recycle inputs to a unit module will be initially undefined. There are

basically two methods of finding convergent solutions to recycle processes: simultaneous and sequential.

In the simultaneous solution procedures, the performance of the individual process units in the flowsheet are linearized around an assumed steady state, and the resulting system of equations are solved simultaneously. New values for the stream variables are used to simulate the individual process unit modules and the flowsheet is again linearized using the new calculated outputs. This procedure is repeated until successive iterations result in no appreciable change in the value of stream variables. The method is sometimes called successive linearization.

Ford (1979) discusses several simultaneous solution methods. Clarke (1986) presents an example using ASPEN PLUS™ where the standard sequential solution method was bypassed and a user-defined simultaneous method was used in its place. The example shows substantial improvement in convergence although Clarke (1986) comments that the increased engineering time required to develop the convergence routine offset the savings in computer time.

The equation-oriented approach to simulation has generally been restricted to specific flowsheeting problems involving multiple distillation columns. It is generally recognized that simulation or design calculations for complex separation systems are more effectively performed using a simultaneous rather than sequential approach. That

is, rather that repeatedly solve a sequence of single columns until a solution to the entire system is obtained, it is preferable to solve all of the columns simultaneously.

The column-modular or Capital-Θ method of Nartker et al.(1966) involves the individual solution of unit modules but these single column problems are converged simultaneously rather than repeatedly one at a time. This was an extension of the single column θ method developed by Lyster et al.(1959a, 1959b, 1959c). The method was later modified by Billingsley (1971) to simplify the multiunit system equations and eliminated the Θ's. An example application of the method is presented by Petryschuk and Johnson (1968).

Browne et al.(1977) proposed considering the system of equations for all unit modules simultaneously. This concept is characteristic of an entire group of methods described by Harclerode and Gentry (1972), Jelinek et al.(1973), Kubiček et al.(1976), Hess et al.(1977), Hofeling and Seader (1978), and Stadtherr and Malachowski (1982).

These methods are well-suited to systems involving distillation units; however, other devices such as vessels in which chemical reactions occur are more nonlinear and more difficult to converge. Large-scale acceptance and implementation of equation-oriented methods for more general flowsheeting problems will require development of improved techniques to manipulate large sparse matrices, to handle

design specifications within each unit module, and to establish a systematic approach to evaluating the Jacobian matrix. In principle, the simultaneous method is computationally more sophisticated than sequential methods but is more difficult to apply and retain flowsheet generality. Moreover, for systems involving highly nonideal vapor-liquid equilibrium, as in alkanolamine systems, the simultaneous approach has a poor record of convergence. Browne (1976) reports that the convergence characteristics for the multicolumn system may be totally different than the same approach applied to a single column.

The most common flowsheet solution technique is the sequential solution method. When used in simulators with distinct process unit modules, it is referred to as the sequential modular approach. In the sequential solution approach, the values of stream variables including composition and flow rates, for certain recycle streams called tear streams, are initially assumed so that the entire flowsheet can be simulated sequentially as a simple flowsheet. Having calculated the values of the recycle stream variables, these may be compared with the assumed values and new estimates made for the next iteration. This procedure is continued until recycle stream variables do not change with successive iterations. Complex flowsheets with many recycle streams may often be decomposed in such a way that several combinations of tear streams are possible.

Shacham (1982) reports that the sequential modular approach has some advantages over other methods for process flowsheeting:

1) Unit modules can be prepared and tested separately and are easily expressed as a computer program subroutine.
2) Each unit module can contain an optimum solution method for that type of problem.
3) Data entering unit modules can easily be checked for completeness and consistency.
4) New unit modules can easily be added or replaced in the simulator as they are developed.

New estimates for the tear-stream variables may be obtained by direct substitution, accelerated substitution or Newton-Raphson methods. Let $X^k = (x_1, x_2, x_3, \ldots x_n)^k$ denote the vector of input tear-stream variables and let $Y^k = (y_1, y_2, y_3, \ldots y_n)^k$ denote the vector of calculated variables at the k-th flowsheet iteration such that

$$Y^k = \psi(X^k) \tag{232}$$

where ψ represents the functionality of the flowsheet configuration. The problem is to find the solution such that

$$||Y^k - X^k|| \leq \epsilon ||X^k|| \tag{233}$$

where $\epsilon > 0$ is the desired tolerance limit and $||X||$ is some norm of the vector X such as $\sqrt{X^T \cdot X}$.

In direct substitution, the calculated tear-stream variables are used as estimates for the next flowsheet iteration.

$$X^{k+1} = Y^k \tag{234}$$

While this method is simple, it is sometimes slow to converge. Accelerated substitution methods such as the Wegstein, dominant eigenvalue or Newton-Raphson methods may be used to improve the rate of convergence of direct substitution. Kliesch (1967) applied Wegstein's method to multivariable systems but found it necessary to bound the acceleration step to ensure stable convergence. Instabilities arise in Wegstein's method because no consideration is given to interaction between variables. Dominant eigenvalue methods developed by Orbach and Crowe (1971), Soliman (1981) and Crowe (1984) are similar in nature to the Wegstein method, but take variable interaction into account.

The convergence characteristics of each of the above mentioned sequential methods are similar to those experienced in other numerical applications. The Newton-Raphson methods converge most rapidly, provided that the initial tear-stream variables are close to the solution

and that the Jacobian matrix is nonsingular at the solution. If the initial guesses are poor, the method will usually diverge. The main drawbacks are the large computer storage requirement for the inverse Jacobian matrix and the additional computational effort required to evaluate the matrix. The Wegstein and direct substitution methods are comparable in simplicity.

A sequential-modular solution procedure was chosen for flowsheet convergence in this study because it would allow for easy future modification to the fixed flowsheet. Considering the strong interaction between the lean amine acid-gas residual loadings, the direct substitution method was chosen because of its stability and simplicity.

8.3 AMine Treating Unit SIMulator, AMSIM

The **AM**ine treating unit **SIM**ulator (**AMSIM**) was initially developed to simulate single-column systems. The advantages of the original program were quickly realized and the scope of the project was expanded to include limited process flowsheeting capabilities. The **AMSIM** system is a completely integrated set of routines written in FORTRAN 77. The use of FORTRAN over other programming languages was considered appropriate so that the system would be portable and easy to modify and maintain. The program has been successfully implemented on the Amdahl 5870 mainframe computer at the

University of Alberta and on IBM PC/XT and PC-AT personal computers.

The AMSIM system presently contains about 12000 lines of FORTRAN 77 source code. The main executive flowsheeting routine only accounts for approximately 3 % of the total line count. Input processing constitutes about 45 % of the entire system. Unit module calculations and supporting convergence routines take up about 32 % of the program and the remaining 20 % is used by report-generating output routines.

Process Unit Modules

AMSIM contains several major process unit modules which numerically simulate the performance of common devices found in gas conditioning facilities. These include:

- Absorber
- Regenerator
- Rigorous Heat Exchanger
- Adiabatic Flash
- Isothermal Flash
- Single Phase Heater/Cooler

The program also contains other minor unit modules required for the interconnecting process streams:

- Single-Phase Stream Addition
- Single-Phase Stream Split
- Two-Phase Stream Addition
- Equate Stream Facility
- Stream Physical Property Generator
- Stream Convergence Method

Considerable attention was given to ensuring a high degree of reliability in all of the unit modules. Extensive testing was performed to locate and resolve problem areas so that the credibility of the system would not be compromised. Each unit module is highly independent, and is partitioned into a hierarchy which gives the program a top-down structure.

Thermodynamic and physico-chemical data required by the unit modules are obtained from the properties package. For example, equilibrium ratios, reaction rate constants, Henry's constants, phase enthalpies or solution densities are provided by subroutines in the properties package. The thermodynamic and physico-chemical properties package is the most critical component of the simulator, particularly from the industrial research standpoint. This was a major reason for undertaking the experimental studies described in Chapter 3. The accuracy of the entire program hinges on the credibility of these routines.

Flowsheet Configuration

With these process unit modules as building blocks, consideration was given to all of the potential flowsheet configurations that might be of industrial interest. Figure 18 shows the flowsheet that was used as the basis for the **AMSIM** program. The logic to solve the recycle calculations for this flowsheet is contained within the program. Other configurations are studied by simplifying this basic flowsheet and instructing **AMSIM** to ignore certain unit modules.

The flowsheet processing executive calls the appropriate subroutines to perform unit module and recycle calculations according to the sequential order of the flowsheet topology. The executive program is exactly the same no matter what is being simulated. This is conceptually similar to the GMB™ system described by Russell (1980) and is termed the "fixed structure" by Motard et al.(1975). The matching of streams to unit modules and the calculation path is determined by data supplied by the user.

This is in contrast to other "variable structure" simulators which create a program of subroutine calls and cause that program to be compiled and linked prior to execution. These programs tend to reduce the memory requirements by only linking the necessary subroutines, but the extra overhead of compilation and linking is included in each run. This may be a relatively small cost percentage

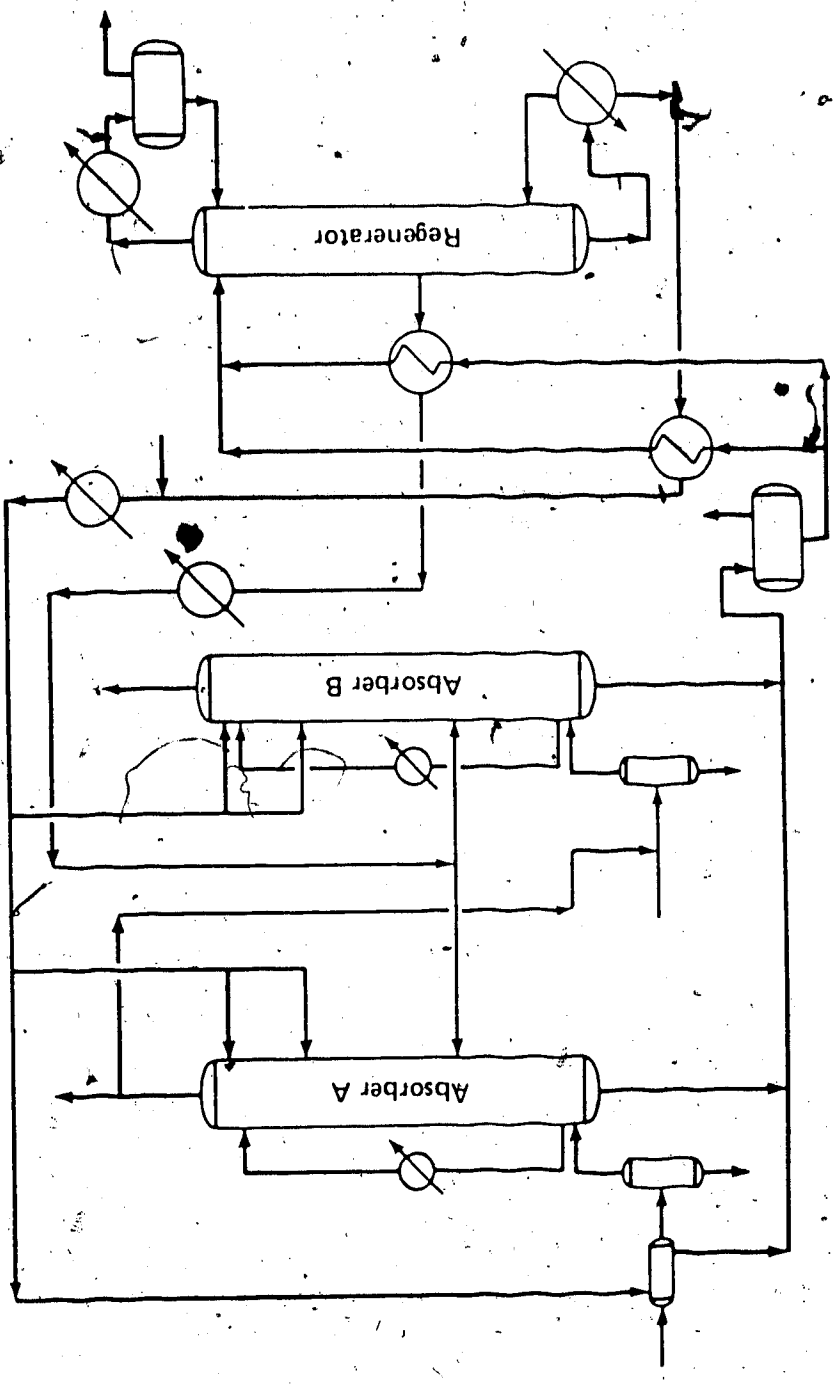

Figure 18. AMSIM Internal Flowsheet

for very large problems but represents a substantial cost for small problems.

With the basic AMSIM flowsheet, it is possible to simulate the following important flow schemes as well as many others:

- Single Absorber
- Single Regenerator
- Absorber - Regenerator System with Rich Amine Flash
- Absorbers in Series with a Common Regenerator
- Parallel Absorbers with a Common Regenerator
- Split-Flow Configurations to either Absorber
- Multiple Lean Amine Feed Points
- Absorbers with Amine Pumparound
- Cocurrent Static Mixing Element

Data Storage

Fundamental to the AMSIM structure is the use of process stream vectors for data storage. These vectors are maintained in an internal "database" and contain stream names, individual component flow rates, pressure, temperature, enthalpy, liquid fraction and additional physical property data. When stream compositions and conditions are required for unit operation calculations, the program retrieves the stream data from the appropriate vector. Similar data areas in memory are reserved to hold

current information about the unit operations. For example, internal phase rate, temperature and composition profiles for multistage devices are saved prior to leaving the absorber/regenerator module. The data storage areas permit the generation of summary reports for each stream and unit module in the flowsheet at the end of the simulation run.

A global data management routine controls the storage and retrieval of information from the process stream vectors and the internal database. During the sequential solution procedure, the data management routine moves data on request from the storage area to a work area which is used by the process unit modules. When a unit module calculation has been completed, the updated data are moved back into storage for future processing. This arrangement relieves subroutines that generate or use problem data from having to know how or where the data are stored. The subroutine need only "see" the data work area.

Data Input

When using the program, the flowsheet topology must first be identified, then the following information must be specified:

1) All components present in the process must be specified.
2) The process operating and design variables such as

the number of stages in a column, the operating pressure of the flash tank, the tray design and dimensions, or the minimum temperature approach in a heat exchanger must be supplied.

3) The composition and condition of each stream which enters the plant must be specified.

The model also requires initial estimates for any recycle streams in the process. From this information the ANSIM program calculates the steady-state operation of the entire plant.

Data is entered into the program in the form of a free-format keyword-oriented command file similar to that described by Rosen and Pauls (1977) for the FLOWTRAN™ system. Data may be entered in either Engineering units (psia, °F, lbmol/h) or in SI units (kPa, °C, kmol/h). Components are identified by mnemonic keywords. An example data file for a combined absorber-regenerator system is listed in Figure 19. The entries are structured in a logical sequence and unit modules are easily identified. Data may appear in virtually any order and may be separated by blank lines or by comment lines as shown in Figure 19. A preprocessor takes this information and converts it into a form which can be used by the main simulator. The data are checked for syntax errors and consistency. Errors in the data file will prevent the execution of the flowsheet simulator. Diagnostic messages are produced to assist the

Figure 19.

Example AMSIM Input Data File

```
            TITLE
Example AMSIM Input Data File
            UNITS
INPUT=IMP OUTPUT=IMP PRINT=LONG
            COMP
H2S H2O CO2 N2 H2 C1 C2 C3 N-C4 I-C4 N-C5 MDEA

*==============================
* Absorber Unit Module
*==============================
            COLUMN
TYPE=ABSA
            SPECS
STAGES=13
PRESS TOP=12.9 DROP=.15
            EST
TEMP TOP=100 BOT=130
            FEED
TYPE=LEAN P=15 T=100 WT=25 FLOW=120 AH2S=.01 ACO2=.01
            FEED
TYPE=GAS P=14.85 T=130
            RATES
7.74 84.64 75.39 405.11 18.7 1.78 .89 .36 .07 .07 .04 0
            EFF
H2S=.5 CO2=.04

*==============================
* Regenerator Unit Module
*==============================
            COLUMN
TYPE=REG
            SPECS
STAGES=16 REB DUTY=5.86E6
PRESS COND=27.4 TOP=29.4 DROP=0.15
TEMP COND=130
            FEED
TYPE=RICH P=30 STAGE=3
            EFF
H2S=1 CO2=.08
            END
```

user in correcting the problem.

Program Output

The calculated results show the pressures, temperatures, phase rates, enthalpies and/or heat duties for each unit module in the flowsheet and the complete composition, condition and fluid properties for every process stream. Data are presented in concise summary reports. Figure 20 contains a process stream summary report for a rich amine stream leaving a contactor. In addition, preliminary mechanical design information is generated for the major unit operations. Diagnostic messages are produced in the event of a nonconverged unit module or flowsheet calculation.

Figure 20.

Example Process Stream Summary Report

AMSIM V3.0 Page 4

Example AMSIM Output for a Rich MDEA Stream

Stream 8 Rich Amine from Absorber A

Component	kmol/h,	mol frc.
H2S	11.533	0.045131
CO2	3.117	0.012195
MDEA	29.050	0.113673
Water	211.537	0.827753
Methane	0.288	0.001128
Ethane	0.022	0.000087
Propane	0.008	0.000031
Nitrogen	0.000	0.000001
Total	255.556	

Temperature	27.872	C
Pressure	5919.000	kPa
Enthalpy	533.754	kW
Mol. Wt.	30.558	
Liquid Fraction	1.000	
Std. Vol. Flow Rate	118.426	L/min
Actual Vol. Flow Rate	118.989	L/min
Weight % amine	47.597	
Std. Density	1099.028	kg/m3
mol H2S/mol amine	0.397	
mol CO2/mol amine	0.107	
Std. Residual H2S	55310.928	mg/L
Std. Residual CO2	19302.962	mg/L
Viscosity	7.655	mPa-s
Heat Capacity	3.196	kJ/kg-C
Thermal Conductivity	0.350	W/m-C

9. MODEL EVALUATION

In this Chapter, five example problems are presented to illustrate the use of the nonequilibrium stage model and the **AMSIM** simulator to analyze the performance of amine treating facilities. The problems involve the use of MEA, DEA and MDEA, and demonstrate the dependence of component stage efficiencies on tray design variables, pressure and the type of alkanolamine used. For consistency, the mass-transfer coefficient models presented by Sharma et al.(1969) were used in all problems. As well, it was assumed that the towers in each example were equipped with bubble-cap trays. Appendix 9 contains sample output from the **AMSIM** program. This should give an indication of the amount of information supplied by the program.

9.1 High-Pressure MDEA Contactor

In this example, sour gas containing 0.44 mol % H_2S and 0.88 mol % CO_2 is treated with a 50 wt % MDEA solution at 6.0 MPa in a multistage contactor that has amine feed nozzles located on stages 1, 5 and 10, numbered from the top tray of the contactor. It is of interest to determine the effect of the number of contacting stages on the composition of the treated gas. The gas and liquid feeds to the contactor are listed in Table 11.

Table 11.

Gas and Liquid Feed Compositions in Example 9.1

Component	Sour Gas (kmol/h)	Lean Amine (kmol/h)
H_2S	10	0.032
CO_2	20	0.096
MDEA	0	31.845
H_2O	2	210.619
C_1	2041	0
C_2	100	0
C_3	50	0
i-C_4	10	0
n-C_4	10	0
n-C_5	10	0
n-C_6	5	0
n-C_7	5	0
N_2	5	0
Total	2268	242.592
Temperature (°C)	35	25

The tower was assumed to have an internal diameter of 1.067 m. The outlet weir dimensions were set to 63.5 mm by 0.6402 m. The active tray area was calculated to be 90 % of the cross-sectional area.

The simulation results indicate that the treated gas contains less than 1.2 ppmv H_2S in each of the three cases, but the amount of CO_2 that passes through the contactor is affected by the number of contacting stages. The predicted CO_2 content of the treated gas is given below:

CO_2 Feed Rate in Sour Gas: 20 kmol/h

Number of Contactor Stages	CO_2 in Treated Gas (kmol/h)	CO_2 Slippage %
10	15.256	76
15	13.330	67
20	11.686	58

This CO_2 slippage rate is in accordance with the performance test data presented by Ammons and Sitton (1981) which was collected from the MDEA contactor at the Waveland Gas Plant in Mississippi.

As expected, the CO_2 stage efficiency varies from about 2 to 3 % throughout the column and is plotted in Figure 21 as a function of contactor stage number for the case with 20

stages. The CO_2 efficiency profile was found to follow the same trend as the temperature profile in the column. This is also to be expected since the value of k_L is a function of k_{ov}, the reaction rate constant. The H_2S stage efficiency remains relatively constant at 91 % on each stage. Average values of K_{og} were 3.6×10^{-6} kmol/m²·s·kPa for H_2S and $3.2\text{-}4.5 \times 10^{-8}$ kmol/m²·s·kPa for CO_2. The predicted value of a was 217 m²/m³.

9.2 Low-Pressure DEA Contactor

This example illustrates the importance of considering component tray efficiencies when designing amine treating facilities. The data in this example are similar to those presented by Donnelly and Henderson (1974). A 20-stage contactor is used to treat a sour solution gas stream containing 8.5 mol % H_2S and 2.2 mol % CO_2 with 20 wt % DEA. The gas is available from the surface separation facilities at 262 kPa and is to be partially sweetened at the low pressure prior to being compressed to line pressures. A second DEA contactor is installed downstream of the compressor for final treating to pipeline specifications. In order to design the high-pressure absorber and select materials for the compression equipment, it is necessary to predict the performance of the low-pressure contactor. The gas and liquid feeds to the low-pressure contactor are

Figure 21.

CO_2 Stage Efficiency as a Function of Stage Number in Example 9.1

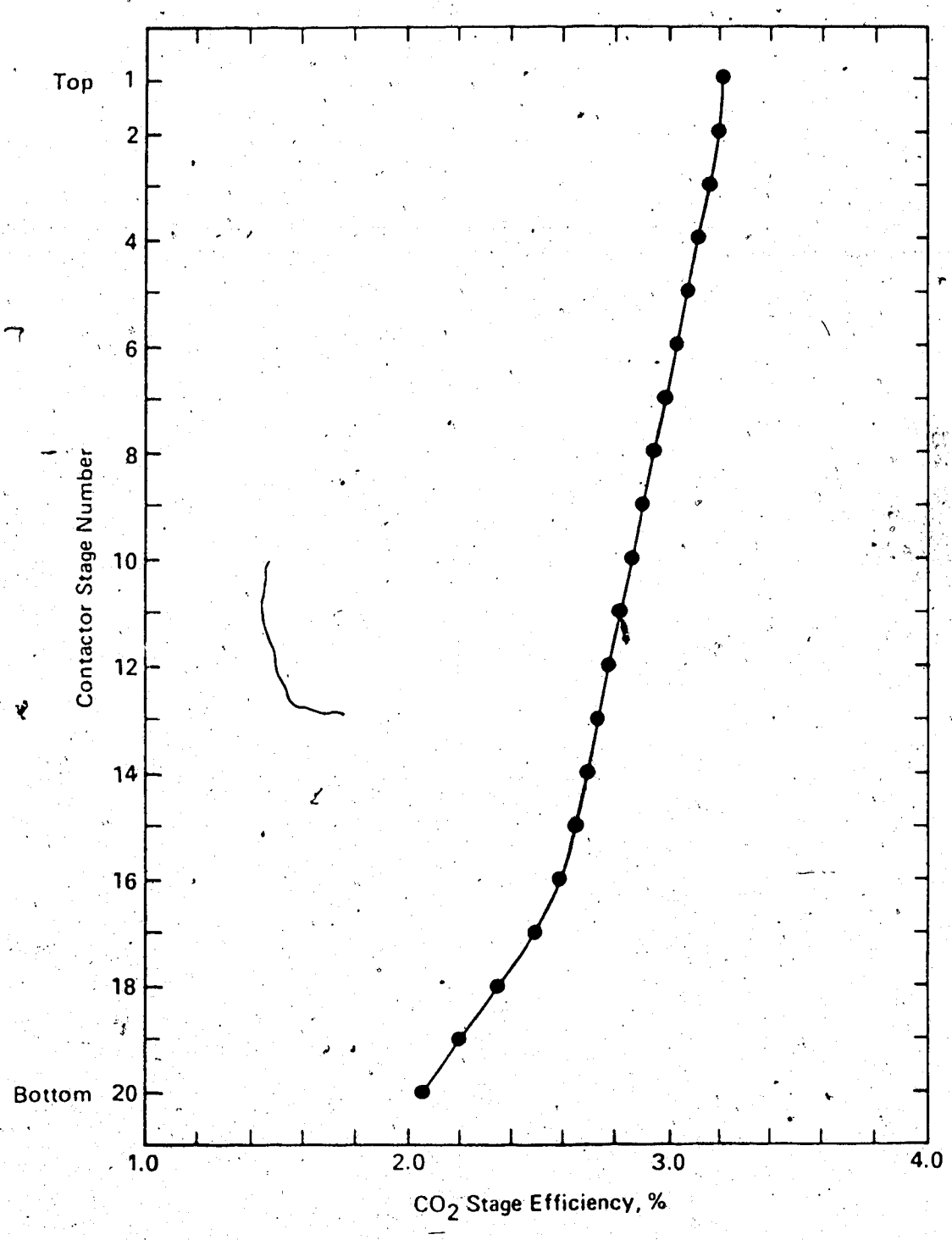

listed in Table 12.

The tower was assumed to have an internal diameter of 1.2 m. The outlet weir dimensions were set to 50.8 mm by 0.90 m. The active tray area was calculated to be 78 % of the total cross-sectional area.

The predicted treated gas composition is 29 ppmv H_2S and 0.154 mol % CO_2. The calculated tray efficiencies are 81 % for H_2S and range from 12.6 to 14.0 % for CO_2. If the contactor is simulated with 20 ideal stages, the treated gas composition is estimated to contain 28 ppmv H_2S and only 6 ppmv CO_2. The model therefore predicts an effect of pressure on the rate of CO_2 absorption under these conditions. Donnelly and Henderson (1974) observed considerable selectivity for H_2S in a similar absorber.

In this example, average values of K_{og} were 5.5×10^{-6} kmol/m^2·s·kPa for H_2S and $4.4\text{-}4.9 \times 10^{-7}$ kmol/m^2·s·kPa for CO_2. The predicted value of $\underline{a}$ was 342 m^2/m^3.

9.3 Low-Pressure MEA Contactor with Amine Pumparound

Amine contactors are occasionally used to recover CO_2 from flue gases in CO_2 production plants. Arnold et al.(1982) presented guideline rules which can be used to design MEA contactors for this purpose. The most striking difference between the operating conditions of a

Table 12.

Gas and Liquid Feed Compositions in Example 9.2

Component	Sour Gas (kmol/h)	Lean Amine (kmol/h)
H_2S	20.58	0.767
CO_2	5.23	1.043
DEA	0	80.214
H_2O	2.90	1092.159
C_1	135.33	0
C_2	32.38	0
C_3	25.63	0
$n\text{-}C_4$	13.49	0
N_2	6.89	0
Total	242.43	1174.183
Temperature (°C)	25	37.2

high-pressure natural gas treater and a low-pressure flue gas absorber is the required amine circulation rate. High pressure absorbers may require about 0.35 L amine solution for every Nm^3 of feed gas while atmospheric towers may use 5.4 L/m^3 gas. The associated regeneration costs become a controlling factor in the operation of flue gas treating facilities.

The large circulation requirement is primarily due to unfavorable CO_2 backpressure from the amine solution. When the CO_2 is absorbed from the gas, the heat of solution raises the temperature of the liquid to a point where the equilibrium partial pressure above the solution approaches that in the gas phase and a "pinch" point occurs in the column. To avoid this effect, large volumes of amine solution are circulated to smooth out this temperature bulge.

In this example, 30 wt % MEA is used to recover CO_2 from a flue gas containing 8.8 mol % CO_2, 81.4 mol % N_2 and the balance water. The gas is available at 105 kPa and 46°C and at a rate of 5875 kmol/h. In order to reduce the total amine circulation to the regenerator, an internal recycle or pumparound circuit is used. The process configuration is shown in Figure 22.

Lean amine at 46°C is fed to the contactor at a rate of 5.8 m^3/min and contains 0.20 mol CO_2/mol MEA. Total liquid is withdrawn from stage 16 and cooled to 46°C. One third of

Figure 22.

Process Configuration for Example 9.3

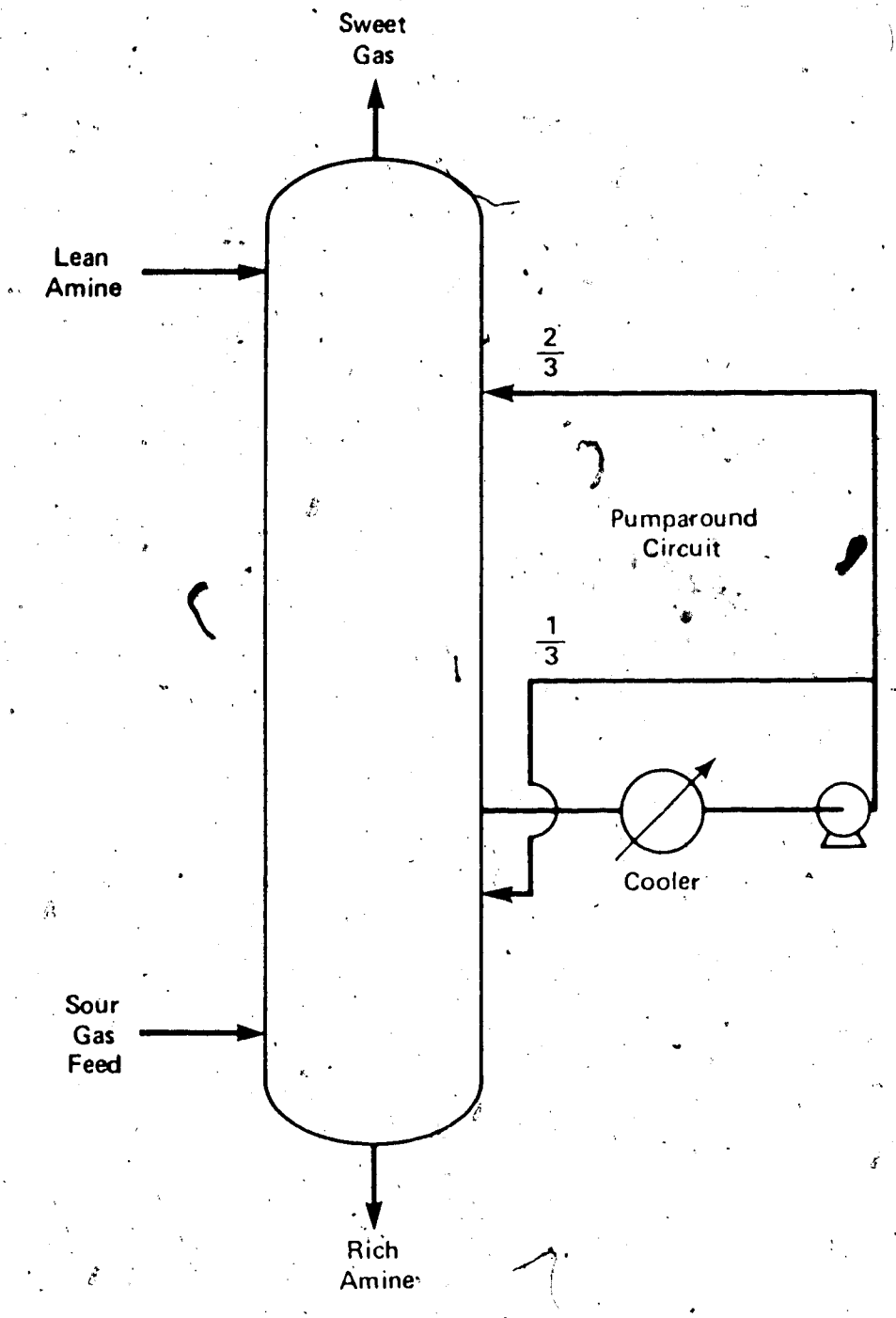

the stream is returned to stage 17 and the remainder is pumped back to stage 5 in the contactor. This arrangement effectively increases the internal circulation of amine from an overall value of 2.5 L/Nm³ gas to 8.2 L/Nm³ on the middle 12 trays in the column. The external cooler that removes the heat of reaction from the system is relatively inexpensive to install and operate as it only treats a single-phase liquid.

The predicted stage efficiency for CO_2 absorption ranges from 20.3 % to 40.3 % and the outlet gas contains 0.04 mol % CO_2 on a dry basis. The CO_2 loading in the circulated pumparound was calculated to be 0.396 mol/mol while the rich amine contains 0.484 mol CO_2/mol MEA. The pumparound cooler heat duty was predicted to be 23.2×10^6 kJ/h. A comparable once-through flow scheme would require 80 % more circulation of amine.

9.4 Multiple-Column Split-Flow DEA System

In this example, the flowsheeting capability of the **AMSIM** program is demonstrated by simulating the performance of the gas conditioning facilities of a western Canadian natural gas processing plant. The flowsheet configuration shown in Figure 23 involves high and medium pressure contactors which treat gas from inlet separators and operate in parallel, receiving amine solution from a common

regenerator. The medium-pressure contactor treats a very sour gas stream and employs the split-flow option. Rich amine from the two contactors is mixed and fed to a flash tank prior to flowing through the heat exchanger train. The rich amine is stripped in the regenerator to produce lean and semi-lean amine streams which are recycled back to the contactors.

The 10-foot internal-diameter high-pressure (HP) contactor contains 20 bubble-cap trays with outlet weir dimensions of 3 inches by 95 inches. The top tray operates at 913 psia and there is a 3.0 psi pressure drop across the column. The 9-foot internal-diameter medium-pressure (MP) contactor contains 16 bubble-cap trays with outlet weir dimensions of 3 inches by 88 inches. The top tray operates at 230 psia and there is a 6.0 psi pressure drop across the column. Semi-lean amine is fed to tray 8 in the MP contactor.

The composition and condition of the two gas streams are given in Table 13. A 33 wt % DEA solution is used in this plant. Sufficient air cooling capacity is available to cool the lean and semi-lean amine streams to 113°F before being fed to the contactors. Lean amine is introduced to the HP contactor at a rate of 1535 US gal/min and 717 US gal/min are directed to the MP contactor. Semi-lean amine is fed to the MP contactor at a rate of 625 US gal/min. The combined rich amine is sent to the flash tank which operates

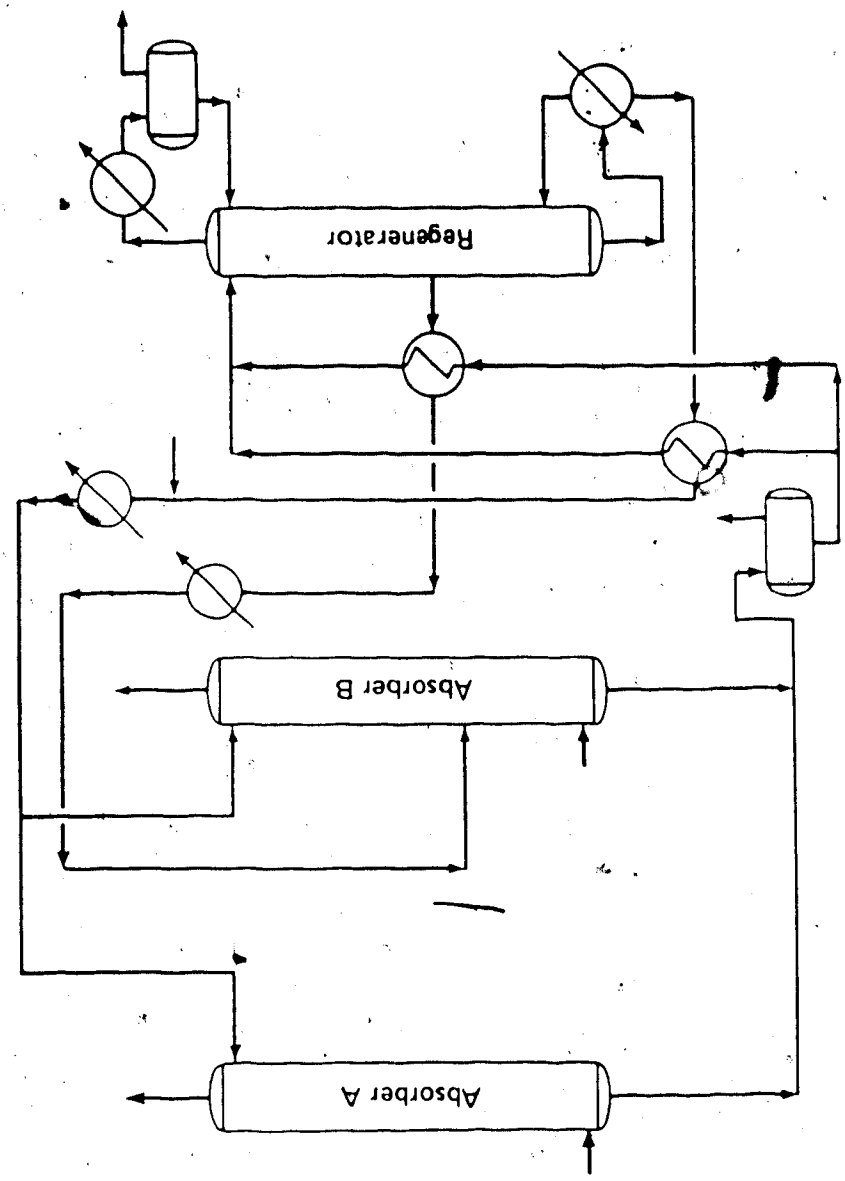

Figure 23. Process Configuration for Example 9.4

Table 13.

Gas Feed Compositions in Example 9.4

Component	HP Gas (lbmol/h)	MP Gas (lbmol/h)
H_2S	1410	1330
CO_2	395	91
H_2O	10	10
C_1	7140	763
C_2	1355	572
C_3	678	565
i-C_4	89	110
n-C_4	166	236
n-C_5	56	72
n-C_6	15	3
n-C_7	20	5
N_2	131	3
Total	11465	3760
Pressure (psia)	930	246
Temperature (°F)	105	106

at 80 psia. The liquid/liquid cross exchangers are specified to run with a 40°F minimum temperature approach. Vaporization losses of DEA and water are made up by injecting these components into the lean amine upstream of the lean amine cooler.

The regenerator contains 19 stages, a condenser and a reboiler. The overhead reflux accumulator operates at 25 psia and 118°F. The top tray pressure is 28 psia and there is a 5.3 psia pressure drop across the column. The reboiler supplies 172 MMBTU/h to the stripping column. Rich amine is fed to the third tray in the column and semi-lean amine is drawn from the 14th tray. A kinetic model to simulate the rate of desorption was not developed in this study, therefore the regenerator was assumed to operate with a H_2S stage efficiency of 80 % and with a CO_2 stage efficiency of 15 %. Experience has shown that when these values are used, the model adequately represents the performance of industrial amine regenerators.

The results of the simulation are summarized in Tables 14 to 16. Although no industrial performance test data are available to evaluate the simulator predictions for this plant, the potential capabilities of the program are demonstrated by this complex example.

Table 14.

Predicted HP and MP Residue Gases in Example 9.4

Component	HP Residue Gas (lbmol/h)	MP Residue Gas (lbmol/h)
H_2S	0.010	0.043
CO_2	0.004	0.100
H_2O	17.693	13.789
C_1	7118.105	760.935
C_2	1351.033	570.516
C_3	676.393	563.798
i-C_4	88.976	109.977
n-C_4	165.955	235.950
n-C_5	55.978	71.978
n-C_6	14.993	2.999
n-C_7	19.989	4.998
N_2	130.790	2.996
Total	9639.921	2338.079
Pressure (psia)	913	230
Temperature (°F)	113.0	113.0

Table 15.

Predicted Flash and Acid Gases in Example 9.4

Component	Flash Gas (lbmol/h)	Acid Gas (lbmol/h)
H_2S	14.205	2728.742
CO_2	2.315	483.581
H_2O	2.957	221.480
C_1	21.612	2.948
C_2	4.938	0.513
C_3	2.589	0.220
$i-C_4$	0.047	0
$n-C_4$	0.094	0.001
$n-C_5$	0.043	0.001
$n-C_6$	0.008	0
$n-C_7$	0.013	0
N_2	0.202	0.012
Total	49.023	3433.898
Pressure (psia)	80	25
Temperature (°F)	163.04	118.0

Table 16.

Additional Calculated Stream Properties in Example 9.4

Property	HP Contactor	MP Contactor
Lean Amine		
H_2S residual (mol/mol)	0.008	0.008
CO_2 residual (mol/mol)	0.005	0.005
Semi-Lean Amine		
H_2S residual (mol/mol)	-	0.019
CO_2 residual (mol/mol)	-	0.015
H_2S Stage Efficiency (%)	95.8	93.5
CO_2 Stage Efficiency (%)	44.1-51.1	33.6-38.6
Rich Amine		
H_2S loading (mol/mol)	0.573	0.666
CO_2 loading (mol/mol)	0.163	0.062
Temperature (°F)	167.97	157.88

	Regenerator
Reflux Ratio (L_1/V_1)	0.669
Condenser Duty (MMBTU/h)	46.669

9.5 Low-Pressure MDEA Contactor

In this final example, the **AMSIM** program was used to predict the performance of MDEA when used in a low-pressure contactor. Harbison and Handwerk (1987) recently presented detailed data for a gas plant operated by Marathon Oil in northern Wyoming. The amine plant was designed to selectively remove H_2S from a gas stream available at 134 psia using 30 wt % MDEA. The plant was inadvertently run with an amine blend containing 21.8 wt % MDEA and 4.2 wt % DEA in water. Therefore, only a qualitative comparison between program predictions and measured data was possible since the **AMSIM** program was not capable of modelling the equilibrium and kinetic properties of amine blends.

The 10-stage contactor has an internal diameter of 36 inches and outlet weir dimensions of 2 inches by 28.5 inches. The active tray area accounts for 72.6 % of the total cross-sectional area of the column. Lean amine residual loadings were measured at 0.004 mol H_2S/mol amine and 0.02 mol CO_2/mol amine. The measured and predicted gas compositions are given in Table 17.

In this example, the predicted H_2S stage efficiency was about 85.5 % while the CO_2 stage efficiency ranged from 2.76 to 3.06 %. The interfacial surface area was estimated to be approximately 280 m^2/m^3. The predicted H_2S content of 33 ppmv is lower than the measured 217 ppm. This discrepancy

Table 17.

Measured and Predicted Gas Compositions in Example 9.5

Component	Measured Contactor Feed Gas (lbmol/h)	Uncorrected Contactor Residue Gas (lbmol/h)	Predicted Contactor Residue Gas (lbmol/h)
H_2S	13.54	0.13	0.02
CO_2	125.12	86.24	93.95
C_1	383.77	380.67	383.57
C_2	55.72	56.79	55.69
C_3	32.18	31.53	32.16
$i\text{-}C_4$	7.58	7.94	7.58
$n\text{-}C_4$	13.67	14.44	13.67
C_5's	9.12	10.05	9.12
C_6	3.49	3.98	3.49
N_2	7.46	7.81	7.46
Total	651.65	599.58	606.71
Temp. (°F)	94	125	120.2

may be due to an overestimation of the value of k_g when the generalized correlation given by Equation (193) is used. Despite the disagreement in the H_2S content, the predicted CO_2 slippage of 75 % is in accordance with the measured 69 % value.

10. DISCUSSION OF MODELLING RESULTS

The original objectives of the work set out in Chapters 6 to 8 included the design and implementation of a new nonequilibrium multistage model for analyzing the performance of amine treating units. The problems presented in Chapter 9 were real-life examples and they demonstrate the potential of the **AMSIM** program to be a valuable engineering tool. In combination with the experimental results of Chapters 4 and 5, the nonequilibrium stage model is capable of simulating the performance of amine units which are governed by reaction kinetics and mass-transfer considerations. It may therefore be stated that the overall objectives were successfully realized.

The use of the component stage efficiency concept in the multistage model has been shown in Chapter 9 to be capable of reproducing existing plant data and may be used to predict the operation of new facilities. The component stage efficiency is known to be a complex function of pressure, temperature, phase compositions, flow rates, physical properties, kinetic and mass-transfer parameters, chemical equilibrium considerations and mechanical tray design and dimensions. Nevertheless, the fundamental model developed in Chapter 7 predicts efficiencies for H_2S and CO_2 absorption that are in accordance with those values required to match the observed performance of amine contactors in selective absorption applications.

An intangible advantage of the Murphree-type efficiency approach is the knowledge that η is constrained to the region in and near the interval from 0.0 to 1.0. In contrast, the vaporization efficiency ranges from 1.0 to ∞ for contactors and from 0.0 to 1.0 for regenerators. This open range makes it difficult to establish guideline efficiencies.

Efficiencies are related to the rate of reaction in the liquid phase. Hydrogen sulphide generally reacts in the instantaneous reaction regime for all alkanolamines; therefore, the predicted H_2S stage efficiencies (η) are similar for MEA, DEA and MDEA solutions. Carbon dioxide, on the other hand, usually reacts in the fast reaction regime. Consequently the rate of absorption is related to the rate of chemical reaction in the liquid. In general, the predicted CO_2 stage efficiency decreases in the following order

$$\eta_{MEA} > \eta_{DEA} > \eta_{MDEA} \qquad (235)$$

according to the value of k_2, the second-order reaction rate constant. The physical significance of the stage efficiency aids in understanding the mass transfer processes that occur on the stage.

The approach to calculate the component stage efficiency developed in this work is relatively simple and there is scope for future improvement. For example, it was

assumed that the liquid on the tray was well mixed and that the vapor passed through the stage in plug flow. Further studies should be undertaken to introduce a liquid mixing model to quantify the effect of backmixing on absorption rates. This would lead to a stage model that would account for composition gradients in the liquid as it passed over the tray.

The calculated component stage efficiencies were affected by the predicted values for mass-transfer coefficients and interfacial surface areas. These quantities were obtained from empirical correlations and thereby introduced uncertainties into the model predictions. No comparison studies were performed in this work to identify differences between correlations. Additional work will be required in the future to properly evaluate the "best" correlation for a given problem type. The structure of the **AMSIM** program makes this relatively simple as side-by-side comparisons of simulation runs using different correlations can be made easily.

The majority of applications of this model will be cases that involve the simultaneous absorption of H_2S and CO_2. The simple mass-transfer model used to estimate local enhancement factors was adequate for evaluation purposes, but a more complex and rigorous model would provide a better indication of the dynamic interaction between the acid gases and alkanolamine during the simultaneous absorption process

in the liquid film. Both H_2S and CO_2 compete for alkanolamine as a reactant.

The expressions given by Equations (219) and (221) used to calculate the CO_2 stage efficiency require estimates for the concentration of OH^- ion and free amine in the liquid film at the gas-liquid interface. There are similar requirements when calculating the H_2S enhancement factor. Thermodynamically - based vapor-liquid equilibrium models such as those discussed by Deshmukh and Mather (1977), Dingman et al.(1983), Chakravarty (1985), Gautam and Wareck (1986), and Vickery and Weiland (1986) offer a rigorous description of the concentration of liquid-phase ionic and molecular species. It would be of interest to combine the Deshmukh-Mather model with a simultaneous absorption rate model to predict the amounts of H_2S and CO_2 that would be absorbed from the gas passing through the liquid dispersion on the tray. The acidic film effect described by Yu and Astarita (1987a) should also be considered. The physico-chemical properties of the liquid film are affected by the presence of absorbed acid gases which tend to reduce the pH of the liquid film.

It is important to note that the model developed in Chapter 7 is capable of reproducing the temperature profiles that are measured in industrial contactors and regenerators. The temperature profile in a contactor is affected by the relative mass flow rates of gas and liquid, the amount of

chemical reaction that occurs on each tray, and by the water saturation of the sour feed gas. Water evaporation and condensation represents a significant heat effect on the bottom few stages in a contactor and can dramatically change the simulated profile if the feed gas water saturation is neglected, particularly at low pressures. All of the feed gases in the examples in Chapter 9 contain water.

The methodology established to obtain a convergent solution to the multistage model equations proved to be very efficient. Absorber and regenerator simulations generally converge in less than 10 column iterations. The procedure was insensitive to initial assumptions and nonconvergence was usually an indication of unrealistic input data rather than a limitation of the method. Future work should focus on calculating the component stage efficiencies as a stage variable in the solution procedure rather than using a decoupled outer loop.

The direct-substitution method of converging the plant flowsheet was found to be sufficient. The nonlinearities in the system acted to destabilize the Wegstein method and cause it to fail. The composition of the lean amine leaving the reboiler is relatively unaffected by small composition changes in the rich amine; therefore, most simulation runs converge in fewer than four flowsheet iterations. Of course, better initial estimates of the tear stream compositions will result in fewer flowsheet iterations.

11. CONCLUSIONS

A single sphere absorber apparatus has been constructed to measure the absorption kinetics of CO_2 in potential gas treating solvents. The equipment has been used to determine the rates of absorption of N_2O and CO_2 in MDEA solutions of industrial interest. The diffusion coefficient of N_2O in MDEA solutions and the second-order rate constant for the reaction between CO_2 and MDEA were obtained from an analysis of the physical absorption and chemical absorption studies respectively.

New data are provided for the second-order reaction rate constant at temperatures ranging from 25° to 75°C and for MDEA concentrations of 20 wt % and 40 wt % in water. The activation energy of the reaction was determined to be 42.7 kJ/mol. The experimental data suggest that MDEA acts as a base catalyst in the CO_2 hydrolysis reaction. The results of this study extend the data of Yu (1985), Versteeg et al.(1986) and Bidarian and Sandall (1986) to higher temperatures and MDEA concentrations. These data are required to predict the rate of absorption of CO_2 in MDEA solutions and to estimate the CO_2 stage efficiency in industrial trayed contactors.

This work also provides new data for the solubility and diffusivity of N_2O in MDEA solutions at temperatures ranging from 25° to 75°C and for MDEA concentrations of 20 wt % and 40 wt % in water. The results extend the work of Haimour

higher MDEA concentration. These data are required when the "N_2O Analogy" is used to interpret the results of corresponding rate measurements using CO_2.

The sphere absorber has been used to measure the effect of piperazine on the rate of absorption of CO_2 in a 40 wt % MDEA solution at 40°C. Experimental data are presented for piperazine concentrations ranging from 0 kmol/m³ to 0.4 kmol/m³. A threefold increase of the CO_2 absorption rate was observed when the MDEA solution contained 0.40 kmol/m³ piperazine. These data represent experimental confirmation of the claims in US Patent #4,336,233 that piperazine is an effective absorption rate-promoting additive that may be used in bulk CO_2 removal processes which employ aqueous MDEA. The mass-transfer rate promotion appears to follow the "shuttle" mechanism.

The single sphere absorber is a complex continuous-flow device that is very difficult to operate, but is capable of permitting accurate absorption rate measurements if proper attention is given to the control of experimental conditions. The diffusion coefficient and second-order rate constant were determined indirectly from experimental absorption rate data and therefore their accuracy depends on the careful control of experimental conditions and the accuracy of gas solubility, solution viscosity and density data. The occurrence of surface rippling was of primary

concern in the operation of the sphere absorber. Additional work is required to establish reliable criteria to estimate the maximum allowable liquid flow rate that will result in a ripple-free spherical film. Further development of the hydrodynamic model is required to include the effects of surface tension and temperature- and composition-dependent physical properties when calculating the solute gas concentration profile in the liquid film.

The results of this work have demonstrated the successful use of the sphere absorber to measure parameters needed to predict the rate of absorption of CO_2 in industrial contactors. Similar studies may be undertaken in the future to measure data for other potential gas treating solvents.

A steady-state nonequilibrium stage model has been developed to permit the rational design of amine contactors when kinetically-selective absorption of H_2S from gases containing CO_2 and H_2S occurs. The stage model incorporates a modified Murphree vapor efficiency which can be related to fundamental kinetic and mass-transfer parameters. The component tray efficiencies are strong functions of these parameters and operating variables such as gas-phase velocities and the interfacial area and dispersion height generated on a tray. The model conveniently makes it possible to evaluate the effect of these variables on contactor performance.

A new algorithm designed to obtain a solution to the multistage model equations was developed to handle the case when the component efficiency is included as a stage variable. Based on the approach of Ishii (1973), the procedure is characterized by rapid and reliable convergence and works well for both absorption and distillation-type problems.

The stage model and solution procedure were combined in a system of integrated programs called **AMSIM** to provide flowsheet simulation capabilities for purposes of engineering analysis and process design. The experimental results of Chapters 4 and 5 were used in the tray efficiency model for MDEA-based systems. Published data were used to supply the kinetic parameters for the other amines in the program. A modified Kent and Eisenberg (1976) model was used to predict the equilibrium solubility of acid gases in the alkanolamine solutions. The **AMSIM** program has been demonstrated to accurately predict the performance of amine treating units that use MEA, DEA, and MDEA solutions.

The program uses a hybrid fixed-flowsheet approach to simulation and solves recycle calculations using a direct substitution method. The sequential-modular simulator contains unit modules to handle the majority of gas conditioning flowsheets. Considerable attention was given to ensuring a high degree of reliability in all of the unit modules. The program contains a global data management

system to effectively move data to and from a work area when solving individual unit modules.

The **AMSIM** program has been developed for use both on mainframe and personal computers. The mainframe program includes an easily understood free-format command file preprocessor which simplifies the organization of input data. The PC version is completely interactive and provides identical capability to the mainframe program without the CPU charges. The **AMSIM** program generates concise technical summary reports of calculated results. The ease of use reduces the engineering time and effort spent on the design of alkanolamine treating units. This allows the designer to investigate complex alternative flow schemes and to arrive at an optimum process design.

The results of this work will provide industry with the technology required to design new facilities which use conventional or selective solvents to treat gas streams containing H_2S and CO_2. In parallel, the **AMSIM** program will provide a reliable methodology to simulate the performance of existing processing equipment for purposes of retrofit modifications.

LITERATURE CITED

1. Akita, K. and F. Yoshida, "Bubble Size, Interfacial Area, and Liquid-Phase Mass Transfer Coefficient in Bubble Columns", *Ind. Eng. Chem. Process Des. Dev.*, 13, 84-91(1974).

2. Alvarez-Fuster, C., N. Midoux, A. Laurent and J.C. Charpentier, "Chemical Kinetics of the Reaction of Carbon Dioxide with Amines in Pseudo m-nth Order Conditions in Aqueous and Organic Solutions", *Chem. Eng. Sci.*, 35, 1717-1723(1980).

3. Alvarez-Fuster, C., N. Midoux, A. Laurent and J.C. Charpentier, "Chemical Kinetics of the Reaction of Carbon Dioxide with Amines in Pseudo m-nth Order Conditions in Polar and Viscous Organic Solutions", *Chem. Eng. Sci.*, 36, 1513-1518(1981).

4. American Petroleum Institute, "Technical Data Book - Petroleum Refining", 2nd Ed., Washington, D.C., 1970.

5. Ammons, H.L. and D.M. Sitton, "Operating Data from a Commercial MDEA Gas Treater", Proceedings of the 31st Annual Gas Conditioning Conference, Norman, Oklahoma, March 2-4, 1981, A1-A11.

6. Appl, M., U. Wagner, H.J. Henrici, K. Kuessner, K. Volkamer and E. Fuerst, "Removal of CO_2 and/or H_2S and/or COS from Gases Containing these Constituents", US Patent #4,336,233, 1982.

7. Arnold, D.S., D.A. Barrett and R.H. Isom, "CO_2 Production from Coal-Fired Boiler Flue Gas by MEA Process", Proceedings of the 32nd Annual Gas Conditioning Conference, Norman, Oklahoma, March 8-10, 1982, A1-A27.

8. Astarita, G., "Mass Transfer with Chemical Reaction", Elsevier Publishing Company, New York, 1967.

9. Astarita, G., D.W. Savage and J.M. Longo, "Promotion of CO_2 Mass Transfer in Carbonate Solutions", *Chem. Eng. Sci.*, 36, 581-588(1981).

10. Astarita, G., D.W. Savage and J.M. Longo, "Promotion of CO_2 Mass Transfer in Carbonate Solutions", *Chem. Eng. Sci.*, 37, 1593(1982).

11. Astarita, G., D.W. Savage and A. Bisio, "Gas Treating with Chemical Solvents", John Wiley and Sons, New

York, 1983.

12. Atwood, K., M.R. Arnold, and R.C. Kindrick, "Equilibria for the System, Ethanolamines - Hydrogen Sulfide - Water", *Ind. Eng. Chem.*, **49**, 1439-1444(1957).

13. Azarnoosh, A. and J.J. McKetta, "The Solubility of Propane in Water", *Pet. Refiner*, **37**, No. 11, 275-278(1958).

14. Barth, D., C. Tondre, G. Lappai and J.-J. Delpuech, "Kinetic Study of Carbon Dioxide Reaction with Tertiary Amines in Aqueous Solutions", *J. Phys. Chem.*, **85**, 3660-3667(1981).

15. Barth, D., C. Tondre and J.-J. Delpuech, "Stopped-Flow Determination of Carbon Dioxide-Diethanolamine Reaction Mechanism : Kinetics of Carbamate Formation", *Int. J. Chem. Kinet.*, **15**, 1147-1160(1983).

16. Barth, D., C. Tondre and J.-J. Delpuech, "Kinetics and Mechanisms of the Reactions of Carbon Dioxide with Alkanolamines : A Discussion Concerning the Cases of MDEA and DEA", *Chem. Eng. Sci.*, **39**, 1753-1757(1984).

17. Bidarian, A. and O.C. Sandall, "Selective Absorption of H_2S from CO_2 Using MDEA in a Packed Column", Paper 103b, Presented at the AIChE Annual Meeting, Miami Beach, Florida, Nov. 2-7, 1986.

18. Billingsley, D.S., "A Simplified Form of Holland's Equations in the Solution of Multicolumn Distillation Systems", *Can. J. Chem. Eng.*, **49**, 672-676(1971).

19. Bird, R.B., W.E. Stewart and E.N. Lightfoot, "Transport Phenomena", John Wiley and Sons, New York, 1960.

20. Blanc, C. and G. Demarais, "Vitesses de la Réaction du CO_2 Avec la Diétnanolamine", *Entropie*, **17**(102), 53-61(1981).

21. Blanc, C., J. Elgue and F. Lallemand, "MDEA Process Selects H_2S", *Hydrocarbon Processing*, **60**, No.8, 111-116(1981).

22. Blauwhoff, P.M.M., G.F. Versteeg and W.P.M. Van Swaaij, "A Study on the Reaction Between CO_2 and Alkanolamines in Aqueous Solutions", *Chem. Eng. Sci.*, **38**, 1411-1429(1983).

23. Blauwhoff, P.M.M., B. Kamphuis, W.P.M. Van Swaaij and K.R. Westerterp, "Absorber Design in Sour Natural Gas Treatment Plants : Impact of Process Variables on Operation and Economics", *Chem. Eng. Process.*, 19, 1-25(1985).

24. Blauwhoff, P.M.M. and W.P.M. Van Swaaij, "Simultaneous Mass Transfer of H_2S and CO_2 with Complex Chemical Reactions in an Aqueous Di-isopropanolamine Solution", *Chem. Eng. Process.*, 19, 67-83(1985).

25. Bourne, J.R., U. von Stockar and G.C. Coggan, "Gas Absorption with Heat Effects. I. A New Computational Method", *Ind. Eng. Chem.*, 13, 115-123(1974).

26. Bibson, C.M. and J.A. Bullin, "Measurement of Carbon Dioxide-MDEA Reaction Rates", Paper 123f, Presented at the AIChE Annual Meeting, Miami Beach, Florida, Nov. 2-7, 1986.

27. Browne, D.W., "Modelling of Amine Units and Multicolumn Systems", M.Sc. Thesis, University of Alberta, 1976.

28. Browne, D.W., Y. Ishii and F.D. Otto, "Solving Multicolumn Equilibrium Stage Operations by Total Linearization", *Can. J. Chem. Eng.*, 55, 307-312(1977).

29. Bucklin, R.W. and K.W. Won, "HIGEE Contactors for Selective H_2S Removal and Superdehydration", Proceedings of the 37th Annual Laurance Reid Gas Conditioning Conference, Norman, Oklahoma, March 2-4, 1987, D1-D16.

30. Bullin, J.A., J.C. Polasek and J.W. Holmes, "Optimization of New and Existing Amine Gas Sweetening Plants by Computer Simulation", Proceedings of the 60th Annual GPA Convention, San Antonio, Texas, March 23-25, 142-148(1981).

31. Bullin, J.A. and J.C. Polasek, "Selective Absorption Using Amines", Proceedings of the 61st Annual GPA Convention, Dallas, Texas, March 15-17, 86-90(1982).

32. Butwell, K.F., D.J. Kubek, and P.W. Sigmund, "Alkanolamine Treating", *Hydrocarbon Processing*, 61, No.3, 108-116(1982).

33. Calderbank, P.H., "Physical Rate Processes in Industrial Fermentation. Part II. - Mass Transfer Coefficients in Gas-Liquid Contacting With and Without Mechanical Agitation", *Trans. Instn. Chem. Engrs.*, 37,

173-185(1959).

34. Chakma, A. and A. Meisen, "MDEA Degradation with CO_2", Presented at the 35th Canadian Chemical Engineering Conference, Calgary, Alberta, October 6-9, 1985.

35. Chakraborty, A.K., G. Astarita and K.B. Bischoff, "CO_2 Absorption in Aqueous Solutions of Hindered Amines", *Chem. Eng. Sci.*, 41, 997-1003(1986).

36. Chakravarty, T., "Solubility Calculations for Acid Gases in Amine Blends", Ph.D. Thesis, Clarkson University, 1985.

37. Chakravarty, T., U.K. Phukan and R.H. Weiland, "Reaction of Acid Gases with Mixtures of Amines", *Chem. Eng. Prog.*, 81, No.4, 32-36(1985).

38. Charpentier, J.C., "What's New in Absorption with Chemical Reaction ?", *Trans. Inst. Chem. Eng.*, 60, 131-156(1982).

39. Chludzinski, G.R., "Recent Commercial Tests of FLEXSORB™ PS Solvent", Presented at the Houston Regional GPA Meeting, Houston, Texas, November 7, 1985.

40. Chludzinski, G.R., "Process Selection Criteria for Gas Treating", Presented at the New Orleans Regional GPA Meeting, New Orleans, Louisiana, January 16, 1986.

41. Clarke, J.K.A., "Kinetics of Absorption of Carbon Dioxide in Monoethanolamine Solutions at Short Contact Times", *Ind. Eng. Chem. Fund.*, 3, 239-245(1964).

42. Clarke, W.M., "Simultaneous Modular Convergence for Sequential Modular Simulators", Paper 50a, Presented at the AIChE Spring National Meeting, New Orleans, Louisiana, April 6-10, 1986.

43. Critchfield, J. and G.T. Rochelle, "CO_2 Absorption into Aqueous MDEA and MDEA/MEA Solutions", Paper 43e, Presented at the AIChE National Meeting, Houston, Texas, March 29 - April 2, 1987.

44. Crowe, C.M., "On a Relationship Between Quasi-Newton and Dominant Eigenvalue Methods for the Numerical Solution of Non-Linear Equations", *Comput. Chem. Eng.*, 8, 35-41(1984).

45. Cullen, E.J. and J.F. Davidson, "Absorption of Gases in

Liquid Jets", *Trans. Farad. Soc.*, 53, 113-120(1957).

46. Danckwerts, P.V., "Gas-Liquid Reactions", McGraw-Hill Book Company, New York, 1970.

47. Danckwerts, P.V., "The Reaction of CO_2 with Ethanolamines", *Chem. Eng. Sci.*, 34, 443-446(1979).

48. Danckwerts, P.V. and M.M. Sharma, "The Absorption of Carbon Dioxide into Solutions of Alkalis and Amines (With some Notes on Hydrogen Sulphide and Carbonyl Sulphide)", *The Chemical Engineer*, No.202, October, CE244-CE279(1966).

49. Davidson, J.F. and E.J. Cullen, "The Determination of Diffusion Coefficients for Sparingly Soluble Gases in Liquids", *Trans. Instn. Chem. Engrs.*, 35, 51-60(1957).

50. Davidson, J.F., E.J. Cullen, D. Hanson and D. Roberts, "The Hold-up and Liquid Film Coefficient of Packed Towers. Part I : Behaviour of a String of Spheres", *Trans. Instn. Chem. Engrs.*, 37, 122-130(1959).

51. Daviet, G.R., R. Sundermann, S.T. Donnelly and J.A. Bullin, "Dome's North Caroline Plant Successful Conversion to MDEA", Proceedings of the 63rd Annual GPA Convention, New Orleans, Louisiana, March 19-21, 69-73(1984).

52. De Leye, L. and G.F. Froment, "Rigorous Simulation and Design of Columns for Gas Absorption and Chemical Reaction I. Packed Columns", *Comput. Chem. Eng.*, 10, 493-504(1986a).

53. De Leye, L. and G.F. Froment, "Rigorous Simulation and Design of Columns for Gas Absorption and Chemical Reaction II. Plate Columns", *Comput. Chem. Eng.*, 10, 505-515(1986b).

54. Deshmukh, R.D., and A.E. Mather, "A Mathematical Model for Equilibrium Solubility of Hydrogen Sulfide and Carbon Dioxide in Aqueous Alkanolamine Solutions", *Chem. Eng. Sci.*, 36, 355-362(1981).

55. Dingman, J.C., "How Acid Gas Loadings Affect Physical Properties of MEA Solution", *Pet. Refiner*, 42, No.9, 189-191(1963).

56. Dingman, J.C., J.L. Jackson, T.F. Moore and J.A. Branson, "Equilibrium Data for the H_2S-CO_2-Diglycolamine® Agent-Water System",

Proceedings of the 62nd Annual GPA Convention, San Francisco, California, March 14-16, 256-268(1983).

57. Donaldson, T.L. and Y.N. Nguyen, "Carbon Dioxide Reaction Kinetics and Transport in Aqueous Amine Membranes", *Ind. Eng. Chem. Fund.*, **19**, 260-266(1980).

58. Donnelly, S.T. and D.R. Henderson, "A New Approach to Amine Selection", Presented at the CNGPA Third Quarterly Meeting, Calgary, Alberta, September 13, 1974.

59. Dow Chemical Company, "Alkanolamines Handbook", Dow Chemical International, 1964.

60. Edwards, T.J., G. Maurer, J. Newman and J.M. Prausnitz, "Vapor-Liquid Equilibria in Multicomponent Aqueous Solutions of Volatile Weak Electrolytes", *A.I.Ch.E. J.*, **24**, 966-976(1978).

61. Fairley, R.E., "Software Engineering Concepts", McGraw-Hill Book Co., New York, 1985.

62. Flynn, A.J., C.B. Wallace, R.G. Christensen and W.T. Knowles, "Shell's Recent Improvements in Gas Treating and Claus Tail Gas Cleanup", Proceedings of the 60th Annual GPA Convention, San Antonio, Texas, March 23-25, 149-151(1981).

63. Ford, M.A., "The Simulation of Ore Dressing Plants", Ph.D. Thesis, University of Alberta, 1979.

64. Frazier, H.D. and A.L. Kohl, "Selective Absorption of Hydrogen Sulfide from Gas Streams", *Ind. Eng. Chem.*, **42**, 2288-2292(1950).

65. Froessling, N., "The Evaporation of Falling Drops", *Gerlands Beitr. z. Geophysik*, **52**, 170-216(1938).

66. Fukushima, S., K. Kusaka and S. Ishii, "Mass Transfer on Multi-Strings of Touching Spheres", *J. Chem. Eng. Japan*, **11**, 33-39(1978).

67. Gazzi, L., C. Rescalli and O. Sguera, "New Amine-Solvent Process for Selective Hydrogen Sulphide Removal", Paper 22b, Presented at the AIChE Spring National Meeting, New Orleans, Louisiana, April 6-10, 1986.

68. Gautam, R. and J.S. Wareck, "Computation of Physical and Chemical Equilibria - Alternate Specifications",

Comput. Chem. Eng., 10, 143-151(1986).

69. Gerhart, P.M. and R.J. Gross, "Fundamentals of Fluid Mechanics", Addison-Wesley, Toronto, 1965.

70. Giavarini, C., M. Moresi and E. Sebastiani, "Absorption of CO_2 in Aqueous Solutions : A Simple Experimental Apparatus for Absorption Measurements", *Ing. Chim. Ital.*, 16, 103-109(1980).

71. Giavarini, C. and M. Moresi, "Absorption of CO_2 into Aqueous Solutions of Neopentanolamine", *Ing. Chim. Ital.*, 18, No.3-4, 21-25(1982a).

72. Giavarini, C. and M. Moresi, "Development of a New Product for Carbon Dioxide Absorption", *Chimica e Industria (Milan)*, 64, 601-603(1982b).

73. Goar, B.G., "Sulfur Recovery from Natural Gas Involves Big Investment", *Oil and Gas J.*, 73, No.28, July 14, 78-85(1975).

74. Goar, B.G., "Selective Gas Treating Produces Better Claus Feeds", *Oil and Gas J.*, 78, No.18, May 5, 239-242(1980).

75. Goddin, C.S., "Comparison of Processes for Treating Gases with High CO_2 Content", Proceedings of the 61st Annual GPA Convention, Dallas, Texas, March 15-17, 60-68(1982).

76. Goel, R.K., R.J. Chen and D.G. Elliot, "Data Requirements in Gas and Liquid Treating", Proceedings of the 61st Annual GPA Convention, Dallas, Texas, March 15-17, 185-193(1982).

77. Goettler, L.A., "The Simultaneous Absorption of Two Gases in a Reactive Liquid", Ph.D. Thesis, University of Delaware, 1967.

78. Goettler, L.A. and R.L. Pigford, "Gas Absorption with Complex Chemical Reaction : The Simultaneous Absorption of Carbon Dioxide and Sulphur Dioxide into Aqueous Solutions of Sodium Hydroxide", Tripartite Chemical Engineering Conference, Symposium on Mass Transfer with Chemical Reaction, September 23, 5(1968).

79. Goldstein, A.M., "FLEXSORB™ SE Commercialization of a New Gas Treating Agent", Presented at the Dallas Regional GPA Meeting, Dallas, Texas, September, 1983.

80. Gyure, D.C. and W.B. Krantz, "Laminar Film Flow over a Sphere", *Ind. Eng. Chem. Fund.*, **22**, 405-410(1983).

81. Haimour, N. and O.C. Sandall, "Molecular Diffusivity of Hydrogen Sulfide in Water", *J. Chem. Eng. Data*, **29**, 20-22(1984).

82. Haimour, N. and O.C. Sandall, "Absorption of Carbon Dioxide into Aqueous Methyldiethanolamine", *Chem. Eng. Sci.*, **39**, 1791-1796(1984).

83. Harbison, J.L. and G.E. Handwerk, "Selective Removal of H_2S Utilizing Generic MDEA", Proceedings of the 37th Annual Laurance Reid Gas Conditioning Conference, Norman, Oklahoma, March 2-4, 1987, H1-H12.

84. Harclerode, H. and J.W. Gentry, "A General Matrix Method for the Steady State Solution of Complex Distillation Assemblies", *Can. J. Chem. Eng.*, **50**, 253-260(1972).

85. Hess, F.E., S.E. Gallun, G.W. Bentzen and C.D. Holland, "Calculational Procedures for Systems of Distillation Columns", Presented at the 83rd AIChE National Meeting, Houston, Texas, 1977.

86. Hikita, H., S. Asai, H. Ishikawa and M. Honda, "The Kinetics of Reactions of Carbon Dioxide with Monoethanolamine, Diethanolamine and Triethanolamine by a Rapid Mixing Method", *Chem. Eng. J.*, **13**, 7-12(1977).

87. Hikita, H., S. Asai, Y. Katsu and S. Ikuno, "Absorption of Carbon Dioxide into Aqueous Monoethanolamine Solutions", *A.I.Ch.E. J.*, **25**, 793-799(1979).

88. Hikita, H., H. Ishikawa, K. Uku and T. Murakami, "Diffusivities of Mono-, Di-, and Triethanolamines in Aqueous Solutions", *J. Chem. Eng. Data*, **25**, 324-325(1980).

89. Hofeling, B.S. and J.D. Seader, "A Modified Naphtali-Sandholm Method for General Systems of Interlinked, Multistaged Separators", *A.I.Ch.E. J.*, **24**, 1131-1134(1978).

90. Holland, C.D., "Fundamentals of Multicomponent Distillation", McGraw-Hill Book Company, New York, 1981.

91. Holmes, J.W., M.L. Spears, and J.A. Bullin, "Sweetening LPG's with Amines", *Chem. Eng. Prog.*, **80**, No.5, 47-50(1984).

92. Isaacs, E.E., F.D. Otto and A.E. Mather, "Solubility of Mixtures of H_2S and CO_2 in a Monoethanolamine Solution at Low Partial Pressures", *J. Chem. Eng. Data*, **25**, 118-120(1980).

93. Ishii, Y., "A New Method for Multistage Multicomponent Separation Calculations", M.Sc. Thesis, University of Alberta, 1973.

94. Ishii, Y., and F.D. Otto, "A General Algorithm for Multistage Multicomponent Separation Calculations", *Can. J. Chem. Eng.*, **51**, 601-605(1973).

95. Jelínek, J., V. Hlaváček and Z. Křivský, "Calculation of Countercurrent Separation Processes - III. Computation of Two Interlinked Columns", *Chem. Eng. Sci.*, **28**, 1833-1838(1973).

96. Jørgensen, E. and C. Faurholt, "Reactions Between Carbon Dioxide and Amino Alcohols", *Acta Chem. Scand.*, **8**, 1141-1144(1954).

97. Joshi, S.V., "Mass Transfer Processes Coupled with Kinetic Phenomena", Ph.D. Thesis, University of Delaware, 1980.

98. Jou, F.-Y., A.E. Mather and F.D. Otto, "Solubility of H_2S and CO_2 in Aqueous Methyldiethanolamine Solutions", *Ind. Eng. Chem. Process Des. Dev.*, **21**, 539-544(1982).

99. Jou, F.-Y., F.D. Otto and A.E. Mather, "Solubility of H_2S and CO_2 in Triethanolamine Solutions", Presented at the AIChE Winter National Meeting, Atlanta, Georgia, March 11-14, 1984.

100. Jou, F.-Y., F.D. Otto and A.E. Mather, "Solubility of N_2O in Methyldiethanolamine Solutions", Presented at the 9th IUPAC Conference on Chemical Thermodynamics, Lisbon, Portugal, July 14-18, 1986.

101. Jou, F.-Y., F.D. Otto and A.E. Mather, "Solubility of Mixtures of H_2S and CO_2 in a Methyldiethanolamine Solution", Paper 140b, Presented at the AIChE Annual Meeting, Miami Beach, Florida, Nov. 2-7, 1986.

102. Kahrim, A., and A.E. Mather, "Enthalpy of Solution of Acid Gases in DEA Solutions", Presented at the 69th

AIChE Annual Meeting, Chicago, Illinois, Nov. 28 - Dec. 2, 1976.

103. Kalra, H., R.G. Moore and F.D. Otto, "The Diffusivity of Hydrogen in Liquid Aminomethane", *Can. J. Chem. Eng.*, 50, 515-519(1972).

104. Kalra, H., "Isotopic Exchange and Diffusivity of Hydrogen in the Hydrogen-Aminomethane System", Ph.D. Thesis, University of Alberta, 1973.

105. Kalra, H. and F.D. Otto, "Rates of Isotopic Exchange Between Hydrogen and Aminomethane Catalyzed by Potassium Methylamide", *Can. J. Chem. Eng.*, 52, 258-262(1974).

106. Katti, S.S., and B.D. Langfitt, "Development of a Simulator for Commercial Absorbers used for Selective Chemical Absorption Based on a Mass Transfer Rate Approach", Proceedings of the 65th Annual GPA Convention, San Antonio, Texas, March 10-12, 158-163(1986).

107. Katti, S.S. and K.A. McDougal, "Rate Approach in the Design and Simulation of Chemical Absorbers : Theory and Practice", Paper 140d, Presented at the AIChE Annual Meeting, Miami Beach, Florida, Nov. 2-7, 1986.

108. Katz, D.L., D. Cornell, R. Kobayashi, F.H. Poettmann, J.A. Vary, J.R. Elenbaas and C.F. Weinaug, "Handbook of Natural Gas Engineering", McGraw-Hill, New York, 1959.

109. Kent, R.L., and B. Eisenberg, "Better Data for Amine Treating", *Hydrocarbon Processing*, 55, No.2, 87-90(1976).

110. Khalil, N., "Simultaneous Absorption of H_2S and CO_2 in Aqueous MDEA", Ph.D. Thesis, University of California, Santa Barbara, 1984.

111. Kim, C.J. and D.W. Savage, "Kinetics of the Carbon Dioxide Reaction with Diethylaminoethanol", Paper 123g, Presented at the AIChE Annual Meeting, Miami Beach, Florida, Nov. 2-7, 1986.

112. Kisala, T.P., J.F. Boston, H.I. Britt, and L.B. Evans, "Successive Quadratic Programming in Sequential Modular Process Optimization", Paper 50b, Presented at the AIChE Spring National Meeting, New Orleans, Louisiana, April 6-10, 1986.

113. Kliesch, H.C., Ph.D. Thesis, Tulane University, 1967.

114. Kobayashi, R. and D.L. Katz, "Vapor-Liquid Equilibria for Binary Hydrocarbon-Water Systems", *Ind. Eng. Chem.*, **45**, 440-451(1953).

115. Kohl, A.L. and F.C. Riesenfeld, "Gas Purification", 4th ed., Gulf Publishing Co., Houston, 1985.

116. Krishnamurthy, R. and R. Taylor, "Application of a Nonequilibrium Stage Model to Absorber Design", Presented at the 34th Canadian Chemical Engineering Conference, Quebec City, Quebec, September, 1984.

117. Krishnamurthy, R. and R. Taylor, "A Nonequilibrium Stage Model of Multicomponent Separation Processes : I. Model Description and Method of Solution", *A.I.Ch.E. J.*, **31**, 449-456(1985a).

118. Krishnamurthy, R. and R. Taylor, "A Nonequilibrium Stage Model of Multicomponent Separation Processes : II. Comparison With Experiment", *A.I.Ch.E. J.*, **31**, 456-465(1985b).

119. Krishnamurthy, R. and R. Taylor, "A Nonequilibrium Stage Model of Multicomponent Separation Processes : III. The Influence of Unequal Component Efficiencies in Process Design Problems", *A.I.Ch.E. J.*, **31**, 1973-1985(1985c).

120. Krishnamurthy, R. and R. Taylor, "Simulation of Packed Distillation and Absorption Columns", *Ind. Eng. Chem. Process Des. Dev.*, **24**, 513-524(1985d).

121. Krishnamurthy, R. and R. Taylor, "Absorber Simulation and Design Using a Nonequilibrium Stage Model", *Can. J. Chem. Eng.*, **64**, 96-105(1986).

122. Kubíček, V. Hlaváček and F. Procháska, "Global Modular Newton-Raphson Technique for Simulation of an Interconnected Plant Applied to Complex Rectification Columns", *Chem. Eng. Sci.*, **31**, 277-284(1976).

123. Laddha, S.S., J.M. Diaz and P.V. Danckwerts, "The N_2O Analogy : The Solubilities of CO_2 and N_2O in Aqueous Solutions of Organic Compounds", *Chem. Eng. Sci.*, **36**, 228-229(1981).

124. Laddha, S.S. and P.V. Danckwerts, "Reaction of CO_2 with

Ethanolamines : Kinetics from Gas-Absorption", *Chem. Eng. Sci.*, 36, 479-482(1981).

125. Laddha, S.S. and P.V. Danckwerts, "Reaction of CO_2 with Diethanolamine at 11°C", *Chem. Eng. Sci.*, 37, 475(1982).

126. Lal, D., E.E. Isaacs, A.E. Mather, and F.D. Otto, "Equilibrium Solubility of Acid Gases in Diethanolamine and Monoethanolamine Solutions at Low Partial Pressures", Proceedings of the 30th Annual Gas Conditioning Conference, Norman, Oklahoma, March 3-5, 1980, I1-I18.

127. Landau, J., J. Boyle, H.G. Gomaa and A.M. Al Taweel, "Comparison of Methods for Measuring Interfacial Areas in Gas-Liquid Dispersions", *Can. J. Chem. Eng.*, 55, 13-18(1977).

128. Lawson, J.D., and A.W. Garst, "Gas Sweetening Data : Equilibrium Solubility of Hydrogen Sulfide and Carbon Dioxide in Aqueous Monoethanolamine and Aqueous Diethanolamine Solutions", *J. Chem. Eng. Data*, 21, 20-30(1976).

129. Lawson, J.D., and A.W. Garst, "Hydrocarbon Gas Solubility in Sweetening Solutions : Methane and Ethane in Aqueous Monoethanolamine and Diethanolamine", *J. Chem. Eng. Data*, 21, 30-32(1976).

130. Lee, J.I., F.D. Otto, and A.E. Mather, "Solubility of Carbon Dioxide in Aqueous Diethanolamine Solutions at High Pressures", *J. Chem. Eng. Data*, 17, 465-468(1972).

131. Lee, J.I., F.D. Otto, and A.E. Mather, "Solubility of Hydrogen Sulfide in Aqueous Diethanolamine Solutions at High Pressures", *J. Chem. Eng. Data*, 18, 71-73(1973a).

132. Lee, J.I., F.D. Otto, and A.E. Mather, "Partial Pressures of Hydrogen Sulfide over Aqueous Diethanolamine Solutions", *J. Chem. Eng. Data*, 18, 420(1973b).

133. Lee, J.I., F.D. Otto, and A.E. Mather, "The Solubility of Mixtures of Carbon Dioxide and Hydrogen Sulphide in Aqueous Diethanolamine Solutions", *Can. J. Chem. Eng.*, 52, 125-127(1974a).

134. Lee, J.I., F.D. Otto and A.E. Mather, "The Solubility of H_2S and CO_2 in Aqueous Monoethanolamine

Solutions", *Can. J. Chem. Eng.*, **52**, 803-805(1974b).

135. Lee, J.I., F.D. Otto and A.E. Mather, "Solubility of Mixtures of Carbon Dioxide and Hydrogen Sulfide in 5.0 N Monoethanolamine Solution", *J. Chem. Eng. Data*, **20**, 161-163(1975).

136. Lee, J.I., F.D. Otto and A.E. Mather, "Equilibrium in Hydrogen Sulfide - Monoethanolamine - Water System", *J. Chem. Eng. Data*, **21**, 207-208(1976a).

137. Lee, J.I., F.D. Otto and A.E. Mather, "The Measurement and Prediction of the Solubility of Mixtures of Carbon Dioxide and Hydrogen Sulphide in a 2.5 N Monoethanolamine Solution", *Can. J. Chem. Eng.*, **54**, 214-219(1976b).

138. Lee, J.I., F.D. Otto and A.E. Mather, "Equilibrium Between Carbon Dioxide and Aqueous Monoethanolamine Solutions", *J. Appl. Chem. Biotechnol.*, **26**, 541-549(1976c).

139. Lee, J.I. and A.E. Mather, "Solubility of Hydrogen Sulfide in Water", *Ber. Bunsenges. Phys. Chem.*, **81**, 1020-1023(1977).

140. Lynn, S., J.R. Straatemeier and H. Kramers, "Absorption Studies in the Light of the Penetration Theory, I. Long Wetted-Wall Columns", *Chem. Eng. Sci.*, **4**, 49-57(1955a).

141. Lynn, S., J.R. Straatemeier and H. Kramers, "Absorption Studies in the Light of the Penetration Theory, II. Absorption by Short Wetted-Wall Columns", *Chem. Eng. Sci.*, **4**, 58-62(1955b).

142. Lynn, S., J.R. Straatemeier and H. Kramers, "Absorption Studies in the Light of the Penetration Theory - III. Absorption by Wetted Spheres, Singly and in Columns", *Chem. Eng. Sci.*, **4**, 63-67(1955c).

143. Lyster, W.N., S.L. Sullivan Jr., D.S. Billingsley and C.D. Holland, "Figure Distillation This New Way : Pt. 1. New Convergence Method Will Handle Many Cases", *Pet. Ref.*, **38**, No. 6, 221-230(1959a).

144. Lyster, W.N., S.L. Sullivan Jr., D.S. Billingsley and C.D. Holland, "Figure Distillation This New Way : Pt. 2. Product Purities Can Set Condition for Column", *Pet. Ref.*, **38**, No. 7, 151-156(1959b).

145. Lyster, W.N., S.L. Sullivan Jr., D.S. Billingsley and

C.D. Holland, "Figure Distillation This New Way : Pt. 3. Consider Multi-feed Columns With Side Streams", *Pet. Ref.*, **38**, No. 10, 139-146(1959c).

146. MacKenzie, D.H., F. Chiraka-Parambil, C.A. Daniels and J.A. Bullin, "Design & Operation of a Selective Sweetening Plant Using MDEA", Paper 32b, Presented at the AIChE Spring National Meeting, New Orleans, Louisiana, April 6-10, 1986.

147. Mahajani, V.V. and P.V. Danckwerts, "The Stripping of CO_2 from Amine-Promoted Potash Solutions at 100°C", *Chem. Eng. Sci.*, **38**, 321-327(1983).

148. Majeed, A., S. Diab, G.J. Mains and R.N. Maddox, "Computer Calculation of Ethanolamine Sweetening", Proceedings of the 32nd Annual Gas Conditioning Conference, Norman, Oklahoma, March 8-11, 1982, G1-G11.

149. Malcolm, J.M., "Rates of Isotopic Exchange Between Hydrogen and Aminomethane Catalysed by Potassium and Lithium Methylamide", M.Sc. Thesis, The University of Alberta, 1977.

150. Marini, L., K. Clement, C. Georgakis and M.M. Suenson, "Experimental and Theoretical Investigation of an Absorber-Stripper Pilot Plant Under Nonequilibrium Conditions", *Ind. Eng. Chem. Fund.*, **24**, 296-301(1985).

151. Martin, J.L., F.D. Otto and A.E. Mather, "Solubility of Hydrogen Sulfide and Carbon Dioxide in a Diglycolamine Solution", *J. Chem. Eng. Data*, **23**, 163-164(1978).

152. Mashelkar, R.A., "Bubble Columns", *Brit. Chem. Eng.*, **15**, 1297-1304(1970).

153. Mason, D.M. and R. Kao, "Correlation of Vapor-Liquid Equilibria of Aqueous Condensates from Coal Processing" in *Thermodynamics of Aqueous Systems with Industrial Applications*, S.A. Newman, Ed., ACS Symp. Ser., **133**, 107-139(1980).

154. McNeil, K.M., "The Measurement of Interfacial Area and Surface-Renewal Rate in a Bubble-Cap Plate", *Can. J. Chem. Eng.*, **48**, 252-254(1970).

155. Meissner III, R.E. and U. Wagner, "Low Energy Process to Recover CO_2 From High Pressure Natural Gas", Presented at the 32nd Canadian Chemical Engineering

Conference, Vancouver, British Columbia, October 3-6, 1982.

156. Meissner III, R.E., "A Low Energy Process for Purifying Natural Gas", Presented at the 33rd Annual Gas Conditioning Conference, Norman, Oklahoma, March 7-9, 1983.

157. Miller, F.E. and A.L. Kohl, "Selective Absorption of Hydrogen Sulfide", *Oil and Gas J.*, 51, No.51, April 27, 175-183(1953).

158. Moore, R.G., "The Solubility and Diffusivity of Hydrogen in Aliphatic Amines", Ph.D. Thesis, University of Alberta, 1971.

159. Motard, R.L., Shacham, M., and E.M. Rosen, "Steady State Chemical Process Simulation", *A.I.Ch.E. J.*, 21, 417-436(1975).

160. Murzin, V.I. and I.L. Leites, "Partial Pressure of Carbon Dioxide over its Dilute Solutions in Aqueous Aminoethanol", *Russ. J. Phys. Chem.*, 45, 230-232(1971).

161. Murzin, V.I., I.L. Leites, L.S. Tyurina and Z.I. Perstina, "Partial Pressure of Carbon Dioxide over Low-Carbonated Aqueous Solutions of Monoethanolamine", *Trudy Gos. Inst. Azot. Prom.*, 10, 26-37(1971).

162. Myers, G.J., "Composite/Structured Design", Van Nostrand Reinhold Co., New York, 1978.

163. Nartker, T.A., J.M. Skrygley and C.D. Holland, "Solution of Problems Involving Systems of Distillation Columns", *Can. J. Chem. Eng.*, 44, 217-226(1966).

164. Nasir, P. and A.E. Mather, "The Measurement and Prediction of the Solubility of Acid Gases in Monoethanolamine Solutions at Low Partial Pressures", *Can. J. Chem. Eng.*, 55, 715-717(1977).

165. Nonhebel, G., "Gas Purification Processes for Air Pollution Control", Newnes-Butterworths, London, 1972.

166. Nysing, R.A.T.O. and H. Kramers, "Absorption of CO_2 in Carbonate Bicarbonate Buffer Solutions in a Wetted Wall Column", *Chem. Eng. Sci.*, 8, 81-89(1958).

167. Olbrich, W.E. and J.D. Wild, "Diffusion from the Free Surface into a Liquid Film in Laminar Flow Over Defined Shapes", *Chem. Eng. Sci.*, **24**, 25-32(1969).

168. Onda, K., H. Takeuchi and Y. Okumoto, "Mass Transfer Coefficients Between Gas and Liquid Phases in Packed Columns", *J. Chem. Eng. Japan*, **1**, 56-62(1968).

169. Onda, K., E. Sada and H. Takeuchi, "Gas Absorption with Chemical Reaction in Packed Columns", *J. Chem. Eng. Japan*, **1**, 62-66(1968).

170. Otto, F.D., A.E. Mather, F.-Y. Jou, and D. Lal, "Solubility of Light Hydrocarbons in Gas Treating Solutions", Paper 21b, Presented at the AIChE Annual Meeting, San Francisco, California, Nov. 25-30, 1984.

171. Orbach, O., and C.M. Crowe, "Convergence Promotion in the Simulation of Chemical Processes with Recycle - The Dominant Eigenvalue Method", *Can. J. Chem. Eng.*, **49**, 509-513(1971).

172. Ouwerkerk, C., "Process Selection for the Treating of Natural Gas", Presented at the Natural Gas Processing and Utilization Conference, Dublin, Ireland, April, 1976.

173. Ouwerkerk, C., "Theory on Mass Transfer with Chemical Reaction Applied in Developing an Absorption Process for Selective H_2S Removal", Presented at the 27th Canadian Chemical Engineering Conference, Calgary, Alberta, 1977.

174. Pearce, R.L., "Hydrogen Sulfide Removal with Methyl Diethanolamine", Proceedings of the 57th Annual GPA Convention, New Orleans, Louisiana, March 20-22, 139-144(1978).

175. Pennwalt Chemicals, "Methyldiethanolamine For Gas Sweetening", Product Information Report S-282, 1980.

176. Penny, D.E. and T.J. Ritter, "Kinetic Study of the Reaction Between Carbon Dioxide and Primary Amines", *J. Chem. Soc., Farad. Trans. 1.*, **79**, 2103-2109(1983).

177. Perry, R.H. and C.H. Chilton, Ed., "Chemical Engineers' Handbook", 5th Edition, McGraw-Hill, New York, 1973.

178. Petryschuk, W.F. and A.I. Johnson, "The Mathematical Representation of a Light Hydrocarbon Refining

Network", *Can. J. Chem. Eng.*, 46, 348-354(1968).

179. Petty, S.D. and B.S. Ho, "Pilot Plant Performance of Triethanolamine for Bulk CO_2 Separation", *J. Pet. Tech.*, 36, 1603-1612(1984).

180. Pinsent, B.R.W., L. Pearson and F.J.W. Roughton, "The Kinetics of Combination of Carbon Dioxide with Hydroxide Ions", *Trans. Farad. Soc.*, 52, 1512-1520(1956).

181. Ratcliff, G.A. and J.G. Holdcroft, "Gas Absorption with First-Order Chemical Reaction in a Spherical Liquid Film", *Chem. Eng. Sci.*, 15, 100-110(1961).

182. Reid, R.C., J.M. Prausnitz and T.K. Sherwood, "The Properties of Gases and Liquids", 3rd Edition, McGraw-Hill, New York, 1977.

183. Ripperger, G. and J. Stover, "MDEA Process for Low-Energy CO_2 Removal", Paper 21e, Presented at the AIChE Spring National Meeting, New Orleans, Louisiana, April 6-10, 1986.

184. Roberts, D. and P.V. Danckwerts, "Kinetics of CO_2 Absorption in Alkaline Solutions - I. Transient Absorption Rates and Catalysis by Arsenite", *Chem. Eng. Sci.*, 17, 961-969(1962).

185. Rosen, E.M., and A.C. Pauls, "Computer Aided Chemical Process Design : The FLOWTRAN System", *Comput. Chem. Eng.*, 1, 11-21(1977).

186. Rowland, C.H. and E.A. Givens II, "Design Absorbers : Use Real Stages", *Hydrocarbon Processing*, 50, No.9, 201-204(1971).

187. Russell, R.A., "Chemical Process Simulation - The GMB System", *Comput. Chem. Eng.*, 4, 167-190(1980).

188. Sada, E., H. Kumazawa and M.A. Butt, "Chemical Absorption Kinetics Over a Wide Range of Contact Time : Absorption of Carbon Dioxide into Aqueous Solutions of Monoethanolamine", *A.I.Ch.E. J.*, 22, 196-198(1976a).

189. Sada, E., H. Kumazawa and M.A. Butt, "Gas Absorption with Consecutive Chemical Reaction : Absorption of Carbon Dioxide into Aqueous Amine Solutions", *Can. J. Chem. Eng.*, 54, 421-424(1976b).

190. Sada, E., H. Kumazawa, M.A. Butt and D. Hayashi, "Simultaneous Absorption of Carbon Dioxide and Hydrogen Sulphide into Aqueous Monoethanolamine Solutions", *Chem. Eng. Sci.*, 31, 839-841(1976).

191. Sada, E., H. Kumazawa, Z.Q. Han and H. Matsuyama, "Chemical Kinetics of the Reaction of Carbon Dioxide with Ethanolamines in Nonaqueous Solvents", *A.I.Ch.E. J.* 31, 1297-1303(1985).

192. Sada, E., H. Kumazawa and Z.Q. Han, "Kinetics of Reaction between Carbon Dioxide and Ethylenediamine in Non-aqueous Solvents", *Chem. Eng. J.*, 31, 109-115(1985).

193. Sada, E., H. Kumazawa and Z.Q. Han, "Chemical Absorption of Carbon Dioxide into Ethanolamine Solutions of Polar Solvent", *A.I.Ch.E. J.*, 32, 347-349(1986).

194. Sardar, H., M.S. Sivasubramanian, and R.H. Weiland, "Simulation of Commercial Amine Treating Units", Presented at the CGPA Second Quarterly Meeting, Calgary, Alberta, June 13, 1985.

195. Sartori, G. and D.W. Savage, "Sterically Hindered Amines for CO_2 Removal from Gases", *Ind. Eng. Chem. Fund.*, 22, 239-249(1983).

196. Savage, D.W., G. Astarita and S. Joshi, "Chemical Absorption and Desorption of Carbon Dioxide from Hot Carbonate Solutions", *Chem. Eng. Sci.*, 35, 1513-1522(1980).

197. Savage, D.W., G. Sartori and G. Astarita, "Amines as Rate Promoters for Carbon Dioxide Hydrolysis", *Farad. Disc. Chem. Soc.*, 77, 17-31(1984).

198. Savage, D.W. and C.J. Kim, "Chemical Kinetics of Carbon Dioxide Reactions with Diethanolamine and Diisopropanolamine in Aqueous Solutions", *A.I.Ch.E. J.*, 31, 296-301(1985).

199. Scheffe, R.D. and R.H. Weiland, "Mass-Transfer Characteristics of Valve Trays", *Ind. Eng. Chem. Res.*, 26, 228-236(1987).

200. Schendel, R.L., "Processing Gases Associated with CO_2 Miscible Flood", Presented at the 33rd Annual Gas Conditioning Conference, Norman, Oklahoma, March 7-9, 1983.

201. Schendel, R.L., "Improved Selective Treating Using the HIGEE Liquid Vapor Contactor", Presented at the AIChE Annual Meeting, Miami Beach, Florida, Nov. 2-7, 1986.

202. Sedelies, R., A. Steiff and P.-M. Weinspach, "Mass Transfer Area in Different Gas-Liquid Reactors as a Function of Liquid Properties", *Chem. Eng. Technol.*, **10**, 1-15(1987).

203. Shacham, M., "Equation Oriented Approach to Process Flowsheeting", *Comput. Chem. Eng.*, **6**, 79-95(1982).

204. Sharma, M.M., R.A. Mashelkar and V.D. Mehta, "Mass Transfer in Plate Columns", *Brit. Chem. Eng.*, **14**, 70-76(1969).

205. Shneerson, A.L. and A.G. Leibush, "Absorption of Carbon Dioxide by Ethanolamines. I. Rate of Absorption of Carbon Dioxide in Solutions of Mono-, Di-, and Triethanolamine", *J. Appl. Chem. (U.S.S.R.)*, **19**, 869-880(1946).

206. Sigmund, P.W., K.F. Butwell and A.J. Wussler, "The HS Process : An Advanced Process for Selective H_2S Removal", Proceedings of the 60th Annual GPA Convention, San Antonio, Texas, March 23-25, 134-141(1981).

207. Sivasubramanian, M.S., H. Sardar and R.H. Weiland, "Simulation Mirrors Commercial Amine Units", *Oil and Gas J.*, **83**, No.40, October 7, 133-143(1985).

208. Smith, B.D., "Design of Equilibrium Stage Processes", McGraw-Hill, New York, 1963.

209. Soliman, M.A., "A Modified General Dominant Eigenvalue Method for Convergence Acceleration of Cyclic Systems", *Can. J. Chem. Eng.*, **59**, 395-397(1981).

210. Sridharan, K. and M.M. Sharma, "New Systems and Methods for the Measurement of Effective Interfacial Area and Mass Transfer Coefficients in Gas-Liquid Contactors", *Chem. Eng. Sci.*, **31**, 767-774(1976).

211. Stadtherr, M.A. and M.A. Malachowski, "On Efficient Solution of Complex Systems of Interlinked Multistage Separators", *Comput. Chem. Eng.*, **6**, 121-130(1982).

212. Stenson, F., "Waste to Wealth - A History of Gas Processing in Canada", Canadian Gas Processors

Association / Canadian Gas Processors Suppliers' Association, 1985.

213. Stogryn, E.L., D.W. Savage and G. Sartori, "Process for Selective Removal of H_2S from Mixtures Containing H_2S and CO_2 with Tertiary Amino Azabicyclic Alcohols", US Patent 4,405,580, 1983.

214. Suenson, M.M., C. Georgakis and L.B. Evans, "Steady-State and Dynamic Modeling of a Gas Absorber-Stripper System", *Ind. Eng. Chem. Fund.*, 24, 288-295(1985).

215. Sweeton, F.H., R.E. Mesmer and C.F. Baes Jr., "Acidity Measurements at Elevated Temperatures VII. Dissociation of Water", *J. Soln. Chem.*, 3, 191-214(1974).

216. Tennyson, R.N. and R.P. Schaaf, "Guidelines Can Help Choose Proper Process for Gas-Treating Plants", *Oil and Gas J.*, 75, No.2, January 10, 78-86(1977).

217. Thomas, J.C., "Practical Applications of UCARSOL™ Solvents", Presented at the Dallas Regional GPA Meeting, Dallas, Texas, October, 1985.

218. Thomas, W.J. and M.J. Adams, "Measurement of the Diffusion Coefficients of Carbon Dioxide and Nitrous Oxide in Water and Aqueous Solutions of Glycerol", *Trans. Farad. Soc.*, 61, 668-673(1965).

219. Thomas, W.J., "The Absorption of Carbon Dioxide in Aqueous Monoethanolamine in a Laminar Jet", *A.I.Ch.E. J.*, 12, 1054-1057(1966).

220. Thompson, R.E., "Energy Conservation in Regenerated Chemical Absorption Processes", Ph.D. Thesis, University of California, Berkeley, 1986.

221. Trass, O. and R.H. Weiland, "Absorption of Carbon Dioxide in Ethylenediamine Solutions II. Pilot Plant Study of Absorption and Regeneration", *Can. J. Chem. Eng.*, 49, 773-781(1971).

222. Tseng, P.C., W.S. Ho and D.W. Savage, "Carbon Dioxide Absorption into Promoted Carbonate Solutions", Paper 123e, Presented at the AIChE Annual Meeting, Miami Beach, Florida, Nov. 2-7, 1986.

223. Union Carbide Corporation, "Gas Treating Chemicals", Union Carbide Petroleum Processing, Chemicals and Additives, 1969.

224. Vaz, R.N., G.J. Mains and R.N. Maddox, "Ethanolamine Process Simulated by Rigorous Calculation", *Hydrocarbon Processing*, **60**, No.4, 139-142(1981).

225. Versteeg, G.F., "Mass Transfer and Chemical Reaction Kinetics in Acid Gas Treating Processes", Ph.D. Thesis, Twente University, 1986.

226. Versteeg, G.F., P.M.M. Blauwhoff and W.P.M. van Swaaij, "The Kinetics Between CO_2 and Alkanolamines. A Study on the Reaction Mechanism", Paper 123d, Presented at the AIChE Annual Meeting, Miami Beach, Florida, Nov. 2-7, 1986.

227. Vickery, D.J. and R.H. Weiland, "Solubility of Acid Gases in Blends of Amines", Paper 140c, Presented at the AIChE Annual Meeting, Miami Beach, Florida, Nov. 2-7, 1986.

228. Vidaurri, F.C. and L.C. Kahre, "Recover H_2S Selectively from Sour Gas Streams", *Hydrocarbon Processing*, **56**, No.11, 333-337(1977).

229. Vidwans, A.D. and M.M. Sharma, "Gas-Side Mass Transfer Coefficient in Packed Columns", *Chem. Eng. Sci.*, **22**, 673-684(1967).

230. Weiland, R.H. and O. Trass, "Absorption of Carbon Dioxide in Ethylenediamine Solutions, I. Absorption Kinetics and Equilibrium", *Can. J. Chem. Eng.*, **49**, 767-772(1971).

231. Wiechert, S., T.M. Gemborys, G. Sartori and F.S. Wu, "Commercialization of FLEXSORB™ PS Gas Treating Agent", Paper 22d, Presented at the AIChE Spring National Meeting, New Orleans, Louisiana, April 6-10, 1986.

232. Wild, J.D. and O.E. Potter, "Gas Absorption with Chemical Reaction into Liquid Flowing on a Sphere", Tripartite Chemical Engineering Conference, Symposium on Mass Transfer with Chemical Reaction, September 23, 34(1968).

233. Wild, J.D. and O.E. Potter, "A Falling Liquid Film on a Sphere", *Chem. Eng. J.*, **4**, 69-76(1972).

234. Yih, S.-M. and C.C. Sun, "Simultaneous Absorption of Hydrogen Sulphide and Carbon Dioxide into Potassium Carbonate Solution with or without Amine Promoters", *Chem. Eng. J.*, **34**, 65-72(1987).

235. Yu, W.-C., Ph.D. Thesis, University of Delaware, 1985.

236. Yu, W.-C., G. Astarita and D.W. Savage, "Kinetics of Carbon Dioxide Absorption in Solutions of Methyldiethanolamine", *Chem. Eng. Sci.*, **40**, 1585-1590(1985).

237. Yu, W.-C. and G. Astarita, "Selective Absorption of Hydrogen Sulphide in Tertiary Amine Solutions", *Chem. Eng. Sci.*, **42**, 419-424(1987a).

238. Yu, W.-C. and G. Astarita, "Design of Packed Towers for Selective Chemical Absorption", *Chem. Eng. Sci.*, **42**, 425-433(1987b).

239. Zioudas, A.P. and Z. Dadach, "Absorption Rates of Carbon Dioxide and Hydrogen Sulphide in Sterically Hindered Amines", *Chem. Eng. Sci.*, **41**, 405-408(1986).

APPENDIX 1

Raw Experimental Data

The raw experimental data that were measured using the sphere absorber apparatus are contained in this appendix. Table A1.1 contains a chronological record of the conditions studied in experiments using N_2O and CO_2 in physical absorption studies. Table A1.2 contains a similar record for experiments using CO_2 in chemical absorption studies.

Table A1.1

Summary of Pertinent System Variables for Experimental Runs Involving Physical Absorption

Date	Gas	MDEA wt %	Teepol wt %	Piper. kmol/m³	Temp. °C
85/11/22	CO_2	0	0.1	0	25 *
86/03/13	CO_2	0	0.1	0	25
86/03/17	CO_2	0	0.1	0	25
86/03/19	CO_2	0	0.1	0	25
86/03/21	CO_2	0	0.1	0	25
86/04/02	CO_2	0	0.1	0	25
86/05/01	N_2O	20	0.01	0	50
86/05/02	N_2O	20	0.01	0	50
86/05/05	N_2O	20	0.01	0	50
86/05/06	N_2O	20	0.01	0	75 *
86/05/07	N_2O	20	0.01	0	75
86/05/08	N_2O	20	0.01	0	75
86/05/12	N_2O	20	0.01	0	25
86/05/13	N_2O	20	0.01	0	25
86/05/23	N_2O	20	0.01	0	25
86/05/28	N_2O	40	0.0075	0	25
86/05/29	N_2O	40	0.0075	0	25
86/06/02	N_2O	40	0.0075	0	50
86/06/03	N_2O	40	0.0075	0	50
86/06/05	N_2O	40	0.0075	0	75
86/06/06	N_2O	40	0.0075	0	75
86/06/09	N_2O	40	0.0075	0	75
86/06/10	N_2O	40	0.0075	0	50

* the effect of liquid take-off level was measured.

Table A1.2

Summary of Pertinent System Variables for Experimental Runs Involving Chemical Absorption

Date	Gas	MDEA wt %	Teepol wt %	Piper. kmol/m³	Temp. °C
86/04/08	CO_2	20	0.01	0	25
86/04/09	CO_2	20	0.01	0	25
86/04/10	CO_2	20	0.01	0	25
86/04/14	CO_2	20	0.01	0	25
86/04/15	CO_2	20	0.01	0	25
86/04/16	CO_2	20	0.01	0	25
86/04/25	CO_2	20	0.01	0	50
86/04/29	CO_2	20	0.01	0	50
86/04/30	CO_2	20	0.01	0	50
86/06/11	CO_2	40	0.0075	0	75
86/06/12	CO_2	40	0.0075	0	75
86/06/13	CO_2	40	0.0075	0	50
86/06/17	CO_2	40	0.0075	0	50
86/06/18	CO_2	40	0.0075	0	25
86/06/19	CO_2	40	0.0075	0	25
86/06/20	CO_2	40	0.0075	0	40
86/06/23	CO_2	40	0.0075	0	40
86/06/25	CO_2	40	0.0075	0.05	40
86/06/26	CO_2	40	0.0075	0.05	40
86/06/27	CO_2	40	0.0075	0.05	40
86/06/30	CO_2	40	0.0075	0.10	40
86/07/01	CO_2	40	0.0075	0.10	40
86/07/03	CO_2	40	0.0075	0.15	40
86/07/04	CO_2	40	0.0075	0.15	40
86/07/08	CO_2	40	0.0075	0.20	40
86/07/09	CO_2	40	0.0075	0.20	40
86/07/11	CO_2	40	0.0075	0.40	40
86/07/28	CO_2	20	0.01	0	50
86/07/29	CO_2	20	0.01	0	50
86/07/30	CO_2	20	0.01	0	50
86/07/31	CO_2	20	0.01	0	75
86/08/01	CO_2	20	0.01	0	75
86/08/13	CO_2	20	0.01	0	60

Date of Experiment 1985/11/18

MDEA Conc	0.0 wt%	Absorbing Gas	CO2
Piperazine Conc	0.0 kmol/m3	Surfactant	0.1000 wt%
Barometric Pressure	711.1 mm Hg	Rotameter Tube	603
Room Temperature	23.0 deg C	Nozzle Diam	0.60 mm
Manometer Right Leg	6.0 in H2O	Thermo Coarse	0.0
Manometer Left Leg	5.3 in H2O	Thermo Fine	0.0
Jet Elevation	88.710 cm	Feed Variac	0.0 %
North Pole	88.525 cm	Circ Variac	0.0 %
South Pole	83.405 cm		
Liquid Take-off	80.995 cm		

Flowmeter	30. mm	60. mm
SFM Volume	15. mL	15. mL

Time 1	50.34 s	40.53 s
Time 2	50.20 s	40.17 s
Time 3	50.88 s	40.45 s
Time 4	50.87 s	40.31 s
Time 5	50.59 s	40.70 s
Time 6	50.87 s	40.42 s
Time 7	50.65 s	40.66 s
Time 8	50.25 s	54.55 s
Time 9	50.51 s	40.66 s
Time 10	50.21 s	40.92 s
Time 11	50.12 s	40.93 s
Time 12	50.62 s	41.07 s
Time 13	50.82 s	41.13 s
Time 14	0.0 s	41.17 s
Time 15	0.0 s	40.92 s

T/C 1 Strt	1.270 mV	1.311 mV
T/C 2 Strt	1.285 mV	1.289 mV
T/C 3 Strt	1.125 mV	1.122 mV
T/C 4 Strt	1.240 mV	1.195 mV
T/C 5 Strt	1.236 mV	1.195 mV
T/C 6 Strt	1.245 mV	1.200 mV
T/C 7 Strt	1.360 mV	1.419 mV
T/C 1 End	1.272 mV	1.320 mV
T/C 2 End	1.290 mV	1.290 mV
T/C 3 End	1.124 mV	1.124 mV
T/C 4 End	1.243 mV	1.185 mV
T/C 5 End	1.245 mV	1.185 mV
T/C 6 End	1.245 mV	1.185 mV
T/C 7 End	1.369 mV	1.430 mV

Start Time	15:50	16:45
End Time	16:25	17:25

Date of Experiment 1985/11/19

MDEA Conc	0.0 wt%	Absorbing Gas	CO2
Piperazine Conc	0.0 kmol/m3	Surfactant	0.1000 wt%
Barometric Pressure	713.9 mm Hg	Rotameter Tube	603
Room Temperature	22.0 deg C	Nozzle Diam	0.60 mm
Manometer Right Leg	6.0 in H2O	Thermo Coarse	0.0
Manometer Left Leg	5.2 in H2O	Thermo Fine	0.0
Jet Elevation	88.730 cm	Feed Variac	0.0 %
North Pole	88.535 cm	Circ Variac	0.0 %
South Pole	83.435 cm		
Liquid Take-off	80.985 cm		

Flowmeter	30. mm	60. mm	40. mm	50. mm
SFM Volume	15. mL	15. mL	15. mL	15. mL
Time 1	50.83 s	41.52 s	47.62 s	45.47 s
Time 2	50.93 s	40.68 s	47.95 s	45.41 s
Time 3	50.88 s	41.14 s	48.38 s	45.24 s
Time 4	50.73 s	41.47 s	48.06 s	45.28 s
Time 5	50.84 s	41.11 s	48.09 s	45.62 s
Time 6	50.35 s	41.33 s	48.06 s	45.51 s
Time 7	51.14 s	41.42 s	48.24 s	45.59 s
Time 8	51.17 s	41.58 s	48.21 s	45.51 s
Time 9	51.35 s	41.70 s	48.20 s	45.82 s
Time 10	51.12 s	41.13 s	48.29 s	45.88 s
Time 11	51.06 s	41.97 s	48.00 s	45.89 s
Time 12	51.26 s	42.12 s	47.41 s	46.02 s
Time 13	51.24 s	41.85 s	48.31 s	0.0 s
T/C 1 Strt	1.225 mV	1.480 mV	1.440 mV	1.450 mV
T/C 2 Strt	1.202 mV	1.452 mV	1.415 mV	1.411 mV
T/C 3 Strt	1.130 mV	1.330 mV	1.325 mV	1.305 mV
T/C 4 Strt	1.168 mV	1.350 mV	1.332 mV	1.315 mV
T/C 5 Strt	1.170 mV	1.350 mV	1.332 mV	1.317 mV
T/C 6 Strt	1.172 mV	1.350 mV	1.340 mV	1.320 mV
T/C 7 Strt	1.312 mV	1.600 mV	1.585 mV	1.595 mV
T/C 1 End	1.119 mV	1.481 mV	1.431 mV	1.453 mV
T/C 2 End	1.186 mV	1.450 mV	1.400 mV	1.415 mV
T/C 3 End	1.125 mV	1.348 mV	1.310 mV	1.293 mV
T/C 4 End	1.142 mV	1.335 mV	1.315 mV	1.312 mV
T/C 5 End	1.144 mV	1.335 mV	1.319 mV	1.313 mV
T/C 6 End	1.145 mV	1.335 mV	1.345 mV	1.312 mV
T/C 7 End	1.335 mV	1.605 mV	1.585 mV	1.598 mV
Start Time	13:17	14:50	15:35	16:15
End Time	13:50	15:15	15:55	16:40

Date of Experiment 1985/11/20

MDEA Conc	0.0 wt%	Absorbing Gas	CO2
Piperazine Conc	0.0 kmol/m3	Surfactant	0.1000 wt%
Barometric Pressure	708.0 mm Hg	Rotameter Tube	603
Room Temperature	22.3 deg C	Nozzle Diam	0.60 mm
Manometer Right Leg	7.1 in H2O	Thermo Coarse	0.0
Manometer Left Leg	5.3 in H2O	Thermo Fine	0.0
Jet Elevation	88.825 cm	Feed V	0.0 %
North Pole	88.650 cm	Circ V	0.0 %
South Pole	83.430 cm		
Liquid Take-off	81.045 cm		

Flowmeter	60. mm	70. mm	50. mm
SFM Volume	15. mL	20. mL	15. mL
Time 1	39.14 s	49.20 s	41.71 s
Time 2	39.50 s	49.26 s	41.91 s
Time 3	39.02 s	49.66 s	41.78 s
Time 4	38.85 s	49.08 s	42.20 s
Time 5	39.34 s	0.0 s	42.22 s
Time 6	39.17 s	0.0 s	41.03 s
Time 7	39.21 s	0.0 s	41.91 s
Time 8	39.59 s	0.0 s	41.73 s
Time 9	39.45 s	0.0 s	42.09 s
Time 10	39.31 s	0.0 s	42.24 s
T/C 1 Strt	1.316 mV	1.325 mV	1.300 mV
T/C 2 Strt	1.311 mV	1.318 mV	1.288 mV
T/C 3 Strt	1.206 mV	1.204 mV	1.206 mV
T/C 4 Strt	1.284 mV	1.260 mV	1.230 mV
T/C 5 Strt	1.285 mV	1.264 mV	1.230 mV
T/C 6 Strt	1.295 mV	1.264 mV	1.230 mV
T/C 7 Strt	1.345 mV	1.376 mV	1.375 mV
T/C 1 End	1.330 mV	1.320 mV	1.294 mV
T/C 2 End	1.320 mV	1.314 mV	1.278 mV
T/C 3 End	1.206 mV	1.205 mV	1.201 mV
T/C 4 End	1.284 mV	1.245 mV	1.220 mV
T/C 5 End	1.285 mV	1.250 mV	1.220 mV
T/C 6 End	1.295 mV	1.250 mV	1.220 mV
T/C 7 End	1.365 mV	1.378 mV	1.376 mV
Start Time	14:10	14:55	15:45
End Time	14:45	15:10	16:20

Date of Experiment 1985/11/21

MDEA Conc	0.0 wt%	Absorbing Gas	CO2
Piperazine Conc	0.0 kmol/m3	Surfactant	0.1000 wt%
Barometric Pressure	713.1 mm Hg	Rotameter Tube	603
Room Temperature	21.5 deg C	Nozzle Diam	0.60 mm
Manometer Right Leg	7.0 in H2O	Thermo Coarse	0.0
Manometer Left Leg	5.0 in H2O	Thermo Fine	0.0
Jet Elevation	88.770 cm	Feed Variac	0.0 %
North Pole	88.600 cm	Circ Variac	0.0 %
South Pole	83.445 cm		
Liquid Take-off	81.065 cm		

Flowmeter	30. mm	50. mm	60. mm	40. mm	30. mm
SFM Volume	15. mL	15. mL	15. mL	15. mL	15. mL
Time 1	52.53 s	43.77 s	41.30 s	48.12 s	53.95 s
Time 2	52.10 s	43.06 s	40.99 s	47.86 s	54.31 s
Time 3	52.95 s	43.66 s	41.11 s	47.84 s	54.39 s
Time 4	53.08 s	43.75 s	41.20 s	48.09 s	53.84 s
Time 5	51.75 s	43.67 s	41.20 s	48.54 s	54.11 s
Time 6	53.32 s	43.89 s	40.63 s	48.54 s	54.40 s
Time 7	53.03 s	43.57 s	40.78 s	47.81 s	54.28 s
Time 8	53.27 s	44.16 s	41.16 s	47.99 s	54.30 s
Time 9	53.92 s	43.80 s	40.86 s	48.02 s	54.40 s
Time 10	53.80 s	43.85 s	40.93 s	48.01 s	54.52 s
Time 11	52.09 s	43.80 s	41.00 s	47.92 s	54.31 s
Time 12	53.36 s	43.49 s	40.87 s	47.86 s	54.09 s
Time 13	0.0 s	0.0 s	0.0 s	48.02 s	54.35 s
Time 14	0.0 s	0.0 s	0.0 s	48.20 s	0.0 s
T/C 1 Strt	1.240 mV	1.286 mV	1.309 mV	1.275 mV	1.250 mV
T/C 2 Strt	1.230 mV	1.273 mV	1.290 mV	1.261 mV	1.239 mV
T/C 3 Strt	1.205 mV	1.230 mV	1.214 mV	1.182 mV	1.172 mV
T/C 4 Strt	1.209 mV	1.230 mV	1.226 mV	1.210 mV	1.203 mV
T/C 5 Strt	1.213 mV	1.238 mV	1.225 mV	1.212 mV	1.203 mV
T/C 6 Strt	1.209 mV	1.233 mV	1.225 mV	1.212 mV	1.203 mV
T/C 7 Strt	1.314 mV	1.345 mV	1.375 mV	1.370 mV	1.356 mV
T/C 1 End	1.250 mV	1.295 mV	1.300 mV	1.275 mV	1.255 mV
T/C 2 End	1.239 mV	1.280 mV	1.283 mV	1.260 mV	1.231 mV
T/C 3 End	1.226 mV	1.232 mV	1.184 mV	1.177 mV	1.160 mV
T/C 4 End	1.218 mV	1.231 mV	1.213 mV	1.210 mV	1.196 mV
T/C 5 End	1.224 mV	1.231 mV	1.215 mV	1.210 mV	1.196 mV
T/C 6 End	1.219 mV	1.231 mV	1.213 mV	1.210 mV	1.210 mV
T/C 7 End	1.326 mV	1.363 mV	1.376 mV	1.374 mV	1.357 mV
Start Time	11:30	12:45	13:50	14:56	15:50
End Time	12:00	13:15	14:30	15:30	16:30

Date of Experiment 1985/11/22

MDEA Conc	0.0 wt%	Absorbing Gas	CO2
Piperazine Conc	0.0 kmol/m3	Surfactant	0.1000 wt%
Barometric Pressure	708.0 mm Hg	Rotameter Tube	603
Room Temperature	22.0 deg C	Nozzle Diam	0.60 mm
Manometer Right Leg	7.0 in H2O	Thermo Coarse	0.0
Manometer Left Leg	4.9 in H2O	Thermo Fine	0.0
Jet Elevation	88.700 cm	Feed Variac	0.0 %
North Pole	88.530 cm	Circ Variac	0.0 %
South Pole	83.335 cm		
Liquid Take-off	82.505 cm		

Flowmeter	40. mm
SFM Volume	15. mL

Time	1	53.41 s
Time	2	54.45 s
Time	3	53.79 s
Time	4	54.38 s
Time	5	53.84 s
Time	6	53.99 s
Time	7	54.17 s
Time	8	54.96 s
Time	9	53.66 s
Time	10	54.09 s
Time	11	53.54 s
Time	12	54.70 s
Time	13	53.64 s
Time	14	54.06 s

T/C	1 Strt	1.245 mV
T/C	2 Strt	1.225 mV
T/C	3 Strt	1.175 mV
T/C	4 Strt	1.198 mV
T/C	5 Strt	1.205 mV
T/C	6 Strt	1.197 mV
T/C	7 Strt	1.316 mV
T/C	1 End	1.241 mV
T/C	2 End	1.230 mV
T/C	3 End	1.180 mV
T/C	4 End	1.190 mV
T/C	5 End	1.189 mV
T/C	6 End	1.190 mV
T/C	7 End	1.318 mV

Start Time	11:40
End Time	12:15

Date of Experiment 1985/11/22

MDEA Conc	0.0 wt%	Absorbing Gas	CO2
Piperazine Conc	0.0 kmol/m3	Surfactant	0.1000 wt%
Barometric Pressure	708.0 mm Hg	Rotameter Tube	603
Room Temperature	22.0 deg C	Nozzle Diam	0.60 mm
Manometer Right Leg	7.0 in H2O	Thermo Coarse	0.0
Manometer Left Leg	4.9 in H2O	Thermo Fine	0.0
Jet Elevation	88.700 cm	Feed Variac	0.0 %
North Pole	88.530 cm	Circ Variac	0.0 %
South Pole	83.335 cm		
Liquid Take-off	82.000 cm		

Flowmeter	40. mm
SFM Volume	15. mL

Time 1	49.86 s
Time 2	49.51 s
Time 3	50.06 s
Time 4	50.01 s
Time 5	49.80 s
Time 6	49.55 s
Time 7	49.95 s
Time 8	50.02 s
Time 9	49.71 s
Time 10	50.07 s
Time 11	50.37 s
Time 12	49.76 s

T/C 1 Strt	1.245 mV
T/C 2 Strt	1.230 mV
T/C 3 Strt	1.177 mV
T/C 4 Strt	1.190 mV
T/C 5 Strt	1.190 mV
T/C 6 Strt	1.190 mV
T/C 7 Strt	1.320 mV
T/C 1 End	1.248 mV
T/C 2 End	1.230 mV
T/C 3 End	1.180 mV
T/C 4 End	1.189 mV
T/C 5 End	1.192 mV
T/C 6 End	1.190 mV
T/C 7 End	1.327 mV

Start Time	12:50
End Time	13:25

Date of Experiment 1985/11/22

MDEA Conc	0.0 wt%	Absorbing Gas	CO2
Piperazine Conc	0.0 kmol/m3	Surfactant	0.1000 wt%
Barometric Pressure	708.0 mm Hg	Rotameter Tube	603
Room Temperature	22.0 deg C	Nozzle Diam	0.60 mm
Manometer Right Leg	7.0 in H2O	Thermo Coarse	0.0
Manometer Left Leg	4.9 in H2O	Thermo Fine	0.0
Jet Elevation	88.700 cm	Feed Variac	0.0 %
North Pole	88.530 cm	Circ Variac	0.0 %
South Pole	83.335 cm		
Liquid Take-off	81.500 cm		

Flowmeter	40. mm
SFM Volume	15. mL

Time 1	47.88 s
Time 2	47.91 s
Time 3	47.61 s
Time 4	47.82 s
Time 5	47.86 s
Time 6	48.53 s
Time 7	47.68 s
Time 8	48.02 s
Time 9	48.62 s
Time 10	47.84 s
Time 11	48.15 s
Time 12	47.84 s

T/C 1 Strt	1.250 mV
T/C 2 Strt	1.236 mV
T/C 3 Strt	1.179 mV
T/C 4 Strt	1.190 mV
T/C 5 Strt	1.190 mV
T/C 6 Strt	1.190 mV
T/C 7 Strt	1.340 mV
T/C 1 End	1.255 mV
T/C 2 End	1.235 mV
T/C 3 End	1.179 mV
T/C 4 End	1.190 mV
T/C 5 End	1.190 mV
T/C 6 End	1.190 mV
T/C 7 End	1.350 mV

Start Time	13:50
End Time	14:25

Date of Experiment 1985/11/22

MDEA Conc	0.0	wt%	Absorbing Gas	CO2	
Piperazine Conc	0.0	kmol/m3	Surfactant	0.1000	wt%
Barometric Pressure	708.0	mm Hg	Rotameter Tube	603	
Room Temperature	22.0	deg C	Nozzle Diam	0.60	mm
Manometer Right Leg	7.0	in H2O	Thermo Coarse	0.0	
Manometer Left Leg	4.9	in H2O	Thermo Fine	0.0	
Jet Elevation	88.700	cm	Feed Variac	0.0	%
North Pole	88.530	cm	Circ Variac	0.0	%
South Pole	83.335	cm			
Liquid Take-off	81.000	cm			

Flowmeter	40.	mm
SFM Volume	15.	mL

Time	1	47.42 s
Time	2	47.67 s
Time	3	47.74 s
Time	4	48.17 s
Time	5	48.35 s
Time	6	47.93 s
Time	7	47.95 s
Time	8	48.14 s
Time	9	47.88 s
Time	10	48.36 s
Time	11	48.38 s
Time	12	48.27 s

T/C 1 Strt	1.258 mV
T/C 2 Strt	1.236 mV
T/C 3 Strt	1.176 mV
T/C 4 Strt	1.190 mV
T/C 5 Strt	1.187 mV
T/C 6 Strt	1.185 mV
T/C 7 Strt	1.355 mV
T/C 1 End	1.265 mV
T/C 2 End	1.240 mV
T/C 3 End	1.186 mV
T/C 4 End	1.192 mV
T/C 5 End	1.192 mV
T/C 6 End	1.187 mV
T/C 7 End	1.363 mV

Start Time	14:55
End Time	15:25

Date of Experiment 1985/11/22

MDEA Conc	0.0 wt%	Absorbing Gas	CO2
Piperazine Conc	0.0 kmol/m3	Surfactant	0.1000 wt%
Barometric Pressure	708.0 mm Hg	Rotameter Tube	603
Room Temperature	22.0 deg C	Nozzle Diam	0.60 mm
Manometer Right Leg	7.0 in H2O	Thermo Coarse	0.0
Manometer Left Leg	4.9 in H2O	Thermo Fine	0.0
Jet Elevation	88.700 cm	Feed Variac	0.0 %
North Pole	88.530 cm	Circ Variac	0.0 %
South Pole	83.335 cm		
Liquid Take-off	80.500 cm		

Flowmeter	40. mm
SFM Volume	15. mL

Time 1	48.04 s
Time 2	48.57 s
Time 3	48.65 s
Time 4	48.77 s
Time 5	48.44 s
Time 6	48.84 s
Time 7	48.34 s
Time 8	48.37 s
Time 9	48.75 s
Time 10	48.47 s
Time 11	48.75 s
Time 12	48.53 s

T/C 1 Strt	1.275 mV
T/C 2 Strt	1.259 mV
T/C 3 Strt	1.190 mV
T/C 4 Strt	1.205 mV
T/C 5 Strt	1.225 mV
T/C 6 Strt	1.234 mV
T/C 7 Strt	1.367 mV
T/C 1 End	1.271 mV
T/C 2 End	1.250 mV
T/C 3 End	1.186 mV
T/C 4 End	1.200 mV
T/C 5 End	1.200 mV
T/C 6 End	1.200 mV
T/C 7 End	1.375 mV

Start Time	16:00
End Time	16:33

Date of Experiment 1985/11/26

MDEA Conc	0.0 wt%	Absorbing Gas	CO2
Piperazine Conc	0.0 kmol/m3	Surfactant	0.1000 wt%
Barometric Pressure	708.6 mm Hg	Rotameter Tube	603
Room Temperature	21.5 deg C	Nozzle Diam	0.60 mm
Manometer Right Leg	7.0 in H2O	Thermo Coarse	0.0
Manometer Left Leg	5.0 in H2O	Thermo Fine	0.0
Jet Elevation	87.765 cm	Feed Variac	0.0 %
North Pole	87.560 cm	Circ Variac	0.0 %
South Pole	82.410 cm		
Liquid Take-off	79.930 cm		

Flowmeter	30. mm	60. mm	40. mm	50. mm	60. mm
SFM Volume	15. mL	15. mL	15. mL	15. mL	15. mL
Time 1	51.41 s	39.67 s	46.65 s	43.07 s	40.02 s
Time 2	51.31 s	40.16 s	46.41 s	42.88 s	40.53 s
Time 3	50.94 s	39.46 s	46.20 s	43.05 s	40.57 s
Time 4	51.69 s	39.91 s	46.46 s	42.83 s	40.38 s
Time 5	51.67 s	39.69 s	46.27 s	43.05 s	40.36 s
Time 6	51.34 s	39.91 s	46.58 s	43.09 s	40.62 s
Time 7	51.30 s	40.06 s	46.16 s	42.87 s	40.50 s
Time 8	51.13 s	40.11 s	46.35 s	43.13 s	40.50 s
Time 9	51.18 s	39.99 s	46.13 s	43.11 s	40.25 s
Time 10	51.36 s	40.11 s	46.05 s	43.09 s	40.69 s
Time 11	51.26 s	40.10 s	46.60 s	42.95 s	40.75 s
Time 12	51.56 s	39.82 s	47.04 s	43.01 s	40.54 s
Time 13	51.34 s	0.0 s	46.43 s	0.0 s	40.63 s
T/C 1 Strt	1.203 mV	1.200 mV	1.182 mV	1.210 mV	1.225 mV
T/C 2 Strt	1.197 mV	1.190 mV	1.170 mV	1.194 mV	1.208 mV
T/C 3 Strt	1.130 mV	1.137 mV	1.140 mV	1.144 mV	1.140 mV
T/C 4 Strt	1.175 mV	1.145 mV	1.130 mV	1.135 mV	1.131 mV
T/C 5 Strt	1.180 mV	1.145 mV	1.130 mV	1.135 mV	1.131 mV
T/C 6 Strt	1.180 mV	1.142 mV	1.130 mV	1.135 mV	1.131 mV
T/C 7 Strt	1.223 mV	1.250 mV	1.260 mV	1.291 mV	1.302 mV
T/C 1 End	1.165 mV	1.200 mV	1.190 mV	1.210 mV	1.228 mV
T/C 2 End	1.165 mV	1.190 mV	1.173 mV	1.194 mV	1.211 mV
T/C 3 End	1.135 mV	1.140 mV	1.138 mV	1.140 mV	1.141 mV
T/C 4 End	1.140 mV	1.139 mV	1.130 mV	1.130 mV	1.132 mV
T/C 5 End	1.140 mV	1.139 mV	1.130 mV	1.130 mV	1.132 mV
T/C 6 End	1.140 mV	1.139 mV	1.130 mV	1.130 mV	1.131 mV
T/C 7 End	1.230 mV	1.258 mV	1.275 mV	1.295 mV	1.307 mV
Start Time	12:10	13:08	14:00	14:55	15:45
End Time	12:38	13:30	14:30	15:23	16:13

Date of Experiment 1985/12/ 3

MDEA Conc	0.0 wt%	Absorbing Gas	CO2
Piperazine Conc	0.0 kmol/m3	Surfactant	0.1000 wt%
Barometric Pressure	694.7 mm Hg	Rotameter Tube	603
Room Temperature	21.5 deg C	Nozzle Diam	0.60 mm
Manometer Right Leg	7.0 in H2O	Thermo Coarse	0.0
Manometer Left Leg	5.0 in H2O	Thermo Fine	0.0
Jet Elevation	87.800 cm	Feed Variac	0.0 %
North Pole	87.595 cm	Circ Variac	0.0 %
South Pole	82.515 cm		
Liquid Take-off	80.055 cm		

Flowmeter	30. mm	40. mm	50. mm	60. mm
SFM Volume	15. mL	15. mL	15. mL	15. mL
Time 1	53.74 s	46.36 s	42.65 s	39.51 s
Time 2	53.80 s	46.51 s	42.11 s	39.71 s
Time 3	53.41 s	46.36 s	42.50 s	39.89 s
Time 4	53.44 s	46.43 s	42.45 s	39.77 s
Time 5	53.83 s	46.49 s	42.52 s	39.91 s
Time 6	53.88 s	46.80 s	42.46 s	39.84 s
Time 7	54.03 s	46.38 s	42.56 s	40.16 s
Time 8	54.09 s	46.66 s	42.66 s	40.29 s
Time 9	54.02 s	46.36 s	42.59 s	39.74 s
Time 10	53.96 s	46.47 s	42.42 s	39.95 s
Time 11	53.83 s	46.57 s	42.63 s	40.05 s
Time 12	54.13 s	46.40 s	42.37 s	40.20 s
Time 13	0.0 s	0.0 s	0.0 s	39.79 s
T/C 1 Strt	1.210 mV	1.237 mV	1.266 mV	1.307 mV
T/C 2 Strt	1.197 mV	1.217 mV	1.248 mV	1.281 mV
T/C 3 Strt	1.161 mV	1.195 mV	1.207 mV	1.196 mV
T/C 4 Strt	1.170 mV	1.186 mV	1.180 mV	1.190 mV
T/C 5 Strt	1.164 mV	1.162 mV	1.161 mV	1.170 mV
T/C 6 Strt	1.175 mV	1.180 mV	1.185 mV	1.191 mV
T/C 7 Strt	1.240 mV	1.267 mV	1.301 mV	1.350 mV
T/C 1 End	1.221 mV	1.246 mV	1.285 mV	1.315 mV
T/C 2 End	1.205 mV	1.228 mV	1.260 mV	1.289 mV
T/C 3 End	1.184 mV	1.210 mV	1.205 mV	1.193 mV
T/C 4 End	1.170 mV	1.180 mV	1.185 mV	1.190 mV
T/C 5 End	1.155 mV	1.160 mV	1.165 mV	1.180 mV
T/C 6 End	1.170 mV	1.181 mV	1.186 mV	1.195 mV
T/C 7 End	1.255 mV	1.280 mV	1.326 mV	1.358 mV
Start Time	12:25	13:25	14:25	15:20
End Time	12:58	13:55	14:50	15:52

Date of Experiment 1986/ 1/ 3

MDEA Conc	0.0 wt%	Absorbing Gas	CO2
Piperazine Conc	0.0 kmol/m3	Surfactant	0.1000 wt%
Barometric Pressure	705.0 mm Hg	Rotameter Tube	603
Room Temperature	22.0 deg C	Nozzle Diam	0.60 mm
Manometer Right Leg	7.0 in H2O	Thermo Coarse	0.0
Manometer Left Leg	5.0 in H2O	Thermo Fine	0.0
Jet Elevation	87.735 cm	Feed Variac	0.0 %
North Pole	87.525 cm	Circ Variac	0.0 %
South Pole	82.445 cm		
Liquid Take-off	79.995 cm		

Flowmeter	30. mm	50. mm	60. mm	40. mm
SFM Volume	15. mL	15. mL	15. mL	15. mL
Time 1	51.68 s	42.65 s	40.58 s	48.03 s
Time 2	51.76 s	42.92 s	40.53 s	48.09 s
Time 3	51.59 s	42.57 s	40.82 s	48.02 s
Time 4	51.77 s	42.77 s	40.99 s	47.82 s
Time 5	52.02 s	42.90 s	41.01 s	48.02 s
Time 6	51.77 s	42.93 s	40.65 s	48.14 s
Time 7	51.74 s	42.91 s	40.67 s	48.34 s
Time 8	52.16 s	42.89 s	40.69 s	47.71 s
Time 9	52.09 s	42.85 s	40.93 s	48.36 s
Time 10	52.09 s	42.64 s	41.02 s	48.53 s
Time 11	52.20 s	42.68 s	40.91 s	48.77 s
Time 12	51.93 s	42.79 s	41.07 s	48.78 s
Time 13	0.0 s	43.07 s	0.0 s	48.13 s
Time 14	0.0 s	0.0 s	0.0 s	48.59 s
T/C 1 Strt	1.165 mV	1.176 mV	1.181 mV	1.189 mV
T/C 2 Strt	1.175 mV	1.176 mV	1.183 mV	1.185 mV
T/C 3 Strt	1.153 mV	1.160 mV	1.170 mV	1.176 mV
T/C 4 Strt	1.163 mV	1.160 mV	1.170 mV	1.173 mV
T/C 5 Strt	1.165 mV	1.164 mV	1.170 mV	1.173 mV
T/C 6 Strt	1.165 mV	1.170 mV	1.171 mV	1.173 mV
T/C 7 Strt	1.181 mV	1.198 mV	1.194 mV	1.200 mV
T/C 1 End	1.169 mV	1.176 mV	1.186 mV	1.188 mV
T/C 2 End	1.170 mV	1.175 mV	1.182 mV	1.185 mV
T/C 3 End	1.143 mV	1.162 mV	1.170 mV	1.185 mV
T/C 4 End	1.152 mV	1.162 mV	1.165 mV	1.174 mV
T/C 5 End	1.155 mV	1.163 mV	1.165 mV	1.175 mV
T/C 6 End	1.155 mV	1.161 mV	1.165 mV	1.175 mV
T/C 7 End	1.200 mV	1.195 mV	1.205 mV	1.200 mV
Start Time	12:00	13:00	14:00	15:00
End Time	12:27	13:30	14:27	15:30

Date of Experiment 1986/ 1/ 6

MDEA Conc	0.0 wt%	Absorbing Gas	CO2
Piperazine Conc	0.0 kmol/m3	Surfactant	0.1000 wt%
Barometric Pressure	702.5 mm Hg	Rotameter Tube	603
Room Temperature	22.0 deg C	Nozzle Diam	0.60 mm
Manometer Right Leg	7.0 in H2O	Thermo Coarse	0.0
Manometer Left Leg	5.0 in H2O	Thermo Fine	0.0
Jet Elevation	87.775 cm	Feed Variac	0.0 %
North Pole	87.525 cm	Circ Variac	0.0 %
South Pole	82.415 cm		
Liquid Take-off	80.025 cm		

Flowmeter		30. mm	60. mm	40. mm	50. mm
SFM Volume		15. mL	15. mL	15. mL	15. mL
Time	1	51.66 s	40.27 s	47.16 s	44.56 s
Time	2	52.52 s	40.08 s	47.04 s	44.52 s
Time	3	52.77 s	40.40 s	47.20 s	44.52 s
Time	4	52.49 s	40.38 s	47.23 s	44.14 s
Time	5	52.53 s	40.42 s	47.61 s	44.46 s
Time	6	52.77 s	40.77 s	47.44 s	44.11 s
Time	7	52.95 s	40.50 s	47.68 s	44.50 s
Time	8	53.08 s	40.41 s	48.08 s	43.89 s
Time	9	52.56 s	40.16 s	48.04 s	44.13 s
Time	10	52.34 s	40.93 s	47.85 s	44.25 s
Time	11	52.72 s	40.53 s	47.78 s	44.45 s
Time	12	53.03 s	40.52 s	47.43 s	44.41 s
Time	13	53.08 s	0.0 s	47.77 s	44.38 s
T/C 1	Strt	1.145 mV	1.145 mV	1.145 mV	1.150 mV
T/C 2	Strt	1.157 mV	1.155 mV	1.144 mV	1.147 mV
T/C 3	Strt	1.136 mV	1.155 mV	1.160 mV	1.150 mV
T/C 4	Strt	1.143 mV	1.131 mV	1.127 mV	1.129 mV
T/C 5	Strt	1.143 mV	1.131 mV	1.129 mV	1.129 mV
T/C 6	Strt	1.143 mV	1.131 mV	1.129 mV	1.129 mV
T/C 7	Strt	1.170 mV	1.155 mV	1.166 mV	1.183 mV
T/C 1	End	1.136 mV	1.151 mV	1.151 mV	1.150 mV
T/C 2	End	1.141 mV	1.150 mV	1.145 mV	1.145 mV
T/C 3	End	1.145 mV	1.157 mV	1.150 mV	1.145 mV
T/C 4	End	1.122 mV	1.125 mV	1.126 mV	1.127 mV
T/C 5	End	1.122 mV	1.125 mV	1.126 mV	1.127 mV
T/C 6	End	1.125 mV	1.125 mV	1.126 mV	1.127 mV
T/C 7	End	1.175 mV	1.161 mV	1.180 mV	1.180 mV
Start	Time	12:20	13:40	14:30	15:33
End	Time	13:10	14:05	15:07	16:07

Date of Experiment 1986/ 2/ 3

MDEA Conc	20.0 wt%	Absorbing Gas	N2O
Piperazine Conc	0.0 kmol/m3	Surfactant	0.0100 wt%
Barometric Pressure	699.8 mm Hg	Rotameter Tube	603
Room Temperature	23.0 deg C	Nozzle Diam	0.60 mm
Manometer Right Leg	6.5 in H2O	Thermo Coarse	0.0
Manometer Left Leg	5.4 in H2O	Thermo Fine	0.0
Jet Elevation	87.330 cm	Feed Variac	0.0 %
North Pole	87.120 cm	Circ Variac	0.0 %
South Pole	81.950 cm		
Liquid Take-off	79.600 cm		

Flowmeter	60. mm
SFM Volume	10. mL

Time	1	66.74 s
Time	2	67.13 s
Time	3	67.38 s
Time	4	67.38 s
Time	5	67.18 s
Time	6	67.64 s
Time	7	66.78 s
Time	8	66.54 s
Time	9	66.38 s
Time	10	66.91 s
Time	11	67.36 s
Time	12	66.17 s
Time	13	66.88 s

T/C 1 Strt	1.195 mV
T/C 2 Strt	1.195 mV
T/C 3 Strt	1.145 mV
T/C 4 Strt	1.190 mV
T/C 5 Strt	1.190 mV
T/C 6 Strt	1.190 mV
T/C 7 Strt	1.215 mV
T/C 1 End	1.193 mV
T/C 2 End	1.193 mV
T/C 3 End	1.145 mV
T/C 4 End	1.180 mV
T/C 5 End	1.180 mV
T/C 6 End	1.180 mV
T/C 7 End	1.212 mV

Start Time	12:45
End Time	13:14

Date of Experiment 1986/ 2/ 3

MDEA Conc	20.0	wt%	Absorbing Gas	H2O
Piperazine Conc	0.0	kmol/m3	Surfactant	0.0100 wt%
Barometric Pressure	699.8	mm Hg	Rotameter Tube	603
Room Temperature	23.0	deg C	Nozzle Diam	0.60 mm
Manometer Right Leg	6.5	in H2O	Thermo Coarse	0.0
Manometer Left Leg	5.4	in H2O	Thermo Fine	0.0
Jet Elevation	87.330	cm	Feed Variac	0.0 %
North Pole	87.120	cm	Circ Variac	0.0 %
South Pole	81.950	cm		
Liquid Take-off	81.120	cm		

Flowmeter	60.	mm
SFM Volume	10.	mL

Time 1	70.75	s
Time 2	71.12	s
Time 3	70.83	s
Time 4	71.19	s
Time 5	69.90	s
Time 6	71.29	s
Time 7	69.95	s
Time 8	70.76	s
Time 9	69.22	s
Time 10	71.56	s
Time 11	71.62	s
Time 12	71.02	s
Time 13	70.40	s
Time 14	69.83	s
Time 15	71.05	s

T/C 1 Strt	1.205	mV
T/C 2 Strt	1.205	mV
T/C 3 Strt	1.145	mV
T/C 4 Strt	1.199	mV
T/C 5 Strt	1.199	mV
T/C 6 Strt	1.207	mV
T/C 7 Strt	1.211	mV
T/C 1 End	1.206	mV
T/C 2 End	1.210	mV
T/C 3 End	1.141	mV
T/C 4 End	1.215	mV
T/C 5 End	1.215	mV
T/C 6 End	1.224	mV
T/C 7 End	1.186	mV

Start Time	13:25
End Time	13:57

Date of Experiment 1986/ 2/ 3

MDEA Conc	20.0 wt%	Absorbing Gas	N2O
Piperazine Conc	0.0 kmol/m3	Surfactant	0.0100 wt%
Barometric Pressure	699.8 mm Hg	Rotameter Tube	603
Room Temperature	23.0 deg C	Nozzle Diam	0.60 mm
Manometer Right Leg	6.5 in H2O	Thermo Coarse	0.0
Manometer Left Leg	5.4 in H2O	Thermo Fine	0.0
Jet Elevation	87.330 cm	Feed Variac	0.0 %
North Pole	87.120 cm	Circ Variac	0.0 %
South Pole	81.950 cm		
Liquid Take-off	80.735 cm		

Flowmeter	60. mm
SFM Volume	10. mL

Time 1	66.66 s
Time 2	66.83 s
Time 3	67.46 s
Time 4	65.67 s
Time 5	67.31 s
Time 6	68.13 s
Time 7	67.40 s
Time 8	67.27 s
Time 9	67.15 s
Time 10	67.99 s
Time 11	68.05 s
Time 12	67.42 s
Time 13	67.32 s
Time 14	66.81 s

T/C 1 Strt	1.170 mV
T/C 2 Strt	1.181 mV
T/C 3 Strt	1.145 mV
T/C 4 Strt	1.180 mV
T/C 5 Strt	1.180 mV
T/C 6 Strt	1.180 mV
T/C 7 Strt	1.178 mV
T/C 1 End	1.185 mV
T/C 2 End	1.185 mV
T/C 3 End	1.146 mV
T/C 4 End	1.170 mV
T/C 5 End	1.170 mV
T/C 6 End	1.170 mV
T/C 7 End	1.200 mV

Start Time	14:50
End Time	15:20

[redacted] Experiment 1986/ 2/ 3

[redacted] Conc	20.0 wt%	Absorbing Gas	N2O
Piperazine Conc	0.0 kmol/m3	Surfactant	0.0100 wt%
Barometric Pressure	699.8 mm Hg	Rotameter Tube	603
Room Temperature	23.0 deg C	Nozzle Diam	0.60 mm
Manometer Right Leg	6.5 in H2O	Thermo Coarse	0.0
Manometer Left Leg	5.4 in H2O	Thermo Fine	0.0
Jet Elevation	87.330 cm	Feed Variac	0.0 %
North Pole	87.120 cm	Circ Variac	0.0 %
South Pole	81.950 cm		
Liquid Take-off	78.690 cm		

Flowmeter	60. mm
SFM Volume	10. mL

Time 1	67.03 s
Time 2	66.50 s
Time 3	67.02 s
Time 4	67.24 s
Time 5	67.52 s
Time 6	66.70 s
Time 7	67.61 s
Time 8	67.82 s
Time 9	67.55 s
Time 10	67.79 s
Time 11	67.22 s
Time 12	68.16 s

T/C 1 Strt	1.180 mV
T/C 2 Strt	1.183 mV
T/C 3 Strt	1.144 mV
T/C 4 Strt	1.170 mV
T/C 5 Strt	1.170 mV
T/C 6 Strt	1.170 mV
T/C 7 Strt	1.196 mV
T/C 1 End	1.190 mV
T/C 2 End	1.190 mV
T/C 3 End	1.146 mV
T/C 4 End	1.167 mV
T/C 5 End	1.167 mV
T/C 6 End	1.168 mV
T/C 7 End	1.210 mV

Start Time	15:30
End Time	15:55

Date of Experiment 1986/ 2/ 3

MDEA Conc	20.0 wt%	Absorbing Gas	N2O
Piperazine Conc	0.0 kmol/m3	Surfactant	0.0100 wt%
Barometric Pressure	699.8 mm Hg	Rotameter Tube	603
Room Temperature	23.0 deg C	Nozzle Diam	0.60 mm
Manometer Right Leg	6.5 in H2O	Thermo Coarse	0.0
Manometer Left Leg	5.4 in H2O	Thermo Fine	0.0
Jet Elevation	87.330 cm	Feed Variac	0.0 %
North Pole	87.120 cm	Circ Variac	0.0 %
South Pole	81.950 cm		
Liquid Take-off	80.115 cm		

Flowmeter	60. mm
SFM Volume	10. mL

Time	1	67.23 s
Time	2	67.57 s
Time	3	67.03 s
Time	4	67.23 s
Time	5	67.95 s
Time	6	67.09 s
Time	7	68.01 s
Time	8	68.30 s
Time	9	68.48 s
Time	10	67.84 s
Time	11	68.39 s
Time	12	67.83 s
Time	13	67.73 s
Time	14	67.43 s
Time	15	66.60 s

T/C 1 Strt	1.180 mV
T/C 2 Strt	1.185 mV
T/C 3 Strt	1.150 mV
T/C 4 Strt	1.165 mV
T/C 5 Strt	1.165 mV
T/C 6 Strt	1.165 mV
T/C 7 Strt	1.186 mV
T/C 1 End	1.175 mV
T/C 2 End	1.176 mV
T/C 3 End	1.147 mV
T/C 4 End	1.160 mV
T/C 5 End	1.160 mV
T/C 6 End	1.161 mV
T/C 7 End	1.195 mV

Start Time	16:10
End Time	16:45

Date of Experiment 1986/ 2/ 7

MDEA Conc	20.0 wt%	Absorbing Gas	N2O
Piperazine Conc	0.0 kmol/m3	Surfactant	0.0100 wt%
Barometric Pressure	710.1 mm Hg	Rotameter Tube	603
Room Temperature	23.0 deg C	Nozzle Diam	0.60 mm
Manometer Right Leg	6.1 in H2O	Thermo Coarse	0.0
Manometer Left Leg	5.8 in H2O	Thermo Fine	0.0
Jet Elevation	87.585 cm	Feed Variac	0.0 %
North Pole	87.380 cm	Circ Variac	0.0 %
South Pole	82.230 cm		
Liquid Take-off	79.860 cm		

Flowmeter	45. mm	75. mm	30. mm	60. mm
SFM Volume	10. mL	10. mL	10. mL	10. mL
Time 1	77.81 s	63.02 s	92.73 s	66.25 s
Time 2	77.95 s	62.86 s	92.07 s	68.01 s
Time 3	77.61 s	62.37 s	93.21 s	67.87 s
Time 4	78.31 s	62.20 s	93.09 s	68.34 s
Time 5	78.03 s	61.79 s	92.54 s	67.80 s
Time 6	77.74 s	62.21 s	93.21 s	67.71 s
Time 7	77.67 s	62.27 s	93.57 s	67.76 s
Time 8	77.89 s	62.87 s	92.78 s	68.23 s
Time 9	75.87 s	63.08 s	93.33 s	67.21 s
Time 10	76.84 s	62.09 s	93.58 s	68.16 s
Time 11	77.05 s	62.[illegible] s	93.87 s	67.58 s
Time 12	76.37 s	62.[illegible] s	93.51 s	67.33 s
Time 13	77.50 s	0.0 s	0.0 s	0.0 s
Time 14	77.55 s	0.0 s	0.0 s	0.0 s
Time 15	77.62 s	0.0 s	0.0 s	0.0 s
Time 16	77.52 s	0.0 s	0.0 s	0.0 s
Time 17	76.32 s	0.0 s	0.0 s	0.0 s
T/C 1 Strt	1.180 mV	1.200 mV	1.170 mV	1.200 mV
T/C 2 Strt	1.180 mV	1.195 mV	1.174 mV	1.195 mV
T/C 3 Strt	1.170 mV	1.171 mV	1.160 mV	1.165 mV
T/C 4 Strt	1.170 mV	1.171 mV	1.160 mV	1.166 mV
T/C 5 Strt	1.170 mV	1.171 mV	1.160 mV	1.170 mV
T/C 6 Strt	1.170 mV	1.171 mV	1.160 mV	1.166 mV
T/C 7 Strt	1.224 mV	1.205 mV	1.210 mV	1.225 mV
T/C 1 End	1.190 mV	1.190 mV	1.175 mV	1.187 mV
T/C 2 End	1.186 mV	1.185 mV	1.171 mV	1.180 mV
T/C 3 End	1.170 mV	1.170 mV	1.165 mV	1.169 mV
T/C 4 End	1.174 mV	1.169 mV	1.163 mV	1.167 mV
T/C 5 End	1.174 mV	1.169 mV	1.163 mV	1.166 mV
T/C 6 End	1.174 mV	1.169 mV	1.163 mV	1.166 mV
T/C 7 End	1.225 mV	1.215 mV	1.235 mV	1.215 mV
Start Time	12:00	13:10	14:02	15:15
End Time	12:47	13:36	14:50	15:45

Date of Experiment 1986/ 3/13

MDEA Conc	0.0 wt%	Absorbing Gas	CO2
Piperazine Conc	0.0 kmol/m3	Surfactant	0.1000 wt%
Barometric Pressure	697.2 mm Hg	Rotameter Tube	603
Room Temperature	25.0 deg C	Nozzle Diam	0.60 mm
Manometer Right Leg	6.5 in H2O	Thermo Coarse	5.02
Manometer Left Leg	5.5 in H2O	Thermo Fine	0.0
Jet Elevation	87.400 cm	Feed Variac	0.0 %
North Pole	87.190 cm	Circ Variac	0.0 %
South Pole	82.060 cm		
Liquid Take-off	79.695 cm		

Flowmeter	30. mm	60. mm
SFM Volume	15. mL	15. mL

Time 1	50.79 s	38.65 s
Time 2	51.15 s	38.66 s
Time 3	50.81 s	38.77 s
Time 4	50.76 s	0.0 s
Time 5	50.82 s	0.0 s
Time 6	51.06 s	0.0 s
Time 7	51.09 s	0.0 s
Time 8	49.96 s	0.0 s
Time 9	50.78 s	0.0 s
Time 10	51.13 s	0.0 s
Time 11	51.09 s	0.0 s
Time 12	51.19 s	0.0 s
Time 13	50.97 s	0.0 s
Time 14	51.13 s	0.0 s

T/C 1 Strt	1.300 mV	1.250 mV
T/C 2 Strt	1.350 mV	1.290 mV
T/C 3 Strt	1.206 mV	1.222 mV
T/C 4 Strt	1.380 mV	1.378 mV
T/C 5 Strt	1.380 mV	1.378 mV
T/C 6 Strt	1.380 mV	1.378 mV
T/C 7 Strt	1.153 mV	1.165 mV
T/C 1 End	1.300 mV	1.250 mV
T/C 2 End	1.340 mV	1.290 mV
T/C 3 End	1.222 mV	1.222 mV
T/C 4 End	1.379 mV	1.378 mV
T/C 5 End	1.375 mV	1.378 mV
T/C 6 End	1.375 mV	1.378 mV
T/C 7 End	1.163 mV	1.165 mV

Start Time	11:45	12:40
End Time	12:20	12:40

Date of Experiment 1986/ 3/14

MDEA Conc	0.0 wt%	Absorbing Gas	CO2
Piperazine Conc	0.0 kmol/m3	Surfactant	0.1000 wt%
Barometric Pressure	698.3 mm Hg	Rotameter Tube	603
Room Temperature	22.5 deg C	Nozzle Diam	0.60 mm
Manometer Right Leg	6.5 in H2O	Thermo Coarse	5.10
Manometer Left Leg	5.5 in H2O	Thermo Fine	0.0
Jet Elevation	87.435 cm	Feed Variac	11.0 %
North Pole	87.225 cm	Circ Variac	0.0 %
South Pole	82.115 cm		
Liquid Take-off	79.700 cm		

Flowmeter	30. mm	60. mm	40. mm	50. mm
SFM Volume	15. mL	15. mL	15. mL	15. mL
Time 1	51.06 s	38.78 s	45.79 s	43.49 s
Time 2	51.12 s	38.83 s	45.09 s	43.59 s
Time 3	50.37 s	38.71 s	44.93 s	42.74 s
Time 4	50.80 s	38.78 s	45.06 s	42.[illegible] s
Time 5	50.57 s	38.75 s	44.33 s	42.[illegible]
Time 6	50.81 s	38.77 s	44.87 s	42.[illegible]
Time 7	50.82 s	38.69 s	45.62 s	42.[illegible]
Time 8	50.53 s	38.67 s	45.27 s	43.[illegible]
Time 9	50.81 s	38.80 s	[illegible]9 s	42.77 s
Time 10	51.00 s	38.93 s	[illegible]53 s	43.20 s
Time 11	50.73 s	39.21 s	[illegible]77 s	42.74 s
Time 12	50.66 s	39.33 s	[illegible]29 s	42.88 s
Time 13	51.17 s	39.27 s	[illegible]5.25 s	43.07 s
Time 14	0.0 s	38.66 s	[illegible]5.80 s	43.23 s
Time 15	0.0 s	38.96 s	45.74 s	43.53 s
Time 16	0.0 s	0.0 s	45.84 s	43.41 s
Time 17	0.0 s	0.0 s	45.94 s	43.56 s
Time 18	0.0 s	0.0 s	0.0 s	43.36 s
Time 19	0.0 s	0.0 s	0.0 s	43.66 s
T/C 1 Strt	1.290 mV	1.295 mV	1.296 mV	1.291 mV
T/C 2 Strt	1.355 mV	1.320 mV	1.330 mV	1.316 mV
T/C 3 Strt	1.240 mV	1.246 mV	1.248 mV	1.248 mV
T/C 4 Strt	1.369 mV	1.390 mV	1.357 mV	1.380 mV
T/C 5 Strt	1.369 mV	1.390 mV	1.358 mV	1.380 mV
T/C 6 Strt	1.375 mV	1.390 mV	1.358 mV	1.380 mV
T/C 7 Strt	1.179 mV	1.195 mV	1.212 mV	1.174 mV
T/C 1 End	1.290 mV	1.295 mV	1.281 mV	1.300 mV
T/C 2 End	1.340 mV	1.325 mV	1.312 mV	1.335 mV
T/C 3 End	1.245 mV	1.249 mV	1.254 mV	1.251 mV
T/C 4 End	1.365 mV	1.390 mV	1.365 mV	1.384 mV
T/C 5 End	1.365 mV	1.390 mV	1.365 mV	1.384 mV
T/C 6 End	1.366 mV	1.390 mV	1.365 mV	1.380 mV
T/C 7 End	1.160 mV	1.214 mV	1.189 mV	1.250 mV
Start Time	12:25	13:20	14:15	15:10
End Time	12:5[illegible]	13:55	14:47	15:50

Date of Experiment 1986/ 3/17

MDEA Conc	0.0 wt%	Absorbing Gas	CO2
Piperazine Conc	0.0 kmol/m3	Surfactant	0.1000 wt%
Barometric Pressure	701.7 mm Hg	Rotameter Tube	603
Room Temperature	23.0 deg C	Nozzle Diam	0.60 mm
Manometer Right Leg	-6.5 in H2O	Thermo Coarse	5.01
Manometer Left Leg	5.5 in H2O	Thermo Fine	0.0
Jet Elevation	87.380 cm	Feed Variac	0.0 %
North Pole	87.170 cm	Circ Variac	0.0 %
South Pole	82.065 cm		
Liquid Take-off	79.600 cm		

Flowmeter	40. mm	50. mm	60. mm
SFM Volume	15. mL	15. mL	20. mL
Time 1	45.26 s	41.71 s	50.99 s
Time 2	44.89 s	40.67 s	51.39 s
Time 3	45.06 s	40.75 s	51.44 s
Time 4	45.05 s	40.84 s	51.35 s
Time 5	44.81 s	41.06 s	51.36 s
Time 6	44.90 s	41.13 s	51.40 s
Time 7	44.73 s	41.52 s	51.42 s
Time 8	44.74 s	41.24 s	51.13 s
Time 9	45.04 s	40.72 s	50.91 s
Time 10	45.14 s	40.95 s	51.05 s
Time 11	45.34 s	41.09 s	50.97 s
Time 12	45.33 s	41.05 s	51.17 s
Time 13	45.40 s	41.85 s	51.15 s
Time 14	45.42 s	41.77 s	51.34 s
Time 15	45.40 s	41.56 s	51.36 s
Time 16	45.49 s	41.46 s	51.37 s
Time 17	45.30 s	41.78 s	51.41 s
Time 18	45.41 s	41.82 s	0.0 s
Time 19	0.0 s	41.69 s	0.0 s
Time 20	0.0 s	41.71 s	0.0 s
T/C 1 Strt	1.260 mV	1.280 mV	1.285 mV
T/C 2 Strt	1.324 mV	1.302 mV	1.306 mV
T/C 3 Strt	1.261 mV	1.269 mV	1.266 mV
T/C 4 Strt	1.365 mV	1.345 mV	1.367 mV
T/C 5 Strt	1.365 mV	1.345 mV	1.367 mV
T/C 6 Strt	1.366 mV	1.344 mV	1.367 mV
T/C 7 Strt	1.157 mV	1.205 mV	1.244 mV
T/C 1 End	1.271 mV	1.280 mV	1.268 mV
T/C 2 End	1.303 mV	1.303 mV	1.296 mV
T/C 3 End	1.267 mV	1.275 mV	1.266 mV
T/C 4 End	1.347 mV	1.358 mV	1.365 mV
T/C 5 End	1.347 mV	1.358 mV	1.365 mV
T/C 6 End	1.346 mV	1.357 mV	1.365 mV
T/C 7 End	1.190 mV	1.230 mV	1.210 mV
Start Time	12:00	13:25	15:00
End Time	12:40	14:10	15:35

Date of Experiment 1986/ 3/18

MDEA Conc	0.0 wt%	Absorbing Gas	CO2
Piperazine Conc	0.0 kmol/m3	Surfactant	0.1000 wt%
Barometric Pressure	703.8 mm Hg	Rotameter Tube	603
Room Temperature	22.5 deg C	Nozzle Diam	0.60 mm
Manometer Right Leg	6.5 in H2O	Thermo Coarse	5.10
Manometer Left Leg	5.5 in H2O	Thermo Fine	0.0
Jet Elevation	87.285 cm	Feed Variac	0.0 %
North Pole	87.060 cm	Circ Variac	0.0 %
South Pole	81.955 cm		
Liquid Take-off	79.540 cm		

Flowmeter	30. mm	40. mm
SFM Volume	25. mL	25. mL

Time 1	89.26 s	77.77 s
Time 2	88.28 s	77.65 s
Time 3	89.02 s	78.63 s
Time 4	88.67 s	78.83 s
Time 5	88.93 s	0.0 s
Time 6	88.92 s	0.0 s
Time 7	89.07 s	0.0 s
Time 8	89.67 s	0.0 s
Time 9	89.63 s	0.0 s
Time 10	89.13 s	0.0 s
Time 11	89.34 s	0.0 s
Time 12	89.27 s	0.0 s

T/C 1 Strt	1.290 mV	1.280 mV
T/C 2 Strt	1.335 mV	1.316 mV
T/C 3 Strt	1.256 mV	1.240 mV
T/C 4 Strt	1.[illegible] mV	1.361 mV
T/C 5 Strt	1.[illegible] mV	1.361 mV
T/C 6 Strt	1.365 mV	1.361 mV
T/C 7 Strt	1.121 mV	1.175 mV
T/C 1 End	1.285 mV	1.280 mV
T/C 2 End	1.321 mV	1.316 mV
T/C 3 End	1.260 mV	1.240 mV
T/C 4 End	1.360 mV	1.361 mV
T/C 5 End	1.360 mV	1.361 mV
T/C 6 End	1.360 mV	1.361 mV
T/C 7 End	1.175 mV	1.175 mV

Start Time	12:00	13:05
End Time	12:30	13:15

Date of Experiment 1986/ 3/19

MDEA Conc	0.0 wt%	Absorbing Gas	CO2
Piperazine Conc	0.0 kmol/m3	Surfactant	0.1000 wt%
Barometric Pressure	706.4 mm Hg	Rotameter Tube	603
Room Temperature	22.5 deg C	Nozzle Diam	0.60 mm
Manometer Right Leg	6.5 in H2O	Thermo Coarse	5.00
Manometer Left Leg	5.5 in H2O	Thermo Fine	0.0
Jet Elevation	87.270 cm	Feed Variac	0.0 %
North Pole	87.060 cm	Circ Variac	0.0 %
South Pole	81.940 cm		
Liquid Take-off	79.590 cm		

Flowmeter	30. mm	40. mm	50. mm
SFM Volume	25. mL	25. mL	25. mL
Time 1	85.45 s	74.05 s	68.08 s
Time 2	85.30 s	74.30 s	68.24 s
Time 3	85.33 s	74.76 s	68.23 s
Time 4	85.57 s	74.83 s	68.35 s
Time 5	85.86 s	74.86 s	68.44 s
Time 6	85.62 s	74.95 s	68.88 s
Time 7	85.46 s	74.92 s	68.38 s
Time 8	85.47 s	75.05 s	68.87 s
Time 9	86.27 s	75.44 s	68.61 s
Time 10	86.34 s	74.87 s	69.07 s
Time 11	85.70 s	75.03 s	69.14 s
Time 12	86.14 s	75.47 s	68.79 s
Time 13	85.92 s	75.57 s	68.86 s
Time 14	86.80 s	75.71 s	68.81 s
Time 15	0.0 s	75.88 s	69.06 s
Time 16	0.0 s	75.59 s	69.45 s
T/C 1 Strt	1.286 mV	1.250 mV	1.275 mV
T/C 2 Strt	1.336 mV	1.280 mV	1.295 mV
T/C 3 Strt	1.265 mV	1.270 mV	1.287 mV
T/C 4 Strt	1.305 mV	1.300 mV	1.305 mV
T/C 5 Strt	1.365 mV	1.300 mV	1.305 mV
T/C 6 Strt	1.365 mV	1.300 mV	1.305 mV
T/C 7 Strt	1.080 mV	1.170 mV	1.255 mV
T/C 1 End	1.287 mV	1.260 mV	1.270 mV
T/C 2 End	1.324 mV	1.280 mV	1.280 mV
T/C 3 End	1.279 mV	1.277 mV	1.285 mV
T/C 4 End	1.365 mV	1.302 mV	1.296 mV
T/C 5 End	1.365 mV	1.302 mV	1.296 mV
T/C 6 End	1.365 mV	1.302 mV	1.296 mV
T/C 7 End	1.180 mV	1.225 mV	1.263 mV
Start Time	12:10	13:30	15:05
End Time	12:50	14:10	15:35

Date of Experiment 1986/ 3/21

MDEA Conc	0.0 wt%	Absorbing Gas	CO2
Piperazine Conc	0.0 kmol/m3	Surfactant	0.1000 wt%
Barometric Pressure	691.9 mm Hg	Rotameter Tube	603
Room Temperature	23.0 deg C	Nozzle Diam	0.60 mm
Manometer Right Leg	6.5 in H2O	Thermo Coarse	5.01
Manometer Left Leg	5.5 in H2O	Thermo Fine	0.0
Jet Elevation	87.270 cm	Feed Variac	0.0 %
North Pole	87.045 cm	Circ Variac	0.0 %
South Pole	81.950 cm		
Liquid Take-off	79.540 cm		

Flowmeter	30. mm	40. mm	50. mm
SFM Volume	15. mL	15. mL	15. mL
Time 1	50.95 s	45.48 s	41.70 s
Time 2	51.38 s	45.56 s	41.92 s
Time 3	51.04 s	45.76 s	41.33 s
Time 4	51.14 s	45.12 s	42.00 s
Time 5	51.01 s	44.91 s	42.02 s
Time 6	51.27 s	45.64 s	41.56 s
Time 7	51.37 s	46.14 s	42.11 s
Time 8	50.82 s	45.63 s	41.99 s
Time 9	51.95 s	45.37 s	42.21 s
Time 10	51.09 s	45.97 s	42.47 s
Time 11	50.87 s	46.09 s	42.46 s
Time 12	51.74 s	45.87 s	42.34 s
Time 13	51.01 s	45.79 s	42.21 s
Time 14	0.0 s	45.43 s	42.38 s
Time 15	0.0 s	45.54 s	42.09 s
Time 16	0.0 s	45.73 s	42.09 s
T/C 1 Strt	1.275 mV	1.267 mV	1.282 mV
T/C 2 Strt	1.325 mV	1.301 mV	1.305 mV
T/C 3 Strt	1.266 mV	1.259 mV	1.279 mV
T/C 4 Strt	1.340 mV	1.332 mV	1.350 mV
T/C 5 Strt	1.340 mV	1.332 mV	1.351 mV
T/C 6 Strt	1.340 mV	1.332 mV	1.351 mV
T/C 7 Strt	1.156 mV	1.165 mV	1.195 mV
T/C 1 End	1.284 mV	1.286 mV	1.285 mV
T/C 2 End	1.309 mV	1.300 mV	1.306 mV
T/C 3 End	1.261 mV	1.260 mV	1.280 mV
T/C 4 End	1.336 mV	1.341 mV	1.346 mV
T/C 5 End	1.336 mV	1.341 mV	1.346 mV
T/C 6 End	1.336 mV	1.341 mV	1.346 mV
T/C 7 End	1.207 mV	1.216 mV	1.250 mV
Start Time	11:50	13:05	14:25
End Time	12:25	13:45	15:00

Date of Experiment 1986/ 3/25

MDEA Conc	0.0 wt%	Absorbing Gas	CO2
Piperazine Conc	0.0 kmol/m3	Surfactant	0.1000 wt%
Barometric Pressure	700.9 mm Hg	Rotameter Tube	603
Room Temperature	22.5 deg C	Nozzle Diam	0.60 mm
Manometer Right Leg	6.5 in H2O	Thermo Coarse	5.01
Manometer Left Leg	5.5 in H2O	Thermo Fine	0.0
Jet Elevation	87.235 cm	Feed Variac	0.0 %
North Pole	87.025 cm	Circ Variac	0.0 %
South Pole	81.860 cm		
Liquid Take-off	79.525 cm		

Flowmeter	30. mm	40. mm	50. mm
SFM Volume	15. mL	15. mL	15. mL
Time 1	50.03 s	44.33 s	40.57 s
Time 2	50.34 s	44.18 s	40.40 s
Time 3	50.41 s	44.24 s	40.56 s
Time 4	50.44 s	44.35 s	40.56 s
Time 5	50.24 s	44.26 s	40.54 s
Time 6	50.31 s	44.57 s	40.56 s
Time 7	50.35 s	44.53 s	40.80 s
Time 8	50.47 s	44.63 s	40.86 s
Time 9	50.60 s	44.34 s	40.27 s
Time 10	50.51 s	44.67 s	40.29 s
Time 11	50.43 s	44.09 s	40.65 s
Time 12	50.63 s	44.27 s	40.55 s
Time 13	50.48 s	44.27 s	40.75 s
Time 14	50.52 s	0.0 s	40.60 s
Time 15	50.24 s	0.0 s	40.23 s
T/C 1 Strt	1.280 mV	1.290 mV	1.296 mV
T/C 2 Strt	1.316 mV	1.306 mV	1.315 mV
T/C 3 Strt	1.253 mV	1.250 mV	1.246 mV
T/C 4 Strt	1.345 mV	1.347 mV	1.337 mV
T/C 5 Strt	1.345 mV	1.347 mV	1.337 mV
T/C 6 Strt	1.345 mV	1.347 mV	1.337 mV
T/C 7 Strt	1.136 mV	1.225 mV	1.274 mV
T/C 1 End	1.285 mV	1.306 mV	1.290 mV
T/C 2 End	1.315 mV	1.325 mV	1.311 mV
T/C 3 End	1.250 mV	1.255 mV	1.246 mV
T/C 4 End	1.345 mV	1.342 mV	1.336 mV
T/C 5 End	1.345 mV	1.342 mV	1.336 mV
T/C 6 End	1.345 mV	1.342 mV	1.336 mV
T/C 7 End	1.201 mV	1.254 mV	1.263 mV
Start Time	11:40	12:50	13:55
End Time	12:05	13:13	14:25

Date of Experiment 1986/ 3/27

MDEA Conc	0.0 wt%	Absorbing Gas	CO2
Piperazine Conc	0.0 kmol/m3	Surfactant	0.1000 wt%
Barometric Pressure	692.0 mm Hg	Rotameter Tube	603
Room Temperature	23.0 deg C	Nozzle Diam	0.60 mm
Manometer Right Leg	6.5 in H2O	Thermo Coarse	5.01
Manometer Left Leg	5.5 in H2O	Thermo Fine	0.0
Jet Elevation	87.265 cm	Feed Variac	0.0 %
North Pole	87.060 cm	Circ Variac	0.0 %
South Pole	81.970 cm		
Liquid Take-off	79.570 cm		

Flowmeter	30. mm
SFM Volume	15. mL

Time 1	50.02 s
Time 2	50.10 s
Time 3	66.25 s
Time 4	66.34 s
Time 5	66.90 s
Time 6	66.56 s
Time 7	67.02 s
Time 8	66.67 s
Time 9	66.61 s
Time 10	67.06 s
Time 11	66.73 s
Time 12	67.08 s
Time 13	67.45 s
Time 14	66.67 s
Time 15	67.02 s
Time 16	66.83 s

T/C 1 Strt	1.291 mV
T/C 2 Strt	1.316 mV
T/C 3 Strt	1.259 mV
T/C 4 Strt	1.335 mV
T/C 5 Strt	1.333 mV
T/C 6 Strt	1.333 mV
T/C 7 Strt	1.211 mV
T/C 1 End	1.290 mV
T/C 2 End	1.314 mV
T/C 3 End	1.260 mV
T/C 4 End	1.333 mV
T/C 5 End	1.333 mV
T/C 6 End	1.333 mV
T/C 7 End	1.246 mV

Start Time	12:00
End Time	12:37

Date of Experiment 1986/ 4/ 2

MDEA Conc	0.0 wt%	Absorbing Gas	CO2
Piperazine Conc	0.0 kmol/m3	Surfactant	0.1000 wt%
Barometric Pressure	708.8 mm Hg	Rotameter Tube	603
Room Temperature	22.0 deg C	Nozzle Diam	0.60 mm
Manometer Right Leg	6.5 in H2O	Thermo Coarse	5.01
Manometer Left Leg	5.5 in H2O	Thermo Fine	0.0
Jet Elevation	87.335 cm	Feed Variac	0.0 %
North Pole	87.130 cm	Circ Variac	0.0 %
South Pole	82.000 cm		
Liquid Take-off	79.570 cm		

Flowmeter	30. mm	40. mm
SFM Volume	15. mL	15. mL

Time 1	51.66 s	45.42 s
Time 2	51.02 s	46.07 s
Time 3	51.60 s	45.83 s
Time 4	50.56 s	46.02 s
Time 5	51.90 s	45.73 s
Time 6	51.70 s	45.74 s
Time 7	51.57 s	45.77 s
Time 8	50.95 s	45.70 s
Time 9	51.19 s	45.58 s
Time 10	50.93 s	45.88 s
Time 11	51.57 s	45.92 s
Time 12	50.77 s	45.84 s
Time 13	51.61 s	0.0 s

T/C 1 Strt	1.265 mV	1.285 mV
T/C 2 Strt	1.302 mV	1.305 mV
T/C 3 Strt	1.229 mV	1.230 mV
T/C 4 Strt	1.336 mV	1.344 mV
T/C 5 Strt	1.336 mV	1.344 mV
T/C 6 Strt	1.336 mV	1.344 mV
T/C 7 Strt	1.110 mV	1.242 mV
T/C 1 End	1.265 mV	1.275 mV
T/C 2 End	1.300 mV	1.300 mV
T/C 3 End	1.229 mV	1.230 mV
T/C 4 End	1.336 mV	1.339 mV
T/C 5 End	1.336 mV	1.339 mV
T/C 6 End	1.336 mV	1.339 mV
T/C 7 End	1.160 mV	1.183 mV

Start Time	11:40	12:51
End Time	12:13	13:15

Date of Experiment 1986/ 4/ 8

MDEA Conc	20.0 wt%	Absorbing Gas	CO2
Piperazine Conc	0.0 kmol/m3	Surfactant	0.0100 wt%
Barometric Pressure	700.6 mm Hg	Rotameter Tube	603
Room Temperature	24.0 deg C	Nozzle Diam	0.60 mm
Manometer Right Leg	6.5 in H2O	Thermo Coarse	5.01
Manometer Left Leg	5.5 in H2O	Thermo Fine	0.0
Jet Elevation	87.525 cm	Feed Variac	0.0 %
North Pole	87.315 cm	Circ Variac	0.0 %
South Pole	82.175 cm		
Liquid Take-off	77.790 cm		

Flowmeter	30. mm	40. mm	50. mm
SFM Volume	25. mL	25. mL	25. mL
Time 1	46.71 s	45.38 s	43.65 s
Time 2	46.79 s	45.54 s	43.66 s
Time 3	46.95 s	45.47 s	43.68 s
Time 4	46.83 s	45.59 s	44.10 s
Time 5	46.74 s	45.64 s	43.99 s
Time 6	46.73 s	45.62 s	43.82 s
Time 7	47.04 s	45.44 s	43.73 s
Time 8	46.82 s	45.60 s	43.90 s
Time 9	46.99 s	45.68 s	43.79 s
Time 10	47.02 s	45.63 s	43.62 s
Time 11	47.00 s	45.60 s	43.80 s
Time 12	47.02 s	45.48 s	43.77 s
Time 13	47.87 s	45.75 s	43.74 s
Time 14	46.91 s	45.68 s	43.88 s
Time 15	46.80 s	0.0 s	43.77 s
Time 16	47.11 s	0.0 s	43.74 s
Time 17	0.0 s	0.0 s	43.59 s
Time 18	0.0 s	0.0 s	43.72 s
T/C 1 Strt	1.270 mV	1.280 mV	1.290 mV
T/C 2 Strt	1.336 mV	1.321 mV	1.325 mV
T/C 3 Strt	1.275 mV	1.296 mV	1.306 mV
T/C 4 Strt	1.305 mV	1.310 mV	1.340 mV
T/C 5 Strt	1.305 mV	1.310 mV	1.340 mV
T/C 6 Strt	1.305 mV	1.310 mV	1.340 mV
T/C 7 Strt	1.176 mV	1.200 mV	1.241 mV
T/C 1 End	1.270 mV	1.290 mV	1.295 mV
T/C 2 End	1.322 mV	1.320 mV	1.326 mV
T/C 3 End	1.275 mV	1.302 mV	1.309 mV
T/C 4 End	1.295 mV	1.334 mV	1.340 mV
T/C 5 End	1.293 mV	1.332 mV	1.340 mV
T/C 6 End	1.295 mV	1.330 mV	1.340 mV
T/C 7 End	1.196 mV	1.205 mV	1.230 mV
Start Time	11:45	13:00	14:20
End Time	12:10	13:30	14:40

Date of Experiment 1986/ 4/ 9

MDEA Conc	20.0 wt%	Absorbing Gas	CO2
Piperazine Conc	0.0 kmol/m3	Surfactant	0.0100 wt%
Barometric Pressure	706.7 mm Hg	Rotameter Tube	603
Room Temperature	23.0 deg C	Nozzle Diam	0.60 mm
Manometer Right Leg	6.5 in H2O	Thermo Coarse	5.01
Manometer Left Leg	5.5 in H2O	Thermo Fine	0.0
Jet Elevation	87.675 cm	Feed Variac	0.0 %
North Pole	87.465 cm	Circ Variac	0.0 %
South Pole	82.315 cm		
Liquid Take-off	79.910 cm		

Flowmeter	40. mm	50. mm	60. mm
SFM Volume	25. mL	25. mL	25. mL
Time 1	45.56 s	44.71 s	43.83 s
Time 2	45.50 s	44.38 s	43.83 s
Time 3	45.31 s	44.71 s	43.79 s
Time 4	45.53 s	44.48 s	43.91 s
Time 5	45.57 s	44.55 s	43.80 s
Time 6	45.66 s	44.30 s	43.91 s
Time 7	45.64 s	44.59 s	43.74 s
Time 8	45.56 s	44.31 s	43.74 s
Time 9	45.63 s	44.48 s	43.81 s
Time 10	45.59 s	44.38 s	43.69 s
Time 11	45.84 s	44.52 s	43.84 s
Time 12	45.59 s	44.52 s	43.77 s
Time 13	45.51 s	44.45 s	43.74 s
Time 14	45.61 s	44.32 s	43.80 s
Time 15	45.63 s	44.45 s	43.81 s
Time 16	0.0 s	44.40 s	43.80 s
T/C 1 Strt	1.279 mV	1.290 mV	1.277 mV
T/C 2 Strt	1.330 mV	1.315 mV	1.312 mV
T/C 3 Strt	1.250 mV	1.250 mV	1.245 mV
T/C 4 Strt	1.335 mV	1.329 mV	1.327 mV
T/C 5 Strt	1.333 mV	1.329 mV	1.327 mV
T/C 6 Strt	1.333 mV	1.329 mV	1.325 mV
T/C 7 Strt	1.132 mV	1.257 mV	1.226 mV
T/C 1 End	1.273 mV	1.290 mV	1.277 mV
T/C 2 End	1.322 mV	1.319 mV	1.312 mV
T/C 3 End	1.255 mV	1.252 mV	1.245 mV
T/C 4 End	1.331 mV	1.327 mV	1.327 mV
T/C 5 End	1.330 mV	1.327 mV	1.327 mV
T/C 6 End	1.330 mV	1.327 mV	1.325 mV
T/C 7 End	1.130 mV	1.250 mV	1.226 mV
Start Time	11:35	12:45	14:05
End Time	11:55	13:15	14:30

Date of Experiment 1986/ 4/10

MDEA Conc	20.0 wt%	Absorbing Gas	CO2
Piperazine Conc	0.0 kmol/m3	Surfactant	0.0100 wt%
Barometric Pressure	704.0 mm Hg	Rotameter Tube	603
Room Temperature	23.0 deg C	Nozzle Diam	0.60 mm
Manometer Right Leg	6.5 in H2O	Thermo Coarse	5.04
Manometer Left Leg	5.5 in H2O	Thermo Fine	0.0
Jet Elevation	87.495 cm	Feed Variac	0.0 %
North Pole	87.285 cm	Circ Variac	0.0 %
South Pole	82.150 cm		
Liquid Take-off	79.785 cm		

Flowmeter	30. mm	40. mm	50. mm
SFM Volume	25. mL	25. mL	25. mL
Time 1	45.50 s	43.42 s	42.73 s
Time 2	45.30 s	43.52 s	42.54 s
Time 3	45.70 s	43.63 s	42.52 s
Time 4	45.70 s	43.48 s	42.41 s
Time 5	45.56 s	43.66 s	42.40 s
Time 6	45.59 s	43.64 s	42.41 s
Time 7	45.58 s	43.68 s	42.43 s
Time 8	45.65 s	43.46 s	42.33 s
Time 9	45.59 s	43.49 s	42.66 s
Time 10	45.66 s	43.51 s	42.68 s
Time 11	45.47 s	43.36 s	42.70 s
Time 12	45.44 s	43.48 s	42.53 s
Time 13	45.58 s	43.52 s	42.60 s
Time 14	45.66 s	43.42 s	42.59 s
Time 15	45.51 s	43.43 s	42.59 s
Time 16	45.63 s	43.55 s	42.59 s
Time 17	45.56 s	0.0 s	42.48 s
Time 18	0.0 s	0.0 s	42.53 s
T/C 1 Strt	1.290 mV	1.275 mV	1.276 mV
T/C 2 Strt	1.300 mV	1.321 mV	1.317 mV
T/C 3 Strt	1.120 mV	1.128 mV	1.118 mV
T/C 4 Strt	1.333 mV	1.345 mV	1.346 mV
T/C 5 Strt	1.337 mV	1.345 mV	1.346 mV
T/C 6 Strt	1.327 mV	1.345 mV	1.344 mV
T/C 7 Strt	1.140 mV	1.170 mV	1.201 mV
T/C 1 End	1.290 mV	1.279 mV	1.266 mV
T/C 2 End	1.320 mV	1.324 mV	1.315 mV
T/C 3 End	1.121 mV	1.125 mV	1.113 mV
T/C 4 End	1.336 mV	1.345 mV	1.346 mV
T/C 5 End	1.340 mV	1.345 mV	1.346 mV
T/C 6 End	1.334 mV	1.345 mV	1.342 mV
T/C 7 End	1.140 mV	1.170 mV	1.206 mV
Start Time	12:20	13:40	14:41
End Time	12:49	14:00	15:05

Date of Experiment 1986/ 4/14

MDEA Conc	20.0 wt%	Absorbing Gas	CO2
Piperazine Conc	0.0 kmol/m3	Surfactant	0.0100 wt%
Barometric Pressure	707.8 mm Hg	Rotameter Tube	603
Room Temperature	23.0 deg C	Nozzle Diam	0.60 mm
Manometer Right Leg	6.5 in H2O	Thermo Coarse	5.04
Manometer Left Leg	5.5 in H2O	Thermo Fine	0.0
Jet Elevation	87.475 cm	Feed Variac	0.0 %
North Pole	87.270 cm	Circ Variac	0.0 %
South Pole	82.120 cm		
Liquid Take-off	79.720 cm		

Flowmeter	30. mm	40. mm	50. mm
SFM Volume	25. mL	25. mL	25. mL
Time 1	45.27 s	43.53 s	42.47 s
Time 2	45.28 s	43.73 s	42.48 s
Time 3	45.14 s	43.66 s	42.49 s
Time 4	45.16 s	43.64 s	42.42 s
Time 5	45.19 s	43.66 s	42.48 s
Time 6	45.31 s	43.38 s	42.38 s
Time 7	45.41 s	43.70 s	42.39 s
Time 8	45.60 s	43.47 s	42.45 s
Time 9	45.48 s	43.45 s	42.24 s
Time 10	45.24 s	43.53 s	42.28 s
Time 11	45.25 s	43.51 s	42.44 s
Time 12	45.34 s	43.53 s	42.36 s
Time 13	45.36 s	43.39 s	42.42 s
Time 14	45.37 s	43.24 s	42.41 s
Time 15	45.39 s	43.38 s	42.38 s
Time 16	45.37 s	43.51 s	42.49 s
Time 17	45.29 s	43.36 s	42.42 s
Time 18	45.35 s	0.0 s	42.39 s
Time 19	0.0 s	0.0 s	42.42 s
T/C 1 Strt	1.275 mV	1.275 mV	1.278 mV
T/C 2 Strt	1.340 mV	1.320 mV	1.321 mV
T/C 3 Strt	1.120 mV	1.125 mV	1.127 mV
T/C 4 Strt	1.330 mV	1.350 mV	1.356 mV
T/C 5 Strt	1.330 mV	1.350 mV	1.356 mV
T/C 6 Strt	1.330 mV	1.350 mV	1.356 mV
T/C 7 Strt	1.070 mV	1.145 mV	1.179 mV
T/C 1 End	1.272 mV	1.280 mV	1.275 mV
T/C 2 End	1.320 mV	1.325 mV	1.325 mV
T/C 3 End	1.122 mV	1.130 mV	1.133 mV
T/C 4 End	1.312 mV	1.355 mV	1.357 mV
T/C 5 End	1.312 mV	1.355 mV	1.358 mV
T/C 6 End	1.312 mV	1.355 mV	1.358 mV
T/C 7 End	1.065 mV	1.169 mV	1.188 mV
Start Time	12:10	13:45	14:55
End Time	13:00	14:07	15:20

Date of Experiment 1986/ 4/15

MDEA Conc	20.0 wt%	Absorbing Gas	CO2
Piperazine Conc	0.0 kmol/m3	Surfactant	0.0100 wt%
Barometric Pressure	700.8 mm Hg	Rotameter Tube	603
Room Temperature	23.0 deg C	Nozzle Diam	0.60 mm
Manometer Right Leg	6.5 in H2O	Thermo Coarse	5.04
Manometer Left Leg	5.5 in H2O	Thermo Fine	0.0
Jet Elevation	87.520 cm	Feed Variac	0.0 %
North Pole	87.300 cm	Circ Variac	0.0 %
South Pole	82.165 cm		
Liquid Take-off	79.770 cm		

Flowmeter	30. mm	40. mm	50. mm
SFM Volume	25. mL	25. mL	25. mL
Time 1	45.25 s	43.84 s	42.40 s
Time 2	45.28 s	43.88 s	42.46 s
Time 3	45.58 s	43.74 s	42.34 s
Time 4	45.20 s	43.68 s	42.49 s
Time 5	45.22 s	43.67 s	42.41 s
Time 6	45.37 s	43.74 s	42.41 s
Time 7	45.32 s	43.63 s	42.39 s
Time 8	45.40 s	43.66 s	42.47 s
Time 9	45.28 s	43.60 s	42.38 s
Time 10	45.44 s	43.65 s	42.48 s
Time 11	45.32 s	43.58 s	42.55 s
Time 12	45.22 s	43.30 s	42.39 s
Time 13	45.27 s	43.62 s	42.31 s
Time 14	45.43 s	43.52 s	42.49 s
Time 15	45.36 s	43.60 s	42.33 s
Time 16	45.27 s	43.63 s	42.40 s
Time 17	45.35 s	43.67 s	42.38 s
Time 18	0.0 s	43.46 s	42.43 s
T/C 1 Strt	1.266 mV	1.276 mV	1.275 mV
T/C 2 Strt	1.330 mV	1.320 mV	1.320 mV
T/C 3 Strt	1.130 mV	1.131 mV	1.128 mV
T/C 4 Strt	1.316 mV	1.350 mV	1.356 mV
T/C 5 Strt	1.316 mV	1.350 mV	1.356 mV
T/C 6 Strt	1.316 mV	1.350 mV	1.356 mV
T/C 7 Strt	1.075 mV	1.152 mV	1.190 mV
T/C 1 End	1.265 mV	1.285 mV	1.276 mV
T/C 2 End	1.320 mV	1.324 mV	1.321 mV
T/C 3 End	1.135 mV	1.132 mV	1.132 mV
T/C 4 End	1.310 mV	1.350 mV	1.355 mV
T/C 5 End	1.310 mV	1.354 mV	1.360 mV
T/C 6 End	1.310 mV	1.350 mV	1.355 mV
T/C 7 End	1.077 mV	1.160 mV	1.190 mV
Start Time	11:15	12:35	13:45
End Time	11:40	13:00	14:10

Date of Experiment 1986/ 4/16

MDEA Conc	20.0	wt%	Absorbing Gas	CO2	
Piperazine Conc	0.0	kmol/m3	Surfactant	0.0100	wt%
Barometric Pressure	695.4	mm Hg	Rotameter Tube	603	
Room Temperature	23.0	deg C	Nozzle Diam	0.60	mm
Manometer Right Leg	6.5	in H2O	Thermo Coarse	5.03	
Manometer Left Leg	5.5	in H2O	Thermo Fine	0.0	
Jet Elevation	87.435	cm	Feed Variac	0.0	%
North Pole	87.215	cm	Circ Variac	0.0	%
South Pole	82.070	cm			
Liquid Take-off	79.660	cm			

Flowmeter	30.	mm
SFM Volume	25.	mL

Time 1	45.37	s
Time 2	45.27	s
Time 3	45.45	s
Time 4	45.28	s
Time 5	45.25	s
Time 6	45.47	s
Time 7	45.33	s
Time 8	45.36	s
Time 9	45.39	s
Time 10	45.35	s
Time 11	45.33	s
Time 12	45.36	s
Time 13	45.34	s
Time 14	45.31	s
Time 15	45.20	s
Time 16	45.21	s
Time 17	45.28	s
Time 18	45.31	s

T/C 1 Strt	1.261	mV
T/C 2 Strt	1.320	mV
T/C 3 Strt	1.140	mV
T/C 4 Strt	1.310	mV
T/C 5 Strt	1.311	mV
T/C 6 Strt	1.311	mV
T/C 7 Strt	1.050	mV
T/C 1 End	1.265	mV
T/C 2 End	1.316	mV
T/C 3 End	1.151	mV
T/C 4 End	1.310	mV
T/C 5 End	1.310	mV
T/C 6 End	1.310	mV
T/C 7 End	1.075	mV

Start Time	10:55
End Time	11:23

Date of Experiment 1986/ 4/18

MDEA Conc	20.0 wt%	Absorbing Gas	CO2
Piperazine Conc	0.0 kmol/m3	Surfactant	0.0100 wt%
Barometric Pressure	700.8 mm Hg	Rotameter Tube	603
Room Temperature	24.0 deg C	Nozzle Diam	0.60 mm
Manometer Right Leg	6.5 in H2O	Thermo Coarse	5.51
Manometer Left Leg	5.5 in H2O	Thermo Fine	0.0
Jet Elevation	87.635 cm	Feed Variac	60.0 %
North Pole	87.420 cm	Circ Variac	105.0 %
South Pole	82.300 cm		
Liquid Take-off	79.875 cm		

Flowmeter	30. mm	40. mm	40. mm	50. mm
SFM Volume	25. mL	25. mL	25. mL	25. mL
Time 1	28.03 s	26.91 s	27.33 s	25.91 s
Time 2	28.13 s	26.95 s	27.41 s	25.94 s
Time 3	28.14 s	26.92 s	27.50 s	25.94 s
Time 4	27.98 s	26.99 s	27.41 s	26.02 s
Time 5	27.96 s	27.10 s	27.39 s	26.07 s
Time 6	28.05 s	27.00 s	27.59 s	25.91 s
Time 7	28.09 s	26.97 s	27.32 s	25.99 s
Time 8	27.95 s	26.99 s	27.42 s	25.99 s
Time 9	28.06 s	26.84 s	27.49 s	26.00 s
Time 10	28.04 s	26.93 s	27.52 s	26.06 s
Time 11	28.11 s	26.91 s	27.59 s	26.03 s
Time 12	28.07 s	26.91 s	27.32 s	26.04 s
Time 13	27.15 s	27.09 s	27.40 s	25.90 s
Time 14	27.95 s	27.07 s	27.29 s	26.02 s
Time 15	27.94 s	0.0 s	27.53 s	25.92 s
Time 16	28.03 s	0.0 s	27.41 s	26.13 s
Time 17	27.94 s	0.0 s	0.0 s	25.87 s
Time 18	27.98 s	0.0 s	0.0 s	26.03 s
Time 19	27.98 s	0.0 s	0.0 s	0.0 s
Time 20	28.06 s	0.0 s	0.0 s	0.0 s
T/C 1 Strt	3.928 mV	3.917 mV	3.916 mV	3.910 mV
T/C 2 Strt	3.965 mV	3.955 mV	3.952 mV	3.946 mV
T/C 3 Strt	1.175 mV	1.160 mV	1.150 mV	1.140 mV
T/C 4 Strt	3.956 mV	3.955 mV	3.957 mV	3.960 mV
T/C 5 Strt	3.990 mV	3.990 mV	3.990 mV	3.990 mV
T/C 6 Strt	3.935 mV	3.935 mV	3.935 mV	3.937 mV
T/C 7 Strt	3.130 mV	3.297 mV	3.285 mV	3.380 mV
T/C 1 End	3.926 mV	3.916 mV	3.916 mV	3.908 mV
T/C 2 End	3.963 mV	3.952 mV	3.955 mV	3.945 mV
T/C 3 End	1.171 mV	1.150 mV	1.147 mV	1.137 mV
T/C 4 End	3.951 mV	3.957 mV	3.957 mV	3.960 mV
T/C 5 End	3.990 mV	3.990 mV	3.990 mV	3.992 mV
T/C 6 End	3.933 mV	3.935 mV	3.933 mV	3.935 mV
T/C 7 End	3.120 mV	3.285 mV	3.283 mV	3.380 mV
Start Time	11:30	12:55	13:15	14:30
End Time	12:00	13:15	13:35	14:55

Date of Experiment 1986/ 4/21

MDEA Conc	20.0 wt%	Absorbing Gas	CO2
Piperazine Conc	0.0 kmol/m3	Surfactant	0.0100 wt%
Barometric Pressure	698.5 mm Hg	Rotameter Tube	603
Room Temperature	23.0 deg C	Nozzle Diam	0.60 mm
Manometer Right Leg	6.5 in H2O	Thermo Coarse	5.51
Manometer Left Leg	5.5 in H2O	Thermo Fine	0.0
Jet Elevation	87.645 cm	Feed Variac	0.0 %
North Pole	87.440 cm	Circ Variac	0.0 %
South Pole	82.325 cm		
Liquid Take-off	79.905 cm		

Flowmeter	30. mm	40. mm	50. mm
SFM Volume	25. mL	25. mL	25. mL
Time 1	27.99 s	26.95 s	26.07 s
Time 2	28.06 s	26.97 s	26.01 s
Time 3	27.98 s	26.81 s	25.95 s
Time 4	28.11 s	26.85 s	25.91 s
Time 5	27.96 s	27.09 s	25.98 s
Time 6	27.91 s	27.01 s	26.03 s
Time 7	27.91 s	26.83 s	26.01 s
Time 8	27.98 s	26.94 s	26.01 s
Time 9	27.87 s	26.93 s	26.10 s
Time 10	27.86 s	26.92 s	25.95 s
Time 11	28.11 s	26.99 s	26.02 s
Time 12	27.93 s	27.13 s	26.06 s
Time 13	27.95 s	27.06 s	25.91 s
Time 14	28.10 s	27.05 s	25.97 s
Time 15	28.13 s	26.95 s	26.13 s
Time 16	28.12 s	27.07 s	25.86 s
Time 17	28.05 s	27.06 s	0.0 s
T/C 1 Strt	3.925 mV	3.924 mV	3.915 mV
T/C 2 Strt	3.965 mV	3.962 mV	3.950 mV
T/C 3 Strt	1.144 mV	1.162 mV	1.175 mV
T/C 4 Strt	3.960 mV	3.960 mV	3.960 mV
T/C 5 Strt	3.987 mV	3.993 mV	3.992 mV
T/C 6 Strt	3.942 mV	3.940 mV	3.940 mV
T/C 7 Strt	3.142 mV	3.306 mV	3.400 mV
T/C 1 End	3.920 mV	3.922 mV	3.915 mV
T/C 2 End	3.962 mV	3.965 mV	3.950 mV
T/C 3 End	1.155 mV	1.170 mV	1.180 mV
T/C 4 End	3.960 mV	3.960 mV	3.962 mV
T/C 5 End	3.991 mV	3.995 mV	3.992 mV
T/C 6 End	3.941 mV	3.940 mV	3.943 mV
T/C 7 End	3.144 mV	3.340 mV	3.395 mV
Start Time	11:15	12:40	13:55
End Time	11:45	13:05	14:25

Date of Experiment 1986/ 4/25

MDEA Conc	20.0 wt%	Absorbing Gas	CO2
Piperazine Conc	0.0. kmol/m3	Surfactant	0.0100 wt%
Barometric Pressure	697.4 mm Hg	Rotameter Tube	603
Room Temperature	24.0 deg C	Nozzle Diam	0.60 mm
Manometer Right Leg	6.4 in H2O	Thermo Coarse	5.27
Manometer Left Leg	5.6 in H2O	Thermo Fine	0.0
Jet Elevation	87.525 cm	Feed Variac	0.0 %
North Pole	87.320 cm	Circ Variac	100.0 %
South Pole	82.180 cm		
Liquid Take-off	79.780 cm		

Flowmeter 50. mm
SFM Volume 25. mL

Time	1	27.20 s
Time	2	27.27 s
Time	3	27.35 s
Time	4	27.25 s
Time	5	27.40 s
Time	6	27.26 s
Time	7	27.34 s
Time	8	27.34 s
Time	9	27.23 s
Time	10	27.16 s
Time	11	27.16 s
Time	12	27.18 s
Time	13	27.30 s
Time	14	27.18 s
Time	15	27.31 s
Time	16	27.28 s
Time	17	27.23 s
Time	18	27.17 s
Time	19	27.28 s

T/C 1	Strt	2.600 mV
T/C 2	Strt	2.625 mV
T/C 3	Strt	1.150 mV
T/C 4	Strt	2.611 mV
T/C 5	Strt	2.621 mV
T/C 6	Strt	2.606 mV
T/C 7	Strt	2.560 mV
T/C 1	End	2.600 mV
T/C 2	End	2.625 mV
T/C 3	End	1.155 mV
T/C 4	End	2.615 mV
T/C 5	End	2.625 mV
T/C 6	End	2.605 mV
T/C 7	End	2.570 mV

Start Time 14:40
End Time 15:10

Date of Experiment 1986/ 4/29

MDEA Conc	20.0 wt%	Absorbing Gas	CO2
Piperazine Conc	0.0 kmol/m3	Surfactant	0.0100 wt%
Barometric Pressure	693.4 mm Hg	Rotameter Tube	603
Room Temperature	23.0 deg C	Nozzle Diam	0.60 mm
Manometer Right Leg	6.4 in H2O	Thermo Coarse	5.27
Manometer Left Leg	5.6 in H2O	Thermo Fine	0.0
Jet Elevation	87.500 cm	Feed Variac	90.0 %
North Pole	87.290 cm	Circ Variac	35.0 %
South Pole	82.175 cm		
Liquid Take-off	79.720 cm		

Flowmeter	30. mm	40. mm	50. mm
SFM Volume	25. mL	25. mL	25. mL
Time 1	28.81 s	27.75 s	27.20 s
Time 2	28.85 s	27.74 s	27.25 s
Time 3	28.77 s	27.74 s	27.20 s
Time 4	28.78 s	27.78 s	27.15 s
Time 5	28.83 s	27.73 s	27.24 s
Time 6	28.88 s	27.74 s	27.16 s
Time 7	28.85 s	27.73 s	27.23 s
Time 8	28.81 s	27.74 s	27.17 s
Time 9	28.85 s	27.74 s	27.24 s
Time 10	28.89 s	27.83 s	27.27 s
Time 11	28.82 s	27.88 s	27.24 s
Time 12	28.81 s	27.80 s	27.31 s
Time 13	28.84 s	27.81 s	27.24 s
Time 14	28.89 s	27.63 s	27.32 s
Time 15	28.79 s	27.80 s	27.29 s
Time 16	28.85 s	27.70 s	27.20 s
Time 17	0.0 s	27.84 s	27.14 s
Time 18	0.0 s	27.81 s	0.0 s
T/C 1 Strt	2.560 mV	2.575 mV	2.580 mV
T/C 2 Strt	2.615 mV	2.615 mV	2.610 mV
T/C 3 Strt	1.126 mV	1.130 mV	1.126 mV
T/C 4 Strt	2.606 mV	2.605 mV	2.605 mV
T/C 5 Strt	2.615 mV	2.616 mV	2.617 mV
T/C 6 Strt	2.597 mV	2.596 mV	2.596 mV
T/C 7 Strt	2.260 mV	2.405 mV	2.470 mV
T/C 1 End	2.566 mV	2.575 mV	2.580 mV
T/C 2 End	2.616 mV	2.611 mV	2.610 mV
T/C 3 End	1.130 mV	1.128 mV	1.127 mV
T/C 4 End	2.605 mV	2.605 mV	2.606 mV
T/C 5 End	2.615 mV	2.616 mV	2.618 mV
T/C 6 End	2.596 mV	2.596 mV	2.597 mV
T/C 7 End	2.270 mV	2.406 mV	2.473 mV
Start Time	11:00	12:10	13:20
End Time	11:30	12:30	13:42

Date of Experiment 1986/ 4/30

MDEA Conc	20.0 wt%	Absorbing Gas	CO2
Piperazine Conc	0.0 kmol/m3	Surfactant	0.0100 wt%
Barometric Pressure	701.9 mm Hg	Rotameter Tube	603
Room Temperature	24.0 deg C	Nozzle Diam	0.60 mm
Manometer Right Leg	6.4 in H2O	Thermo Coarse	5.27
Manometer Left Leg	5.6 in H2O	Thermo Fine	0.0
Jet Elevation	87.440 cm	Feed Variac	36.5 %
North Pole	87.235 cm	Circ Variac	90.0 %
South Pole	82.120 cm		
Liquid Take-off	79.710 cm		

Flowmeter	30. mm	40. mm	50. mm
SFM Volume	25. mL	25. mL	25. mL
Time 1	28.80 s	27.79 s	27.21 s
Time 2	28.75 s	27.76 s	27.23 s
Time 3	28.89 s	27.79 s	27.24 s
Time 4	28.84 s	27.73 s	27.20 s
Time 5	28.78 s	27.69 s	27.23 s
Time 6	28.91 s	27.83 s	27.21 s
Time 7	28.95 s	27.69 s	27.20 s
Time 8	28.75 s	27.75 s	27.27 s
Time 9	28.74 s	27.77 s	27.24 s
Time 10	28.85 s	27.90 s	27.27 s
Time 11	28.85 s	27.81 s	27.20 s
Time 12	28.75 s	27.81 s	27.19 s
Time 13	28.70 s	27.75 s	27.20 s
Time 14	28.80 s	27.85 s	27.13 s
Time 15	28.98 s	27.98 s	27.35 s
Time 16	28.79 s	27.94 s	27.21 s
Time 17	28.89 s	27.76 s	0.0 s
Time 18	28.91 s	0.0 s	0.0 s
T/C 1 Strt	2.575 mV	2.581 mV	2.586 mV
T/C 2 Strt	2.615 mV	2.620 mV	2.616 mV
T/C 3 Strt	1.150 mV	1.160 mV	1.160 mV
T/C 4 Strt	2.605 mV	2.609 mV	2.606 mV
T/C 5 Strt	2.615 mV	2.620 mV	2.620 mV
T/C 6 Strt	2.595 mV	2.600 mV	2.599 mV
T/C 7 Strt	2.265 mV	2.415 mV	2.491 mV
T/C 1 End	2.575 mV	2.580 mV	2.580 mV
T/C 2 End	2.615 mV	2.616 mV	2.610 mV
T/C 3 End	1.156 mV	1.160 mV	1.159 mV
T/C 4 End	2.603 mV	2.605 mV	2.606 mV
T/C 5 End	2.615 mV	2.617 mV	2.617 mV
T/C 6 End	2.596 mV	2.600 mV	2.598 mV
T/C 7 End	2.270 mV	2.420 mV	2.486 mV
Start Time	10:55	12:00	13:06
End Time	11:20	12:20	13:33

Date of Experiment 1986/ 5/ 1

MDEA Conc	20.0 wt%	Absorbing Gas	N2O
Piperazine Conc	0.0 kmol/m3	Surfactant	0.0100 wt%
Barometric Pressure	710.5 mm Hg	Rotameter Tube	603
Room Temperature	24.0 deg C	Nozzle Diam	0.60 mm
Manometer Right Leg	6.4 in H2O	Thermo Coarse	5.27
Manometer Left Leg	5.6 in H2O	Thermo Fine	0.0
Jet Elevation	87.600 cm	Feed Variac	36.0 %
North Pole	87.390 cm	Circ Variac	90.0 %
South Pole	82.240 cm		
Liquid Take-off	79.855 cm		

Flowmeter	30. mm	40. mm	50. mm
SFM Volume	10. mL	10. mL	10. mL
Time 1	97.99 s	86.80 s	79.65 s
Time 2	98.21 s	87.45 s	79.28 s
Time 3	98.26 s	88.48 s	79.42 s
Time 4	98.62 s	87.98 s	79.74 s
Time 5	101.09 s	87.63 s	79.58 s
Time 6	100.55 s	88.67 s	81.33 s
Time 7	99.25 s	87.27 s	80.65 s
Time 8	99.31 s	87.49 s	80.20 s
Time 9	100.99 s	87.60 s	78.84 s
Time 10	99.86 s	87.45 s	80.13 s
Time 11	99.74 s	87.60 s	78.93 s
Time 12	101.16 s	87.95 s	81.03 s
Time 13	100.62 s	88.56 s	78.43 s
Time 14	99.13 s	88.42 s	80.18 s
Time 15	98.70 s	88.66 s	80.33 s
Time 16	101.04 s	88.27 s	80.70 s
Time 17	0.0 s	0.0 s	80.66 s
T/C 1 Strt	2.575 mV	2.593 mV	2.592 mV
T/C 2 Strt	2.590 mV	2.600 mV	2.600 mV
T/C 3 Strt	1.147 mV	1.163 mV	1.138 mV
T/C 4 Strt	2.605 mV	2.606 mV	2.606 mV
T/C 5 Strt	2.615 mV	2.616 mV	2.616 mV
T/C 6 Strt	2.598 mV	2.600 mV	2.595 mV
T/C 7 Strt	2.281 mV	2.413 mV	2.475 mV
T/C 1 End	2.580 mV	2.594 mV	2.590 mV
T/C 2 End	2.590 mV	2.599 mV	2.595 mV
T/C 3 End	1.168 mV	1.150 mV	1.137 mV
T/C 4 End	2.605 mV	2.605 mV	2.601 mV
T/C 5 End	2.615 mV	2.615 mV	2.615 mV
T/C 6 End	2.596 mV	2.595 mV	2.595 mV
T/C 7 End	2.285 mV	2.421 mV	2.472 mV
Start Time	10:30	11:50	13:05
End Time	11:10	12:25	13:40

Date of Experiment 1986/ 5/ 2

MDEA Conc	20.0 wt%	Absorbing Gas	N2O
Piperazine Conc	0.0 kmol/m3	Surfactant	0.0100 wt%
Barometric Pressure	705.3 mm Hg	Rotameter Tube	603
Room Temperature	23.5 deg C	Nozzle Diam	0.60 mm
Manometer Right Leg	6.4 in H2O	Thermo Coarse	5.27
Manometer Left Leg	5.6 in H2O	Thermo Fine	0.0
Jet Elevation	87.540 cm	Feed Variac	90.0 %
North Pole	87.320 cm	Circ Variac	37.5 %
South Pole	82.200 cm		
Liquid Take-off	79.770 cm		

Flowmeter	30. mm	40. mm	50. mm
SFM Volume	10. mL	10. mL	10. mL
Time 1	102.12 s	88.62 s	81.16 s
Time 2	101.75 s	89.20 s	80.28 s
Time 3	101.24 s	89.45 s	80.55 s
Time 4	100.44 s	89.60 s	79.06 s
Time 5	100.43 s	89.24 s	80.78 s
Time 6	98.24 s	88.31 s	80.59 s
Time 7	100.74 s	88.99 s	81.05 s
Time 8	101.13 s	89.72 s	81.32 s
Time 9	99.31 s	89.84 s	81.63 s
Time 10	100.81 s	88.61 s	81.56 s
Time 11	100.66 s	88.33 s	80.50 s
Time 12	100.44 s	89.36 s	80.79 s
Time 13	101.03 s	89.16 s	81.48 s
Time 14	101.38 s	89.26 s	79.84 s
Time 15	100.66 s	89.56 s	81.16 s
Time 16	100.30 s	89.09 s	80.74 s
Time 17	100.61 s	0.0 s	0.0 s
T/C 1 Strt	2.586 mV	2.598 mV	2.590 mV
T/C 2 Strt	2.591 mV	2.600 mV	2.595 mV
T/C 3 Strt	1.153 mV	1.145 mV	1.150 mV
T/C 4 Strt	2.605 mV	2.606 mV	2.607 mV
T/C 5 Strt	2.615 mV	2.616 mV	2.617 mV
T/C 6 Strt	2.597 mV	2.599 mV	2.600 mV
T/C 7 Strt	2.265 mV	2.407 mV	2.470 mV
T/C 1 End	2.585 mV	2.600 mV	2.590 mV
T/C 2 End	2.590 mV	2.605 mV	2.595 mV
T/C 3 End	1.148 mV	1.150 mV	1.153 mV
T/C 4 End	2.600 mV	2.605 mV	2.607 mV
T/C 5 End	2.611 mV	2.616 mV	2.618 mV
T/C 6 End	2.593 mV	2.598 mV	2.600 mV
T/C 7 End	2.265 mV	2.418 mV	2.475 mV
Start Time	10:00	11:25	12:45
End Time	10:36	12:00	13:15

Date of Experiment 1986/ 5/ 5

MDEA Conc	20.0 wt%	Absorbing Gas	N2O
Piperazine Conc	0.0 kmol/m3	Surfactant	0.0100 wt%
Barometric Pressure	696.7 mm Hg	Rotameter Tube	603
Room Temperature	24.0 deg C	Nozzle Diam	0.60 mm
Manometer Right Leg	6.4 in H2O	Thermo Coarse	5.27
Manometer Left Leg	5.6 in H2O	Thermo Fine	0.0
Jet Elevation	87.485 cm	Feed Variac	37.0 %
North Pole	87.275 cm	Circ Variac	100.0 %
South Pole	82.145 cm		
Liquid Take-off	79.760 cm		

Flowmeter	30. mm	40. mm	50. mm
SFM Volume	10. mL	10. mL	10. mL
Time 1	100.61 s	88.81 s	81.46 s
Time 2	100.99 s	89.53 s	82.09 s
Time 3	101.08 s	89.30 s	81.60 s
Time 4	100.51 s	88.29 s	82.13 s
Time 5	101.04 s	88.74 s	81.34 s
Time 6	101.49 s	88.30 s	81.50 s
Time 7	101.83 s	88.86 s	81.63 s
Time 8	101.99 s	88.71 s	81.24 s
Time 9	101.79 s	89.01 s	81.12 s
Time 10	100.99 s	88.53 s	82.01 s
Time 11	101.83 s	88.96 s	81.81 s
Time 12	102.49 s	88.93 s	81.15 s
Time 13	100.20 s	88.27 s	81.47 s
Time 14	101.03 s	88.92 s	80.84 s
Time 15	101.46 s	88.47 s	81.21 s
Time 16	101.57 s	88.63 s	81.33 s
Time 17	0.0 s	89.59 s	0.0 s
Time 18	0.0 s	89.59 s	0.0 s
Time 19	0.0 s	88.98 s	0.0 s
T/C 1 Strt	2.578 mV	2.601 mV	2.595 mV
T/C 2 Strt	2.592 mV	2.601 mV	2.598 mV
T/C 3 Strt	1.120 mV	1.150 mV	1.155 mV
T/C 4 Strt	2.605 mV	2.607 mV	2.610 mV
T/C 5 Strt	2.615 mV	2.620 mV	2.620 mV
T/C 6 Strt	2.597 mV	2.600 mV	2.601 mV
T/C 7 Strt	2.255 mV	2.420 mV	2.490 mV
T/C 1 End	2.581 mV	2.601 mV	2.595 mV
T/C 2 End	2.594 mV	2.601 mV	2.600 mV
T/C 3 End	1.146 mV	1.160 mV	1.151 mV
T/C 4 End	2.605 mV	2.606 mV	2.606 mV
T/C 5 End	2.617 mV	2.616 mV	2.619 mV
T/C 6 End	2.594 mV	2.598 mV	2.600 mV
T/C 7 End	2.278 mV	2.434 mV	2.487 mV
Start Time	10:45	12:10	13:45
End Time	11:30	12:42	14:00

Date of Experiment 1986/ 5/ 6

MDEA Conc	20.0 wt%	Absorbing Gas	N2O
Piperazine Conc	0.0 kmol/m3	Surfactant	0.0100 wt%
Barometric Pressure	700.9 mm Hg	Rotameter Tube	603
Room Temperature	24.0 deg C	Nozzle Diam	0.60 mm
Manometer Right Leg	6.4 in H2O	Thermo Coarse	5.51
Manometer Left Leg	5.6 in H2O	Thermo Fine	0.0
Jet Elevation	87.615 cm	Feed Variac	60.0 %
North Pole	87.410 cm	Circ Variac	100.0 %
South Pole	82.260 cm		
Liquid Take-off	78.820 cm		

Flowmeter	40. mm
SFM Volume	5. mL

Time 1	65.85 s
Time 2	64.10 s
Time 3	67.47 s
Time 4	66.52 s
Time 5	66.83 s
Time 6	68.49 s
Time 7	69.43 s
Time 8	68.83 s
Time 9	68.61 s
Time 10	69.66 s
Time 11	68.64 s
Time 12	62.51 s
Time 13	65.89 s
Time 14	68.91 s

T/C 1 Strt	3.930 mV
T/C 2 Strt	3.930 mV
T/C 3 Strt	1.158 mV
T/C 4 Strt	3.960 mV
T/C 5 Strt	3.990 mV
T/C 6 Strt	3.935 mV
T/C 7 Strt	3.290 mV
T/C 1 End	3.938 mV
T/C 2 End	3.946 mV
T/C 3 End	1.176 mV
T/C 4 End	3.983 mV
T/C 5 End	4.000 mV
T/C 6 End	3.976 mV
T/C 7 End	3.273 mV

Start Time	11:15
End Time	12:15

Date of Experiment 1986/ 5/ 6

MDEA Conc	20.0	wt%	Absorbing Gas	N2O	
Piperazine Conc	0.0	kmol/m3	Surfactant	0.0100	wt%
Barometric Pressure	700.9	mm Hg	Rotameter Tube	603	
Room Temperature	24.0	deg C	Nozzle Diam	0.60	mm
Manometer Right Leg	6.4	in H2O	Thermo Coarse	5.51	
Manometer Left Leg	5.6	in H2O	Thermo Fine	0.0	
Jet Elevation	87.615	cm	Feed Variac	60.0	%
North Pole	87.410	cm	Circ Variac	100.0	%
South Pole	82.260	cm			
Liquid Take-off	79.810	cm			

Flowmeter	40.	mm
SFM Volume	5.	mL

Time	1	65.41	s
Time	2	63.04	s
Time	3	64.07	s
Time	4	63.31	s
Time	5	64.40	s
Time	6	64.19	s
Time	7	64.40	s
Time	8	65.00	s
Time	9	67.45	s
Time	10	64.88	s
Time	11	66.48	s
Time	12	66.61	s

T/C 1 Strt	3.930	mV
T/C 2 Strt	3.948	mV
T/C 3 Strt	1.183	mV
T/C 4 Strt	3.985	mV
T/C 5 Strt	3.996	mV
T/C 6 Strt	3.978	mV
T/C 7 Strt	3.275	mV
T/C 1 End	3.920	mV
T/C 2 End	3.941	mV
T/C 3 End	1.185	mV
T/C 4 End	3.985	mV
T/C 5 End	4.000	mV
T/C 6 End	3.981	mV
T/C 7 End	3.266	mV

Start Time	12:45
End Time	13:15

Date of Experiment 1986/ 5/ 6

MDEA Conc	20.0	wt%	Absorbing Gas	N2O	
Piperazine Conc	0.0	kmol/m3	Surfactant	0.0100	wt%
Barometric Pressure	700.9	mm Hg	Rotameter Tube	603	
Room Temperature	24.0	deg C	Nozzle Diam	0.60	mm
Manometer Right Leg	6.4	in H2O	Thermo Coarse	5.51	
Manometer Left Leg	5.6	in H2O	Thermo Fine	0.0	
Jet Elevation	87.615	cm	Feed Variac	60.0	%
North Pole	87.410	cm	Circ Variac	100.0	%
South Pole	82.260	cm			
Liquid Take-off	80.325	cm			

Flowmeter	40.	mm
SFM Volume	5.	mL

Time	1	66.10 s
Time	2	67.21 s
Time	3	65.31 s
Time	4	64.04 s
Time	5	65.21 s
Time	6	61.86 s
Time	7	64.94 s
Time	8	67.71 s
Time	9	64.46 s
Time	10	66.70 s

T/C 1 Strt	3.920	mV
T/C 2 Strt	3.949	mV
T/C 3 Strt	1.180	mV
T/C 4 Strt	3.986	mV
T/C 5 Strt	4.000	mV
T/C 6 Strt	3.981	mV
T/C 7 Strt	3.265	mV
T/C 1 End	3.939	mV
T/C 2 End	3.950	mV
T/C 3 End	1.180	mV
T/C 4 End	3.990	mV
T/C 5 End	4.001	mV
T/C 6 End	3.981	mV
T/C 7 End	3.266	mV

Start Time	13:40
End Time	14:05

Date of Experiment 1986/ 5/ 6

MDEA Conc	20.0 wt%	Absorbing Gas	N2O
Piperazine Conc	0.0 kmol/m3	Surfactant	0.0100 wt%
Barometric Pressure	700.9 mm Hg	Rotameter Tube	603
Room Temperature	24.0 deg C	Nozzle Diam	0.60 mm
Manometer Right Leg	6.4 in H2O	Thermo Coarse	5.51
Manometer Left Leg	5.6 in H2O	Thermo Fine	0.0
Jet Elevation	87.615 cm	Feed Variac	60.0 %
North Pole	87.410 cm	Circ. Variac	100.0 %
South Pole	82.260 cm		
Liquid Take-off	80.905 cm		

Flowmeter	40. mm
SFM Volume	5. mL

Time	1	65.00 s
Time	2	66.06 s
Time	3	67.92 s
Time	4	65.24 s
Time	5	65.83 s
Time	6	68.68 s
Time	7	66.13 s
Time	8	65.85 s
Time	9	69.16 s
Time	10	68.06 s
Time	11	65.91 s
Time	12	69.11 s
Time	13	68.91 s
Time	14	65.76 s
Time	15	66.35 s

T/C 1	Strt	3.930 mV
T/C 2	Strt	3.951 mV
T/C 3	Strt	1.180 mV
T/C 4	Strt	3.990 mV
T/C 5	Strt	4.001 mV
T/C 6	Strt	3.983 mV
T/C 7	Strt	3.262 mV
T/C 1	End	3.931 mV
T/C 2	End	3.953 mV
T/C 3	End	1.176 mV
T/C 4	End	3.990 mV
T/C 5	End	4.004 mV
T/C 6	End	3.985 mV
T/C 7	End	3.255 mV

Start Time	14:25
End Time	14:55

Date of Experiment 1986/ 5/ 6

MDEA Conc	20.0 wt%	Absorbing Gas	N2O
Piperazine Conc	0.0 kmol/m3	Surfactant	0.0100 wt%
Barometric Pressure	700.9 mm Hg	Rotameter Tube	603
Room Temperature	24.0 deg C	Nozzle Diam	0.60 mm
Manometer Right Leg	6.4 in H2O	Thermo Coarse	5.51
Manometer Left Leg	5.6 in H2O	Thermo Fine	0.0
Jet Elevation	87.615 cm	Feed Variac	60.0 %
North Pole	87.410 cm	Circ Variac	100.0 %
South Pole	82.260 cm		
Liquid Take-off	81.505 cm		

Flowmeter	40. mm
SFM Volume	5. mL

Time 1	70.88 s
Time 2	71.88 s
Time 3	71.85 s
Time 4	71.88 s
Time 5	74.22 s
Time 6	71.81 s
Time 7	71.44 s
Time 8	73.88 s
Time 9	70.78 s
Time 10	73.53 s
Time 11	73.22 s
Time 12	72.66 s
Time 13	71.19 s
Time 14	72.27 s

T/C 1 Strt	3.928 mV
T/C 2 Strt	3.951 mV
T/C 3 Strt	1.176 mV
T/C 4 Strt	3.991 mV
T/C 5 Strt	4.005 mV
T/C 6 Strt	3.985 mV
T/C 7 Strt	3.253 mV
T/C 1 End	3.922 mV
T/C 2 End	3.945 mV
T/C 3 End	1.179 mV
T/C 4 End	3.990 mV
T/C 5 End	4.004 mV
T/C 6 End	3.985 mV
T/C 7 End	3.247 mV

Start Time	15:15
End Time	15:45

Date of Experiment 1986/ 5/ 7

MDEA Conc	20.0 wt%	Absorbing Gas	N2O
Piperazine Conc	0.0 kmol/m3	Surfactant	0.0100 wt%
Barometric Pressure	700.7 mm Hg	Rotameter Tube	603
Room Temperature	25.0 deg C	Nozzle Diam	0.60 mm
Manometer Right Leg	6.4 in H2O	Thermo Coarse	5.51
Manometer Left Leg	5.6 in H2O	Thermo Fine	0.0
Jet Elevation	87.525 cm	Feed Variac	60.0 %
North Pole	87.310 cm	Circ Variac	90.0 %
South Pole	82.180 cm		
Liquid Take-off	79.770 cm		

Flowmeter	30. mm	30. mm	40. mm	50. mm
SFM Volume	5. mL	5. mL	5. mL	5. mL
Time 1	76.38 s	73.02 s	67.69 s	59.65 s
Time 2	76.63 s	71.77 s	66.93 s	59.70 s
Time 3	75.47 s	72.08 s	65.07 s	59.18 s
Time 4	75.70 s	72.28 s	67.27 s	58.07 s
Time 5	76.96 s	72.14 s	67.29 s	59.06 s
Time 6	77.95 s	74.86 s	66.11 s	59.45 s
Time 7	76.26 s	71.87 s	68.03 s	60.01 s
Time 8	78.75 s	73.08 s	65.44 s	60.01 s
Time 9	75.84 s	73.98 s	65.43 s	62.05 s
Time 10	76.62 s	72.49 s	64.33 s	60.08 s
Time 11	76.14 s	71.84 s	63.00 s	59.69 s
Time 12	76.13 s	72.56 s	66.00 s	60.18 s
Time 13	0.0 s	74.40 s	66.06 s	59.92 s
Time 14	0.0 s	72.41 s	65.16 s	58.88 s
Time 15	0.0 s	73.13 s	66.21 s	58.95 s
Time 16	0.0 s	71.67 s	66.07 s	57.91 s
Time 17	0.0 s	0.0 s	0.0 s	57.67 s
Time 18	0.0 s	0.0 s	0.0 s	59.27 s
T/C 1 Strt	3.930 mV	3.921 mV	3.932 mV	3.921 mV
T/C 2 Strt	3.940 mV	3.939 mV	3.935 mV	3.935 mV
T/C 3 Strt	1.160 mV	1.190 mV	1.205 mV	1.233 mV
T/C 4 Strt	3.961 mV	3.964 mV	3.961 mV	3.963 mV
T/C 5 Strt	3.991 mV	3.994 mV	3.991 mV	3.995 mV
T/C 6 Strt	3.935 mV	3.940 mV	3.938 mV	3.945 mV
T/C 7 Strt	3.080 mV	3.062 mV	3.225 mV	3.345 mV
T/C 1 End	3.921 mV	3.915 mV	3.933 mV	3.929 mV
T/C 2 End	3.939 mV	3.933 mV	3.945 mV	3.940 mV
T/C 3 End	1.190 mV	1.196 mV	1.220 mV	1.240 mV
T/C 4 End	3.964 mV	3.963 mV	3.966 mV	3.965 mV
T/C 5 End	3.994 mV	3.991 mV	3.995 mV	3.995 mV
T/C 6 End	3.940 mV	3.939 mV	3.940 mV	3.945 mV
T/C 7 End	3.062 mV	3.060 mV	3.225 mV	3.350 mV
Start Time	11:00	11:35	13:00	14:40
End Time	11:30	12:00	13:35	15:10

Date of Experiment 1986/ 5/ 8

MDEA Conc	20.0 wt%	Absorbing Gas	N2O
Piperazine Conc	0.0 kmol/m3	Surfactant	0.0100 wt%
Barometric Pressure	705.3 mm Hg	Rotameter Tube	603
Room Temperature	25.0 deg C	Nozzle Diam	0.60 mm
Manometer Right Leg	6.4 in H2O	Thermo Coarse	5.51
Manometer Left Leg	5.6 in H2O	Thermo Fine	0.0
Jet Elevation	87.440 cm	Feed Variac	62.0 %
North Pole	87.225 cm	Circ Variac	95.0 %
South Pole	82.120 cm		
Liquid Take-off	79.700 cm		

Flowmeter	30. mm	40. mm	50. mm
SFM Volume	5. mL	5. mL	5. mL
Time 1	72.94 s	68.24 s	58.84 s
Time 2	70.75 s	66.30 s	60.49 s
Time 3	73.87 s	67.20 s	60.08 s
Time 4	69.84 s	66.39 s	60.61 s
Time 5	74.93 s	63.41 s	59.66 s
Time 6	70.89 s	66.06 s	61.00 s
Time 7	71.37 s	63.48 s	58.93 s
Time 8	72.50 s	64.40 s	58.75 s
Time 9	75.06 s	66.45 s	59.14 s
Time 10	71.76 s	67.45 s	60.18 s
Time 11	74.17 s	63.65 s	60.16 s
Time 12	74.12 s	64.14 s	60.09 s
Time 13	72.80 s	65.74 s	60.03 s
Time 14	73.25 s	64.06 s	59.84 s
Time 15	72.38 s	66.10 s	59.39 s
Time 16	70.33 s	65.95 s	58.40 s
Time 17	72.63 s	64.85 s	60.38 s
Time 18	72.82 s	63.59 s	59.51 s
Time 19	74.91 s	63.74 s	0.0 s
Time 20	0.0 s	66.24 s	0.0 s
T/C 1 Strt	3.929 mV	3.935 mV	3.925 mV
T/C 2 Strt	3.940 mV	3.940 mV	3.931 mV
T/C 3 Strt	1.160 mV	1.196 mV	1.205 mV
T/C 4 Strt	3.962 mV	3.964 mV	3.961 mV
T/C 5 Strt	3.992 mV	3.991 mV	3.991 mV
T/C 6 Strt	3.940 mV	3.945 mV	3.940 mV
T/C 7 Strt	3.066 mV	3.232 mV	3.346 mV
T/C 1 End	3.920 mV	3.930 mV	3.928 mV
T/C 2 End	3.932 mV	3.936 mV	3.935 mV
T/C 3 End	1.174 mV	1.200 mV	1.211 mV
T/C 4 End	3.962 mV	3.961 mV	3.965 mV
T/C 5 End	3.993 mV	3.992 mV	3.995 mV
T/C 6 End	3.937 mV	3.942 mV	3.941 mV
T/C 7 End	3.050 mV	3.227 mV	3.350 mV
Start Time	11:15	12:55	14:15
End Time	11:55	13:30	14:50

Date of Experiment 1986/ 5/12

MDEA Conc	20.0 wt%	Absorbing Gas	N2O
Piperazine Conc	0.0 kmol/m3	Surfactant	0.0100 wt%
Barometric Pressure	696.5 mm Hg	Rotameter Tube	603
Room Temperature	23.5 deg C	Nozzle Diam	0.60 mm
Manometer Right Leg	6.4 in H2O	Thermo Coarse	5.04
Manometer Left Leg	5.6 in H2O	Thermo Fine	0.0
Jet Elevation	87.635 cm	Feed Variac	0.0 %
North Pole	87.430 cm	Circ Variac	0.0 %
South Pole	82.265 cm		
Liquid Take-off	79.915 cm		

Flowmeter	30. mm	40. mm	50. mm
SFM Volume	5. mL	5. mL	10. mL
Time 1	45.92 s	39.27 s	69.42 s
Time 2	45.76 s	39.29 s	69.24 s
Time 3	45.50 s	39.13 s	70.14 s
Time 4	46.04 s	38.84 s	68.88 s
Time 5	46.00 s	38.52 s	70.43 s
Time 6	45.79 s	38.45 s	69.96 s
Time 7	45.35 s	38.99 s	69.95 s
Time 8	46.27 s	38.92 s	69.57 s
Time 9	46.31 s	38.56 s	69.99 s
Time 10	46.21 s	38.85 s	69.45 s
Time 11	46.20 s	38.75 s	69.77 s
Time 12	47.66 s	39.49 s	69.61 s
Time 13	45.05 s	39.29 s	69.77 s
Time 14	46.45 s	38.44 s	69.66 s
Time 15	46.70 s	38.73 s	0.0 s
Time 16	46.49 s	39.35 s	0.0 s
Time 17	46.02 s	39.02 s	0.0 s
Time 18	46.92 s	38.90 s	0.0 s
T/C 1 Strt	1.293 mV	1.266 mV	1.274 mV
T/C 2 Strt	1.336 mV	1.300 mV	1.301 mV
T/C 3 Strt	1.121 mV	1.139 mV	1.145 mV
T/C 4 Strt	1.351 mV	1.351 mV	1.350 mV
T/C 5 Strt	1.352 mV	1.351 mV	1.349 mV
T/C 6 Strt	1.352 mV	1.351 mV	1.349 mV
T/C 7 Strt	1.015 mV	1.140 mV	1.210 mV
T/C 1 End	1.283 mV	1.274 mV	1.276 mV
T/C 2 End	1.325 mV	1.308 mV	1.305 mV
T/C 3 End	1.126 mV	1.145 mV	1.150 mV
T/C 4 End	1.346 mV	1.351 mV	1.350 mV
T/C 5 End	1.346 mV	1.351 mV	1.350 mV
T/C 6 End	1.345 mV	1.351 mV	1.350 mV
T/C 7 End	1.015 mV	1.137 mV	1.201 mV
Start Time	11:22	12:50	13:59
End Time	11:54	13:11	14:25

Date of Experiment 1986/ 5/13

MDEA Conc	20.0 wt%	Absorbing Gas	N2O
Piperazine Conc	0.0 kmol/m3	Surfactant	0.0100 wt%
Barometric Pressure	686.9 mm Hg	Rotameter Tube	603
Room Temperature	23.5 deg C	Nozzle Diam	0.60 mm
Manometer Right Leg	6.4 in H2O	Thermo Coarse	5.04
Manometer Left Leg	5.6 in H2O	Thermo Fine	0.0
Jet Elevation	87.770 cm	Feed Variac	0.0 %
North Pole	87.560 cm	Circ Variac	0.0 %
South Pole	82.430 cm		
Liquid Take-off	80.000 cm		

Flowmeter	30. mm	40. mm	50. mm
SFM Volume	10. mL	10. mL	10. mL
Time 1	93.06 s	77.57 s	68.47 s
Time 2	92.12 s	78.38 s	70.32 s
Time 3	92.99 s	78.10 s	68.98 s
Time 4	90.50 s	77.02 s	70.07 s
Time 5	91.28 s	77.86 s	70.17 s
Time 6	92.89 s	77.31 s	69.57 s
Time 7	93.04 s	78.10 s	68.51 s
Time 8	92.86 s	77.93 s	69.85 s
Time 9	91.74 s	78.01 s	69.30 s
Time 10	92.44 s	76.72 s	69.62 s
Time 11	91.82 s	77.75 s	69.96 s
Time 12	92.40 s	77.25 s	69.84 s
Time 13	92.02 s	78.11 s	69.5[illegible] s
Time 14	92.31 s	77.29 s	69.90 s
Time 15	91.76 s	0.0 s	69.87 s
T/C 1 Strt	1.290 mV	1.272 mV	1.275 mV
T/C 2 Strt	1.330 mV	1.305 mV	1.303 mV
T/C 3 Strt	1.120 mV	1.134 mV	1.144 mV
T/C 4 Strt	1.352 mV	1.355 mV	1.356 mV
T/C 5 Strt	1.352 mV	1.355 mV	1.356 mV
T/C 6 Strt	1.352 mV	1.355 mV	1.356 mV
T/C 7 Strt	1.010 mV	1.125 mV	1.196 mV
T/C 1 End	1.289 mV	1.281 mV	1.283 mV
T/C 2 End	1.328 mV	1.310 mV	1.308 mV
T/C 3 End	1.125 mV	1.140 mV	1.146 mV
T/C 4 End	1.352 mV	1.355 mV	1.356 mV
T/C 5 End	1.352 mV	1.355 mV	1.357 mV
T/C 6 End	1.352 mV	1.355 mV	1.356 mV
T/C 7 End	1.028 mV	1.153 mV	1.205 mV
Start Time	10:40	11:50	12:50
End Time	11:10	12:20	13:30

Date of Experiment 1986/ 5/14

MDEA Conc	20.0 wt%	Absorbing Gas	CO2
Piperazine Conc	0.0 kmol/m3	Surfactant	0.0100 wt%
Barometric Pressure	693.4 mm Hg	Rotameter Tube	603
Room Temperature	24.0 deg C	Nozzle Diam	0.60 mm
Manometer Right Leg	5.4 in H2O	Thermo Coarse	5.14
Manometer Left Leg	5.6 in H2O	Thermo Fine	0.0
Jet Elevation	87.810 cm	Feed Variac	0.0 %
North Pole	87.610 cm	Circ Variac	0.0 %
South Pole	82.475 cm		
Liquid Take-off	80.055 cm		

Flowmeter	30. mm	40. mm	50. mm
SFM Volume	25. mL	25. mL	25. mL
Time 1	34.22 s	33.27 s	32.34 s
Time 2	34.32 s	33.24 s	32.27 s
Time 3	34.52 s	33.36 s	32.42 s
Time 4	34.31 s	33.34 s	32.59 s
Time 5	34.48 s	33.19 s	32.30 s
Time 6	34.21 s	33.38 s	32.34 s
Time 7	34.09 s	33.13 s	32.20 s
Time 8	34.38 s	33.31 s	32.57 s
Time 9	34.47 s	33.32 s	32.20 s
Time 10	34.20 s	33.27 s	32.47 s
Time 11	34.44 s	33.37 s	32.29 s
Time 12	34.38 s	33.06 s	32.31 s
Time 13	34.09 s	33.36 s	32.38 s
Time 14	34.28 s	33.17 s	32.12 s
Time 15	34.50 s	33.38 s	32.23 s
Time 16	34.28 s	33.17 s	32.36 s
Time 17	34.35 s	33.10 s	32.10 s
Time 18	0.0 s	33.41 s	32.40 s
Time 19	0.0 s	33.24 s	32.24 s
T/C 1 Strt	1.785 mV	1.780 mV	1.790 mV
T/C 2 Strt	1.870 mV	1.847 mV	1.845 mV
T/C 3 Strt	1.165 mV	1.168 mV	1.165 mV
T/C 4 Strt	1.889 mV	1.889 mV	1.886 mV
T/C 5 Strt	1.892 mV	1.894 mV	1.894 mV
T/C 6 Strt	1.885 mV	1.885 mV	1.884 mV
T/C 7 Strt	1.664 mV	1.745 mV	1.786 mV
T/C 1 End	1.786 mV	1.782 mV	1.790 mV
T/C 2 End	1.865 mV	1.850 mV	1.845 mV
T/C 3 End	1.170 mV	1.170 mV	1.169 mV
T/C 4 End	1.889 mV	1.888 mV	1.887 mV
T/C 5 End	1.892 mV	1.894 mV	1.892 mV
T/C 6 End	1.884 mV	1.885 mV	1.883 mV
T/C 7 End	1.665 mV	1.746 mV	1.790 mV
Start Time	10:45	11:45	12:40
End Time	11:08	12:07	13:05

Date of Experiment 1986/ 5/15

MDEA Conc	20.0 wt%	Absorbing Gas	CO2
Piperazine Conc	0.0 kmol/m3	Surfactant	0.0100 wt%
Barometric Pressure	701.3 mm Hg	Rotameter Tube	603
Room Temperature	24.0 deg C	Nozzle Diam	0.60 mm
Manometer Right Leg	6.4 in H2O	Thermo Coarse	14
Manometer Left Leg	5.6 in H2O	Thermo Fine	.0
Jet Elevation	87.955 cm	Feed Variac	0.0 %
North Pole	87.740 cm	Circ Variac	0.0 %
South Pole	82.620 cm		
Liquid Take-off	80.185 cm		

Flowmeter	30. mm	40. mm	50. mm
SFM Volume	25. mL	25. mL	25. mL
Time 1	34.33 s	33.26 s	32.46 s
Time 2	34.27 s	33.29 s	32.36 s
Time 3	34.15 s	33.38 s	32.29 s
Time 4	34.24 s	33.11 s	32.43 s
Time 5	34.43 s	33.20 s	32.45 s
Time 6	34.32 s	33.34 s	32.36 s
Time 7	34.43 s	33.32 s	32.42 s
Time 8	34.49 s	33.09 s	32.47 s
Time 9	34.49 s	33.21 s	32.49 s
Time 10	34.32 s	33.28 s	32.43 s
Time 11	34.60 s	33.33 s	32.57 s
Time 12	34.47 s	33.26 s	32.66 s
Time 13	34.35 s	33.32 s	32.45 s
Time 14	34.41 s	33.31 s	32.41 s
Time 15	34.21 s	33.45 s	32.15 s
Time 16	34.51 s	33.23 s	32.62 s
Time 17	34.42 s	33.34 s	32.40 s
Time 18	0.0 s	33.39 s	32.36 s
Time 19	0.0 s	33.33 s	0.0 s
Time 20	0.0 s	33.19 s	0.0 s
T/C 1 Strt	1.776 mV	1.772 mV	1.786 mV
T/C 2 Strt	1.850 mV	1.835 mV	1.835 mV
T/C 3 Strt	1.152 mV	1.140 mV	1.162 mV
T/C 4 Strt	1.875 mV	1.874 mV	1.878 mV
T/C 5 Strt	1.875 mV	1.880 mV	1.881 mV
T/C 6 Strt	1.870 mV	1.870 mV	1.873 mV
T/C 7 Strt	1.663 mV	1.747 mV	1.790 mV
T/C 1 End	1.779 mV	1.775 mV	1.784 mV
T/C 2 End	1.850 mV	1.837 mV	1.836 mV
T/C 3 End	1.156 mV	1.160 mV	1.158 mV
T/C 4 End	1.876 mV	1.876 mV	1.876 mV
T/C 5 End	1.880 mV	1.880 mV	1.880 mV
T/C 6 End	1.872 mV	1.873 mV	1.870 mV
T/C 7 End	1.669 mV	1.750 mV	1.790 mV
Start Time	10:08	11:00	12:05
End Time	10:28	11:23	12:30

Date of Experiment 1986/ 5/16

MDEA Conc	20.0 wt%	Absorbing Gas	CO2
Piperazine Conc	0.0 kmol/m3	Surfactant	0.0100 wt%
Barometric Pressure	706.0 mm Hg	Rotameter Tube	603
Room Temperature	23.0 deg C	Nozzle Diam	0.60 mm
Manometer Right Leg	6.4 in H2O	Thermo Coarse	5.08
Manometer Left Leg	5.6 in H2O	Thermo Fine	0.0
Jet Elevation	88.005 cm	Feed Variac	0.0 %
North Pole	87.800 cm	Circ Variac	0.0 %
South Pole	82.670 cm		
Liquid Take-off	80.215 cm		

Flowmeter	30. mm	40. mm	50. mm
SFM Volume	25. mL	25. mL	25. mL
Time 1	37.63 s	36.74 s	35.74 s
Time 2	37.76 s	36.77 s	35.74 s
Time 3	37.66 s	36.78 s	35.79 s
Time 4	37.84 s	36.74 s	35.80 s
Time 5	37.77 s	36.78 s	35.83 s
Time 6	37.83 s	36.74 s	35.81 s
Time 7	37.80 s	36.81 s	35.78 s
Time 8	37.88 s	36.65 s	35.73 s
Time 9	37.84 s	36.63 s	35.82 s
Time 10	37.84 s	36.69 s	35.84 s
Time 11	37.91 s	36.70 s	35.77 s
Time 12	37.79 s	36.69 s	35.72 s
Time 13	37.97 s	36.74 s	35.72 s
Time 14	37.83 s	36.61 s	35.80 s
Time 15	37.75 s	36.74 s	35.76 s
Time 16	38.03 s	36.65 s	35.73 s
Time 17	37.73 s	36.74 s	35.77 s
Time 18	37.82 s	36.70 s	35.70 s
Time 19	37.77 s	36.68 s	35.70 s
Time 20	37.70 s	0.0 s	0.0 s
T/C 1 Strt	1.545 mV	1.535 mV	1.545 mV
T/C 2 Strt	1.601 mV	1.583 mV	1.585 mV
T/C 3 Strt	1.141 mV	1.124 mV	1.132 mV
T/C 4 Strt	1.610 mV	1.602 mV	1.605 mV
T/C 5 Strt	1.610 mV	1.606 mV	1.608 mV
T/C 6 Strt	1.605 mV	1.601 mV	1.603 mV
T/C 7 Strt	1.466 mV	1.510 mV	1.550 mV
T/C 1 End	1.543 mV	1.538 mV	1.545 mV
T/C 2 End	1.599 mV	1.585 mV	1.585 mV
T/C 3 End	1.132 mV	1.130 mV	1.139 mV
T/C 4 End	1.601 mV	1.605 mV	1.605 mV
T/C 5 End	1.605 mV	1.606 mV	1.607 mV
T/C 6 End	1.601 mV	1.601 mV	1.601 mV
T/C 7 End	1.455 mV	1.515 mV	1.551 mV
Start Time	09:50	10:50	11:50
End Time	10:10	11:10	12:15

Date of Experiment 1986/ 5/20

MDEA Conc	20.0 wt%	Absorbing Gas	CO2
Piperazine Conc	0.0 kmol/m3	Surfactant	0.0100 wt%
Barometric Pressure	691.8 mm Hg	Rotameter Tube	603
Room Temperature	25.0 deg C	Nozzle Diam	0.60 mm
Manometer Right Leg	6.4 in H2O	Thermo Coarse	5.08
Manometer Left Leg	5.6 in H2O	Thermo Fine	0.0
Jet Elevation	87.970 cm	Feed Variac	0.0 %
North Pole	87.760 cm	Circ Variac	0.0 %
South Pole	82.620 cm		
Liquid Take-off	80.165 cm		

Flowmeter	30. mm	40. mm	50. mm	50. mm
SFM Volume	25. mL	25. mL	25. mL	25. mL
Time 1	37.63 s	36.11 s	35.17 s	35.45 s
Time 2	37.57 s	36.15 s	35.13 s	35.40 s
Time 3	37.66 s	35.95 s	35.20 s	35.48 s
Time 4	37.75 s	36.06 s	35.14 s	35.40 s
Time 5	37.71 s	36.03 s	35.23 s	35.66 s
Time 6	37.59 s	36.21 s	35.08 s	35.38 s
Time 7	37.70 s	36.16 s	35.15 s	35.44 s
Time 8	37.59 s	36.14 s	35.31 s	35.54 s
Time 9	37.66 s	36.13 s	35.27 s	35.31 s
Time 10	37.95 s	36.24 s	35.24 s	35.29 s
Time 11	37.72 s	36.12 s	35.24 s	35.31 s
Time 12	37.84 s	36.08 s	35.40 s	35.26 s
Time 13	37.66 s	36.13 s	35.38 s	35.48 s
Time 14	37.75 s	36.16 s	0.0 s	35.58 s
Time 15	37.72 s	36.22 s	0.0 s	35.25 s
Time 16	37.62 s	36.11 s	0.0 s	35.44 s
Time 17	37.66 s	36.18 s	0.0 s	35.28 s
Time 18	37.69 s	36.16 s	0.0 s	0.0 s

T/C 1 Strt	1.555 mV	1.560 mV	1.550 mV	1.546 mV
T/C 2 Strt	1.609 mV	1.601 mV	1.596 mV	1.590 mV
T/C 3 Strt	1.178 mV	1.200 mV	1.230 mV	1.230 mV
T/C 4 Strt	1.610 mV	1.610 mV	1.610 mV	1.610 mV
T/C 5 Strt	1.610 mV	1.611 mV	1.615 mV	1.611 mV
T/C 6 Strt	1.608 mV	1.606 mV	1.610 mV	1.609 mV
T/C 7 Strt	1.492 mV	1.564 mV	1.525 mV	1.530 mV
T/C 1 End	1.557 mV	1.565 mV	1.550 mV	1.550 mV
T/C 2 End	1.610 mV	1.602 mV	1.590 mV	1.590 mV
T/C 3 End	1.194 mV	1.212 mV	1.230 mV	1.235 mV
T/C 4 End	1.611 mV	1.610 mV	1.610 mV	1.611 mV
T/C 5 End	1.615 mV	1.611 mV	1.611 mV	1.611 mV
T/C 6 End	1.609 mV	1.606 mV	1.609 mV	1.609 mV
T/C 7 End	1.505 mV	1.570 mV	1.530 mV	1.550 mV

Start Time	09:40	10:45	12:00	12:20
End Time	10:00	11:05	12:20	12:40

Date of Experiment 1986/ 5/21

MDEA Conc	20.0 wt%	Absorbing Gas	CO2
Piperazine Conc	0.0 kmol/m3	Surfactant	0.0100 wt%
Barometric Pressure	692.4 mm Hg	Rotameter Tube	603
Room Temperature	24.0 deg C	Nozzle Diam	0.60 mm
Manometer Right Leg	6.4 in H2O	Thermo Coarse	5.03
Manometer Left Leg	5.6 in H2O	Thermo Fine	0.0
Jet Elevation	88.605 cm	Feed Variac	0.0 %
North Pole	87.800 cm	Circ Variac	0.0 %
South Pole	82.675 cm		
Liquid Take-off	80.280 cm		

Flowmeter	30. mm	40. mm	50. mm
SFM Volume	25. mL	25. mL	25. mL
Time 1	42.56 s	40.89 s	39.84 s
Time 2	42.45 s	40.83 s	39.74 s
Time 3	42.39 s	41.03 s	39.65 s
Time 4	42.45 s	41.02 s	39.83 s
Time 5	42.29 s	41.03 s	39.69 s
Time 6	42.36 s	40.99 s	39.61 s
Time 7	42.44 s	40.87 s	39.53 s
Time 8	42.33 s	40.98 s	39.89 s
Time 9	42.24 s	40.86 s	39.82 s
Time 10	42.34 s	40.81 s	39.63 s
Time 11	42.22 s	40.81 s	39.53 s
Time 12	42.42 s	40.83 s	39.82 s
Time 13	42.39 s	40.81 s	39.74 s
Time 14	42.27 s	40.95 s	39.82 s
Time 15	42.38 s	40.86 s	39.79 s
Time 16	42.20 s	40.96 s	39.75 s
T/C 1 Strt	1.277 mV	1.265 mV	1.270 mV
T/C 2 Strt	1.325 mV	1.300 mV	1.300 mV
T/C 3 Strt	1.167 mV	1.177 mV	1.180 mV
T/C 4 Strt	1.315 mV	1.311 mV	1.314 mV
T/C 5 Strt	1.315 mV	1.314 mV	1.314 mV
T/C 6 Strt	1.315 mV	1.312 mV	1.314 mV
T/C 7 Strt	1.126 mV	1.195 mV	1.240 mV
T/C 1 End	1.275 mV	1.275 mV	1.278 mV
T/C 2 End	1.323 mV	1.307 mV	1.303 mV
T/C 3 End	1.173 mV	1.180 mV	1.181 mV
T/C 4 End	1.315 mV	1.315 mV	1.315 mV
T/C 5 End	1.315 mV	1.315 mV	1.315 mV
T/C 6 End	1.315 mV	1.315 mV	1.315 mV
T/C 7 End	1.122 mV	1.220 mV	1.238 mV
Start Time	10:00	11:05	12:07
End Time	10:21	11:27	12:30

Date of Experiment 1986/ 5/22

MDEA Conc	20.0 wt%	Absorbing Gas	CO2
Piperazine Conc	0.0 kmol/m3	Surfactant	0.0100 wt%
Barometric Pressure	697.2 mm Hg	Rotameter Tube	603
Room Temperature	23.0 deg C	Nozzle Diam	0.60 mm
Manometer Right Leg	6.4 in H2O	Thermo Coarse	5.03
Manometer Left Leg	5.6 in H2O	Thermo Fine	0.0
Jet Elevation	87.990 cm	Feed Variac	0.0 %
North Pole	87.780 cm	Circ Variac	0.0 %
South Pole	82.635 cm		
Liquid Take-off	80.235 cm		

Flowmeter	30. mm	40. mm	50. mm
SFM Volume	25. mL	25. mL	25. mL
Time 1	43.02 s	40.91 s	39.86 s
Time 2	43.27 s	40.95 s	40.05 s
Time 3	43.14 s	40.84 s	40.05 s
Time 4	43.17 s	41.06 s	39.99 s
Time 5	43.04 s	41.05 s	39.97 s
Time 6	43.25 s	40.96 s	39.88 s
Time 7	42.98 s	40.94 s	39.74 s
Time 8	42.98 s	41.09 s	40.00 s
Time 9	42.94 s	41.01 s	39.93 s
Time 10	42.97 s	40.94 s	39.84 s
Time 11	43.06 s	40.95 s	39.76 s
Time 12	43.06 s	41.05 s	39.80 s
Time 13	43.04 s	41.01 s	39.90 s
Time 14	43.11 s	41.00 s	39.98 s
Time 15	43.03 s	40.94 s	39.71 s
Time 16	42.98 s	41.05 s	39.91 s
Time 17	43.06 s	0.0 s	0.0 s
T/C 1 Strt	1.260 mV	1.276 mV	1.280 mV
T/C 2 Strt	1.313 mV	1.305 mV	1.306 mV
T/C 3 Strt	1.111 mV	1.115 mV	1.116 mV
T/C 4 Strt	1.309 mV	1.306 mV	1.310 mV
T/C 5 Strt	1.310 mV	1.307 mV	1.310 mV
T/C 6 Strt	1.310 mV	1.305 mV	1.310 mV
T/C 7 Strt	1.095 mV	1.261 mV	1.284 mV
T/C 1 End	1.261 mV	1.276 mV	1.282 mV
T/C 2 End	1.313 mV	1.306 mV	1.308 mV
T/C 3 End	1.111 mV	1.115 mV	1.117 mV
T/C 4 End	1.306 mV	1.306 mV	1.310 mV
T/C 5 End	1.310 mV	1.308 mV	1.311 mV
T/C 6 End	1.306 mV	1.305 mV	1.310 mV
T/C 7 End	1.110 mV	1.265 mV	1.281 mV
Start Time	10:10	11:45	12:46
End Time	10:30	12:05	13:06

Date of Experiment 1986/ 5/23

MDEA Conc	20.0 wt%	Absorbing Gas	N2O
Piperazine Conc	0.0 kmol/m3	Surfactant	0.0100 wt%
Barometric Pressure	702.8 mm Hg	Rotameter Tube	603
Room Temperature	23.5 deg C	Nozzle Diam	0.60 mm
Manometer Right Leg	6.4 in H2O	Thermo Coarse	5.03
Manometer Left Leg	5.6 in H2O	Thermo Fine	0.0
Jet Elevation	87.915 cm	Feed Variac	0.0 %
North Pole	87.710 cm	Circ Variac	0.0 %
South Pole	82.605 cm		
Liquid Take-off	80.165 cm		

Flowmeter	30. mm	40. mm	50. mm
SFM Volume	10. mL	10. mL	10. mL
Time 1	91.37 s	77.52 s	69.91 s
Time 2	91.40 s	77.34 s	69.79 s
Time 3	90.73 s	78.13 s	69.38 s
Time 4	91.94 s	77.18 s	70.13 s
Time 5	90.41 s	77.29 s	69.05 s
Time 6	90.40 s	77.62 s	69.68 s
Time 7	90.41 s	76.98 s	69.90 s
Time 8	91.08 s	77.09 s	69.30 s
Time 9	90.38 s	77.27 s	70.34 s
Time 10	91.21 s	77.07 s	69.74 s
Time 11	90.73 s	77.31 s	69.90 s
Time 12	90.51 s	76.89 s	69.76 s
Time 13	90.88 s	77.09 s	69.57 s
Time 14	91.08 s	76.93 s	0.0 s
Time 15	92.33 s	0.0 s	0.0 s
Time 16	91.87 s	0.0 s	0.0 s
T/C 1 Strt	1.280 mV	1.280 mV	1.280 mV
T/C 2 Strt	1.310 mV	1.296 mV	1.300 mV
T/C 3 Strt	1.124 mV	1.150 mV	1.154 mV
T/C 4 Strt	1.329 mV	1.325 mV	1.325 mV
T/C 5 Strt	1.329 mV	1.325 mV	1.325 mV
T/C 6 Strt	1.329 mV	1.325 mV	1.325 mV
T/C 7 Strt	1.095 mV	1.235 mV	1.250 mV
T/C 1 End	1.277 mV	1.287 mV	1.288 mV
T/C 2 End	1.308 mV	1.304 mV	1.303 mV
T/C 3 End	1.137 mV	1.155 mV	1.157 mV
T/C 4 End	1.325 mV	1.326 mV	1.328 mV
T/C 5 End	1.325 mV	1.326 mV	1.328 mV
T/C 6 End	1.324 mV	1.325 mV	1.328 mV
T/C 7 End	1.090 mV	1.237 mV	1.265 mV
Start Time	09:40	11:00	12:05
End Time	10:15	11:22	12:30

Date of Experiment 1986/ 5/28

MDEA Conc	40.0 wt%	Absorbing Gas	N2O
Piperazine Conc	0.0 kmol/m3	Surfactant	0.0075 wt%
Barometric Pressure	702.2 mm Hg	Rotameter Tube	603
Room Temperature	24.0 deg C	Nozzle Diam	0.60 mm
Manometer Right Leg	6.4 in H2O	Thermo Coarse	5.03
Manometer Left Leg	5.6 in H2O	Thermo Fine	0.0
Jet Elevation	87.955 cm	Feed Variac	0.0 %
North Pole	87.750 cm	Circ Variac	0.0 %
South Pole	82.615 cm		
Liquid Take-off	80.225 cm		

Flowmeter	45. mm	60. mm	70. mm
SFM Volume	5. mL	5. mL	5. mL
Time 1	78.74 s	65.95 s	59.02 s
Time 2	78.06 s	65.78 s	60.00 s
Time 3	78.43 s	66.08 s	59.83 s
Time 4	79.08 s	65.86 s	60.10 s
Time 5	78.74 s	65.68 s	59.71 s
Time 6	78.66 s	66.45 s	59.44 s
Time 7	79.13 s	65.59 s	60.00 s
Time 8	77.87 s	65.64 s	59.61 s
Time 9	78.59 s	64.90 s	58.74 s
Time 10	78.07 s	65.75 s	58.93 s
Time 11	78.73 s	65.25 s	60.12 s
Time 12	78.81 s	65.48 s	59.87 s
Time 13	78.89 s	64.84 s	59.55 s
Time 14	0.0 s	0.0 s	59.04 s
Time 15	0.0 s	0.0 s	60.00 s
Time 16	0.0 s	0.0 s	59.13 s
Time 17	0.0 s	0.0 s	60.47 s
T/C 1 Strt	1.290 mV	1.270 mV	1.284 mV
T/C 2 Strt	1.315 mV	1.296 mV	1.300 mV
T/C 3 Strt	1.155 mV	1.170 mV	1.185 mV
T/C 4 Strt	1.325 mV	1.325 mV	1.325 mV
T/C 5 Strt	1.325 mV	1.325 mV	1.325 mV
T/C 6 Strt	1.325 mV	1.325 mV	1.325 mV
T/C 7 Strt	1.091 mV	1.172 mV	1.250 mV
T/C 1 End	1.290 mV	1.278 mV	1.292 mV
T/C 2 End	1.314 mV	1.300 mV	1.306 mV
T/C 3 End	1.164 mV	1.176 mV	1.190 mV
T/C 4 End	1.325 mV	1.325 mV	1.325 mV
T/C 5 End	1.325 mV	1.325 mV	1.325 mV
T/C 6 End	1.325 mV	1.325 mV	1.325 mV
T/C 7 End	1.090 mV	1.200 mV	1.265 mV
Start Time	09:50	11:00	12:05
End Time	10:18	11:25	12:37

Date of Experiment 1986/ 5/29

MDEA Conc	40.0 wt%	Absorbing Gas	N2O
Piperazine Conc	0.0 kmol/m3	Surfactant	0.0075 wt%
Barometric Pressure	702.2 mm Hg	Rotameter Tube	603
Room Temperature	24.5 deg C	Nozzle Diam	0.60 mm
Manometer Right Leg	6.4 in H2O	Thermo Coarse	5.03
Manometer Left Leg	5.6 in H2O	Thermo Fine	0.0
Jet Elevation	87.825 cm	Feed Variac	0.0 %
North Pole	87.620 cm	Circ Variac	0.0 %
South Pole	82.500 cm		
Liquid Take-off	80.055 cm		

Flowmeter	45. mm	60. mm	70. mm
SFM Volume	5. mL	5. mL	5. mL
Time 1	77.99 s	65.88 s	60.84 s
Time 2	77.79 s	65.60 s	59.45 s
Time 3	79.20 s	65.30 s	58.69 s
Time 4	77.91 s	65.42 s	59.52 s
Time 5	78.45 s	65.64 s	59.34 s
Time 6	78.19 s	65.28 s	59.49 s
Time 7	78.16 s	64.93 s	59.75 s
Time 8	78.83 s	65.26 s	60.15 s
Time 9	78.18 s	64.81 s	60.00 s
Time 10	78.37 s	64.99 s	59.74 s
Time 11	77.90 s	65.14 s	60.03 s
Time 12	78.50 s	65.07 s	60.80 s
Time 13	78.39 s	65.90 s	59.71 s
Time 14	79.32 s	65.28 s	59.48 s
Time 15	79.02 s	0.0 s	58.99 s
T/C 1 Strt	1.289 mV	1.275 mV	1.290 mV
T/C 2 Strt	1.315 mV	1.297 mV	1.305 mV
T/C 3 Strt	1.164 mV	1.176 mV	1.190 mV
T/C 4 Strt	1.325 mV	1.323 mV	1.325 mV
T/C 5 Strt	1.325 mV	1.324 mV	1.325 mV
T/C 6 Strt	1.325 mV	1.324 mV	1.325 mV
T/C 7 Strt	1.095 mV	1.192 mV	1.240 mV
T/C 1 End	1.289 mV	1.285 mV	1.285 mV
T/C 2 End	1.315 mV	1.301 mV	1.303 mV
T/C 3 End	1.170 mV	1.185 mV	1.196 mV
T/C 4 End	1.325 mV	1.325 mV	1.325 mV
T/C 5 End	1.325 mV	1.325 mV	1.325 mV
T/C 6 End	1.325 mV	1.325 mV	1.325 mV
T/C 7 End	1.195 mV	1.237 mV	1.250 mV
Start Time	09:45	10:53	11:55
End Time	10:07	11:15	12:20

Date of Experiment 1986/ 6/ 2

MDEA Conc	40.0 wt%	Absorbing Gas	N2O
Piperazine Conc	0.0 kmol/m3	Surfactant	0.0075 wt%
Barometric Pressure	700.2 mm Hg	Rotameter Tube	603
Room Temperature	24.0 deg C	Nozzle Diam	0.60 mm
Manometer Right Leg	6.4 in H2O	Thermo Coarse	5.27
Manometer Left Leg	5.6 in H2O	Thermo Fine	0.0
Jet Elevation	87.930 cm	Feed Variac	30.0 %
North Pole	87.720 cm	Circ Variac	100.0 %
South Pole	82.605 cm		
Liquid Take-off	80.200 cm		

Flowmeter	45. mm	45. mm	60. mm	70. mm
SFM Volume	5. mL	5. mL	5. mL	5. mL
Time 1	60.62 s	64.78 s	53.43 s	50.24 s
Time 2	61.59 s	65.33 s	53.24 s	50.41 s
Time 3	61.09 s	64.35 s	52.42 s	50.62 s
Time 4	59.49 s	64.19 s	53.37 s	50.00 s
Time 5	61.12 s	64.28 s	53.65 s	51.28 s
Time 6	61.33 s	62.88 s	53.59 s	50.14 s
Time 7	61.79 s	62.75 s	53.74 s	50.33 s
Time 8	62.34 s	64.52 s	53.65 s	50.74 s
Time 9	0.0 s	63.97 s	53.88 s	50.75 s
Time 10	0.0 s	63.96 s	53.70 s	50.73 s
Time 11	0.0 s	62.99 s	54.16 s	51.03 s
Time 12	0.0 s	62.80 s	53.69 s	50.27 s
Time 13	0.0 s	63.10 s	54.25 s	50.32 s
Time 14	0.0 s	62.86 s	0.0 s	0.0 s
T/C 1 Strt	2.590 mV	2.595 mV	2.596 mV	2.593 mV
T/C 2 Strt	2.612 mV	2.610 mV	2.609 mV	2.600 mV
T/C 3 Strt	1.120 mV	1.137 mV	1.205 mV	1.198 mV
T/C 4 Strt	2.627 mV	2.627 mV	2.623 mV	2.625 mV
T/C 5 Strt	2.636 mV	2.636 mV	2.633 mV	2.635 mV
T/C 6 Strt	2.616 mV	2.615 mV	2.615 mV	2.618 mV
T/C 7 Strt	2.412 mV	2.425 mV	2.584 mV	2.645 mV
T/C 1 End	2.595 mV	2.593 mV	2.590 mV	2.596 mV
T/C 2 End	2.610 mV	2.610 mV	2.600 mV	2.605 mV
T/C 3 End	1.137 mV	1.155 mV	1.210 mV	1.196 mV
T/C 4 End	2.627 mV	2.625 mV	2.622 mV	2.625 mV
T/C 5 End	2.636 mV	2.635 mV	2.632 mV	2.635 mV
T/C 6 End	2.615 mV	2.611 mV	2.610 mV	2.615 mV
T/C 7 End	2.425 mV	2.430 mV	2.587 mV	2.654 mV
Start Time	09:45	10:00	11:10	12:13
End Time	10:00	10:20	11:30	12:49

Date of Experiment 1986/ 6/ 3

MDEA Conc	40.0 wt%	Absorbing Gas	N2O
Piperazine Conc	0.0 kmol/m3	Surfactant	0.0075 wt%
Barometric Pressure	705.7 mm Hg	Rotameter Tube	603
Room Temperature	24.5 deg C	Nozzle Diam	0.60 mm
Manometer Right Leg	6.4 in H2O	Thermo Coarse	5.27
Manometer Left Leg	5.6 in H2O	Thermo Fine	0.0
Jet Elevation	88.135 cm	Feed Variac	30.0 %
North Pole	87.925 cm	Circ Variac	100.0 %
South Pole	82.810 cm		
Liquid Take-off	80.355 cm		

Flowmeter	45. mm	60. mm	70. mm
SFM Volume	5. mL	5. mL	5. mL
Time 1	63.33 s	55.10 s	52.63 s
Time 2	62.79 s	55.20 s	52.82 s
Time 3	63.31 s	54.12 s	51.16 s
Time 4	63.67 s	55.41 s	50.96 s
Time 5	63.63 s	54.95 s	52.50 s
Time 6	62.16 s	55.53 s	52.33 s
Time 7	62.82 s	55.50 s	52.38 s
Time 8	63.15 s	55.49 s	52.32 s
Time 9	63.46 s	55.65 s	52.15 s
Time 10	64.20 s	54.41 s	50.94 s
Time 11	63.37 s	56.57 s	51.63 s
Time 12	62.58 s	56.20 s	52.67 s
Time 13	62.63 s	55.81 s	52.32 s
Time 14	0.0 s	55.80 s	52.49 s
Time 15	0.0 s	56.09 s	52.03 s
Time 16	0.0 s	55.49 s	52.37 s
T/C 1 Strt	2.582 mV	2.585 mV	2.589 mV
T/C 2 Strt	2.600 mV	2.595 mV	2.600 mV
T/C 3 Strt	1.162 mV	1.185 mV	1.185 mV
T/C 4 Strt	2.625 mV	2.625 mV	2.625 mV
T/C 5 Strt	2.635 mV	2.635 mV	2.635 mV
T/C 6 Strt	2.615 mV	2.615 mV	2.619 mV
T/C 7 Strt	2.381 mV	2.558 mV	2.620 mV
T/C 1 End	2.585 mV	2.590 mV	2.591 mV
T/C 2 End	2.600 mV	2.600 mV	2.600 mV
T/C 3 End	1.170 mV	1.190 mV	1.185 mV
T/C 4 End	2.624 mV	2.625 mV	2.628 mV
T/C 5 End	2.635 mV	2.635 mV	2.635 mV
T/C 6 End	2.615 mV	2.615 mV	2.620 mV
T/C 7 End	2.390 mV	2.565 mV	2.625 mV
Start Time	09:45	10:50	12:00
End Time	10:05	11:20	12:25

Date of Experiment 1986/ 6/ 5

MDEA Conc	40.0 wt%	Absorbing Gas	N2O
Piperazine Conc	0.0 kmol/m3	Surfactant	0.0075 wt%
Barometric Pressure	701.2 mm Hg	Rotameter Tube	603
Room Temperature	24.0 deg C	Nozzle Diam	0.60 mm
Manometer Right Leg	6.4 in H2O	Thermo Coarse	5.51
Manometer Left Leg	5.6 in H2O	Thermo Fine	0.0
Jet Elevation	88.205 cm	Feed Variac	60.0 %
North Pole	87.995 cm	Circ Variac	110.0 %
South Pole	82.895 cm		
Liquid Take-off	80.470 cm		

Flowmeter	45. mm	60. mm	60. mm	70. mm
SFM Volume	5. mL	5. mL	5. mL	5. mL
Time 1	75.69 s	69.88 s	69.25 s	63.50 s
Time 2	75.27 s	71.94 s	68.96 s	63.90 s
Time 3	75.46 s	69.91 s	67.94 s	64.46 s
Time 4	75.62 s	70.79 s	67.93 s	62.58 s
Time 5	76.19 s	70.82 s	68.16 s	63.80 s
Time 6	76.37 s	69.70 s	68.55 s	64.75 s
Time 7	75.06 s	0.0 s	68.73 s	64.16 s
Time 8	75.62 s	0.0 s	69.37 s	62.77 s
Time 9	76.49 s	0.0 s	68.65 s	62.83 s
Time 10	76.07 s	0.0 s	68.35 s	63.99 s
Time 11	75.82 s	0.0 s	69.37 s	64.13 s
Time 12	0.0 s	0.0 s	68.07 s	62.54 s
Time 13	0.0 s	0.0 s	0.0 s	62.96 s
T/C 1 Strt	3.933 mV	3.938 mV	3.930 mV	3.935 mV
T/C 2 Strt	3.935 mV	3.940 mV	3.940 mV	3.940 mV
T/C 3 Strt	1.155 mV	1.165 mV	1.170 mV	1.177 mV
T/C 4 Strt	3.960 mV	3.960 mV	3.961 mV	3.961 mV
T/C 5 Strt	3.990 mV	3.990 mV	3.996 mV	3.993 mV
T/C 6 Strt	3.935 mV	3.935 mV	3.935 mV	3.945 mV
T/C 7 Strt	3.314 mV	3.454 mV	3.450 mV	3.500 mV
T/C 1 End	3.930 mV	3.930 mV	3.930 mV	3.935 mV
T/C 2 End	3.935 mV	3.940 mV	3.940 mV	3.943 mV
T/C 3 End	1.160 mV	1.170 mV	1.170 mV	1.178 mV
T/C 4 End	3.960 mV	3.961 mV	3.961 mV	3.965 mV
T/C 5 End	3.990 mV	3.996 mV	3.991 mV	3.995 mV
T/C 6 End	3.932 mV	3.935 mV	3.935 mV	3.938 mV
T/C 7 End	3.310 mV	3.450 mV	3.446 mV	3.501 mV
Start Time	10:05	11:20	11:30	12:38
End Time	10:35	11:30	11:55	13:05

Date of Experiment 1986/ 6/ 6

MDEA Conc	40.0 wt%	Absorbing Gas	N2O
Piperazine Conc	0.0 kmol/m3	Surfactant	0.0075 wt%
Barometric Pressure	698.2 mm Hg	Rotameter Tube	603
Room Temperature	25.0 deg C	Nozzle Diam	0.60 mm
Manometer Right Leg	6.4 in H2O	Thermo Coarse	5.51
Manometer Left Leg	5.6 in H2O	Thermo Fine	0.0
Jet Elevation	88.245 cm	Feed Variac	59.0 %
North Pole	88.025 cm	Circ Variac	110.0 %
South Pole	82.910 cm		
Liquid Take-off	80.475 cm		

Flowmeter	45. mm	45. mm	60. mm	70. mm
SFM Volume	5. mL	5. mL	5. mL	5. mL
Time 1	76.30 s	72.72 s	68.73 s	63.34 s
Time 2	76.46 s	72.80 s	68.80 s	62.31 s
Time 3	74.02 s	72.36 s	69.96 s	64.63 s
Time 4	75.37 s	72.80 s	69.94 s	64.16 s
Time 5	75.83 s	72.37 s	69.21 s	64.20 s
Time 6	75.36 s	72.07 s	67.89 s	64.39 s
Time 7	75.79 s	72.32 s	67.09 s	64.45 s
Time 8	75.87 s	71.63 s	69.09 s	63.77 s
Time 9	75.63 s	71.34 s	68.64 s	64.27 s
Time 10	76.37 s	72.77 s	67.93 s	63.37 s
Time 11	74.79 s	73.92 s	68.44 s	64.20 s
Time 12	74.89 s	73.77 s	69.17 s	61.03 s
Time 13	0.0 s	73.15 s	67.15 s	63.92 s
T/C 1 Strt	3.930 mV	3.925 mV	3.934 mV	3.936 mV
T/C 2 Strt	3.935 mV	3.940 mV	3.940 mV	3.946 mV
T/C 3 Strt	1.210 mV	1.221 mV	1.226 mV	1.225 mV
T/C 4 Strt	3.960 mV	3.961 mV	3.961 mV	3.966 mV
T/C 5 Strt	3.990 mV	3.991 mV	3.992 mV	3.995 mV
T/C 6 Strt	3.934 mV	3.940 mV	3.940 mV	3.940 mV
T/C 7 Strt	3.318 mV	3.314 mV	3.460 mV	3.515 mV
T/C 1 End	3.925 mV	3.921 mV	3.940 mV	3.930 mV
T/C 2 End	3.940 mV	3.935 mV	3.950 mV	3.941 mV
T/C 3 End	1.221 mV	1.224 mV	1.230 mV	1.228 mV
T/C 4 End	3.961 mV	3.961 mV	3.961 mV	3.969 mV
T/C 5 End	3.991 mV	3.990 mV	3.995 mV	3.997 mV
T/C 6 End	3.940 mV	3.935 mV	3.940 mV	3.943 mV
T/C 7 End	3.314 mV	3.312 mV	3.460 mV	3.513 mV
Start Time	10:00	10:30	11:30	12:40
End Time	10:30	10:50	12:00	13:20

Date of Experiment 1986/ 6/ 9

MDEA Conc	40.0 wt%	Absorbing Gas	N2O
Piperazine Conc	0.0 kmol/m3	Surfactant	0.0075 wt%
Barometric Pressure	704.3 mm Hg	Rotameter Tube	603
Room Temperature	24.5 deg C	Nozzle Diam	0.60 mm
Manometer Right Leg	6.4 in H2O	Thermo Coarse	5.51
Manometer Left Leg	5.6 in H2O	Thermo Fine	0.0
Jet Elevation	88.180 cm	Feed Variac	59.0 %
North Pole	87.975 cm	Circ Variac	110.0 %
South Pole	82.850 cm		
Liquid Take-off	80.425 cm		

Flowmeter	45. mm	60. mm	70. mm
SFM Volume	5. mL	5. mL	5. mL
Time 1	74.54 s	69.34 s	62.50 s
Time 2	74.73 s	67.12 s	62.53 s
Time 3	76.24 s	69.49 s	63.47 s
Time 4	75.06 s	69.07 s	62.78 s
Time 5	75.70 s	68.37 s	63.03 s
Time 6	73.94 s	67.93 s	62.70 s
Time 7	75.90 s	67.16 s	63.37 s
Time 8	75.75 s	67.08 s	62.53 s
Time 9	75.56 s	69.37 s	63.81 s
Time 10	73.95 s	69.93 s	62.66 s
Time 11	75.21 s	68.27 s	63.72 s
Time 12	75.12 s	67.28 s	62.07 s
Time 13	0.0 s	68.74 s	62.57 s
Time 14	0.0 s	69.85 s	0.0 s
T/C 1 Strt	3.932 mV	3.936 mV	3.930 mV
T/C 2 Strt	3.942 mV	3.946 mV	3.943 mV
T/C 3 Strt	1.175 mV	1.195 mV	1.225 mV
T/C 4 Strt	3.964 mV	3.966 mV	3.968 mV
T/C 5 Strt	3.992 mV	3.995 mV	3.995 mV
T/C 6 Strt	3.940 mV	3.940 mV	3.943 mV
T/C 7 Strt	3.317 mV	3.461 mV	3.510 mV
T/C 1 End	3.935 mV	3.935 mV	3.929 mV
T/C 2 End	3.945 mV	3.946 mV	3.940 mV
T/C 3 End	1.185 mV	1.210 mV	1.228 mV
T/C 4 End	3.965 mV	3.970 mV	3.966 mV
T/C 5 End	3.995 mV	3.998 mV	3.995 mV
T/C 6 End	3.940 mV	3.941 mV	3.945 mV
T/C 7 End	3.310 mV	3.460 mV	3.500 mV
Start Time	10:15	11:35	12:45
End Time	10:45	12:00	13:20

Date of Experiment 1986/ 6/10

MDEA Conc	40.0 wt%	Absorbing Gas	N2O
Piperazine Conc	0.0 kmol/m3	Surfactant	0.0075 wt%
Barometric Pressure	703.3 mm Hg	Rotameter Tube	603
Room Temperature	25.0 deg C	Nozzle Diam	0.60 mm
Manometer Right Leg	6.4 in H2O	Thermo Coarse	5.27
Manometer Left Leg	5.6 in H2O	Thermo Fine	0.0
Jet Elevation	88.170 cm	Feed Variac	30.0 %
North Pole	87.960 cm	Circ Variac	100.0 %
South Pole	82.830 cm		
Liquid Take-off	80.360 cm		

Flowmeter	45. mm	60. mm	70. mm
SFM Volume	5. mL	5. mL	5. mL
Time 1	60.23 s	54.99 s	52.86 s
Time 2	60.87 s	55.99 s	52.56 s
Time 3	60.27 s	55.29 s	52.58 s
Time 4	61.29 s	56.10 s	52.78 s
Time 5	60.46 s	56.20 s	53.10 s
Time 6	61.57 s	55.61 s	52.44 s
Time 7	60.25 s	55.51 s	53.26 s
Time 8	61.34 s	56.21 s	53.17 s
Time 9	61.74 s	56.06 s	52.86 s
Time 10	61.85 s	55.50 s	53.16 s
Time 11	61.73 s	54.93 s	53.09 s
Time 12	62.05 s	54.87 s	53.10 s
Time 13	62.37 s	55.37 s	52.89 s
Time 14	61.74 s	55.68 s	52.16 s
Time 15	62.53 s	0.0 s	52.68 s
Time 16	0.0 s	0.0 s	52.57 s
Time 17	0.0 s	0.0 s	52.75 s
T/C 1 Strt	2.595 mV	2.593 mV	2.596 mV
T/C 2 Strt	2.610 mV	2.600 mV	2.603 mV
T/C 3 Strt	1.195 mV	1.210 mV	1.224 mV
T/C 4 Strt	2.620 mV	2.619 mV	2.620 mV
T/C 5 Strt	2.630 mV	2.630 mV	2.630 mV
T/C 6 Strt	2.610 mV	2.610 mV	2.610 mV
T/C 7 Strt	2.425 mV	2.597 mV	2.650 mV
T/C 1 End	2.587 mV	2.598 mV	2.595 mV
T/C 2 End	2.602 mV	2.605 mV	2.605 mV
T/C 3 End	1.195 mV	1.220 mV	1.230 mV
T/C 4 End	2.620 mV	2.620 mV	2.620 mV
T/C 5 End	2.630 mV	2.631 mV	2.630 mV
T/C 6 End	2.610 mV	2.611 mV	2.611 mV
T/C 7 End	2.427 mV	2.600 mV	2.655 mV
Start Time	10:00	11:15	12:25
End Time	10:30	11:40	12:55

Date of Experiment 1986/ 6/11

MDEA Conc	40.0 wt%	Absorbing Gas	CO2
Piperazine Conc	0.0 kmol/m3	Surfactant	0.0075 wt%
Barometric Pressure	700.1 mm Hg	Rotameter Tube	603
Room Temperature	25.0 deg C	Nozzle Diam	0.60 mm
Manometer Right Leg	6.4 in H2O	Thermo Coarse	5.51
Manometer Left Leg	5.6 in H2O	Thermo Fine	0.0
Jet Elevation	88.235 cm	Feed Variac	60.0 %
North Pole	88.020 cm	Circ Variac	110.0 %
South Pole	82.905 cm		
Liquid Take-off	80.510 cm		

Flowmeter	45. mm	60. mm	70. mm	50. mm	50. mm
SFM Volume	25. mL	25. mL	25. mL	25. mL	25. mL
Time 1	20.17 s	19.18 s	19.34 s	19.66 s	19.14 s
Time 2	19.79 s	19.14 s	19.32 s	19.64 s	19.37 s
Time 3	20.06 s	19.16 s	19.14 s	19.66 s	19.06 s
Time 4	20.06 s	19.18 s	19.13 s	19.82 s	19.09 s
Time 5	19.81 s	19.18 s	19.20 s	19.56 s	19.26 s
Time 6	20.12 s	19.09 s	19.04 s	19.67 s	19.21 s
Time 7	19.83 s	19.00 s	19.20 s	19.42 s	19.32 s
Time 8	20.25 s	19.36 s	19.25 s	19.67 s	19.28 s
Time 9	19.93 s	19.27 s	19.28 s	19.66 s	19.13 s
Time 10	20.10 s	19.27 s	19.07 s	19.53 s	19.20 s
Time 11	19.84 s	19.31 s	19.27 s	19.79 s	19.31 s
Time 12	19.76 s	19.19 s	19.34 s	19.52 s	19.25 s
Time 13	19.88 s	19.17 s	19.34 s	19.74 s	19.20 s
Time 14	19.93 s	19.02 s	19.21 s	19.52 s	19.24 s
Time 15	19.91 s	19.31 s	19.18 s	0.0 s	0.0 s
Time 16	19.94 s	19.34 s	19.14 s	0.0 s	0.0 s
T/C 1 Strt	3.940 mV	3.935 mV	3.935 mV	3.910 mV	3.910 mV
T/C 2 Strt	3.964 mV	3.972 mV	3.973 mV	3.970 mV	3.965 mV
T/C 3 Strt	1.165 mV	1.175 mV	1.192 mV	1.182 mV	1.185 mV
T/C 4 Strt	3.950 mV	3.955 mV	3.980 mV	3.962 mV	3.960 mV
T/C 5 Strt	3.980 mV	3.990 mV	3.995 mV	3.994 mV	3.992 mV
T/C 6 Strt	3.923 mV	3.933 mV	3.974 mV	3.940 mV	3.940 mV
T/C 7 Strt	3.284 mV	3.440 mV	3.490 mV	3.321 mV	3.320 mV
T/C 1 End	3.942 mV	3.935 mV	3.925 mV	3.912 mV	3.913 mV
T/C 2 End	3.980 mV	3.975 mV	3.965 mV	3.966 mV	3.967 mV
T/C 3 End	1.170 mV	1.187 mV	1.194 mV	1.185 mV	1.187 mV
T/C 4 End	3.956 mV	3.960 mV	3.980 mV	3.960 mV	3.960 mV
T/C 5 End	3.987 mV	3.991 mV	3.995 mV	3.993 mV	3.991 mV
T/C 6 End	3.927 mV	3.935 mV	3.986 mV	3.942 mV	3.940 mV
T/C 7 End	3.285 mV	3.437 mV	3.489 mV	3.320 mV	3.327 mV
Start Time	10:00	11:00	11:50	12:50	13:10
End Time	10:20	11:20	12:15	13:10	13:27

Date of Experiment 1986/ 6/12

MDEA Conc	40.0 wt%	Absorbing Gas	CO2
Piperazine Conc	0.0 kmol/m3	Surfactant	0.0075 wt%
Barometric Pressure	706.6 mm Hg	Rotameter Tube	603
Room Temperature	24.5 deg C	Nozzle Diam	0.60 mm
Manometer Right Leg	6.4 in H2O	Thermo Coarse	5.51
Manometer Left Leg	5.6 in H2O	Thermo Fine	0.0
Jet Elevation	88.025 cm	Feed Variac	59.5 %
North Pole	87.820 cm	Circ Variac	110.0 %
South Pole	82.685 cm		
Liquid Take-off	80.295 cm		

Flowmeter	45. mm	60. mm	40. mm
SFM Volume	25. mL	25. mL	25. mL
Time 1	19.96 s	19.06 s	20.06 s
Time 2	19.93 s	19.03 s	19.86 s
Time 3	19.84 s	19.14 s	19.89 s
Time 4	19.84 s	19.12 s	20.01 s
Time 5	19.67 s	19.34 s	20.07 s
Time 6	19.87 s	18.92 s	20.20 s
Time 7	19.64 s	18.82 s	20.14 s
Time 8	20.02 s	18.99 s	19.89 s
Time 9	20.01 s	19.09 s	19.94 s
Time 10	19.80 s	19.19 s	20.14 s
Time 11	19.99 s	19.20 s	20.18 s
Time 12	20.00 s	19.03 s	19.85 s
Time 13	20.11 s	18.92 s	20.02 s
Time 14	19.93 s	18.95 s	0.0 s
Time 15	19.87 s	19.25 s	0.0 s
Time 16	20.27 s	19.45 s	0.0 s
Time 17	0.0 s	19.13 s	0.0 s
T/C 1 Strt	3.926 mV	3.915 mV	3.911 mV
T/C 2 Strt	3.955 mV	3.960 mV	3.980 mV
T/C 3 Strt	1.157 mV	1.185 mV	1.205 mV
T/C 4 Strt	3.940 mV	3.960 mV	3.965 mV
T/C 5 Strt	3.974 mV	3.991 mV	3.995 mV
T/C 6 Strt	3.915 mV	3.935 mV	3.943 mV
T/C 7 Strt	3.275 mV	3.435 mV	3.188 mV
T/C 1 End	3.926 mV	3.911 mV	3.913 mV
T/C 2 End	3.962 mV	3.957 mV	3.980 mV
T/C 3 End	1.163 mV	1.191 mV	1.210 mV
T/C 4 End	3.947 mV	3.956 mV	3.965 mV
T/C 5 End	3.985 mV	3.991 mV	3.996 mV
T/C 6 End	3.924 mV	3.935 mV	3.941 mV
T/C 7 End	3.275 mV	3.430 mV	3.186 mV
Start Time	10:05	11:07	12:02
End Time	10:25	11:25	12:18

[redacted] 1986/ 6/13

MDEA Conc	40.0 wt%	Absorbing Gas	CO2
Piperazine Conc	0.0 kmol/m3	Surfactant	0.0075 wt%
Barometric Pressure	707.5 mm Hg	Rotameter Tube	603
Room Temperature	24.0 deg C	Nozzle Diam	0.60 mm
Manometer Right Leg	6.[redacted] in H2O	Thermo Coarse	5.27
Manometer Left Leg	5.6 in H2O	Thermo Fine	0.0
Jet Elevation	87.990 cm	Feed Variac	32.0 %
North Pole	87.785 cm	Circ Variac	110.0 %
South Pole	82.655 cm		
Liquid Take-off	80.255 cm		

Flowmeter	40. mm	50. mm	60. mm
SFM Volume	25. mL	25. mL	25. mL
Time 1	26.18 s	25.67 s	25.28 s
Time 2	26.40 s	25.65 s	25.16 s
Time 3	26.25 s	25.59 s	25.18 s
Time 4	26.38 s	25.72 s	25.17 s
Time 5	26.52 s	25.37 s	25.18 s
Time 6	26.50 s	25.76 s	25.16 s
Time 7	26.34 s	25.63 s	25.23 s
Time 8	26.53 s	25.77 s	25.27 s
Time 9	26.46 s	25.77 s	25.38 s
Time 10	26.56 s	25.76 s	25.36 s
Time 11	26.38 s	25.71 s	25.14 s
Time 12	26.07 s	25.80 s	25.27 s
Time 13	26.50 s	25.77 s	25.19 s
Time 14	26.56 s	25.72 s	25.16 s
Time 15	26.51 s	25.67 s	25.21 s
Time 16	26.39 s	25.79 s	25.13 s
Time 17	26.47 s	0.0 s	0.0 s
T/C 1 Strt	2.595 mV	2.580 mV	2.595 mV
T/C 2 Strt	2.640 mV	2.631 mV	2.628 mV
T/C 3 Strt	1.150 mV	1.165 mV	1.171 mV
T/C 4 Strt	2.616 mV	2.617 mV	2.620 mV
T/C 5 Strt	2.630 mV	2.630 mV	2.631 mV
T/C 6 Strt	2.606 mV	2.610 mV	2.611 mV
T/C 7 Strt	2.305 mV	2.455 mV	2.559 mV
T/C 1 End	2.594 mV	2.580 mV	2.595 mV
T/C 2 End	2.640 mV	2.622 mV	2.629 mV
T/C 3 End	1.160 mV	1.170 mV	1.174 mV
T/C 4 End	2.619 mV	2.620 mV	2.620 mV
T/C 5 End	2.630 mV	2.632 mV	2.633 mV
T/C 6 End	2.609 mV	2.611 mV	2.611 mV
T/C 7 End	2.310 mV	2.460 mV	2.565 mV
Start Time	09:30	10:25	11:20
End Time	09:47	10:45	11:35

Date of Experiment 1986/ 6/17

MDEA Conc	40.0 wt%	Absorbing Gas	CO2
Piperazine Conc	0.0 kmol/m3	Surfactant	0.0075 wt%
Barometric Pressure	700.7 mm Hg	Rotameter Tube	603
Room Temperature	24.0 deg C	Nozzle Diam	0.60 mm
Manometer Right Leg	6.4 in H2O	Thermo Coarse	5.27
Manometer Left Leg	5.6 in H2O	Thermo Fine	0.0
Jet Elevation	87.925 cm	Feed Variac	30.0 %
North Pole	87.715 cm	Circ Variac	110.0 %
South Pole	82.605 cm		
Liquid Take-off	80.205 cm		

Flowmeter	40. mm	50. mm	60. mm
SFM Volume	25. mL	25. mL	25. mL
Time 1	26.54 s	25.70 s	25.25 s
Time 2	26.47 s	25.72 s	25.32 s
Time 3	26.59 s	25.81 s	25.34 s
Time 4	26.46 s	25.63 s	25.27 s
Time 5	26.63 s	25.78 s	25.21 s
Time 6	26.49 s	25.83 s	25.31 s
Time 7	26.56 s	25.97 s	25.23 s
Time 8	26.48 s	25.66 s	25.17 s
Time 9	26.41 s	25.81 s	25.29 s
Time 10	26.54 s	25.85 s	25.31 s
Time 11	26.59 s	25.59 s	25.37 s
Time 12	26.61 s	25.83 s	25.38 s
Time 13	26.41 s	25.73 s	25.31 s
Time 14	26.57 s	25.74 s	25.23 s
Time 15	26.50 s	25.77 s	25.27 s
Time 16	0.0 s	25.66 s	25.18 s
T/C 1 Strt	2.587 mV	2.580 mV	2.595 mV
T/C 2 Strt	2.628 mV	2.621 mV	2.628 mV
T/C 3 Strt	1.159 mV	1.162 mV	1.170 mV
T/C 4 Strt	2.610 mV	2.610 mV	2.611 mV
T/C 5 Strt	2.620 mV	2.620 mV	2.625 mV
T/C 6 Strt	2.600 mV	2.601 mV	2.605 mV
T/C 7 Strt	2.315 mV	2.470 mV	2.571 mV
T/C 1 End	2.590 mV	2.585 mV	2.598 mV
T/C 2 End	2.630 mV	2.622 mV	2.628 mV
T/C 3 End	1.160 mV	1.166 mV	1.175 mV
T/C 4 End	2.610 mV	2.610 mV	2.613 mV
T/C 5 End	2.620 mV	2.621 mV	2.625 mV
T/C 6 End	2.600 mV	2.600 mV	2.605 mV
T/C 7 End	2.320 mV	2.475 mV	2.575 mV
Start Time	09:35	10:25	11:15
End Time	09:50	10:40	11:42

Date of Experiment 1986/ 6/18

MDEA Conc	40.0 wt%	Absorbing Gas	CO2
Piperazine Conc	0.0 kmol/m3	Surfactant	0.0075 wt%
Barometric Pressure	698.2 mm Hg	Rotameter Tube	603
Room Temperature	24.0 deg C	Nozzle Diam	0.60 mm
Manometer Right Leg	6.4 in H2O	Thermo Coarse	5.03
Manometer Left Leg	5.6 in H2O	Thermo Fine	0.0
Jet Elevation	88.070 cm	Feed Variac	0.0 %
North Pole	87.860 cm	Circ Variac	0.0 %
South Pole	82.740 cm		
Liquid Take-off	80.365 cm		

Flowmeter	45. mm	60. mm	70. mm
SFM Volume	25. mL	25. mL	25. mL
Time 1	44.95 s	44.84 s	43.31 s
Time 2	45.09 s	45.09 s	43.42 s
Time 3	45.11 s	44.66 s	43.47 s
Time 4	45.02 s	44.72 s	43.41 s
Time 5	44.95 s	44.69 s	43.52 s
Time 6	44.83 s	44.82 s	43.63 s
Time 7	44.99 s	44.79 s	43.45 s
Time 8	44.97 s	44.73 s	43.65 s
Time 9	45.09 s	44.85 s	43.56 s
Time 10	44.85 s	44.80 s	43.68 s
Time 11	44.88 s	44.52 s	43.47 s
Time 12	44.85 s	44.57 s	43.34 s
Time 13	45.01 s	44.75 s	43.52 s
Time 14	0.0 s	44.71 s	43.54 s
T/C 1 Strt	1.317 mV	1.260 mV	1.270 mV
T/C 2 Strt	1.375 mV	1.332 mV	1.322 mV
T/C 3 Strt	1.185 mV	1.190 mV	1.205 mV
T/C 4 Strt	1.355 mV	1.345 mV	1.356 mV
T/C 5 Strt	1.355 mV	1.345 mV	1.346 mV
T/C 6 Strt	1.355 mV	1.345 mV	1.354 mV
T/C 7 Strt	1.005 mV	0.972 mV	1.154 mV
T/C 1 End	1.314 mV	1.260 mV	1.272 mV
T/C 2 End	1.372 mV	1.330 mV	1.320 mV
T/C 3 End	1.190 mV	1.195 mV	1.208 mV
T/C 4 End	1.350 mV	1.344 mV	1.340 mV
T/C 5 End	1.350 mV	1.344 mV	1.340 mV
T/C 6 End	1.350 mV	1.344 mV	1.340 mV
T/C 7 End	1.000 mV	0.996 mV	1.165 mV
Start Time	09:40	10:40	11:40
End Time	10:00	11:00	12:00

Date of Experiment 1986/ 6/19

MDEA Conc	40.0 wt%	Absorbing Gas	CO2
Piperazine Conc	0.0 kmol/m3	Surfactant	0.0075 wt%
Barometric Pressure	694.1 mm Hg	Rotameter Tube	603
Room Temperature	23.0 deg C	Nozzle Diam	0.60 mm
Manometer Right Leg	6.4 in H2O	Thermo Coarse	5.03
Manometer Left Leg	5.6 in H2O	Thermo Fine	0.0
Jet Elevation	88.090 cm	Feed Variac	0.0 %
North Pole	87.885 cm	Circ Variac	0.0 %
South Pole	82.755 cm		
Liquid Take-off	80.375 cm		

Flowmeter	45. mm	60. mm	70. mm
SFM Volume	25. mL	25. mL	25. mL
Time 1	45.14 s	44.25 s	42.41 s
Time 2	44.99 s	43.91 s	42.56 s
Time 3	44.95 s	43.95 s	42.63 s
Time 4	45.12 s	44.25 s	42.52 s
Time 5	44.93 s	44.13 s	42.74 s
Time 6	44.88 s	44.11 s	42.76 s
Time 7	44.91 s	44.13 s	42.71 s
Time 8	44.76 s	43.74 s	42.49 s
Time 9	44.82 s	43.91 s	42.53 s
Time 10	45.00 s	44.06 s	42.62 s
Time 11	44.66 s	43.93 s	42.50 s
Time 12	44.66 s	43.89 s	42.57 s
Time 13	44.93 s	43.67 s	42.61 s
Time 14	44.98 s	43.78 s	42.49 s
Time 15	0.0 s	0.0 s	42.58 s
T/C 1 Strt	1.300 mV	1.270 mV	1.290 mV
T/C 2 Strt	1.350 mV	1.323 mV	1.330 mV
T/C 3 Strt	1.145 mV	1.145 mV	1.150 mV
T/C 4 Strt	1.336 mV	1.333 mV	1.336 mV
T/C 5 Strt	1.337 mV	1.333 mV	1.336 mV
T/C 6 Strt	1.336 mV	1.333 mV	1.336 mV
T/C 7 Strt	1.050 mV	1.141 mV	1.255 mV
T/C 1 End	1.296 mV	1.279 mV	1.295 mV
T/C 2 End	1.350 mV	1.325 mV	1.330 mV
T/C 3 End	1.150 mV	1.149 mV	1.155 mV
T/C 4 End	1.335 mV	1.335 mV	1.335 mV
T/C 5 End	1.335 mV	1.335 mV	1.335 mV
T/C 6 End	1.335 mV	1.335 mV	1.335 mV
T/C 7 End	1.072 mV	1.188 mV	1.270 mV
Start Time	09:30	10:20	11:17
End Time	09:45	10:43	11:40

Date of Experiment 1986/ 6/20

MDEA Conc	40.0 wt%	Absorbing Gas	CO2
Piperazine Conc	0.0 kmol/m3	Surfactant	0.0075 wt%
Barometric Pressure	698.5 mm Hg	Rotameter Tube	603
Room Temperature	24.5 deg C	Nozzle Diam	0.60 mm
Manometer Right Leg	6.4 in H2O	Thermo Coarse	5.19
Manometer Left Leg	5.6 in H2O	Thermo Fine	0.0
Jet Elevation	88.295 cm	Feed Variac	25.0 %
North Pole	88.095 cm	Circ Variac	0.0 %
South Pole	82.980 cm		
Liquid Take-off	80.590 cm		

Flowmeter	45. mm	50. mm	60. mm
SFM Volume	25. mL	25. mL	25. mL
Time 1	31.31 s	31.06 s	30.48 s
Time 2	31.33 s	31.07 s	30.56 s
Time 3	31.46 s	31.08 s	30.61 s
Time 4	31.37 s	31.11 s	30.41 s
Time 5	31.41 s	31.07 s	30.59 s
Time 6	31.35 s	31.07 s	30.46 s
Time 7	31.44 s	31.11 s	30.40 s
Time 8	31.65 s	31.16 s	30.51 s
Time 9	31.46 s	31.02 s	30.56 s
Time 10	31.31 s	31.08 s	30.47 s
Time 11	31.45 s	31.16 s	30.56 s
Time 12	31.32 s	31.12 s	30.52 s
Time 13	31.30 s	31.11 s	30.45 s
Time 14	31.35 s	0.0 s	30.51 s
Time 15	0.0 s	0.0 s	30.48 s
T/C 1 Strt	2.085 mV	2.072 mV	2.076 mV
T/C 2 Strt	2.119 mV	2.125 mV	2.122 mV
T/C 3 Strt	1.170 mV	1.181 mV	1.195 mV
T/C 4 Strt	2.133 mV	2.131 mV	2.135 mV
T/C 5 Strt	2.139 mV	2.140 mV	2.140 mV
T/C 6 Strt	2.126 mV	2.125 mV	2.130 mV
T/C 7 Strt	1.833 mV	1.870 mV	1.933 mV
T/C 1 End	2.080 mV	2.076 mV	2.076 mV
T/C 2 End	2.137 mV	2.128 mV	2.121 mV
T/C 3 End	1.175 mV	1.187 mV	1.205 mV
T/C 4 End	2.135 mV	2.132 mV	2.134 mV
T/C 5 End	2.140 mV	2.140 mV	2.139 mV
T/C 6 End	2.127 mV	2.125 mV	2.129 mV
T/C 7 End	1.825 mV	1.872 mV	1.938 mV
Start Time	09:35	10:30	11:20
End Time	09:55	10:48	11:40

Date of Experiment 1986/ 6/23

MDEA Conc	40.0 wt%	Absorbing Gas	CO2
Piperazine Conc	0.0 kmol/m3	Surfactant	0.0075 wt%
Barometric Pressure	703.0 mm Hg	Rotameter Tube	603
Room Temperature	25.0 deg C	Nozzle Diam	0.60 mm
Manometer Right Leg	6.6 in H2O	Thermo Coarse	5.19
Manometer Left Leg	5.4 in H2O	Thermo Fine	0.0
Jet Elevation	88.370 cm	Feed Variac	20.0 %
North Pole	88.160 cm	Circ Variac	0.0 %
South Pole	83.040 cm		
Liquid Take-off	80.620 cm		

Flowmeter	45. mm	50. mm	50. mm	60. mm
SFM Volume	25. mL	25. mL	25. mL	25. mL
Time 1	31.46 s	31.16 s	31.31 s	30.56 s
Time 2	31.47 s	31.22 s	31.27 s	30.62 s
Time 3	31.56 s	30.95 s	31.37 s	30.61 s
Time 4	31.49 s	31.19 s	31.29 s	30.52 s
Time 5	31.45 s	31.22 s	31.32 s	30.59 s
Time 6	31.52 s	31.26 s	31.32 s	30.60 s
Time 7	31.45 s	31.25 s	31.37 s	30.58 s
Time 8	31.48 s	31.29 s	31.43 s	30.49 s
Time 9	31.52 s	31.27 s	31.37 s	30.56 s
Time 10	31.61 s	31.27 s	31.49 s	30.56 s
Time 11	31.65 s	31.16 s	31.35 s	30.60 s
Time 12	31.50 s	31.16 s	31.37 s	30.52 s
Time 13	31.56 s	31.16 s	31.38 s	30.58 s
Time 14	31.53 s	31.13 s	31.30 s	30.57 s
Time 15	0.0 s	31.01 s	0.0 s	30.59 s
T/C 1 Strt	2.065 mV	2.065 mV	2.063 mV	2.065 mV
T/C 2 Strt	2.135 mV	2.125 mV	2.125 mV	2.120 mV
T/C 3 Strt	1.205 mV	1.213 mV	1.213 mV	1.225 mV
T/C 4 Strt	2.143 mV	2.143 mV	2.140 mV	2.143 mV
T/C 5 Strt	2.150 mV	2.149 mV	2.147 mV	2.149 mV
T/C 6 Strt	2.140 mV	2.139 mV	2.137 mV	2.138 mV
T/C 7 Strt	1.835 mV	1.904 mV	1.900 mV	1.960 mV
T/C 1 End	2.060 mV	2.063 mV	2.063 mV	2.066 mV
T/C 2 End	2.135 mV	2.125 mV	2.125 mV	2.120 mV
T/C 3 End	1.206 mV	1.213 mV	1.215 mV	1.226 mV
T/C 4 End	2.143 mV	2.140 mV	2.140 mV	2.141 mV
T/C 5 End	2.149 mV	2.147 mV	2.146 mV	2.150 mV
T/C 6 End	2.139 mV	2.137 mV	2.136 mV	2.137 mV
T/C 7 End	1.839 mV	1.900 mV	1.902 mV	1.961 mV
Start Time	09:30	10:25	10:45	11:30
End Time	09:50	10:45	11:00	12:00

Date of Experiment 1986/ 6/25

MDEA Conc	40.0 wt%	Absorbing Gas	CO2
Piperazine Conc	0.05 kmol/m3	Surfactant	0.0075 wt%
Barometric Pressure	699.6 mm Hg	Rotameter Tube	603
Room Temperature	24.0 deg C	Nozzle Diam	0.60 mm
Manometer Right Leg	6.7 in H2O	Thermo Coarse	5.19
Manometer Left Leg	5.3 in H2O	Thermo Fine	0.0
Jet Elevation	88.300 cm	Feed Variac	22.0 %
North Pole	88.100 cm	Circ Variac	0.0 %
South Pole	82.980 cm		
Liquid Take-off	80.575 cm		

Flowmeter	45. mm	50. mm	60. mm
SFM Volume	25. mL	25. mL	25. mL
Time 1	27.58 s	26.80 s	25.81 s
Time 2	27.60 s	26.82 s	25.81 s
Time 3	27.66 s	26.82 s	25.86 s
Time 4	27.63 s	26.85 s	25.83 s
Time 5	27.62 s	26.78 s	25.79 s
Time 6	27.57 s	26.82 s	25.84 s
Time 7	27.58 s	26.77 s	25.87 s
Time 8	27.61 s	26.79 s	25.86 s
Time 9	27.57 s	26.86 s	25.84 s
Time 10	27.64 s	26.78 s	25.79 s
Time 11	27.62 s	26.84 s	25.89 s
Time 12	27.52 s	26.75 s	25.88 s
Time 13	27.59 s	26.85 s	25.82 s
Time 14	27.61 s	26.80 s	25.79 s
T/C 1 Strt	2.045 mV	2.052 mV	2.052 mV
T/C 2 Strt	2.121 mV	2.121 mV	2.115 mV
T/C 3 Strt	1.180 mV	1.180 mV	1.176 mV
T/C 4 Strt	2.135 mV	2.135 mV	2.135 mV
T/C 5 Strt	2.140 mV	2.142 mV	2.140 mV
T/C 6 Strt	2.130 mV	2.130 mV	2.130 mV
T/C 7 Strt	1.786 mV	1.865 mV	1.930 mV
T/C 1 End	2.046 mV	2.054 mV	2.055 mV
T/C 2 End	2.123 mV	2.124 mV	2.115 mV
T/C 3 End	1.180 mV	1.180 mV	1.180 mV
T/C 4 End	2.135 mV	2.135 mV	2.135 mV
T/C 5 End	2.140 mV	2.142 mV	2.140 mV
T/C 6 End	2.130 mV	2.130 mV	2.130 mV
T/C 7 End	1.798 mV	1.867 mV	1.930 mV
Start Time	09:45	10:40	11:30
End Time	10:05	10:55	11:45

Date of Experiment 1986/ 6/26

MDEA Conc	40.0 wt%	Absorbing Gas	CO2
Piperazine Conc	0.05 kmol/m3	Surfactant	0.0075 wt%
Barometric Pressure	702.5 mm Hg	Rotameter Tube	603
Room Temperature	24.0 deg C	Nozzle Diam	0.60 mm
Manometer Right Leg	6.8 in H2O	Thermo Coarse	5.19
Manometer Left Leg	5.2 in H2O	Thermo Fine	0.0
Jet Elevation	88.270 cm	Feed Variac	22.0 %
North Pole	88.070 cm	Circ Variac	0.0 %
South Pole	82.955 cm		
Liquid Take-off	80.535 cm		

Flowmeter	45. mm	50. mm	60. mm
SFM Volume	25. mL	25. mL	25. mL
Time 1	27.44 s	26.81 s	26.00 s
Time 2	27.42 s	26.92 s	25.99 s
Time 3	27.51 s	26.90 s	26.02 s
Time 4	27.53 s	26.82 s	25.82 s
Time 5	27.56 s	26.85 s	25.95 s
Time 6	27.46 s	26.74 s	26.05 s
Time 7	27.37 s	26.80 s	25.93 s
Time 8	27.40 s	26.81 s	25.95 s
Time 9	27.30 s	26.85 s	26.02 s
Time 10	27.49 s	26.93 s	25.91 s
Time 11	27.38 s	26.69 s	26.05 s
Time 12	27.37 s	26.83 s	26.02 s
Time 13	27.50 s	26.72 s	26.03 s
Time 14	27.38 s	26.84 s	26.05 s
Time 15	27.41 s	26.78 s	26.02 s
T/C 1 Strt	2.050 mV	2.055 mV	2.045 mV
T/C 2 Strt	2.125 mV	2.124 mV	2.115 mV
T/C 3 Strt	1.160 mV	1.170 mV	1.165 mV
T/C 4 Strt	2.135 mV	2.135 mV	2.125 mV
T/C 5 Strt	2.140 mV	2.140 mV	2.132 mV
T/C 6 Strt	2.128 mV	2.130 mV	2.120 mV
T/C 7 Strt	1.810 mV	1.869 mV	1.918 mV
T/C 1 End	2.054 mV	2.055 mV	2.045 mV
T/C 2 End	2.130 mV	2.125 mV	2.105 mV
T/C 3 End	1.165 mV	1.175 mV	1.170 mV
T/C 4 End	2.135 mV	2.135 mV	2.125 mV
T/C 5 End	2.140 mV	2.140 mV	2.130 mV
T/C 6 End	2.128 mV	2.128 mV	2.120 mV
T/C 7 End	1.816 mV	1.870 mV	1.920 mV
Start Time	09:30	10:20	11:12
End Time	09:47	10:40	11:30

Date of Experiment 1986/ 6/27

MDEA Conc	40.0 wt%	Absorbing Gas	CO2
Piperazine Conc	0.05 kmol/m3	Surfactant	0.0075 wt%
Barometric Pressure	704.7 mm Hg	Rotameter Tube	603
Room Temperature	24.0 deg C	Nozzle Diam	0.60 mm
Manometer Right Leg	6.8 in H2O	Thermo Coarse	5.19
Manometer Left Leg	5.2 in H2O	Thermo Fine	0.0
Jet Elevation	88.340 cm	Feed Variac	22.0 %
North Pole	88.130 cm	Circ Variac	0.0 %
South Pole	83.015 cm		
Liquid Take-off	80.615 cm		

Flowmeter	45. mm	50. mm	60. mm
SFM Volume	25. mL	25. mL	25. mL
Time 1	27.55 s	26.92 s	25.84 s
Time 2	27.52 s	26.77 s	25.95 s
Time 3	27.64 s	26.84 s	25.97 s
Time 4	27.53 s	26.82 s	25.96 s
Time 5	27.48 s	26.90 s	25.94 s
Time 6	27.47 s	26.91 s	25.97 s
Time 7	27.42 s	26.82 s	25.88 s
Time 8	27.45 s	26.84 s	26.01 s
Time 9	27.45 s	26.89 s	25.99 s
Time 10	27.43 s	26.86 s	25.99 s
Time 11	27.46 s	26.74 s	25.96 s
Time 12	27.52 s	26.70 s	25.99 s
Time 13	27.40 s	26.85 s	25.89 s
Time 14	27.38 s	26.73 s	26.02 s
Time 15	27.43 s	26.92 s	25.96 s
Time 16	0.0 s	26.83 s	0.0 s
T/C 1 Strt	2.045 mV	2.045 mV	2.047 mV
T/C 2 Strt	2.120 mV	2.115 mV	2.110 mV
T/C 3 Strt	1.150 mV	1.160 mV	1.165 mV
T/C 4 Strt	2.128 mV	2.125 mV	2.128 mV
T/C 5 Strt	2.135 mV	2.133 mV	2.132 mV
T/C 6 Strt	2.121 mV	2.120 mV	2.122 mV
T/C 7 Strt	1.797 mV	1.860 mV	1.915 mV
T/C 1 End	2.050 mV	2.049 mV	2.047 mV
T/C 2 End	2.122 mV	2.115 mV	2.110 mV
T/C 3 End	1.156 mV	1.163 mV	1.168 mV
T/C 4 End	2.126 mV	2.125 mV	2.126 mV
T/C 5 End	2.135 mV	2.131 mV	2.134 mV
T/C 6 End	2.120 mV	2.120 mV	2.120 mV
T/C 7 End	1.810 mV	1.861 mV	1.913 mV
Start Time	09:20	10:10	11:00
End Time	09:38	10:27	11:17

Date of Experiment 1986/ 6/30

MDEA Conc	40.0 wt%	Absorbing Gas	CO2
Piperazine Conc	0.10 kmol/m3	Surfactant	0.0075 wt%
Barometric Pressure	701.7 mm Hg	Rotameter Tube	603
Room Temperature	23.5 deg C	Nozzle Diam	0.60 mm
Manometer Right Leg	6.8 in H2O	Thermo Coarse	5.19
Manometer Left Leg	5.2 in H2O	Thermo Fine	0.0
Jet Elevation	88.525 cm	Feed Variac	22.5 %
North Pole	88.325 cm	Circ Variac	0.0 %
South Pole	83.180 cm		
Liquid Take-off	80.795 cm		

Flowmeter	45. mm	50. mm	60. mm
SFM Volume	25. mL	25. mL	25. mL
Time 1	23.53 s	22.56 s	21.56 s
Time 2	23.47 s	22.60 s	21.56 s
Time 3	23.56 s	22.52 s	21.52 s
Time 4	23.35 s	22.59 s	21.52 s
Time 5	23.43 s	22.60 s	21.53 s
Time 6	23.23 s	22.49 s	21.54 s
Time 7	23.20 s	22.46 s	21.53 s
Time 8	23.18 s	22.55 s	21.57 s
Time 9	23.19 s	22.56 s	21.48 s
Time 10	23.17 s	22.46 s	21.63 s
Time 11	23.28 s	22.47 s	21.51 s
Time 12	23.29 s	22.52 s	21.47 s
Time 13	23.21 s	22.64 s	21.56 s
Time 14	23.21 s	22.57 s	21.52 s
Time 15	23.27 s	22.49 s	0.0 s
Time 16	23.23 s	22.47 s	0.0 s
Time 17	23.24 s	0.0 s	0.0 s
Time 18	23.24 s	0.0 s	0.0 s
T/C 1 Strt	2.036 mV	2.045 mV	2.050 mV
T/C 2 Strt	2.125 mV	2.125 mV	2.116 mV
T/C 3 Strt	1.157 mV	1.155 mV	1.160 mV
T/C 4 Strt	2.130 mV	2.125 mV	2.130 mV
T/C 5 Strt	2.135 mV	2.133 mV	2.135 mV
T/C 6 Strt	2.122 mV	2.121 mV	2.125 mV
T/C 7 Strt	1.750 mV	1.835 mV	1.910 mV
T/C 1 End	2.048 mV	2.048 mV	2.050 mV
T/C 2 End	2.130 mV	2.126 mV	2.117 mV
T/C 3 End	1.160 mV	1.157 mV	1.162 mV
T/C 4 End	2.129 mV	2.130 mV	2.130 mV
T/C 5 End	2.135 mV	2.135 mV	2.135 mV
T/C 6 End	2.120 mV	2.125 mV	2.121 mV
T/C 7 End	1.770 mV	1.841 mV	1.910 mV
Start Time	09:30	10:20	11:12
End Time	09:48	10:37	11:30

Date of Experiment 1986/ 7/ 1

MDEA Conc	40.0 wt%	Absorbing Gas	CO2
Piperazine Conc	0.10 kmol/m3	Surfactant	0.0075 wt%
Barometric Pressure	702.9 mm Hg	Rotameter Tube	603
Room Temperature	24.0 deg C	Nozzle Diam	0.60 mm
Manometer Right Leg	6.8 in H2O	Thermo Coarse	5.19
Manometer Left Leg	5.2 in H2O	Thermo Fine	0.0
Jet Elevation	87.975 cm	Feed Variac	20.0 %
North Pole	87.775 cm	Circ Variac	0.0 %
South Pole	82.630 cm		
Liquid Take-off	80.245 cm		

Flowmeter	45. mm	50. mm	60. mm
SFM Volume	25. mL	25. mL	25. mL
Time 1	23.07 s	22.49 s	21.56 s
Time 2	23.07 s	22.45 s	21.50 s
Time 3	23.16 s	22.54 s	21.55 s
Time 4	23.09 s	22.59 s	21.46 s
Time 5	23.08 s	22.68 s	21.49 s
Time 6	23.07 s	22.62 s	21.47 s
Time 7	23.17 s	22.54 s	21.49 s
Time 8	23.12 s	22.64 s	21.51 s
Time 9	23.12 s	22.59 s	21.54 s
Time 10	23.14 s	22.47 s	21.55 s
Time 11	23.12 s	22.60 s	21.46 s
Time 12	23.11 s	22.52 s	21.52 s
Time 13	23.12 s	22.45 s	21.50 s
Time 14	23.15 s	22.61 s	0.0 s
Time 15	23.14 s	22.52 s	0.0 s
T/C 1 Strt	2.040 mV	2.035 mV	2.043 mV
T/C 2 Strt	2.130 mV	2.125 mV	2.112 mV
T/C 3 Strt	1.158 mV	1.173 mV	1.176 mV
T/C 4 Strt	2.131 mV	2.126 mV	2.130 mV
T/C 5 Strt	2.140 mV	2.135 mV	2.135 mV
T/C 6 Strt	2.127 mV	2.120 mV	2.124 mV
T/C 7 Strt	1.796 mV	1.865 mV	1.928 mV
T/C 1 End	2.045 mV	2.036 mV	2.045 mV
T/C 2 End	2.136 mV	2.120 mV	2.115 mV
T/C 3 End	1.175 mV	1.176 mV	1.180 mV
T/C 4 End	2.130 mV	2.127 mV	2.126 mV
T/C 5 End	2.133 mV	2.135 mV	2.135 mV
T/C 6 End	2.123 mV	2.122 mV	2.121 mV
T/C 7 End	1.816 mV	1.866 mV	1.925 mV
Start Time	09:10	10:00	10:50
End Time	09:30	10:15	11:08

Date of Experiment 1986/ 7/ 3

MDEA Conc	40.0 wt%	Absorbing Gas	CO2
Piperazine Conc	0.15 kmol/m3	Surfactant	0.0075 wt%
Barometric Pressure	695.5 mm Hg	Rotameter Tube	603
Room Temperature	24.0 deg C	Nozzle Diam	0.60 mm
Manometer Right Leg	6.8 in H2O	Thermo Coarse	5.18
Manometer Left Leg	5.2 in H2O	Thermo Fine	0.0
Jet Elevation	87.925 cm	Feed Variac	15.0 %
North Pole	87.715 cm	Circ Variac	0.0 %
South Pole	82.585 cm		
Liquid Take-off	80.195 cm		

Flowmeter	45. mm	50. mm	60. mm
SFM Volume	40. mL	40. mL	40. mL
Time 1	31.55 s	30.61 s	28.93 s
Time 2	31.31 s	30.55 s	28.92 s
Time 3	31.70 s	30.53 s	28.91 s
Time 4	31.57 s	30.63 s	28.91 s
Time 5	31.43 s	30.56 s	29.00 s
Time 6	31.57 s	30.49 s	28.79 s
Time 7	31.56 s	30.72 s	28.98 s
Time 8	31.48 s	30.57 s	28.76 s
Time 9	31.68 s	30.67 s	28.94 s
Time 10	31.61 s	30.61 s	28.91 s
Time 11	31.71 s	30.57 s	29.03 s
Time 12	31.33 s	30.49 s	28.84 s
Time 13	31.69 s	30.67 s	28.91 s
Time 14	31.52 s	30.42 s	28.84 s
Time 15	0.0 s	30.60 s	28.99 s
Time 16	0.0 s	30.55 s	28.79 s
T/C 1 Strt	2.050 mV	2.045 mV	2.045 mV
T/C 2 Strt	2.160 mV	2.146 mV	2.135 mV
T/C 3 Strt	1.166 mV	1.195 mV	1.213 mV
T/C 4 Strt	2.156 mV	2.155 mV	2.155 mV
T/C 5 Strt	2.163 mV	2.162 mV	2.162 mV
T/C 6 Strt	2.151 mV	2.152 mV	2.151 mV
T/C 7 Strt	1.820 mV	1.880 mV	1.950 mV
T/C 1 End	2.050 mV	2.048 mV	2.046 mV
T/C 2 End	2.162 mV	2.150 mV	2.135 mV
T/C 3 End	1.180 mV	1.200 mV	1.225 mV
T/C 4 End	2.156 mV	2.156 mV	2.155 mV
T/C 5 End	2.163 mV	2.162 mV	2.160 mV
T/C 6 End	2.152 mV	2.152 mV	2.150 mV
T/C 7 End	1.825 mV	1.885 mV	1.950 mV
Start Time	09:15	10:00	10:45
End Time	09:30	10:15	11:00

Date of Experiment 1986/ 7/ 4

MDEA Conc	40.0 wt%	Absorbing Gas	CO2
Piperazine Conc	0.15 kmol/m3	Surfactant	0.0075 wt%
Barometric Pressure	692.8 mm Hg	Rotameter Tube	603
Room Temperature	24.0 deg C	Nozzle Diam	0.60 mm
Manometer Right Leg	6.8 in H2O	Thermo Coarse	5.18
Manometer Left Leg	5.2 in H2O	Thermo Fine	0.0
Jet Elevation	87.780 cm	Feed Variac	15.0 %
North Pole	87.580 cm	Circ Variac	0.0 %
South Pole	82.470 cm		
Liquid Take-off	80.080 cm		

Flowmeter	45. mm	45. mm	50. mm	60. mm
SFM Volume	40. mL	40. mL	40. mL	40. mL
Time 1	32.04 s	31.67 s	30.44 s	28.91 s
Time 2	31.94 s	31.66 s	30.45 s	28.80 s
Time 3	31.99 s	31.69 s	30.45 s	28.77 s
Time 4	32.03 s	31.69 s	30.47 s	28.77 s
Time 5	31.84 s	31.63 s	30.40 s	28.89 s
Time 6	31.84 s	31.51 s	30.43 s	28.91 s
Time 7	31.85 s	31.54 s	30.45 s	28.88 s
Time 8	31.77 s	31.56 s	30.48 s	28.77 s
Time 9	31.76 s	31.43 s	30.38 s	28.83 s
Time 10	31.83 s	31.58 s	30.42 s	28.71 s
Time 11	31.64 s	31.47 s	30.45 s	28.79 s
Time 12	31.70 s	31.64 s	30.41 s	28.77 s
Time 13	31.66 s	31.45 s	30.49 s	28.84 s
Time 14	31.77 s	0.0 s	30.43 s	28.75 s
Time 15	31.62 s	0.0 s	0.0 s	28.86 s
Time 16	31.72 s	0.0 s	0.0 s	28.76 s
T/C 1 Strt	2.045 mV	2.045 mV	2.055 mV	2.046 mV
T/C 2 Strt	2.146 mV	2.146 mV	2.150 mV	2.135 mV
T/C 3 Strt	1.218 mV	1.218 mV	1.222 mV	1.230 mV
T/C 4 Strt	2.155 mV	2.155 mV	2.155 mV	2.153 mV
T/C 5 Strt	2.160 mV	2.160 mV	2.160 mV	2.160 mV
T/C 6 Strt	2.150 mV	2.150 mV	2.148 mV	2.146 mV
T/C 7 Strt	1.773 mV	1.773 mV	1.878 mV	1.946 mV
T/C 1 End	2.056 mV	2.056 mV	2.050 mV	2.050 mV
T/C 2 End	2.159 mV	2.159 mV	2.150 mV	2.135 mV
T/C 3 End	1.220 mV	1.220 mV	1.231 mV	1.231 mV
T/C 4 End	2.155 mV	2.155 mV	2.155 mV	2.155 mV
T/C 5 End	2.160 mV	2.160 mV	2.160 mV	2.160 mV
T/C 6 End	2.149 mV	2.149 mV	2.149 mV	2.147 mV
T/C 7 End	1.805 mV	1.805 mV	1.880 mV	1.947 mV
Start Time	09:10	09:10	10:05	10:50
End Time	09:35	09:35	10:20	11:10

Date of Experiment 1986/ 7/ 8

MDEA Conc	40.0 wt%	Absorbing Gas	CO2
Piperazine Conc	0.20 kmol/m3	Surfactant	0.0075 wt%
Barometric Pressure	704.0 mm Hg	Rotameter Tube	603
Room Temperature	24.5 deg C	Nozzle Diam	0.60 mm
Manometer Right Leg	6.8 in H2O	Thermo Coarse	5.18
Manometer Left Leg	5.2 in H2O	Thermo Fine	0.0
Jet Elevation	87.910 cm	Feed Variac	15.0 %
North Pole	87.705 cm	Circ Variac	0.0 %
South Pole	82.580 cm		
Liquid Take-off	80.200 cm		

Flowmeter	45. mm	50. mm	60. mm	50. mm
SFM Volume*	40. mL	40. mL	40. mL	40. mL
Time 1	27.06 s	26.06 s	24.48 s	26.01 s
Time 2	27.04 s	25.81 s	24.31 s	26.10 s
Time 3	27.34 s	25.99 s	24.41 s	26.00 s
Time 4	27.12 s	25.89 s	24.20 s	26.09 s
Time 5	27.24 s	26.13 s	24.46 s	26.08 s
Time 6	27.30 s	25.94 s	24.46 s	25.96 s
Time 7	27.24 s	26.09 s	24.48 s	25.99 s
Time 8	27.04 s	25.86 s	24.26 s	26.03 s
Time 9	27.29 s	26.02 s	24.38 s	26.13 s
Time 10	27.16 s	25.95 s	24.33 s	26.01 s
Time 11	27.26 s	26.05 s	24.32 s	26.23 s
Time 12	27.07 s	25.99 s	24.39 s	25.95 s
Time 13	27.16 s	25.77 s	24.39 s	26.06 s
Time 14	27.30 s	25.92 s	24.40 s	25.94 s
Time 15	27.06 s	26.05 s	24.20 s	26.06 s
Time 16	0.0 s	25.77 s	0.0 s	0.0 s
Time 17	0.0 s	25.96 s	0.0 s	0.0 s
Time 18	0.0 s	25.89 s	0.0 s	0.0 s
T/C 1 Strt	2.053 mV	2.047 mV	2.054 mV	2.060 mV
T/C 2 Strt	2.169 mV	2.159 mV	2.146 mV	2.165 mV
T/C 3 Strt	1.191 mV	1.225 mV	1.240 mV	1.241 mV
T/C 4 Strt	2.145 mV	2.146 mV	2.149 mV	2.147 mV
T/C 5 Strt	2.151 mV	2.166 mV	2.156 mV	2.154 mV
T/C 6 Strt	2.139 mV	2.139 mV	2.145 mV	2.144 mV
T/C 7 Strt	1.826 mV	1.896 mV	1.966 mV	1.906 mV
T/C 1 End	2.050 mV	2.053 mV	2.054 mV	2.055 mV
T/C 2 End	2.164 mV	2.166 mV	2.146 mV	2.160 mV
T/C 3 End	1.195 mV	1.235 mV	1.240 mV	1.249 mV
T/C 4 End	2.144 mV	2.149 mV	2.148 mV	2.146 mV
T/C 5 End	2.150 mV	2.169 mV	2.155 mV	2.154 mV
T/C 6 End	2.139 mV	2.140 mV	2.143 mV	2.143 mV
T/C 7 End	1.843 mV	1.904 mV	1.966 mV	1.906 mV
Start Time	10:00	11:00	11:55	12:30
End Time	10:25	11:20	12:10	12:55

Date of Experiment 1986/ 7/ 9

MDEA Conc	40.0 wt%	Absorbing Gas	CO2
Piperazine Conc	0.20 kmol/m3	Surfactant	0.0075 wt%
Barometric Pressure	701.0 mm Hg	Rotameter Tube	603
Room Temperature	24.5 deg C	Nozzle Diam	0.60 mm
Manometer Right Leg	6.8 in H2O	Thermo Coarse	5.18
Manometer Left Leg	5.2 in H2O	Thermo Fine	0.0
Jet Elevation	87.880 cm	Feed Variac	14.0 %
North Pole	87.680 cm	Circ Variac	0.0 %
South Pole	82.545 cm		
Liquid Take-off	80.165 cm		

Flowmeter	45. mm	50. mm	60. mm
SFM Volume	40. mL	40. mL	40. mL
Time 1	27.23 s	25.96 s	24.42 s
Time 2	27.06 s	26.01 s	24.41 s
Time 3	27.20 s	26.04 s	24.47 s
Time 4	27.13 s	25.96 s	24.33 s
Time 5	27.15 s	25.98 s	24.46 s
Time 6	27.20 s	25.99 s	24.37 s
Time 7	27.25 s	26.01 s	24.36 s
Time 8	27.12 s	26.02 s	24.36 s
Time 9	27.13 s	25.93 s	24.39 s
Time 10	27.21 s	26.02 s	24.28 s
Time 11	27.05 s	26.09 s	24.50 s
Time 12	27.06 s	26.06 s	24.39 s
Time 13	27.16 s	25.90 s	24.35 s
Time 14	27.13 s	25.99 s	24.38 s
Time 15	0.0 s	25.97 s	24.52 s
Time 16	0.0 s	0.0 s	24.34 s
Time 17	0.0 s	0.0 s	24.40 s
Time 18	0.0 s	0.0 s	24.43 s
T/C 1 Strt	2.037 mV	2.042 mV	2.043 mV
T/C 2 Strt	2.160 mV	2.151 mV	2.141 mV
T/C 3 Strt	1.235 mV	1.249 mV	1.260 mV
T/C 4 Strt	2.150 mV	2.150 mV	2.153 mV
T/C 5 Strt	2.155 mV	2.156 mV	2.158 mV
T/C 6 Strt	2.145 mV	2.144 mV	2.149 mV
T/C 7 Strt	1.805 mV	1.883 mV	1.952 mV
T/C 1 End	2.043 mV	2.041 mV	2.044 mV
T/C 2 End	2.165 mV	2.151 mV	2.140 mV
T/C 3 End	1.247 mV	1.250 mV	1.261 mV
T/C 4 End	2.148 mV	2.149 mV	2.150 mV
T/C 5 End	2.155 mV	2.158 mV	2.156 mV
T/C 6 End	2.143 mV	2.146 mV	2.146 mV
T/C 7 End	1.820 mV	1.888 mV	1.955 mV
Start Time	09:50	10:32	11:30
End Time	10:05	10:56	11:55

Date of Experiment 1986/ 7/11

MDEA Conc	40.0 wt%	Absorbing Gas	CO2
Piperazine Conc	0.40 kmol/m3	Surfactant	0.0075 wt%
Barometric Pressure	695.0 mm Hg	Rotameter Tube	603
Room Temperature	24.0 deg C	Nozzle Diam	0.60 mm
Manometer Right Leg	6.3 in H2O	Thermo Coarse	5.18
Manometer Left Leg	5.7 in H2O	Thermo Fine	0.0
Jet Elevation	88.040 cm	Feed Variac	14.0 %
North Pole	87.835 cm	Circ Variac	0.0 %
South Pole	82.705 cm		
Liquid Take-off	80.315 cm		

Flowmeter	45. mm	50. mm	60. mm
SFM Volume	80. mL	80. mL	80. mL
Time 1	35.71 s	33.79 s	31.48 s
Time 2	35.74 s	33.70 s	31.50 s
Time 3	35.74 s	33.83 s	31.46 s
Time 4	35.63 s	33.84 s	31.65 s
Time 5	35.59 s	33.75 s	31.39 s
Time 6	35.75 s	33.70 s	31.51 s
Time 7	35.66 s	33.84 s	31.47 s
Time 8	35.62 s	33.77 s	31.53 s
Time 9	35.50 s	33.73 s	31.53 s
Time 10	35.54 s	33.70 s	31.36 s
Time 11	[illegible]63 s	33.74 s	31.52 s
Time 12	[illegible]9 s	33.67 s	31.40 s
Time 13	[illegible]3 s	33.76 s	31.56 s
Time 14	[illegible] s	33.78 s	31.45 s
Time 15	[illegible] s	33.70 s	31.66 s
Time 16	[illegible]2 s	33.70 s	31.31 s
Time 17	35.55 s	0.0 s	31.34 s
Time 18	35.70 s	0.0 s	31.31 s
Time 19	0.0 s	0.0 s	31.62 s
T/C 1 Strt	2.027 mV	2.035 mV	2.038 mV
T/C 2 Strt	2.198 mV	2.190 mV	2.170 mV
T/C 3 Strt	1.224 mV	1.231 mV	1.234 mV
T/C 4 Strt	2.143 mV	2.141 mV	2.141 mV
T/C 5 Strt	2.150 mV	2.150 mV	2.150 mV
T/C 6 Strt	2.138 mV	2.136 mV	2.139 mV
T/C 7 Strt	1.741 mV	1.875 mV	1.947 mV
T/C 1 End	2.040 mV	2.036 mV	2.035 mV
T/C 2 End	2.205 mV	2.190 mV	2.170 mV
T/C 3 End	1.237 mV	1.240 mV	1.235 mV
T/C 4 End	2.141 mV	2.141 mV	2.141 mV
T/C 5 End	2.149 mV	2.150 mV	2.150 mV
T/C 6 End	2.135 mV	2.136 mV	2.135 mV
T/C 7 End	1.810 mV	1.878 mV	1.945 mV
Start Time	09:40	10:40	11:30
End Time	10:10	10:58	11:55

Date of Experiment 1986/ 7/23

MDEA Conc	20.0 wt%	Absorbing Gas	CO2
Piperazine Conc	0.0 kmol/m3	Surfactant	0.0100 wt%
Barometric Pressure	699.5 mm Hg	Rotameter Tube	603
Room Temperature	24.5 deg C	Nozzle Diam	0.60 mm
Manometer Right Leg	6.2 in H2O	Thermo Coarse	0.0
Manometer Left Leg	5.9 in H2O	Thermo Fine	0.0
Jet Elevation	88.025 cm	Feed Variac	0.0 %
North Pole	87.810 cm	Circ Variac	0.0 %
South Pole	82.720 cm		
Liquid Take-off	80.290 cm		

Flowmeter	30. mm	40. mm	50. mm
SFM Volume	30. mL	30. mL	30. mL
Time 1	49.89 s	46.99 s	45.18 s
Time 2	49.71 s	47.02 s	45.04 s
Time 3	49.26 s	46.92 s	45.19 s
Time 4	49.36 s	47.30 s	44.88 s
Time 5	49.27 s	47.07 s	44.80 s
Time 6	49.12 s	47.03 s	45.06 s
Time 7	48.86 s	47.02 s	45.16 s
Time 8	48.77 s	47.02 s	45.13 s
Time 9	48.78 s	46.89 s	45.13 s
Time 10	48.81 s	47.26 s	45.34 s
Time 11	48.97 s	47.06 s	44.88 s
Time 12	49.23 s	46.88 s	44.88 s
Time 13	48.95 s	0.0 s	45.09 s
Time 14	48.93 s	0.0 s	45.23 s
Time 15	48.69 s	0.0 s	45.03 s
Time 16	48.97 s	0.0 s	45.19 s
Time 17	48.87 s	0.0 s	45.08 s
Time 18	49.07 s	0.0 s	0.0 s
T/C 1 Strt	1.276 mV	1.260 mV	1.304 mV
T/C 2 Strt	1.360 mV	1.300 mV	1.319 mV
T/C 3 Strt	1.245 mV	1.252 mV	1.249 mV
T/C 4 Strt	1.342 mV	1.303 mV	1.300 mV
T/C 5 Strt	1.340 mV	1.302 mV	1.301 mV
T/C 6 Strt	1.343 mV	1.302 mV	1.300 mV
T/C 7 Strt	1.035 mV	1.222 mV	1.338 mV
T/C 1 End	1.271 mV	1.279 mV	1.304 mV
T/C 2 End	1.355 mV	1.306 mV	1.317 mV
T/C 3 End	1.259 mV	1.251 mV	1.250 mV
T/C 4 End	1.340 mV	1.298 mV	1.299 mV
T/C 5 End	1.336 mV	1.299 mV	1.302 mV
T/C 6 End	1.338 mV	1.299 mV	1.300 mV
T/C 7 End	1.015 mV	1.284 mV	1.330 mV
Start Time	11:10	12:50	13:52
End Time	11:40	13:20	14:30

Date of Experiment 1986/ 7/24

MDEA Conc	20.0 wt%	Absorbing Gas	CO2
Piperazine Conc	0.0 kmol/m3	Surfactant	0.0100 wt%
Barometric Pressure	701.5 mm Hg	Rotameter Tube	603
Room Temperature	24.0 deg C	Nozzle Diam	0.60 mm
Manometer Right Leg	6.1 in H2O	Thermo Coarse	0.0
Manometer Left Leg	5.9 in H2O	Thermo Fine	0.0
Jet Elevation	88.065 cm	Feed Variac	0.0 %
North Pole	87.860 cm	Circ Variac	0.0 %
South Pole	82.720 cm		
Liquid Take-off	80.335 cm		

Flowmeter	30. mm	40. mm	50. mm
SFM Volume	30. mL	30. mL	30. mL
Time 1	50.34 s	47.13 s	44.78 s
Time 2	50.35 s	47.45 s	44.67 s
Time 3	50.29 s	47.27 s	45.00 s
Time 4	50.13 s	47.23 s	44.91 s
Time 5	49.79 s	47.14 s	44.87 s
Time 6	50.26 s	47.31 s	45.15 s
Time 7	50.16 s	47.28 s	44.95 s
Time 8	50.10 s	47.06 s	45.16 s
Time 9	50.16 s	47.11 s	44.99 s
Time 10	50.17 s	47.23 s	44.87 s
Time 11	49.78 s	47.14 s	45.02 s
Time 12	50.07 s	47.12 s	44.95 s
Time 13	50.21 s	47.46 s	44.85 s
Time 14	49.89 s	47.01 s	0.0 s
Time 15	49.95 s	47.28 s	0.0 s
T/C 1 Strt	1.249 mV	1.276 mV	1.311 mV
T/C 2 Strt	1.294 mV	1.301 mV	1.321 mV
T/C 3 Strt	1.214 mV	1.228 mV	1.234 mV
T/C 4 Strt	1.286 mV	1.294 mV	1.300 mV
T/C 5 Strt	1.286 mV	1.295 mV	1.304 mV
T/C 6 Strt	1.285 mV	1.291 mV	1.300 mV
T/C 7 Strt	1.125 mV	1.274 mV	1.320 mV
T/C 1 End	1.260 mV	1.289 mV	1.299 mV
T/C 2 End	1.295 mV	1.309 mV	1.314 mV
T/C 3 End	1.216 mV	1.234 mV	1.238 mV
T/C 4 End	1.288 mV	1.298 mV	1.301 mV
T/C 5 End	1.288 mV	1.299 mV	1.304 mV
T/C 6 End	1.285 mV	1.295 mV	1.300 mV
T/C 7 End	1.202 mV	1.304 mV	1.325 mV
Start Time	10:45	11:55	13:05
End Time	11:20	12:23	13:32

Date of Experiment 1986/ 7/28

MDEA Conc	20.0 wt%	Absorbing Gas	CO2
Piperazine Conc	0.0 kmol/m3	Surfactant	0.0100 wt%
Barometric Pressure	698.4 mm Hg	Rotameter Tube	603
Room Temperature	25.0 deg C	Nozzle Diam	0.60 mm
Manometer Right Leg	6.1 in H2O	Thermo Coarse	5.27
Manometer Left Leg	5.9 in H2O	Thermo Fine	0.0
Jet Elevation	88.150 cm	Feed Variac	0.0 %
North Pole	87.945 cm	Circ Variac	0.0 %
South Pole	82.845 cm		
Liquid Take-off	80.435 cm		

Flowmeter	30. mm	40. mm	50. mm
SFM Volume	30. mL	30. mL	30. mL
Time 1	33.04 s	30.31 s	29.50 s
Time 2	32.97 s	30.48 s	29.55 s
Time 3	33.25 s	30.57 s	29.76 s
Time 4	33.12 s	30.60 s	29.65 s
Time 5	33.09 s	30.62 s	29.70 s
Time 6	33.27 s	30.61 s	29.78 s
Time 7	33.20 s	30.46 s	29.88 s
Time 8	33.43 s	30.58 s	29.69 s
Time 9	33.41 s	30.60 s	29.69 s
Time 10	33.31 s	30.36 s	29.54 s
Time 11	33.34 s	30.47 s	29.62 s
Time 12	33.25 s	30.60 s	29.53 s
Time 13	33.17 s	30.54 s	29.56 s
Time 14	33.36 s	0.0 s	29.64 s
Time 15	33.36 s	0.0 s	29.53 s
Time 16	33.33 s	0.0 s	29.59 s
Time 17	33.22 s	0.0 s	0.0 s
Time 18	33.22 s	0.0 s	0.0 s
T/C 1 Strt	2.575 mV	2.576 mV	2.594 mV
T/C 2 Strt	2.650 mV	2.630 mV	2.640 mV
T/C 3 Strt	1.225 mV	1.240 mV	1.253 mV
T/C 4 Strt	2.665 mV	2.661 mV	2.665 mV
T/C 5 Strt	2.675 mV	2.674 mV	2.676 mV
T/C 6 Strt	2.655 mV	2.654 mV	2.656 mV
T/C 7 Strt	2.387 mV	2.516 mV	2.600 mV
T/C 1 End	2.554 mV	2.579 mV	2.595 mV
T/C 2 End	2.633 mV	2.634 mV	2.636 mV
T/C 3 End	1.235 mV	1.253 mV	1.260 mV
T/C 4 End	2.664 mV	2.664 mV	2.665 mV
T/C 5 End	2.675 mV	2.675 mV	2.675 mV
T/C 6 End	2.655 mV	2.655 mV	2.655 mV
T/C 7 End	2.384 mV	2.523 mV	2.605 mV
Start Time	10:51	11:40	12:45
End Time	11:06	12:03	13:08

Date of Experiment 1986/ 7/29

MDEA Conc	20.0 wt%	Absorbing Gas	CO2
Piperazine Conc	0.0 kmol/m3	Surfactant	0.0100 wt%
Barometric Pressure	699.5 mm Hg	Rotameter Tube	603
Room Temperature	24.5 deg C	Nozzle Diam	0.60 mm
Manometer Right Leg	6.1 in H2O	Thermo Coarse	5.27
Manometer Left Leg	5.9 in H2O	Thermo Fine	0.0
Jet Elevation	88.135 cm	Feed Variac	30.0 %
North Pole	87.930 cm	Circ Variac	90.0 %
South Pole	82.845 cm		
Liquid Take-off	80.425 cm		

Flowmeter	30. mm	40. mm	50. mm
SFM Volume	30. mL	30. mL	30. mL
Time 1	33.16 s	31.82 s	31.02 s
Time 2	33.17 s	31.85 s	31.10 s
Time 3	33.21 s	32.03 s	31.15 s
Time 4	33.20 s	31.97 s	30.97 s
Time 5	33.40 s	32.02 s	31.09 s
Time 6	33.37 s	31.85 s	30.99 s
Time 7	33.32 s	31.92 s	31.13 s
Time 8	33.34 s	31.89 s	31.16 s
Time 9	33.17 s	31.91 s	31.07 s
Time 10	33.36 s	32.01 s	30.96 s
Time 11	33.34 s	31.90 s	31.24 s
Time 12	33.22 s	31.94 s	31.08 s
Time 13	33.33 s	31.69 s	30.91 s
Time 14	33.34 s	31.82 s	31.09 s
Time 15	33.43 s	32.02 s	31.04 s
Time 16	0.0 s	0.0 s	31.04 s
Time 17	0.0 s	0.0 s	31.12 s
T/C 1 Strt	2.584 mV	2.570 mV	2.585 mV
T/C 2 Strt	2.639 mV	2.624 mV	2.631 mV
T/C 3 Strt	1.204 mV	1.223 mV	1.225 mV
T/C 4 Strt	2.656 mV	2.658 mV	2.659 mV
T/C 5 Strt	2.668 mV	2.670 mV	2.671 mV
T/C 6 Strt	2.648 mV	2.650 mV	2.651 mV
T/C 7 Strt	2.345 mV	2.495 mV	2.579 mV
T/C 1 End	2.589 mV	2.575 mV	2.585 mV
T/C 2 End	2.645 mV	2.628 mV	2.629 mV
T/C 3 End	1.218 mV	1.229 mV	1.230 mV
T/C 4 End	2.659 mV	2.660 mV	2.660 mV
T/C 5 End	2.670 mV	2.670 mV	2.671 mV
T/C 6 End	2.649 mV	2.651 mV	2.651 mV
T/C 7 End	2.364 mV	2.504 mV	2.585 mV
Start Time	10:33	11:50	12:57
End Time	11:02	12:16	13:30

Date of Experiment 1986/ 7/30

MDEA Conc	20.0 wt%	Absorbing Gas	CO2
Piperazine Conc	0.0 kmol/m3	Surfactant	0.0100 wt%
Barometric Pressure	704.4 mm Hg	Rotameter Tube	603
Room Temperature	25.0 deg C	Nozzle Diam	0.60 mm
Manometer Right Leg	6.1 in H2O	Thermo Coarse	5.27.
Manometer Left Leg	5.9 in H2O	Thermo Fine	0.0
Jet Elevation	88.170 cm	Feed Variac	27.0 %
North Pole	87.960 cm	Circ Variac	90.0 %
South Pole	82.860 cm		
Liquid Take-off	80.450 cm		

Flowmeter	30. mm	40. mm	50. mm
SFM Volume	30. mL	30. mL	30. mL
Time 1	33.16 s	31.65 s	30.87 s
Time 2	33.20 s	31.38 s	30.82 s
Time 3	32.89 s	31.59 s	31.07 s
Time 4	32.66 s	31.44 s	30.78 s
Time 5	32.66 s	31.61 s	30.98 s
Time 6	32.93 s	31.70 s	30.94 s
Time 7	33.25 s	31.55 s	30.87 s
Time 8	32.63 s	31.54 s	30.98 s
Time 9	33.12 s	31.54 s	30.70 s
Time 10	32.75 s	31.80 s	31.12 s
Time 11	32.99 s	31.60 s	31.06 s
Time 12	32.70 s	31.45 s	30.98 s
Time 13	33.18 s	31.68 s	30.99 s
Time 14	33.06 s	31.67 s	31.06 s
Time 15	32.92 s	31.48 s	30.97 s
Time 16	32.91 s	31.38 s	30.99 s
Time 17	32.91 s	31.60 s	30.84 s
Time 18	33.05 s	31.66 s	30.99 s
Time 19	0.0 s	31.67 s	0.0 s
T/C 1 Strt	2.570 mV	2.580 mV	2.580 mV
T/C 2 Strt	2.636 mV	2.632 mV	2.630 mV
T/C 3 Strt	1.226 mV	1.243 mV	1.259 mV
T/C 4 Strt	2.656 mV	2.656 mV	2.658 mV
T/C 5 Strt	2.678 mV	2.676 mV	2.680 mV
T/C 6 Strt	2.650 mV	2.644 mV	2.645 mV
T/C 7 Strt	2.346 mV	2.494 mV	2.584 mV
T/C 1 End	2.571 mV	2.585 mV	2.579 mV
T/C 2 End	2.640 mV	2.635 mV	2.626 mV
T/C 3 End	1.239 mV	1.260 mV	1.251 mV
T/C 4 End	2.656 mV	2.660 mV	2.656 mV
T/C 5 End	2.676 mV	2.681 mV	2.677 mV
T/C 6 End	2.645 mV	2.646 mV	2.643 mV
T/C 7 End	2.360 mV	2.508 mV	2.585 mV
Start Time	10:34	11:40	12:46
End Time	11:01	12:05	13:12

Date of Experiment 1986/ 7/31

MDEA Conc	20.0 wt%	Absorbing Gas	CO2
Piperazine Conc	0.0 kmol/m3	Surfactant	0.0100 wt%
Barometric Pressure	706.2 mm Hg	Rotameter Tube	603
Room Temperature	25.0 deg C	Nozzle Diam	0.60 mm
Manometer Right Leg	6.1 in H2O	Thermo Coarse	5.51
Manometer Left Leg	5.9 in H2O	Thermo Fine	0.0
Jet Elevation	88.500 cm	Feed Variac	57.0 %
North Pole	88.290 cm	Circ Variac	100.0 %
South Pole	83.180 cm		
Liquid Take-off	80.755 cm		

Flowmeter	30. mm	40. mm	50. mm
SFM Volume	30. mL	30. mL	30. mL
Time 1	30.43 s	29,88 s	28.03 s
Time 2	30.36 s	29.84 s	28.09 s
Time 3	30.44 s	29.68 s	28.49 s
Time 4	30.56 s	29.79 s	28.41 s
Time 5	30.65 s	29,72 s	28.20 s
Time 6	30.64 s	30.06 s	28.08 s
Time 7	30.64 s	29.92 s	28.17 s
Time 8	30.61 s	30.03 s	28.25 s
Time 9	30.66 s	29.79 s	28.18 s
Time 10	30.57 s	29.88 s	28.17 s
Time 11	30.63 s	29.90 s	28.04 s
Time 12	30.61 s	29.65 s	28.08 s
Time 13	30.59 s	29.88 s	28.24 s
Time 14	30.69 s	29.89 s	28.17 s
Time 15	0.0 s	29.66 s	28.25 s
Time 16	0.0 s	0.0 s	28.15 s
Time 17	0.0 s	0.0 s	28.18 s
T/C 1 Strt	3.900 mV	3.916 mV	3.900 mV
T/C 2 Strt	3.966 mV	3.971 mV	3.950 mV
T/C 3 Strt	1.239 mV	1.256 mV	1.261 mV
T/C 4 Strt	4.010 mV	4.018 mV	4.014 mV
T/C 5 Strt	4.036 mV	4.049 mV	4.045 mV
T/C 6 Strt	3.985 mV	3.995 mV	3.990 mV
T/C 7 Strt	3.177 mV	3.344 mV	3.431 mV
T/C 1 End	3.900 mV	3.910 mV	3.899 mV
T/C 2 End	3.970 mV	3.970 mV	3.950 mV
T/C 3 End	1.242 mV	1.260 mV	1.267 mV
T/C 4 End	4.010 mV	4.016 mV	4.015 mV
T/C 5 End	4.040 mV	4.046 mV	4.045 mV
T/C 6 End	3.980 mV	3.995 mV	3.991 mV
T/C 7 End	3.178 mV	3.338 mV	3.416 mV
Start Time	11:00	12:30	13:32
End Time	11:25	13:01	14:03

Date of Experiment 1986/ 8/ 1

MDEA Conc	20.0 wt%	Absorbing Gas	CO2
Piperazine Conc	0.0 kmol/m3	Surfactant	0.0100 wt%
Barometric Pressure	706.6 mm Hg	Rotameter Tube	603
Room Temperature	25.5 deg C	Nozzle Diam	0.60 mm
Manometer Right Leg	6.1 in H2O	Thermo Coarse	5.51
Manometer Left Leg	5.9 in H2O	Thermo Fine	0.0
Jet Elevation	87.990 cm	Feed Variac	56.0 %
North Pole	87.785 cm	Circ Variac	100.0 %
South Pole	82.695 cm		
Liquid Take-off	80.265 cm		

Flowmeter	30. mm	40. mm	50. mm
SFM Volume	30. mL	30. mL	30. mL
Time 1	30.29 s	29.21 s	28.09 s
Time 2	30.27 s	29.05 s	27.84 s
Time 3	30.33 s	29.16 s	28.09 s
Time 4	30.41 s	28.84 s	28.06 s
Time 5	30.35 s	28.89 s	28.04 s
Time 6	30.40 s	29.05 s	28.13 s
Time 7	30.38 s	28.99 s	28.06 s
Time 8	30.32 s	29.02 s	27.94 s
Time 9	30.56 s	29.20 s	28.03 s
Time 10	30.20 s	29.03 s	27.85 s
Time 11	30.46 s	29.07 s	27.98 s
Time 12	30.41 s	29.15 s	28.17 s
Time 13	30.46 s	29.13 s	28.03 s
Time 14	30.38 s	29.05 s	28.31 s
Time 15	30.42 s	28.96 s	27.95 s
Time 16	30.30 s	0.0 s	0.0 s
T/C 1 Strt	3.900 mV	3.905 mV	3.914 mV
T/C 2 Strt	3.971 mV	3.965 mV	3.960 mV
T/C 3 Strt	1.270 mV	1.289 mV	1.298 mV
T/C 4 Strt	4.018 mV	4.015 mV	4.020 mV
T/C 5 Strt	4.045 mV	4.046 mV	4.048 mV
T/C 6 Strt	3.989 mV	3.995 mV	3.997 mV
T/C 7 Strt	3.201 mV	3.341 mV	3.430 mV
T/C 1 End	3.905 mV	3.905 mV	3.908 mV
T/C 2 End	3.976 mV	3.967 mV	3.960 mV
T/C 3 End	1.281 mV	1.297 mV	1.300 mV
T/C 4 End	4.015 mV	4.020 mV	4.020 mV
T/C 5 End	4.048 mV	4.049 mV	4.047 mV
T/C 6 End	3.989 mV	3.992 mV	3.998 mV
T/C 7 End	3.190 mV	3.336 mV	3.420 mV
Start Time	10:33	12:05	13:02
End Time	11:12	12:35	13:41

Date of Experiment 1986/ 8/13

MDEA Conc	20.0 wt%	Absorbing Gas	CO2
Piperazine Conc	0.0 kmol/m3	Surfactant	0.0100 wt%
Barometric Pressure	701.5 mm Hg	Rotameter Tube	603
Room Temperature	25.0 deg C	Nozzle Diam	0.60 mm
Manometer Right Leg	6.1 in H2O	Thermo Coarse	5.36
Manometer Left Leg	5.9 in H2O	Thermo Fine	0.0
Jet Elevation	88.110 cm	Feed Variac	40.0 %
North Pole	87.910 cm	Circ Variac	100.0 %
South Pole	82.790 cm		
Liquid Take-off	80.380 cm		

Flowmeter		30. mm	40. mm	50. mm
SFM Volume		50. mL	50. mL	50. mL
Time	1	51.86 s	49.73 s	48.39 s
Time	2	51.74 s	49.61 s	48.28 s
Time	3	51.70 s	49.48 s	48.22 s
Time	4	51.86 s	49.46 s	48.23 s
Time	5	51.94 s	49.52 s	48.37 s
Time	6	51.65 s	49.76 s	48.12 s
Time	7	51.67 s	49.42 s	48.22 s
Time	8	51.83 s	49.62 s	48.23 s
Time	9	51.86 s	49.53 s	48.22 s
Time	10	52.07 s	49.76 s	48.16 s
Time	11	51.77 s	49.57 s	48.37 s
Time	12	51.59 s	49.51 s	48.33 s
Time	13	51.91 s	0.0 s	48.37 s
Time	14	51.71 s	0.0 s	47.90 s
Time	15	0.0 s	0.0 s	48.30 s
T/C 1	Strt	3.109 mV	3.109 mV	3.121 mV
T/C 2	Strt	3.181 mV	3.163 mV	3.159 mV
T/C 3	Strt	1.260 mV	1.268 mV	1.280 mV
T/C 4	Strt	3.196 mV	3.189 mV	3.186 mV
T/C 5	Strt	3.210 mV	3.203 mV	3.202 mV
T/C 6	Strt	3.191 mV	3.176 mV	3.180 mV
T/C 7	Strt	2.700 mV	2.851 mV	2.945 mV
T/C 1	End	3.102 mV	3.119 mV	3.120 mV
T/C 2	End	3.170 mV	3.165 mV	3.161 mV
T/C 3	End	1.274 mV	1.276 mV	1.286 mV
T/C 4	End	3.191 mV	3.187 mV	3.189 mV
T/C 5	End	3.205 mV	3.203 mV	3.205 mV
T/C 6	End	3.179 mV	3.176 mV	3.180 mV
T/C 7	End	2.707 mV	2.858 mV	2.949 mV
Start	Time	10:18	11:08	12:12
End	Time	10:38	11:38	12:44

APPENDIX 2

Equipment Details

This appendix contains additional detail about the sphere absorber apparatus and the operating procedure. Figure A2.1 contains a schematic diagram of the constant head reservoir, described in Chapters 3.2.3 and 3.2.4, showing the construction of the device and the plumbing arrangement. Figure A2.2 contains a schematic diagram of the amine regenerator described in Chapter 3.2.6. Table A2.1 contains a brief description and identifying code for each valve associated with the sphere absorber apparatus. Table A2.2 contains the detailed description of the operating procedure used to obtain the experimental measurements. Table A2.3 describes the method used to regenerate amine which had passed through the absorption chamber.

Figure A2.1.

Schematic Diagram of the Constant Head Reservoir

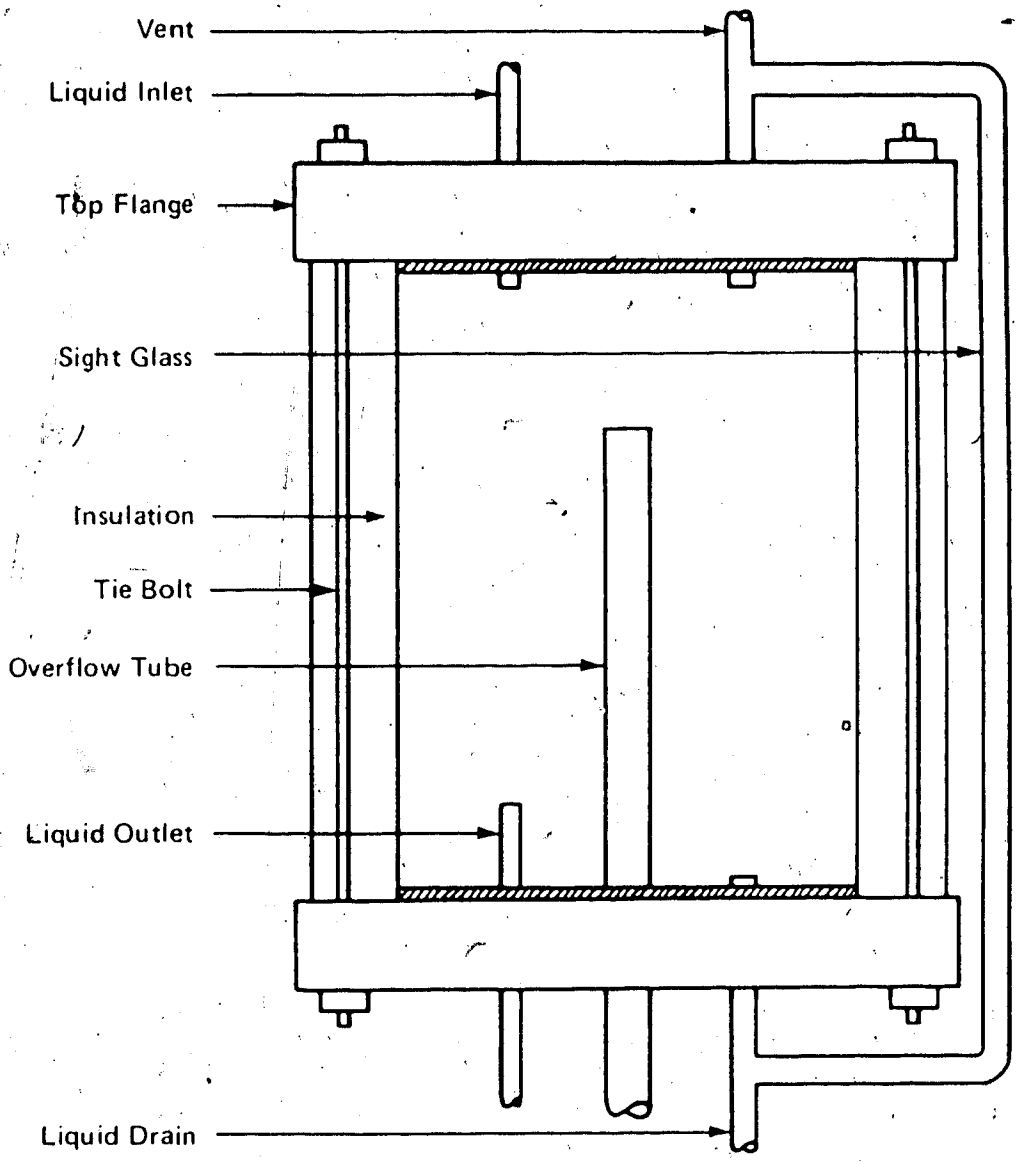

Figure A2.2.

Schematic Diagram of the Amine Regenerator

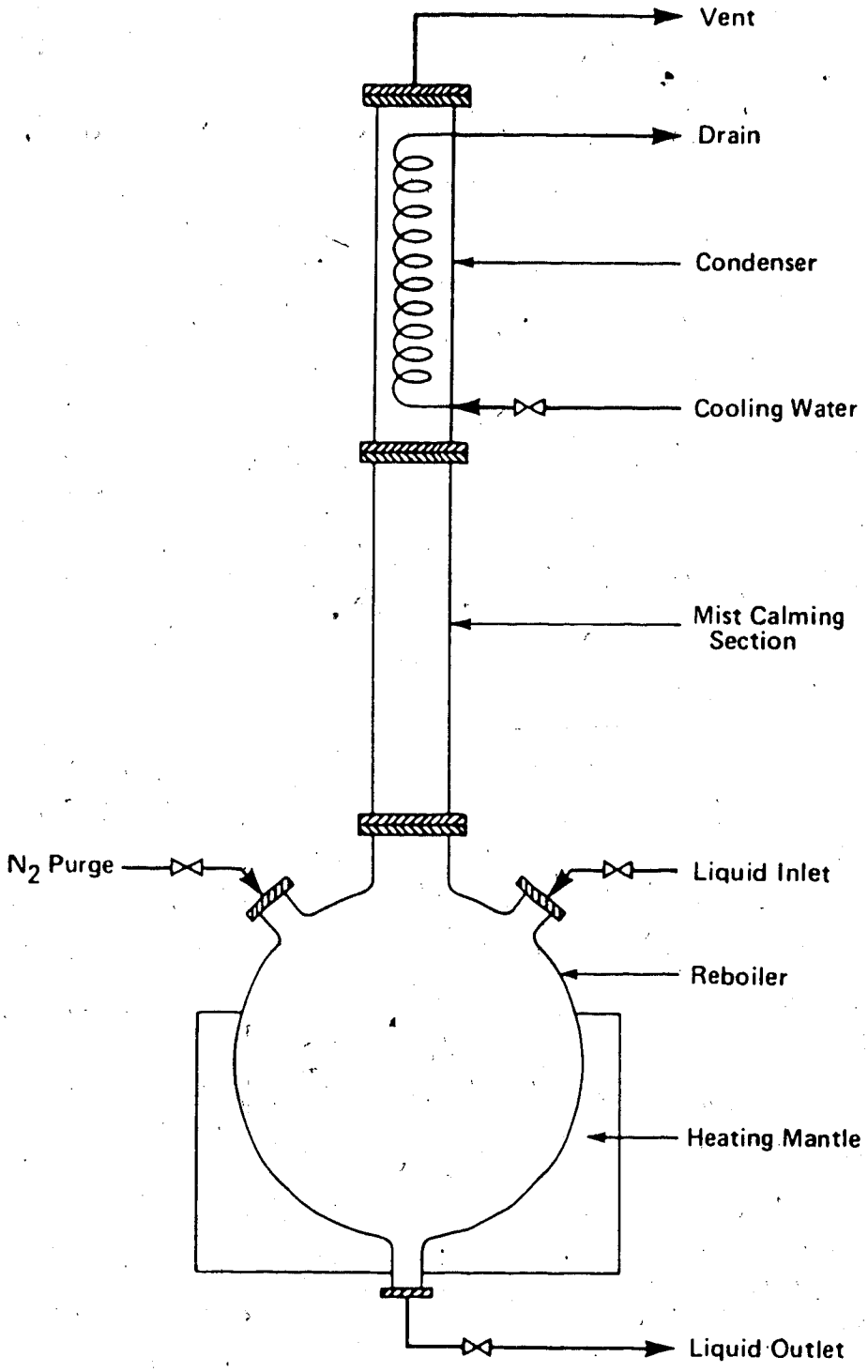

Table A2.1

Description of Valves on Sphere Absorber Apparatus

Valve	Description
V1	Helium to constant head reservoir
V2	Constant head reservoir drain
V3	Manometer isolation
V4	CO_2/N_2O to absorber
V5	Lean amine to feed tank
V6	Liquid circulation pump regulating valve
V7	Absorber bypass
V8	Lean amine to absorber
V9	Rich amine shut-off
V10	Rich amine flow control
V11	Helium to helium reservoir
V12	CO_2/N_2O inlet to gas circulation pump
V13	CO_2/N_2O outlet from gas circulation pump
V14	Gas circulation pump vent to atmosphere
V15	Gas circulation pump bypass
V16	Amine feed tank drain
V17	Liquid to liquid circulation pump
V18	Rich amine drain valve
V19	Feed tank vent
V20	Feed tank vacuum
V21	Helium to feed tank
V22	CO_2/N_2O purge to absorber

V23	Gas out of absorber
V24	Gas out of base of knockout bomb
V25	Saturator gas to absorber
V26	Reboiler base port
V27	Amine transfer from reboiler to feed tank
V28	Absorber slide valve

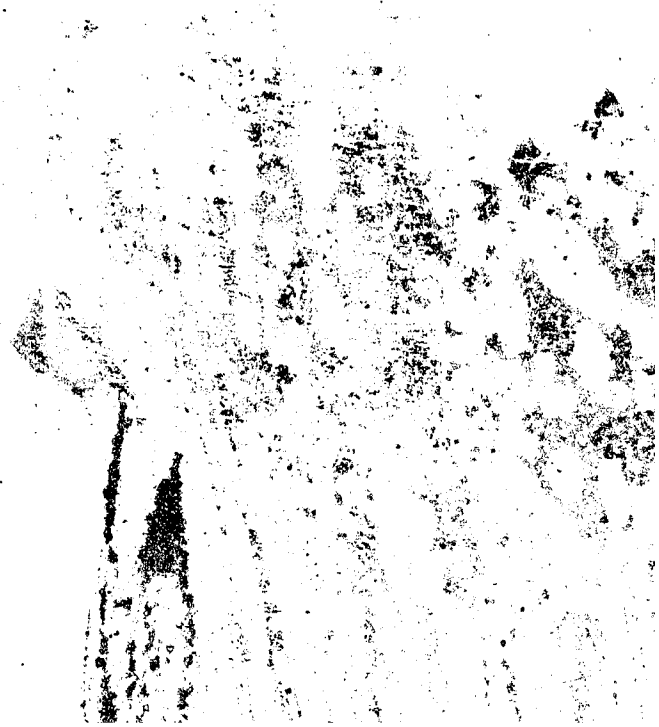

Table A2.2

Detailed Operating Procedure for Sphere Absorber

1) Open CO_2/N_2O cylinder and He cylinder main regulators.

2) Purge overhead tank with He for approximately 1/2 h by opening valve V1 slightly.

3) Purge CO_2/N_2O soap film meter by opening the top soap trap temporarily.

4) Open valve V22 to maintain pressure in the absorption chamber. Let the system equilibrate for approximately 15 minutes.

5) Open valve V3.

6) Increase chamber pressure to 24 inches of water by adjusting the low-pressure bleed regulator on the control panel.

7) Close valve V22.

8) At low temperatures, let the system reach thermal equilibrium for about 15 minutes.

9) Check for pressure drop in the system.

10) Close valve V1.

11) Open valve V11 to the He reservoir and valve V21 to the amine feed tank.

12) Open valve V19 to release any internal He pressure in the amine feed tank.

13) Close valve V21.

14) Open valve V17 between the amine feed tank and the liquid circulation pump.

15) Open valve V6 about 4 turns.

16) Open valve V5 to allow liquid overflow to return the the amine feed tank.

17) Start liquid circulation pump.

18) Set Variac 2 on the liquid circulation line to the desired setting.

19) Open/close valve V2 repeatedly to remove trapped bubbles in the sight glass and to ensure proper operation.

20) Close valve V2 when the sight glass operates properly.

21) As the liquid level approaches the overflow level, close valve V6 to approximately 1 1/2 turns open. If more turns are required, check the liquid feed filter for clogging.

22) Check the in-line sight glass inside the air bath for proper liquid flow. If no flow is visible, check valve V5.

23) Open valve V8 to allow liquid to enter the absorption chamber.

24) Adjust the liquid flow to obtain a rotameter setting of approximately 30 to 40 mm.

25) Set Variac 1 on the liquid feed line to the desired setting.

26) Open valve V10 about 5 turns and check that valve V9 is open.

27) If the sphere needs to be wet manually,

27.1) Turn off the air bath fan.

27.2) Open the absorption chamber slide valve V28.

27.3) Open valve V10 to prevent the take-off tube from overflowing.

27.4) Wet the sp[illegible]arefully by rotating the support ro[illegible] spreading the liquid with a spatula. Take care not to scratch the surface of the sphere.

27.5) Close valve V28 and ensure that the liquid film covers the entire surface of the sphere.

27.6) Maintain a liquid flow rate of 30 to 40 mm on the liquid rotameter to prevent the film from rupturing.

28) Adjust valve V10 to maintain a take-off height of about 3 cm.

29) Open valve V23 inside the air bath.

30) Open valve V12 on the control panel.

31) Open valve V14.

32) Open valve V10 to maintain a 3 cm level in the take-off tube.

33) Purge the system for 20 minutes with pure CO_2/N_2O..

34) Adjust the sphere elevation to obtain a jet length of approximately 2 mm.

35) Take the cathetometer measurements.

36) Close valve V14. The liquid take-off level will go

down.

37) Open valve V13 and valve V24 at the bottom of the saturated gas knockout bomb.

38) Purge the system for 10 minutes. The gas rotameter will read about 20 to 30 % on the linear scale.

39) Close valve V24.

40) Open valve V25 between the knockout bomb and the absorption chamber fully open.

41) Ensure that valve V15 is fully open.

42) Close valve V13.

43) Start the gas circulation pump.

44) Open valve V13 fully open.

45) Adjust the circulation pump bypass valve V15 to obtain a circulation rate of about 50 % on the gas rotameter.

46) Adjust the CO_2/N_2O pressure in the absorption chamber to read about 12 inches of water on the manometer. The liquid take-off level will rise and must be controlled by opening valve V10.

47) Open valve V4 at the soap film meter.

48) Close valve V22 at the back of the air bath.

49) Make the final adjustment of liquid flow rate using valve V8.

50) Adjust the liquid take-off level using valve V10 so that the meniscus is at the change of diameter on the support rod.

51) Run the gas saturator for 15 minutes.

If the gas saturator is run during the experiment, proceed to step 57.

52) Open valve V15 fully open.

53) Close valve V13.

54) Shut off the gas circulation pump.

55) Close the two block valves V23 and V25 to isolate the absorption chamber.

56) Run the system for 15 minutes to allow the flowing temperatures to equilibrate.

57) Control the lean amine feed temperature T_1 with Variac 1 and fine tune to the desired level.

58) Condition the soap film meter by passing several soap bubbles through it.

59) **Measure all the data, taking 15 readings of absorption rate for each liquid flow rate. Measure T_1 to T_7 before and after each liquid rate. Ensure that the take-off height is steady by controlling valve V10. Record all pressures.**

60) Open valve V22.

61) Close valve V4.

62) Open valve V23.

63) Open valve V12.

64) Open valve V13.

65) Open valve V24.

66) Watch the liquid level in the take-off tube to prevent an overflow. Control the level with valve V10.

67) Purge the system for 5 minutes. This will expel inerts which have accumulated in the absorption chamber over the last hour.

68) Close valve V24.

69) Open valve V15.

70) Close valve V13.

71) <u>Open valve V25 between the knockout bomb and the absorption chamber fully open.</u>

72) Start the gas circulation pump.

73) Open valve V13.

74) Close the bypass valve V15 to maintain a rotameter setting of approximately 50 %.

74.1) Saturate the system for 5 minutes.

74.2) Repeat steps 52 to 56.

75) Open valve V4.

76) Close valve V22.

77) Adjust the liquid flow rate carefully to the next setting using valve V8.

78) Maintain the liquid level using valve V10.

79) Adjust Variac 1 to control temperature T_1.

80) Repeat procedure from step 56 to collect data for all liquid flow rates.

81) When finished, shut off both Variacs.

82) Close valve V8 to stop liquid feed to the absorber.

83) Stop the amine circulation pump.

84) Close valves V17 and V6.

85) Isolate the manometer by closing valve V3.

86) Drain the constant head reservoir and close valve V21 when the tank has emptied.

87) When the liquid has drained from the rich amine line, close valve V10.

88) Close valve V5 to isolate the amine feed tank.

89) Close valve V4 to isolate the soap film meter.

90) Shut the regulators and close all main valves on the gas supply cylinders.

91) Close valve V19.

92) Shut off the He supply.

93) Close valve V11.

Table A2.3

Detailed Operating Procedure for Amine Regenerator

1) Ensure that valve V10 is closed.

2) Connect the low-pressure He supply line to the amine vent port on the rich amine tank.

3) Open the He supply and pressurize the tank to 10 psig.

4) Open valve V18.

5) Fill the reboiler approximately 1/2 full. Make sure that enough liquid is present to cover the glass exposed to the mantle. If there is not enough liquid, postpone the regeneration step.

6) Close valve V18.

7) Shut off the He supply.

8) Depressurize the rich amine tank by carefully disconnecting the He supply line.

9) Reconnect the rich amine tank vent line to the port.

10) Slowly start cooling water circulating through the overhead condenser.

11) Power up both heating mantles.

12) Heat for approximately 1 to 1 1/2 h until the solution comes to a rolling boil.

13) Power down the top element in the heating mantle.

14) Regenerate the solution for at least 1 h.

15) Power down both heating mantle elements.

16) Let the system stand for 15 minutes.

17) Open the N_2 supply.

18) Purge the regenerator with N_2 for 2 minutes.

19) Start the vacuum transfer pump.

20) Open valve V20 slowly.

21) Maintain vacuum in the amine feed tank at approximately 28 in. Hg on the indicator gauge.

22) Fill the bucket with ice or water, depending on the temperature of the air bath.

23) Place the cooling coil in the bucket.

24) Open valve V26.

25) Open valve V27.

26) If necessary, maintain the ice level in the bucket.

27) When the reboiler empties, close valve V26.

28) Turn off the N_2 purge.

29) Close valve V27.

30) Continue vacuum for 10 minutes.

31) Close valve V20.

32) Shut off the vacuum pump.

33) Open the He supply to 10 psig on the regulator.

34) Open valve V21 at the back of the air bath for approximately 3 minutes.

35) Open valve V19.

36) Close valve V21.

37) Shut off the He supply.

38) Close valve V19.

39) Turn off the condenser cooling water.

APPENDIX 3

Calibration Data

This appendix contains information regarding the calibration of thermocouples, rotameters and soap film meters. For a more detailed account of the instrument calibration, the reader is referred to the sphere absorber reference material which is available in the laboratory.

Calibration of Thermocouples

Type J iron-constantan thermocouples were used to determine the temperature of key process streams in the sphere absorber apparatus. The thermocouples numbered UA8410 through UA8419 were calibrated with the platinum resistance thermometer (PRT) #UA0120831 in the Instrument Shop Standards Laboratory (E404), over a range of temperatures from 0° to 200°C. The actual calibration tables may be found in the reference material in the laboratory. The following nomenclature was used to refer to process temperatures

Temperature	Thermocouple	Description
T_1	UA8414	Amine to Absorption Chamber
T_2	UA8415	Amine from Absorption Chamber
T_3	UA8410	Gas at Soap Film Meter
T_4	UA8411	Gas at Absorption Chamber
T_5	UA8413	Gas from Circulation Pump
T_6	UA8419	Gas to Circulation Pump
T_7	UA8412	Amine at Rotameter
T_0	UA8417	Reference Junction

The standard EMF tables for converting from mV to °C were correlated with the following expression

$$T = a_0 + a_1\epsilon + a_2\epsilon^2 + a_3\epsilon^3 + a_4/\epsilon + a_5 \ln \epsilon$$

The following coefficients were used

a_0	-0.2902502066
a_1	17.31101383
a_2	0.07400533679
a_3	-0.004800534311
a_4	2.572484
a_5	4.377872676

where T is in °C and ϵ is in mV using a reference junction maintained at 0°C. The above correlation is valid from 20° to 120°C and has a maximum error of -0.376 % (-0.09°) at 24°C.

To calculate the temperature of the test thermocouple with a measured potential of $\epsilon_i^{T/C}$, the following expressions were used

$$T_i = f(\epsilon_i^{STD})$$

where

$$f = a_0 + a_1\epsilon + a_2\epsilon^2 + a_3\epsilon^3 + a_4/\epsilon + a_5 \ln \epsilon$$

$$\epsilon_i^{STD} = [\epsilon_i^{T/C} + \epsilon^{REF}] + g(\epsilon_i^{T/C} + \epsilon^{REF})$$

$$\epsilon^{REF} = \epsilon_{UA8417} \text{ at } 0°C = +0.0061 \text{ mV}$$

and

$$g = \beta_0 + \beta_1 e + \beta_2 e^2 + \beta_3 e^3$$

Values of g were calculated by using the PRT thermocouple calibrations and the standard EMF tables. The values of β_0-β_3 were obtained by least-squares regression analysis and are listed in Table A3.1.

Table A3.1

Error Correction for Thermocouple EMF

Thermocouple No. UA	β_0	β_1	β_2	β_3
8410	-5.3460	-17.1750	+0.3300	+0.4408
8411	-7.6516	-14.9870	-0.3151	+0.54015
8412	-7.4650	-15.3803	-0.4767	+0.53053
8413	-6.7735	-18.0780	+1.6850	+0.2497
8414	-7.0530	-12.8770	+2.0390	+0.7763
8415	-6.0775	-20.9390	+3.8254	-0.0603
8416	-4.9756	-16.5360	+0.0450	+0.45061
8417	-5.9118	-19.5580	+2.3734	+0.13940
8418	-6.7965	-16.5790	-0.1467	+0.5442
8419	-5.4220	-15.8000	-0.7680	+0.6216

where

$$g = \beta_0 + \beta_1 \epsilon + \beta_2 \epsilon^2 + \beta_3 \epsilon^3$$

ϵ is in mV

g is in μV

Calibration of Rotameters

Liquid feed rate was measured using a Matheson 150 mm rotameter with a #603 tube equipped with glass and stainless steel floats. A reliable correlation was required to convert the scale reading of the rotameter float to volumetric flow rate in the absorption chamber. A direct gravimetric technique was used to obtain the calibration for each solution at each operating temperature. This eliminated the need to estimate the effect of liquid composition and viscosity on the rotameter reading.

The temperature of the flowing liquid was recorded at the rotameter and at the approach tube in the absorption chamber. The volumetric flow rate of liquid in the absorption chamber was estimated by dividing the calibrated mass flow rate by the solution density at the absorber temperature. Mass flow rates at temperatures between those for which direct calibration existed were estimated by linear interpolation.

A detailed account of the gravimetric technique used to obtain the calibration curves can be found in the sphere absorber reference material. The calibration curves were each correlated with a fifth-order polynomial of the form

$$f = a_0 + a_1x + a_2x^2 + a_3x^3 + a_4x^4 + a_5x^5$$

where f is the mass flow rate in g/s and x is the scale

reading in mm from the stainless steel rotameter float. The values of $a_o - a_s$ for each calibration are presented in Tables A3.2 to A3.4.

Table A3.2

Parameters for Water Flow-Correlation

25°C

a_0	2.6342815
a_1	-0.2726597
a_2	1.252393×10^{-2}
a_3	-2.615804×10^{-4}
a_4	2.67175×10^{-6}
a_5	-1.07274×10^{-8}

where

$$f = a_0 + a_1 x + a_2 x^2 + a_3 x^3 + a_4 x^4 + a_5 x^5$$

f is in g/s

x is the stainless steel float reading in mm

Table A3.3

Parameters for 20 wt% MDEA Flow-Correlation

	25°C	50°C	75°C
a_0	1.078327×10^{-2}	-5.31112×10^{-1}	2.382154
a_1	9.427604×10^{-3}	5.99597×10^{-2}	-2.450092×10^{-1}
a_2	3.11711×10^{-4}	-1.395817×10^{-3}	1.134012×10^{-2}
a_3	-4.414908×10^{-6}	2.477809×10^{-5}	-2.34374×10^{-4}
a_4	2.178295×10^{-8}	-2.241557×10^{-7}	2.35895×10^{-6}
a_5	$-2.572552 \times 10^{-11}$	7.899346×10^{-10}	-9.323651×10^{-9}

where

$$f = a_0 + a_1 x + a_2 x^2 + a_3 x^3 + a_4 x^4 + a_5 x^5$$

f is in g/s

x is the stainless steel float reading in mm

Table A3.4

Parameters for 40 wt% MDEA Flow-Correlation

	25°C	50°C	75°C
a_0	-0.448478	-0.388295	-0.492547
a_1	1.951922×10^{-2}	1.965263×10^{-2}	3.736211×10^{-2}
a_2	1.661114×10^{-5}	3.014302×10^{-4}	-2.470948×10^{-4}
a_3	-2.822739×10^{-6}	-8.171372×10^{-6}	-7.132243×10^{-9}
a_4	4.109065×10^{-8}	7.449426×10^{-8}	1.771181×10^{-8}
a_5	$-1.899019 \times 10^{-10}$	$-2.393638 \times 10^{-10}$	$-9.032819 \times 10^{-11}$

where

$$f = a_0 + a_1 x + a_2 x^2 + a_3 x^3 + a_4 x^4 + a_5 x^5$$

f is in g/s

x is the stainless steel float reading in mm

Calibration of Soap Film Meters

The rate of absorption of solute gas into the liquid flowing over the sphere was measured with a soap film meter (SFM). The internal volumes of each SFM were measured using gravimetric analysis with water as the test fluid. A measured volume of water at a known temperature was delivered through the SFM, collected and weighed. The density of water was used to convert the delivered mass to volume.

Each SFM was found to deliver volumes well within acceptable limits (< 0.1 %). A detailed account of the calibration results can be found in the sphere absorber reference ma

APPENDIX 4

Correlation of Physical Properties

The correlations used in the analysis of the raw data are contained in this appendix. The properties include:

1) Density of MDEA solutions
2) Kinematic viscosity of MDEA solutions
3) Equilibrium solubility of N_2O in MDEA solutions

Density of MDEA Solutions

The density of aqueous solutions of MDEA was assumed to agree with the figures published by Pennwalt Chemicals. The density of pure water was taken from Table 3-29 in Perry and Chilton (1973). Selected points were taken from these sources and used to obtain a polynomial expression of the form

$$\rho = a_0 + a_1 T + a_2 T^2 + a_3 T^3 + a_4 T^4 + a_5 T^5$$

The coefficients obtained are listed in Table A4.1. The above correlation is valid for temperatures ranging from 20° to 85°C. The presence of residual carbon dioxide (~0.03 mol CO_2/mol MDEA) was assumed not to significantly affect the density of the solution.

Table A4.1

Correlation of MDEA Solution Density

	0 wt%	10 wt%	20 wt%
a_0	1.000244355	1.0142473	1.0256906
a_1	1.941636×10^{-5}	-0.457723×10^{-3}	-0.494247×10^{-3}
a_2	-6.543792×10^{-6}	0.119919×10^{-4}	0.123157×10^{-4}
a_3	2.984752×10^{-8}	-0.252978×10^{-6}	-0.324908×10^{-6}
a_4	-8.223252×10^{-11}	0.127470×10^{-8}	0.278452×10^{-8}
a_5	0	0.200840×10^{-12}	-0.831680×10^{-11}

	30 wt%	40 wt%	50 wt%
a_0	1.0322227	1.0459222	1.0654460
a_1	-0.872888×10^{-4}	-0.482704×10^{-3}	-0.143623×10^{-2}
a_2	-0.352015×10^{-5}	0.117230×10^{-4}	0.382244×10^{-4}
a_3	-0.109310×10^{-6}	-0.490963×10^{-6}	-0.835901×10^{-6}
a_4	0.172301×10^{-8}	0.640395×10^{-8}	0.838608×10^{-8}
a_5	-0.747054×10^{-11}	-0.286903×10^{-10}	-0.323155×10^{-10}

$$\rho = a_0 + a_1T + a_2T^2 + a_3T^3 + a_4T^4 + a_5T^5$$

where T is in °C and ρ is in g/cm³. To obtain density in kg/m³ the value of ρ must be multiplied by 1000.

Kinematic Viscosity of MDEA Solutions

The kinematic viscosity of aqueous solutions of MDEA was determined experimentally using the Cannon-Fenske Routine Viscometer in the Instrument Shop Standards Laboratory (E404). In principle, a known volume of liquid is allowed to flow by gravity through a capillary tube. The efflux time is a direct measure of the kinematic viscosity of the liquid. The standard procedure outlined in ASTM D-445 was used to measure the viscosity of 10, 20, 30, 40, and 60 wt % MDEA solutions at temperatures ranging from 25° to 75°C. Additional detail on the experimental procedure and methods used to calculate the viscosity may be found in the sphere absorber reference material. The results of the experimental measurements are contained in Table A4.2.

The kinematic viscosity data were correlated with a polynomial function of the form

$$\ln \nu = a_0 + \frac{a_1}{T} + \frac{a_2}{T^2}$$

The coefficients obtained are given in Table A4.3. This correlation is valid over a temperature range of 20° to 100°C, and an amine concentration range from 0 wt % to 60 wt % MDEA. The presence of residual carbon dioxide (~0.03 mol CO_2/mol MDEA) was assumed not to significantly affect the kinematic viscosity of the solution.

Table A4.2

Raw Data from Viscosity Experiment

wt % MDEA	Tube #	T (°C)	Constant o	Efflux Time (s)	Viscosity (cs)
0	F50-442	23.3	0.0025771	360.87	0.93
0	F50-442	23.3	0.0025733	361.41	0.93
0	F50-442	23.3	0.0025780	360.75	0.93
0	F50-442	39.15	0.0025262	261.66	0.661
0	F50-442	39.15	0.0025244	261.84	0.661
0	F50-442	39.15	0.0025251	261.77	0.661
0	F50-442	77.2	0.0024841	150.96	0.375
0	F50-442	77.2	0.0024882	150.71	0.375
0	F50-442	77.3	0.0024809	150.75	0.374
0	F50-442	77.3	0.0024819	150.69	0.374
0	F25-25	77.6	0.0017808	209.46	0.373
0	F25-25	77.7	0.0017661	210.63	0.372
0	F25-25	77.7	0.0017715	209.99	0.372
10.000	F50-442	23.3	0.0025767	517.76	1.33
10.000	F50-442	23.3	0.0025767	517.53	1.33
10.000	F50-442	23.3	0.0025767	517.64	1.33
10.000	F50-442	39.15	0.0025252	357.76	0.903
10.000	F50-442	39.15	0.0025252	357.57	0.903
10.000	F50-442	39.15	0.0025252	357.64	0.903
10.000	F25-25	77.2	0.0017728	270.20	0.479
10.000	F25-25	77.2	0.0017728	268.75	0.476
10.000	F25-25	77.3	0.0017728	269.05	0.477
19.994	F50-442	23.3	0.0025767	785.52	2.02
19.994	F50-442	23.3	0.0025767	780.21	2.01
19.994	F50-442	23.3	0.0025767	781.13	2.01
19.994	F50-442	39.15	0.0025252	511.17	1.29
19.994	F50-442	39.20	0.0025252	510.00	1.29
19.994	F50-442	39.20	0.0025252	510.63	1.29
19.994	F25-25	77.6	0.0017728	351.04	0.622
19.994	F25-25	77.7	0.0017728	351.10	0.622
19.994	F25-25	77.7	0.0017728	351.09	0.622
29.993	C100-J871	25.2	0.0136388	225.09	3.07
29.993	C100-J871	25.2	0.0136388	224.96	3.07
29.993	C100-J871	25.2	0.0136388	224.28	3.06
29.993	F50-442	40.0	0.0025232	771.52	1.95
29.993	F50-442	40.0	0.0025232	766.19	1.93
29.993	F50-442	40.0	0.0025232	748.71	1.89
29.993	F50-442	77.7	0.0024833	334.52	0.831
29.993	F50-442	77.7	0.0024833	332.84	0.827
29.993	F50-442	77.8	0.0024833	333.00	0.827
29.993	F25-25	77.7	0.0017728	475.16	0.842
29.993	F25-25	77.7	0.0017728	473.64	0.840
29.993	F25-25	77.8	0.0017728	474.04	0.840

40.010	C100-J871	25.2	0.0136388	370.72	5.06
40.010	C100-J871	25.2	0.0136388	373.63	5.10
40.010	C100-J871	25.2	0.0136388	374.07	5.10
40.010	C100-J871	40.0	0.0136283	220.63	3.01
40.010	C100-J871	40.0	0.0136283	220.65	3.01
40.010	C100-J871	40.0	0.0136283	220.63	3.01
40.010	F50-442	77.6	0.0024833	464.47	1.15
40.010	F50-442	77.7	0.0024833	468.15	1.16
40.010	F50-442	77.7	0.0024833	462.56	1.15
49.998	C100-J871	25.2	0.0136388	658.16	8.98
49.998	C100-J871	25.2	0.0136388	660.13	9.00
49.998	C100-J871	25.2	0.0136388	661.84	9.03
49.998	C100-J871	39.9	0.0136283	360.86	4.92
49.998	C100-J871	40.0	0.0136283	360.22	4.91
49.998	C100-J871	40.0	0.0136283	362.10	4.93
49.998	F50-442	77.6	0.0024833	659.05	1.64
49.998	F50-442	77.6	0.0024833	663.94	1.65
49.998	F50-442	77.7	0.0024833	660.16	1.64

Table A4.3

Correlation of MDEA Solution Kinematic Viscosity

wt % MDEA	a_0	a_1	a_2
0	0.6641	-2549.5	[illegible]
10	1.6001	-3183.1	[illegible]
20	2.6484	-3920.3	[illegible]
30	2.2170	-3762.1	[illegible]4841
40	1.5084	-3404.2	[illegible]026178
50	2.7418	-4344.8	1247827

$$\ln \nu = a_0 + \frac{a_1}{T} + \frac{a_2}{T^2}$$

where ν is in cs and T is in K. To obtain viscosity in m^2/s, the value of ν must be multiplied by 1.0×10^{-6}. The absolute viscosity of a solution, μ, may be calculated by multiplying the kinematic viscosity by the density (i.e. $\mu = \nu\rho$).

Physical Solubility of Nitrous Oxide in MDEA Solutions

The physical solubility of nitrous oxide (N_2O) in aqueous solutions of MDEA was determined experimentally with a visual equilibrium cell. The measurements were taken by Dr. F.-Y. Jou at temperatures ranging from 25° to 125°C and for 0 wt %, 20 wt % and 40 wt % MDEA solutions. Jou et al.(1986) describe the experimental apparatus and procedure that were used. The results of these experiments are given in the form of Henry's constants in Table A4.4.

The Henry's constants were correlated with an equation of the form

$$\ln H = a_0 + a_1 T + \frac{a_2}{T}$$

The coefficients for this equation are given in Table A4.5. This correlation is valid over a temperature range of 20° to 130°C, and an amine concentration of 0 wt % to 50 wt % MDEA.

The data have been compared to those of Blauwhoff et al.(1983) and Haimour and Sandall (1984). The sets agree at 25°C, although the results of this work span a much larger temperature range. The Henry's constant was found to be a strong function of temperature. The data of Haimour and Sandall (1984) suggest that H varies linearly with inverse temperature. The results of this study show that the Henry's constant must be represented by a higher order polynomial in inverse temperature.

A comparison between the experimental and predicted Henry's constant is illustrated in Figure A4.1.

Table A4.4

Henry's Constant for N_2O in MDEA Solutions

Temperature °C	Water	20 wt % MDEA	40 wt % MDEA
25	228.3	212.6	191.6
50	407.4	352.1	292.9
75	606.6	475.6	371.9
100	764.8	583.5	420.8
125	858.7	627.1	434.2

where the Henry's constant is in MPa/mole fraction.

Table A4.5

Correlation of N_2O Henry's Constant in MDEA Solutions

wt % MDEA	a_0	a_1	a_2
0	31.6847	-0.0301286	-5149.67
20	28.7470	-0.0274130	-4535.4
40	27.8522	-0.0278120	-4263.8

where

$$\ln H = a_0 + a_1 T + \frac{a_2}{T}$$

and H is in MPa, T is in K.

Figure A4.1.

Henry's Constant for N_2O in MDEA Solutions

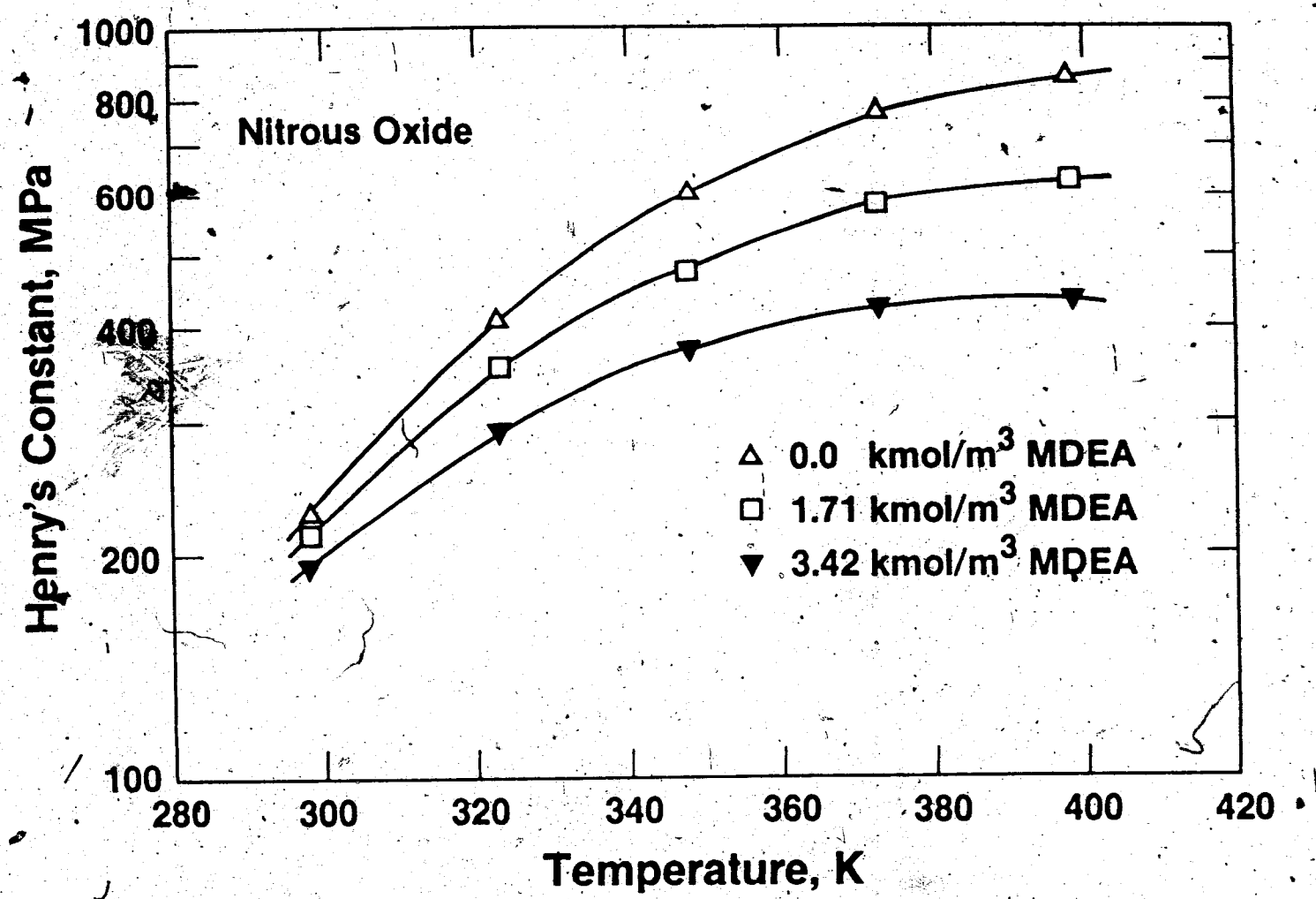

APPENDIX 5

Error Analysis

For any function $F(x_1, x_2, x_3, x_4)$ the standard error σ_F^2 in F is given by

$$\sigma_F^2 = \left(\frac{\partial F}{\partial x_1}\right)^2 \sigma_{x_1}^2 + \left(\frac{\partial F}{\partial x_2}\right)^2 \sigma_{x_2}^2 + \left(\frac{\partial F}{\partial x_3}\right)^2 \sigma_{x_3}^2 + \left(\frac{\partial F}{\partial x_4}\right)^2 \sigma_{x_4}^2 \qquad \text{(A5.1)}$$

where σ_{x_1}, σ_{x_2}, σ_{x_3} and σ_{x_4} are the standard errors in the means of x_1, x_2, x_3 and x_4.

Molecular Diffusion Coefficient

The rate of physical absorption of solute gas into the liquid film on the sphere absorber is given by Equation (50)-

$$G_s = L(C_i - C_o)\left[1 - \sum_i \beta_i e^{-\gamma_i \alpha}\right]$$

$$= L(C_i - C_o)f \qquad (50)$$

where

$$\alpha = 3.3653\pi\left(\frac{2\pi g}{3\nu}\right)^{1/3} D\, R^{7/3}\, L^{-4/3} \qquad (51)$$

Equation (50) may be expressed in general as

$$G_s = E(L, (C_i - C_o), D, \nu) \qquad (A5.2)$$

Applying Equation (A5.1) to Equation (A5.2) gives

$$\sigma_{Gs}^2 = (\partial G_s/\partial L)^2\sigma_L^2 + (\partial G_s/\partial(C_i - C_o))^2\,\sigma_{(Ci-Co)}^2 + (\partial G_s/\partial D)^2\sigma_D^2 + (\partial G_s/\partial\nu)^2\sigma_\nu^2 \qquad (A5.3)$$

Now

$$\partial G_s/\partial L = (C_i - C_o)f + L(C_i - C_o)\left(\frac{\partial f}{\partial L}\right) \qquad (A5.4)$$

but

$$f = 1 - \Sigma\beta e^{-\gamma\alpha} \qquad (A5.5)$$

therefore

$$\frac{\partial f}{\partial L} = \frac{\partial \alpha}{\partial L}\, g \qquad (A5.6)$$

where

$$g = \Sigma\beta\gamma e^{-\gamma\alpha} \qquad (A5.7)$$

and

$$\frac{\partial \alpha}{\partial L} = 3.3653\pi\left(\frac{2\pi g}{3\nu}\right)^{1/3} D\, R^{7/3}\left(\frac{-4}{3} L^{-7/3}\right) = \frac{-4\alpha}{3L} \qquad (A5.8)$$

Therefore

$$\partial G_s/\partial L = (C_i - C_o)[f - 4\alpha g/3] \qquad (A5.9)$$

In a similar manner, the following may be derived

$$\partial G_s/\partial(C_i - C_o) = Lf \qquad (A5.10)$$

$$\partial G_s / \partial D = L(C_i - C_o)\, g\alpha / D \qquad \text{(A5.11)}$$

$$\partial G_s / \partial \nu = L(C_i - C_o)\left(\frac{-g\alpha}{3\nu}\right) \qquad \text{(A5.12)}$$

Substituting Equations (A5.9) to (A5.12) into Equation (A5.3) gives

$$\sigma_{Gs}^2 = \{(C_i - C_o)[f - \tfrac{4\alpha g}{3}]\}^2 \sigma_L^2 + \{Lf\}^2 \sigma_{(Ci-Co)}^2 + \{L(C_i - C_o) g\alpha / D\}^2 \sigma_D^2 + \{L(C_i - C_o)\tfrac{g\alpha}{3\nu}\}^2 \sigma_\nu^2 \qquad \text{(A5.13)}$$

Dividing Equation (A5.13) by G_s^2 to obtain fractional errors and rearranging (assuming all errors are additive) gives

$$(\sigma_D / D)^2 = \{(f - \tfrac{4\alpha g}{3})/g\alpha\}^2 (\sigma_L / L)^2 + \{f/g\alpha\}^2 (\sigma_{(Ci-Co)} / (C_i - C_o))^2 + \{1/3\}^2 (\sigma_\nu / \nu)^2 + \{f/g\alpha\}^2 (\sigma_{Gs} / G_s)^2 \qquad \text{(A5.14)}$$

Reaction Rate Constant

The rate of chemical absorption of solute gas into the liquid film on the sphere absorber is given by Equation (68)

$$G_s = 4\pi R^2 \sqrt{k_{ov} D}\,(G_i - C_{eq}) \qquad (68)$$

Equation (68) may be expressed in general as

$$G_s = F(k_{ov}, D, (C_i - C_{eq})) \qquad (A5.15)$$

Note that C_{eq} was assumed to equal zero. Applying Equation (A5.1) to Equation (A5.15) gives

$$\sigma_{Gs}^2 = (\partial G_s/\partial k_{ov})^2 \sigma_{kov}^2 + (\partial G_s/\partial D)^2 \sigma_D^2 + (\partial G_s/\partial (C_i - C_{eq}))^2 \sigma_{(Ci-Ceq)}^2 \qquad (A5.16)$$

Now

$$\partial G_s/\partial k_{ov} = 4\pi R^2 \sqrt{k_{ov} D}(C_i - C_{eq})/2k_{ov} \qquad (A5.17)$$

$$\partial G_s/\partial D = 4\pi R^2 \sqrt{k_{ov} D}(C_i - C_{eq})/2D \qquad (A5.18)$$

$$\partial G_s/\partial (C_i - C_{eq}) = 4\pi R^2 \sqrt{k_{ov} D} \qquad (A5.19)$$

Substituting Equations (A5.17) to (A5.19) into Equation (A5.16) gives

$$\sigma_{Gs}^2 = \{4\pi R^2 \sqrt{k_{ov} D}(C_i - C_{eq})/2k_{ov}\}^2 \sigma_{kov}^2 + \{4\pi R^2 \sqrt{k_{ov} D}(C_i - C_{eq})/2D\}^2 \sigma_D^2 + \{4\pi R^2 \sqrt{k_{ov} D}\}^2 \sigma_{(Ci-Ceq)}^2 \qquad (A5.20)$$

Dividing Equation (A5.20) by G_s^2 to obtain fractional errors and rearranging (assuming all errors are additive) gives

$$(\sigma_{kov}/k_{ov})^2 = 4(\sigma_{Gs}/G_s)^2 + (\sigma_D/D)^2 + 4(\sigma_{(Ci-Ceq)})/(C_i - C_{eq}))^2 \qquad (A5.21)$$

APPENDIX 6

Computer Programs

This appendix contains listings of the computer programs used to calculate the molecular diffusion coefficient and the second order rate constant from raw experimental data.

Program 1 - Analysis for Diffusion Coefficient

Program 2 - Analysis for Reaction Rate Constant

```
C PROGRAM 1
C
C     Program to determine the molecular diffusion coefficient
C      using experimental data from the sphere absorber
C
C
      IMPLICIT REAL*8(A-H,O-Z)
      CHARACTER*4 TOD(2),DATE(3)
      CHARACTER*8 MONTH,BLANK,GAS,FILE,COMMNT
      CHARACTER*1 NO,NO2,IANS
      REAL*8 JETLTH
      DIMENSION G(20)
      DIMENSION FLOW(5),TCS(7,5),TCF(7,5),TIMES(5),TIMEF(5)
      DIMENSION SWVOL(20,5),SWTIM(20,5),MEAS(5),GAS(2)
      DIMENSION COMMNT(10,10),MONTH(2,12),FILE(3)
      DIMENSION TEMPS(7),TEMPF(7),TEMPA(7)
      COMMON/IO/IIN,IOUT,JIN,JOUT,LOUT
      COMMON/FNAME/FILE
      COMMON/DATES1/MONTH,TOD,DATE
      COMMON/DATES2/IYEAR,IMONTH,IDAY
      COMMON/NUMB/PI,GRAVTY,E1,E2,E3,E4,E5,R
      COMMON/FLUID/QLIQ,DENS,VISCK,WT
      COMMON/CONC/CI,CO
      COMMON/EQUIP/RS
      DATA BLANK/'        '/,NO/'N'/,NO2/'n'/
      DATA GAS/'N2O     ','CO2     '/
C
      CALL TIME(O)
      CALL TIME(4,O,TOD)
      CALL TIME(5,O,DATE)
C
      KIN=9
C
      E1=1.D+00/6.D+00
      E2=7.D+00/6.D+00
      E3=1.D+00/3.D+00
      E4=7.D+00/3.D+00
      E5=-4.D+00/3.D+00
      DIAM=50.8D-03
C
      DO 100 J=1,10
      DO 100 I=1,10
         COMMNT(I,J)=BLANK
100   CONTINUE
      READ(KIN,1009)(FILE(I),I=1,3)
```

```
1009  FORMAT(1X,9A8)
      IRES=1
      WRITE(IOUT,2004)
2004  FORMAT(' Analysis for Molecular Diffusivity Begins...')
C
C
C
C
9000  READ(JIN,1000)IROUTE
1000  FORMAT(20I5)
      READ(JIN,1001)OPNAME
1001  FORMAT(10A8)
      READ(JIN,1000)IYEAR,IMONTH,IDAY,IGAS,ITUBE,ICOMM
      READ(JIN,1002)WT,TEEP
      READ(JIN,1002)DNOZ,PBARO,TROOM
      READ(JIN,1002)CELLPR,CELLPL
      READ(JIN,1002)HJET,HNORTH,HSOUTH,HTAKE
      READ(JIN,1002)COARSE,FINE,VFEED,VCIRC
      READ(JIN,1000)NFLOW
      DO 1005 J=1,NFLOW
          READ(JIN,1002)FLOW(J)
          READ(JIN,1000)NMEAS
          MEAS(J)=NMEAS
          READ(JIN,1002)(SWVOL(I,J),I=1,NMEAS)
          READ(JIN,1002)(SWTIM(I,J),I=1,NMEAS)
          READ(JIN,1006)(TCS(I,J),I=1,7)
          READ(JIN,1006)(TCF(I,J),I=1,7)
          READ(JIN,1001)TIMES(J),TIMEF(J)
1005  CONTINUE
      IF(ICOMM.EQ.1)THEN
          DO 1008 J=1,10
              READ(JIN,1001)(COMMNT(I,J),I=1,10)
1008      CONTINUE
1002      FORMAT(5F15.6)
1006      FORMAT(7F10.6)
      ENDIF
1007  READ(JIN,1000)IEND
C
C
      CALL NEWPGE
      WRITE(JOUT,2000)
2000  FORMAT(////,' Comments :',//)
      IF(ICOMM.EQ.0)THEN
          WRITE(JOUT,2002)
2002      FORMAT(' None.')
```

```
      ELSE
         DO 2003 J=1,10
            WRITE(JOUT,1001)(COMMNT(I,J),I=1,10)
2003     CONTINUE
      ENDIF
C
C
3000  CONTINUE
      CALL NEWPGE
      WRITE(JOUT,2006)
2006  FORMAT(/,' Echo of Raw Experimental Data.',//)
      WRITE(JOUT,2007)WT
2007  FORMAT(' Amine Concentration (wt % MDEA)',T50,F15.4)
      WRITE(JOUT,2008)TEEP
2008  FORMAT(' Surfactant Concentration (wt % SLS "Teepol")',
     %T50,F15.4)
      WRITE(JOUT,2009)GAS(IGAS)
2009  FORMAT(' Absorbing Gas',T57,A8)
      WRITE(JOUT,2010)OPNAME
2010  FORMAT(' Process Operator',T57,A8)
      WRITE(JOUT,2011)
2011  FORMAT(//)
      WRITE(JOUT,2012)PBARO
2012  FORMAT(' Atmospheric Pressure (mm Hg)',T50,F15.4)
      WRITE(JOUT,2013)TROOM
2013  FORMAT(' Atmospheric Temperature (deg C)',T50,F15.4)
      WRITE(JOUT,2011)
      WRITE(JOUT,2014)ITUBE
2014  FORMAT(' Rotameter Tube #',T50,I15)
      WRITE(JOUT,2015)DNOZ
2015  FORMAT(' Jet Nozzle Throat Diameter (mm)',T50,F15.4)
      WRITE(JOUT,2011)
      WRITE(JOUT,2016)CELLPR
2016  FORMAT(' Cell Pressure Manometer Right Leg (in. H20)',
     %T50,F15.4)
      WRITE(JOUT,2017)CELLPL
2017  FORMAT(' Cell Pressure Manometer Left Leg  (in. H20)',
     %T50,F15.4)
      WRITE(JOUT,2011)
      WRITE(JOUT,2018)HJET
2018  FORMAT(' Jet Nozzle Elevation (cm)',T50,F15.4)
      WRITE(JOUT,2019)HNORTH
2019  FORMAT(' Sphere North Pole Elevation (cm)',T50,F15.4)
      WRITE(JOUT,2020)HSOUTH
2020  FORMAT(' Sphere South Pole Elevation (cm)',T50,F15.4)
```

```
      WRITE(JOUT,2021)HTAKE
2021  FORMAT(' Liquid Take-off Elevation (cm)',T50,F15.4)
      WRITE(JOUT,2011)
      WRITE(JOUT,2022)COARSE
2022  FORMAT(' Thermotrol Coarse Setting',T50,F15.4)
      WRITE(JOUT,2023)FINE
2023  FORMAT(' Thermotrol Fine Setting',T50,F15.4)
      WRITE(JOUT,2024)VFEED
2024  FORMAT(' Amine Feed Preheater Variac Setting',T50,F15.4)
      WRITE(JOUT,2025)VCIRC
2025  FORMAT(' Amine Circulation Heater Variac Setting',T50,F15.4)
      WRITE(JOUT,2011)
C
      JETLTH=(HJET-HNORTH)*0.01D+00
      DNOZ=DNOZ*1.D-03
      TAKOFF=(HSOUTH-HTAKE)*0.01D+00
      IF(TAKOFF.LT.0.02D+00)WRITE(JOUT,2035)TAKOFF
2035  FORMAT(/,' **** Take-off length is ',F8.5,' m',/,
     %' **** Stagnant layer may affect the absorption rate.',//)
C
      PBARO=(PBARO/760.D+00)*101.325D+00
      PMANO=(CELLPR+CELLPL)*0.24848D+00
      PCELL=PBARO+PMANO
C
C
      DO 3001 IFLOW=1,NFLOW
         NMEAS=MEAS(IFLOW)
         CALL NEWPGE
         WRITE(JOUT,2006)
         WRITE(JOUT,2026)IFLOW
2026     FORMAT(' These data are for amine flow rate ',I3)
         WRITE(JOUT,2011)
         WRITE(JOUT,2027)FLOW(IFLOW)
2027     FORMAT(' Rotameter Scale Reading (mm)',T50,F15.4)
         WRITE(JOUT,2011)
         WRITE(JOUT,2028)TIMES(IFLOW)
2028     FORMAT(' Start Time (HH:MM)',T60,2A8)
         WRITE(JOUT,2029)TIMEF(IFLOW)
2029     FORMAT(' End Time   (HH:MM)',T60,2A8)
         WRITE(JOUT,2011)
         WRITE(JOUT,2030)
2030     FORMAT(5X,'Measurement',5X,'Sweep Volume (mL)',5X,
     %   'Sweep Time (s)',/,1X,60('-'),/)
         DO 3002 IMEAS=1,NMEAS
            WRITE(JOUT,2031)IMEAS,SWVOL(IMEAS,IFLOW),
```

```
     %        SWTIM(IMEAS,IFLOW)
2031          FORMAT(5X,I5,14X,F7.2,14X,F8.2)
3002       CONTINUE
           WRITE(JOUT,2032)
2032       FORMAT(/,1X,60('-'))
           WRITE(JOUT,2011)
           WRITE(JOUT,2033)
2033       FORMAT(' Thermocouple Readings (mV)',/,4X,'T/C',4X,
     %     'Start',6X,'End',/,1X,60('-'),/)
           DO 3003 IC=1,7
              WRITE(JOUT,2034)IC,TCS(IC,IFLOW),TCF(IC,IFLOW)
2034          FORMAT(1X,I5,2F10.3)
3003       CONTINUE
           WRITE(JOUT,2032)
3001    CONTINUE
C
        CALL MOLEFC(XW)
        DO 3004 IFLOW=1,NFLOW
           WRITE(IOUT,2049)IFLOW
2049       FORMAT('      Calculations for Flow Rate ',I3,' Begin...')
           NMEAS=MEAS(IFLOW)
           CALL NEWPGE
           WRITE(JOUT,2026)IFLOW
           DO 3005 IC=1,7
              TEMPS(IC)=TCOUPL(IC,TCS(IC,IFLOW))
              TEMPF(IC)=TCOUPL(IC,TCF(IC,IFLOW))
              TEMPA(IC)=(TEMPS(IC)+TEMPF(IC))*0.5D+00
3005       CONTINUE
           TCELL=(TEMPA(1)+TEMPA(2))*0.5D+00
C
           CALL DENSL(TCELL)
           CONC=10.D+00*WT*DENS/119.17D+00
           CALL CELLP(TCELL,PCELL,XW,PGAS)
           CALL HENRY(IGAS,TCELL,HCOEFF)
           CALL AKG(IRES,IGAS,TCELL,PCELL,PGAS,XKG)
           CALL KINVSC(TCELL)
           VISCA=VISCK*DENS*1.D+03
           DDENS=DENS*1.D+03
           GAVG=0.D+00
           DO 3006 IMEAS=1,NMEAS
              G(IMEAS)=(PCELL*SWVOL(IMEAS,IFLOW)*1.D-06)/
     %          (R*(TEMPA(3)+273.15D+00)*SWTIM(IMEAS,IFLOW))
              GAVG=GAVG+G(IMEAS)
3006       CONTINUE
           GAVG=GAVG/DBLE(FLOAT(NMEAS))
```

```
      CALL ROTAM(TCELL,FLOW(IFLOW))
      CO=0.D+00
      CALL AKB(DNOZ,JETLTH,GAVG,HCOEFF,PGAS,XKG,RESIST)
      PCSAT=GAVG*100.D+00/(QLIQ*CI)
      RES=2.D+00*QLIQ/(PI*RS*VISCK)
      REJ=4.D+00*QLIQ/(PI*DNOZ*VISCK)
C
      ZSPH=4.49D+00*(2.D+00*PI*GRAVTY/(3.E+00*VISCK))**E1
     %    *(RS**E2)*(QLIQ**E3)
      ZJET=4.D+00*DSQRT(JETLTH*QLIQ)
      FSPH=ZSPH/(ZSPH+ZJET)
      FJET=ZJET/(ZSPH+ZJET)
      GSPH=GAVG*FSPH
      GJET=GAVG-GSPH
      CIO=0.D+00
      CO=GJET/QLIQ
      DGAS=(GSPH/(ZSPH*(CI-CO)))**2
      DOLD=0.D+00
      ERRORD=0.D+00
      JTERD=0
C
      DELTAP=(3.D+00*QLIQ*VISCK/(2.D+00*PI*RS*GRAVTY))**E3
      ACORR=1.D+00+(2.58712D+00*DELTAP/RS)
C
3010  GSPH=GSPH/ACORR
C
      ITERD=0
      DLOW=DGAS/2.D+00
      DHI=DGAS*2.D+00
      CALL ABSORB(DLOW,GCALC)
      F1=GSPH-GCALC
      CALL ABSORB(DHI,GCALC)
      F2=GSPH-GCALC
3008  CONTINUE
      IF(ITERD.GT.50)THEN
         WRITE(JOUT,6009)
6009     FORMAT(/,' ** More than 50 iterations required',
     %        ' for the inner loop **')
         GO TO 3012
      ENDIF
      ITERD=ITERD+1
      DGAS=0.5D+00*(DHI+DLOW)
      DELTAD=DHI-DLOW
      IF((DABS(DELTAD)/DGAS).LT.1.D-05)GO TO 3009
      CALL ABSORB(DGAS,GCALC)
```

```
      FUNC=GSPH-GCALC
      FSIGN=FUNC*F1
      IF(FSIGN.LT.0.D+00)THEN
          DHI=DGAS
          F2=FUNC
      ELSE
          DLOW=DGAS
          F1=FUNC
      ENDIF
      GO TO 3008
3009  GJET=4.D+00*(CI-CIO)*DSQRT(JETLTH*QLIQ*DGAS)
      CO=CIO+(GJET/QLIQ)
      GSPH=GAVG-GJET
      JTERD=JTERD+1
C
      IF(JTERD.EQ.1)GO TO 3010
      IF(JTERD.GT.25)THEN
          WRITE(JOUT,6010)
6010      FORMAT(/,' ** More than 25 iterations required',
     %         ' for the outer loop **')
          GO TO 3012
      ENDIF
      ERRORD=DABS(DGAS-DOLD)/DGAS
      IF(ERRORD.LT.1.D-04)GO TO 3012
      DOLD=DGAS
      GO TO 3010
C
3012  CONTINUE
      WRITE(JOUT,6004)PCELL,GAS(IGAS),PGAS,TCELL,QLIQ
6004  FORMAT(/,5X,'------Absorber Conditions------',/,
     %  ' Total P',T15,F15.2,
     %  ' kPa',T40,'P',A8,T54,F15.2,' kPa',/,' Temperature',T15,
     %  F15.2,' deg C',T40,'Liquid Flow',T54,D15.5,' m3/s')
      WRITE(JOUT,6005)WT,CONC,VISCA,VISCK,DDENS
6005  FORMAT(5X,'------Fluid Properties------',/,
     %  ' Wt % Amine',T15,F15.2,
     %  T40,'Amine Conc.',T54,F15.3,' kmol/m3',/,' Viscosity',
     %  T15,E15.5,' kg/m-s',T40,'Viscosity',T54,E15.5,' m2/s',/,
     %  ' Density',T15,F15.3,' kg/m3')
      WRITE(JOUT,6006)DIAM,DELTAP,RES,REJ,DNOZ,JETLTH,TAKOFF
6006  FORMAT(5X,'------Sphere Data------',/,
     %  ' Diameter',T15,F15.5,' m',T40,'Film Thick.',T54,D15.5,' m',
     %  /,' Sphere Re',T15,F15.2,T40,'Jet Re',T54,F15.2,/,
     %  ' Jet Diameter',T15,D15.4,' m',T40,'Jet Length',
     %  T54,D15.5,' m',/,' Take-off',T15,F15.5,' m')
```

```
      WRITE(JOUT,6007)JTERD,GSPH,GJET,GAVG,DGAS,ERRORD,
     %  CI,HCOEFF,PCSAT,CIO,CO,XKG,RESIST
6007  FORMAT(5X,'------Absorption Data------',/,
     %  ' After ',I4,' Iterations :',/,' Sphere Rate',T15,
     %  D15.5,' kmol/s',T40,'Jet Rate',T54,D15.5,' kmol/s',/,
     %  ' Measured Rate',T15,D15.5,' kmol/s',/,
     %  ' Predicted D',T15,D15.5,' m2/s',T40,'Error',T54,F15.5,' %',
     %  /,' Int. Conc.',T15,F15.7,' kmol/m3',T40,'Henry''s Const.',
     %  T54,F15.3,' kPa-m3/kmol',/,
     %  ' Saturation',T15,F15.3,' %',/,' Jet Inlet',T15,F15.7,
     %  ' kmol/m3',T40,'Sphere Inlet',T54,F15.7,' kmol/m3',/,
     %  ' kg',T15,D15.5,' kmol/s...',T40,'% Vap. Resist.',
     %  T54,F15.3,' %')
      WRITE(LOUT,6011)(MONTH(J,IMONTH),J=1,2),IDAY,IYEAR,IFLOW,
     %  GAS(IGAS)
6011  FORMAT(' ',2A8,I3,', ',I5,' Flowrate : ',I3,' Gas : ',A8)
      WRITE(LOUT,6012)PCELL,PGAS,TCELL,QLIQ
6012  FORMAT(5D15.7)
      WRITE(LOUT,6012)TEEP
      WRITE(LOUT,6012)WT,CONC,VISCA,VISCK,DDENS
      WRITE(LOUT,6012)RS,DELTAP,DNOZ,JETLTH,TAKOFF
      WRITE(LOUT,6012)GAVG,GSPH,DGAS
      WRITE(LOUT,6012)CI,CIO,HCOEFF,XKG,RESIST
3004  CONTINUE
      IF(IEND.EQ.-9)GO TO 999
      GO TO 9000
C
C
999   CONTINUE
      WRITE(IOUT,2005)
2005  FORMAT(' Analysis Finished.')
      STOP
      END
C
C
C
      SUBROUTINE NEWPGE
      IMPLICIT REAL*8(A-H,O-Z)
      CHARACTER*4 TOD(2),DATE(3)
      CHARACTER*8 MONTH,FILE
      DIMENSION MONTH(2,12),FILE(3)
      COMMON/IO/IIN,IOUT,JIN,JOUT,LOUT
      COMMON/FNAME/FILE
      COMMON/DATES1/MONTH,TOD,DATE
      COMMON/DATES2/IYEAR,IMONTH,IDAY
```

```
      WRITE(JOUT,1000)
1000  FORMAT('1SPHERE ABSORBER DATA ANALYSIS PROGRAM I. ',45('-'),
     %' DETERMINATION OF MOLECULAR DIFFUSIVITY.')
      WRITE(JOUT,1001)TOD(1),TOD(2),(DATE(I),I=1,3),
     %(MONTH(J,IMONTH),J=1,2),IDAY,IYEAR,(FILE(K),K=1,3)
1001  FORMAT(' Analysis at ',2A4,' on ',3A4,10X,'Experiment on ',
     %2A8,I3,',',I5,10X,'Data File ',3A8,/)
      RETURN
      END
C
C
C
      REAL FUNCTION TCOUPL(ITC,EMF)
      IMPLICIT REAL*8(A-H,O-Z)
      DIMENSION ALPHA(7),BETA(7),GAMMA(7),DELTA(7)
      DATA ALPHA/-7.053D+00,-6.0775D+00,-5.346D+00,-7.6516D+00,
     %-6.7735D+00,-5.422D+00,-7.4650D+00/
      DATA BETA/-12.877D+00,-20.939D+00,-17.175D+00,
     %-14.987D+00,-18.078D+00,-15.800D+00,-15.3803D+00/
      DATA GAMMA/-2.039D+00,3.8254D+00,0.33D+00,-0.3151D+00,
     %1.685D+00,-0.768D+00,-0.4767D+00/
      DATA DELTA/0.7763D+00,-0.0603D+00,0.4408D+00,0.54015D+00,
     %0.2497D+00,0.6216D+00,0.53053D+00/
      EACTUL=EMF+0.0061D+00
      GCORR=ALPHA(ITC)+(BETA(ITC)+(GAMMA(ITC)+(DELTA(ITC)
     %*EACTUL))*EACTUL)*EACTUL
      GCORR=GCORR*1.D-03
      ESTD=EACTUL+GCORR
      ARG=-0.2902502066D+00+(17.31101383D+00+(0.74005336790-01
     %-0.48005343110-02*ESTD)*ESTD)*ESTD
      ARG=ARG+2.572484D+00/ESTD+4.377872676D+00*DLOG(ESTD)
      TCOUPL=ARG
      RETURN
      END
C
C
C
      SUBROUTINE ROTAM(TC,SCALE)
      IMPLICIT REAL*8(A-H,O-Z)
      COMMON/FLUID/QLIQ,DENS,VISCK,WT
      QLIQ=0.D+00
      IF(WT.LT.10.D+00)THEN
          ICORR=1
      ELSEIF(WT.LT.30.D+00)THEN
          ICORR=2
```

```
      ELSEIF(WT.LT.50.D+00)THEN
          ICORR=3
      ELSE
          RETURN
      ENDIF
C
      GO TO (4100,4200,4300),ICORR
C
C     Water at 25 deg C
C
4100  QLIQ=2.6342815D+00+(-2.7265972D-01+(1.2523934D-02
     %+(-2.6158035D-04+(2.6717540D-06+(-1.0727432D-08*SCALE))
     %*SCALE)*SCALE)*SCALE)*SCALE
      GO TO 5000
C
4200  CONTINUE
C
C     20 wt% MDEA
C
          Q25=1.0783276D-02+(9.4276038D-03+(3.1471087D-04
     %    +(-4.4149080D-06+(2.1782946D-08+(-2.5725522D-11*SCALE))
     %    *SCALE)*SCALE)*SCALE)*SCALE
C
          Q50=-5.3111207D-01+(5.9959681D-02+(-1.3958166D-03
     %    +(2.4778085D-05+(-2.2415571D-07+(7.8993462D-10*SCALE))
     %    *SCALE)*SCALE)*SCALE)*SCALE
C
          Q75=2.3821535D+00+(-2.4500919D-01+(1.1340119D-02
     %    +(-2.3437403D-04+(2.3589534D-06+(-9.3236513D-09*SCALE))
     %    *SCALE)*SCALE)*SCALE)*SCALE
C
      IF(TC.LE.25.D+00)THEN
          SLOPE=(Q50-Q25)/25.D+00
          QLIQ=Q25+SLOPE*(TC-25.D+00)
      ELSEIF(TC.LE.50.D+00)THEN
          SLOPE=(Q50-Q25)/25.D+00
          QLIQ=Q25+SLOPE*(TC-25.D+00)
      ELSEIF(TC.LE.75.D+00)THEN
          SLOPE=(Q75-Q50)/25.D+00
          QLIQ=Q50+SLOPE*(TC-50.D+00)
      ELSE
          SLOPE=(Q75-Q50)/25.D+00
          QLIQ=Q75+SLOPE*(TC-75.D+00)
      ENDIF
      GO TO 5000
```

```
C
4300  CONTINUE
C
C     40 wt% MDEA
C
      Q25=-0.44847841D+00+(1.9519216D-02+(1.6611137D-05
     %    +(-2.8227395D-06+(4.1090646D-08+(-1.8990185D-10*SCALE))
     %    *SCALE)*SCALE)*SCALE)*SCALE
C
      Q50=-0.38829569D+00+(1.9652628D-02+(3.01430180D-04
     %    +(-8.1713716D-06+(7.4494260D-08+(-2.3936380D-10*SCALE))
     %    *SCALE)*SCALE)*SCALE)*SCALE
C
      Q75=-0.49254667D+00+(3.7362110D-02+(-2.4709480D-04
     %    +(-7.1322431D-09+(1.7711812D-08+(-9.0328190D-11*SCALE))
     %    *SCALE)*SCALE)*SCALE)*SCALE
C
      IF(TC.LE.25.D+00)THEN
          SLOPE=(Q50-Q25)/25.D+00
          QLIQ=Q25+SLOPE*(TC-25.D+00)
      ELSEIF(TC.LE.50.D+00)THEN
          SLOPE=(Q50-Q25)/25.D+00
          QLIQ=Q25+SLOPE*(TC-25.D+00)
      ELSEIF(TC.LE.75.D+00)THEN
          SLOPE=(Q75-Q50)/25.D+00
          QLIQ=Q50+SLOPE*(TC-50.D+00)
      ELSE
          SLOPE=(Q75-Q50)/25.D+00
          QLIQ=Q75+SLOPE*(TC-75.D+00)
      ENDIF
      GO TO 5000
C
5000  QLIQ=QLIQ*1.D-06/DENS
      RETURN
      END
C
C
C
      SUBROUTINE DENSL(TC)
      IMPLICIT REAL*8(A-H,O-Z)
      DIMENSION A0(6),A1(6),A2(6),A3(6),A4(6),A5(6),PCT(6)
      COMMON/FLUID/QLIQ,DENS,VISCK,WT
      DATA A0/1.000244355D+00,1.0142473D+00,1.0256906D+00,
     %    1.0322227D+00,1.0459222D+00,1.0654460D+00/
      DATA A1/1.941636116D-05,-0.45772313D-03,-0.49424711D-03,
```

```
     %     -0.87288832D-04,-0.48270445D-03,-0.14362947D-02/
      DATA A2/-6.543792186D-06,0.11991943D-04,0.12315728D-04,
     %     -0.35201506D-05,0.11723010D-04,0.38224393D-04/
      DATA A3/2.984752134D-08,-0.25297787D-06,-0.32490784D-06,
     %     -0.10930976D-06,-0.49096279D-06,-0.83590164D-06/
      DATA A4/-8.223252092D-11,0.12746992D-08,0.27845152D-08,
     %     0.17230108D-08,0.64039493D-08,0.83860837D-08/
      DATA A5/0.D+00,0.20084018D-12,-0.83167968D-11,
     %     -0.74705420D-11,-0.28690296D-10,-0.32315523D-10/
      DATA PCT/0.D+00,10.D+00,20.D+00,30.D+00,40.D+00,50.D+00/
C
      DO 10 I=2,6
          IHI=I
          IF(WT.LE.PCT(I))THEN
              ILO=IHI-1
              GO TO 30
          ENDIF
10    CONTINUE
      IHI=6
      ILO=5
C
30    CONTINUE
      XHI=A0(IHI)+(A1(IHI)+(A2(IHI)+(A3(IHI)+(A4(IHI)+A5(IHI)*TC)*
     %     TC)*TC)*TC)*TC
      XLO=A0(ILO)+(A1(ILO)+(A2(ILO)+(A3(ILO)+(A4(ILO)+A5(ILO)*TC)*
     %     TC)*TC)*TC)*TC
      DENS=XLO+((XHI-XLO)/(PCT(IHI)-PCT(ILO)))*(WT-PCT(ILO))
C
      RETURN
      END
C
C
C
      SUBROUTINE KINVSC(TC)
      IMPLICIT REAL*8(A-H,O-Z)
      DIMENSION AK(6),BK(6),CK(6),PCT(6)
      COMMON/FLUID/QLIQ,DENS,VISCK,WT
      DATA AK/0.6641D+00,1.6001D+00,2.6484D+00,2.217D+00,
     %1.5084D+00,2.7418D+00/
      DATA BK/-2549.5D+00,-3183.1D+00,-3920.3D+00,-3762.1D+00,
     %-3404.2D+00,-4344.8D+00/
      DATA CK/691053.D+00,828076.D+00,990917.D+00,
     %1024841.D+00,1026178.D+00,1247827.D+00/
      DATA PCT/0.D+00,10.D+00,19.994D+00,29.993D+00,40.01D+00,
     %49.998D+00/
```

```
C
      DO 10 I=2,6
          IHI=I
          IF(WT.LE.PCT(I))THEN
              ILO=IHI-1
              GO TO 30
          ENDIF
10    CONTINUE
      IHI=6
      ILO=5
C
30    CONTINUE
      T=TC+273.15D+00
      XHI=AK(IHI)+(BK(IHI)/T)+(CK(IHI)/(T*T))
      XLO=AK(ILO)+(BK(ILO)/T)+(CK(ILO)/(T*T))
      XMID=XLO+((XHI-XLO)/(PCT(IHI)-PCT(ILO)))*(WT-PCT(ILO))
      VISCK=DEXP(XMID)*1.D-06
C
      RETURN
      END
C
C
C
      SUBROUTINE HENRY(IGAS,TC,HCOEFF)
      IMPLICIT REAL*8(A-H,O-Z)
      DIMENSION AH(3),BH(3),CH(3),PCT(3)
      COMMON/FLUID/QLIQ,DENS,VISCK,WT
      DATA AH/31.6847D+00,28.747D+00,27.8522D+00/
      DATA BH/-0.301286D-01,-0.27413D-01,-0.27812D-01/
      DATA CH/-5149.67D+00,-4535.4D+00,-4263.8D+00/
      DATA PCT/0.D+00,20.D+00,40.D+00/
C
      TK=TC+273.15D+00
      DUMD=DENS
      DUMWT=WT
      WT=0.D+00
      CALL DENSL(TC)
      DENS0=DENS
      WT=20.D+00
      CALL DENSL(TC)
      DENS20=DENS
      WT=40.D+00
      CALL DENSL(TC)
      DENS40=DENS
      HON20=18.018D+00*DEXP(AH(1)+BH(1)*TK+CH(1)/TK)/DENS0
```

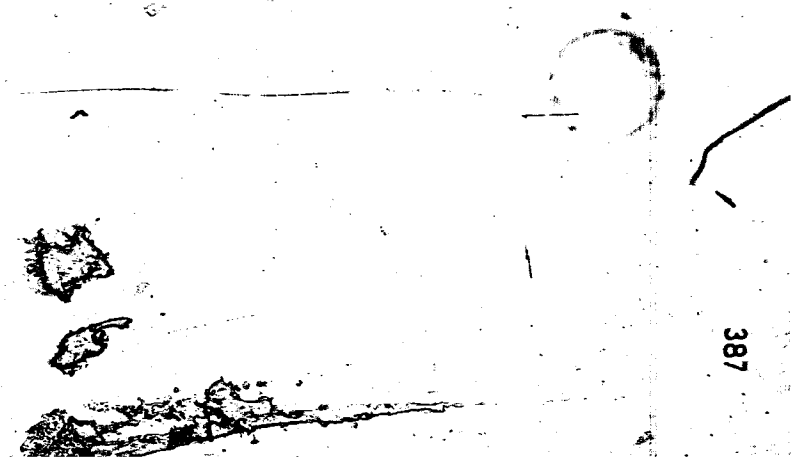

```
C
      IF(DUMWT.LE.20.D+00)THEN
     &    H2ON20=21.70218053D+00*DEXP(AH(2)+BH(2)*TK+CH(2)/TK)/DENS20
          SLOPE=(DLOG(H2ON20)-DLOG(HON20))/(20.D+00-0.D+00)
          HN20=DEXP(DLOG(HON20)+SLOPE*(DUMWT-0.D+00))
      ELSEIF(DUMWT.LE.40.D+00)THEN
          H2ON20=21.70218053D+00*DEXP(AH(2)+BH(2)*TK+CH(2)/TK)/DENS20
          H4ON20=27.28022976D+00*DEXP(AH(3)+BH(3)*TK+CH(3)/TK)/DENS40
          SLOPE=(DLOG(H4ON20)-DLOG(H2ON20))/(40.D+00-20.D+00)
          HN20=DEXP(DLOG(H2ON20)+SLOPE*(DUMWT-20.D+00))
      ELSE
          H2ON20=21.70218053D+00*DEXP(AH(2)+BH(2)*TK+CH(2)/TK)/DENS20
          H4ON20=27.28022976D+00*DEXP(AH(3)+BH(3)*TK+CH(3)/TK)/DENS40
          SLOPE=(DLOG(H4ON20)-DLOG(H2ON20))/(40.D+00-20.D+00)
          HN20=DEXP(DLOG(H2ON20)+SLOPE*(DUMWT-20.D+00))
      ENDIF
C
      IF(IGAS.EQ.1)THEN
          HCOEFF=HN20
          WT=DUMWT
          DENS=DUMD
          RETURN
      ELSE
C
C     Henry's constant correlation from Mason and Kao (1980)
C     Units are atm/molality
C
          TRED=TK/100.D+00
          TRED2=TRED*TRED
          HOCO2=3.822D+00-7.8665D-04*DEXP(TRED)
     %         -0.04145D+00*TRED2-17.457D+00/TRED2
          HOCO2=101.325D+00*(10.D+00**HOCO2)/DENSO
          HCO2=HOCO2*(HN20/HON20)
          HCOEFF=HCO2
          WT=DUMWT
          DENS=DUMD
          RETURN
      ENDIF
      RETURN
      END
```

```
C
C
C
      SUBROUTINE ABSORB(DGAS,GCALC)
      IMPLICIT REAL*8(A-H,O-Z)
      DIMENSION B(10),BETA(10)
      COMMON/NUMB/PI,GRAVTY,E1,E2,E3,E4,E5,R
      COMMON/EQUIP/RS
      COMMON/FLUID/QLIQ,DENS,VISCK,WT
      COMMON/SERIES/B,BETA
      COMMON/CONC/CI,CO
C
      FACTOR=QLIQ*(CI-CO)
      ALPHA=3.36525D+00*PI
     %     *(2.D+00*PI*GRAVTY/(3.D+00*VISCK))**E3
     %     *(RS**E4)*(QLIQ**E5)*DGAS
      GCALC=FACTOR
      DO 3007 JTERM=1,10
          GCALC=GCALC-FACTOR*B(JTERM)*DEXP(-BETA(JTERM)*ALPHA)
3007  CONTINUE
      RETURN
      END
C
C
C
      SUBROUTINE CELLP(TCELL,PCELL,XW,PGAS)
      IMPLICIT REAL*8(A-H,O-Z)
          TK=TCELL+273.16D+00
          TR=647.27D+00-TK
          SAVE1=(TR*TR*1.1702379D-08+5.86826D-03)*TR+3.2437814D+00
          SAVE1=SAVE1*TR/(TK*(1.D+00+2.1878462D-03*TR))
          PWATER=10.D+00**SAVE1
          PWATER=(218.167D+00/PWATER)*101.325D+00
      PWATER=XW*PWATER
      PGAS=PCELL-PWATER
      RETURN
      END
C
C
C
      SUBROUTINE MOLEFC(XWATER)
      IMPLICIT REAL*8(A-H,O-Z)
      COMMON/FLUID/QLIQ,DENS,VISCK,WT
      XA=WT/119.17D+00
      XW=(100.D+00-WT)/18.018D+00
```

```
      XWATER=XW/(XA+XW)
      RETURN
      END
C
C
C
      SUBROUTINE AKG(IRES,IGAS,TCELL,PCELL,PGAS,XKG)
      IMPLICIT REAL*8(A-H,O-Z)
      DIMENSION SIG(3),EOK(3),XM(3)
      COMMON/NUMB/PI,GRAVTY,E1,E2,E3,E4,E5,R
      COMMON/EQUIP/RS
      DATA SIG/3.828D+00,3.941D+00,2.641D+00/
      DATA EOK/232.4D+00,195.2D+00,809.1D+00/
      DATA XM/44.013D+00,44.01D+00,18.018D+00/
C
      IF(IRES.EQ.1)THEN
          SIGMA=(SIG(IGAS)+SIG(3))*0.5D+00
          EK=DSQRT(EOK(IGAS)*EOK(3))
          TK=TCELL+273.15D+00
          TSTAR=TK/EK
          OMEGAD=(1.06036D+00/(TSTAR**0.15610D+00)) +
     %        (0.19300D+00/DEXP(0.47635D+00*TSTAR)) +
     %        (1.03587D+00/DEXP(1.52996D+00*TSTAR)) +
     %        (1.76474D+00/DEXP(3.89411D+00*TSTAR))
          FACTOR=DSQRT((XM(IGAS)+XM(3))/(XM(IGAS)*XM(3)))
          FACT2=0.00217D+00-0.00050D+00*FACTOR
          DAB=FACT2*(TK**1.5D+00)*FACTOR*1.D-04
          DAB=DAB*101.325D+00/(PCELL*SIGMA*SIGMA*OMEGAD)
C
          TSTAR=TK/EOK(IGAS)
          OMEGAV=(1.16145D+00/(TSTAR**0.14874D+00)) +
     %        (0.52487D+00/DEXP(0.77320D+00*TSTAR)) +
     %        (2.16178D+00/DEXP(2.43787D+00*TSTAR))
          VISC1=26.69D-07*DSQRT(XM(IGAS)*TK)
          VISC1=VISC1/(SIG(IGAS)*SIG(IGAS)*OMEGAV)
          TSTAR=TK/EOK(3)
          OMEGAV=(1.16145D+00/(TSTAR**0.14874D+00)) +
     %        (0.52487D+00/DEXP(0.77320D+00*TSTAR)) +
     %        (2.16178D+00/DEXP(2.43787D+00*TSTAR))
          VISC2=26.69D-07*DSQRT(XM(3)*TK)
          VISC2=VISC2/(SIG(3)*SIG(3)*OMEGAV)
          Y1=PGAS/PCELL
          Y2=1.D+00-Y1
          PAR1=VISC1/VISC2
          PAR2=XM(IGAS)/XM(3)
```

```
      PHI12=(1.D+00+(PAR1**0.5D+00)/(PAR2**0.25D+00))**2
      PHI12=PHI12/DSQRT(8.D+00*(1.D+00+PAR2))
      PHI21=PHI12*PAR2/PAR1
      VISC=Y1*VISC1/(Y1+Y2*PHI12)+Y2*VISC2/(Y2+Y1*PHI21)
      VELG=8.7D-03
      WT=Y1*XM(IGAS)+Y2*XM(3)
      RHOG=WT*PCELL/(R*TK)
      SCG=VISC/(RHOG*DAB)
      REG=2.D+00*RHOG*VELG*RS/VISC
      SHG=2.D+00+0.556D+00*DSQRT(REG)*(SCG**0.3333333333D+00)
C
      XKG=SHG*DAB/(2.D+00*R*TK*RS)
      RETURN
    ELSE
      XKG=1.D+20
      RETURN
    ENDIF
    RETURN
    END
C
C
C
    SUBROUTINE AKL(DNOZ,JETLTH,GAVG,HCOEFF,PGAS,XKG,RESIST)
    IMPLICIT REAL*8(A-H,O-Z)
    REAL*8 JETLTH
    COMMON/NUMB/PI,GRAVTY,E1,E2,E3,E4,E5,R
    COMMON/EQUIP/RS
    COMMON/FLUID/QLIQ,DENS,VISCK,WT
    COMMON/CONC/CI,CO
    DELTAP=(3.D+00*QLIQ*VISCK/(2.D+00*PI*RS*GRAVTY))**E3
    ACORR=1.D+00+(2.58712D+00*DELTAP/RS)
    AREA=PI*(DNOZ*JETLTH+4.D+00*RS*RS*ACORR)
    CAPKL=GAVG/(AREA*(PGAS/HCOEFF))
    XKL=1.D+00/((1.D+00/CAPKL)-(1.D+00/(HCOEFF*XKG)))
    RESIST=100.D+00*CAPKL/(HCOEFF*XKG)
    CI=(XKG*PGAS+XKL*CO)/(XKL+HCOEFF*XKG)
    RETURN
    END
```

```
C
C
C
      BLOCK DATA
      IMPLICIT REAL*8(A-H,O-Z)
      CHARACTER*4 TOD(2),DATE(3)
      CHARACTER*8 MONTH,FILE
      DIMENSION MONTH(2,12),FILE(3),B(10),BETA(10)
      COMMON/IO/IIN,IOUT,JIN,JOUT,LOUT
      COMMON/FNAME/FILE
      COMMON/DATES1/MONTH,TOD,DATE
      COMMON/DATES2/IYEAR,IMONTH,IDAY
      COMMON/NUMB/PI,GRAVTY,E1,E2,E3,E4,E5,R
      COMMON/EQUIP/RS
      COMMON/FLUID/QLIQ,DENS,VISCK,WT
      COMMON/SERIES/B,BETA
      COMMON/CONC/CI,CO
      DATA MONTH/'January ','        ','February','
     %     'March   ','        ','April   ','        ',
     %     'May     ','        ','June    ','        ',
     %     'July    ','        ','August  ','        ',
     %     'Septembe','r       ','October ','        ',
     %     'November','        ','December','        '/
      DATA B/0.7897026D+00,0.09725511D+00,0.03609362D+00,
     %0.01868637D+00,0.011401760D+00,0.007675970D+00,
     %0.005517943D+00,0.004157034D+00,0.003243974D+00,
     %0.002601795D+00/
      DATA BETA/3.414446D+00,26.440559D+00,70.832821D+00,
     %136.57071D+00,223.64880D+00,332.06472D+00,
     %421.81720D+00,612.90545D+00,785.32896D+00,
     %979.08735D+00/
      DATA IIN,IOUT,JIN,JOUT,LOUT/5,6,7,8,10/
      DATA GRAVTY/9.80665D+00/,PI/3.141592653589793D+00/
      DATA R/8.31434D+00/,RS/0.0254D+00/
      END
```

```
C PROGRAM 2
C
C     Program to determine the second-order reaction rate
C      constant using experimental data from the sphere absorber
C
C
      IMPLICIT REAL*8(A-H,O-Z)
      CHARACTER*4 TOD(2),DATE(3)
      CHARACTER*8 MONTH,BLANK,GAS,FILE,COMMNT
      CHARACTER*1 NO,NO2,NOTE,SPACE,STAR,IANS
      REAL*8 JETLTH,K1,M,KTMAX,JETF1,JETF2,KOLD,KLOW,KHI
      REAL*8 KW,KP,KOH,KAPP,K2
      DIMENSION G(20)
      DIMENSION FLOW(5),TCS(7,5),TCF(7,5),TIMES(5),TIMEF(5)
      DIMENSION SWVOL(20,5),SWTIM(20,5),MEAS(5),GAS(2)
      DIMENSION COMMNT(10,10),MONTH(2,12),FILE(3)
      DIMENSION TEMPS(7),TEMPF(7),TEMPA(7)
      LOGICAL FLAG
      COMMON/IO/IIN,IOUT,JIN,JOUT,LOUT
      COMMON/FNAME/FILE
      COMMON/DATES1/MONTH,TOD,DATE
      COMMON/DATES2/IYEAR,IMONTH,IDAY
      COMMON/NUMB/PI,GRAVTY,E1,E2,E3,E4,E5,R
      COMMON/FLUID/QLIQ,DENS,VISCK,WT
      COMMON/CONC/CI,CO,CIO
      COMMON/EQUIP/RS
      COMMON/VAPOR/DGAS
      COMMON/HYDRO/DELTAP,KTMAX,TMAX
      DATA BLANK/'        '/,NO/'N'/,NO2/'n'/
      DATA GAS/'N2O     ','CO2     '/
      DATA SPACE/' '/,STAR/'*'/
C
      CALL TIME(0)
      CALL TIME(4,O,TOD)
      CALL TIME(5,O,DATE)
C
      KIN=9
C
      E1=1.D+00/6.D+00
      E2=7.D+00/6.D+00
      E3=1.D+00/3.D+00
      E4=7.D+00/3.D+00
      E5=-4.D+00/3.D+00
      FLAG=.FALSE.
      DIAM=50.8D-03
```

```
C
      DO 100 J=1,10
      DO 100 I=1,10
         COMMNT(I,J)=BLANK
100   CONTINUE
      READ(KIN,1009)(FILE(I),I=1,3)
1009  FORMAT(1X,9A8)
      IRES=1
      WRITE(IOUT,2004)
2004  FORMAT(' Analysis for Kinetic Rate Constant Begins...')
C
C
C
C
9000  READ(JIN,1000)IROUTE
1000  FORMAT(20I5)
      READ(JIN,1001)OPNAME
1001  FORMAT(10A8)
      READ(JIN,1000)IYEAR,IMONTH,IDAY,IGAS,ITUBE,ICOMM
      READ(JIN,1002)WT,TEEP,PIPER
      READ(JIN,1002)DNOZ,PBARO,TROOM
      READ(JIN,1002)CELLPR,CELLPL
      READ(JIN,1002)HJET,HNORTH,HSOUTH,HTAKE
      READ(JIN,1002)COARSE,FINE,VFEED,VCIRC
      READ(JIN,1000)NFLOW
      DO 1005 J=1,NFLOW
         READ(JIN,1002)FLOW(J)
         READ(JIN,1000)NMEAS
         MEAS(J)=NMEAS
         READ(JIN,1002)(SWVOL(I,J),I=1,NMEAS)
         READ(JIN,1002)(SWTIM(I,J),I=1,NMEAS)
         READ(JIN,1006)(TCS(I,J),I=1,7)
         READ(JIN,1006)(TCF(I,J),I=1,7)
         READ(JIN,1001)TIMES(J),TIMEF(J)
1005  CONTINUE
      IF(ICOMM.EQ.1)THEN
         DO 1008 J=1,10
            READ(JIN,1001)(COMMNT(I,J),I=1,10)
1008     CONTINUE
1002     FORMAT(5F15.6)
1006     FORMAT(7F10.6)
      ENDIF
1007  READ(JIN,1000)IEND
C
C
```

```
      CALL NEWPGE
      WRITE(JOUT,2000)
2000  FORMAT(/////,' Comments :',//)
      IF(ICOMM.EQ.0)THEN
          WRITE(JOUT,2002)
2002      FORMAT(' None.')
      ELSE
          DO 2003 J=1,10
              WRITE(JOUT,1001)(COMMNT(I,J),I=1,10)
2003      CONTINUE
      ENDIF
C
C
3000  CONTINUE
      CALL NEWPGE
      WRITE(JOUT,2006)
2006  FORMAT(/,' Echo of Raw Experimental Data.',//)
      WRITE(JOUT,2007)WT
2007  FORMAT(' Amine Concentration (wt % MDEA)',T50,F15.4)
      WRITE(JOUT,2008)TEEP
2008  FORMAT(' Surfactant Concentration (wt % SLS "Teepol")',
     %T50,F15.4)
      WRITE(JOUT,2050)PIPER
2050  FORMAT(' Promoter Concentration (kmol/m3 Piperazine)',
     %T50,F15.4)
      WRITE(JOUT,2009)GAS(IGAS)
2009  FORMAT(' Absorbing Gas',T57,A8)
      WRITE(JOUT,2010)OPNAME
2010  FORMAT(' Process Operator',T57,A8)
      WRITE(JOUT,2011)
2011  FORMAT(//)
      WRITE(JOUT,2012)PBARO
2012  FORMAT(' Atmospheric Pressure (mm Hg)',T50,F15.4)
      WRITE(JOUT,2013)TROOM
2013  FORMAT(' Atmospheric Temperature (deg C)',T50,F15.4)
      WRITE(JOUT,2011)
      WRITE(JOUT,2014)ITUBE
2014  FORMAT(' Rotameter Tube #',T50,I15)
      WRITE(JOUT,2015)DNOZ
2015  FORMAT(' Jet Nozzle Throat Diameter (mm)',T50,F15.4)
      WRITE(JOUT,2011)
      WRITE(JOUT,2016)CELLPR
2016  FORMAT(' Cell Pressure Manometer Right Leg (in. H2O)',
     %T50,F15.4)
      WRITE(JOUT,2017)CELLPL
```

```
 Cell Pressure Manometer Left Leg  (in. H2O)',
1)
JT,2011)
JT,2018)HJET
 Jet Nozzle Elevation (cm)',T50,F15.4)
JT,2019)HNORTH
 Sphere North Pole Elevation (cm)',T50,F15.4)
JT,2020)HSOUTH
 Sphere South Pole Elevation (cm)',T50,F15.4)
JT,2021)HTAKE
 Liquid Take-off Elevation (cm)',T50,F15.4)
JT,2011)
JT,2022)COARSE
 Thermotrol Coarse Setting',T50,F15.4)
JT,2023)FINE
 Thermotrol Fine Setting',T50,F15.4)
JT,2024)VFEED
 Amine Feed Preheater Variac Setting',T50,F15.4)
JT,2025)VCIRC
 Amine Circulation Heater Variac Setting',T50,F15.4)
JT,2011)

HJET-HNORTH)*0.01D+00
Z*1.D-03
HSOUTH-HTAKE)*0.01D+00
F.LT.0.02D+00)WRITE(JOUT,2035)TAKOFF
,' **** Take-off length is ',F8.5,' m',/,
tagnant layer may affect the absorption rate.',//)

BARO/760.D+00)*101.325D+00
ELLPR+CELLPL)*0.24848D+00
ARO+PMANO


IFLOW=1,NFLOW
S=MEAS(IFLOW)
 NEWPGE
E(JOUT,2006)
E(JOUT,2026)IFLOW
AT(' These data are for amine flow rate ',I3)
E(JOUT,2011)
E(JOUT,2027)FLOW(IFLOW)
AT(' Rotameter Scale Reading (mm)',T50,F15.4)
E(JOUT,2011)
E(JOUT,2028)TIMES(IFLOW)
```

```
2028      FORMAT(' Start Time (HH:MM)',T60,2A8)
          WRITE(JOUT,2029)TIMEF(IFLOW)
2029      FORMAT(' End Time   (HH:MM)',T60,2A8)
          WRITE(JOUT,2011)
          WRITE(JOUT,2030)
2030      FORMAT(5X,'Measurement',5X,'Sweep Volume (mL)',5X,
     %    'Sweep Time (s)',/,1X,60('-'),/)
          DO 3002 IMEAS=1,NMEAS
              WRITE(JOUT,2031)IMEAS,SWVOL(IMEAS,IFLOW),
     %        SWTIM(IMEAS,IFLOW)
2031          FORMAT(5X,I5,14X,F7.2,14X,F8.2)
3002      CONTINUE
          WRITE(JOUT,2032)
2032      FORMAT(/,1X,60('-'))
          WRITE(JOUT,2011)
          WRITE(JOUT,2033)
2033      FORMAT(' Thermocouple Readings (mV)',/,4X,'T/C',4X,
     %    'Start',6X,'End',/,1X,60('-'),/)
          DO 3003 IC=1,7
              WRITE(JOUT,2034)IC,TCS(IC,IFLOW),TCF(IC,IFLOW)
2034          FORMAT(1X,I5,2F10.3)
3003      CONTINUE
          WRITE(JOUT,2032)
3001  CONTINUE
C
      CALL MOLEFC(XW)
      DO 3004 IFLOW=1,NFLOW
          WRITE(IOUT,2049)IFLOW
2049      FORMAT('      Calculations for Flow Rate ',I3,' Begin...')
          NMEAS=MEAS(IFLOW)
          CALL NEWPGE
          WRITE(JOUT,2026)IFLOW
          DO 3005 IC=1,7
              TEMPS(IC)=TCOUPL(IC,TCS(IC,IFLOW))
              TEMPF(IC)=TCOUPL(IC,TCF(IC,IFLOW))
              TEMPA(IC)=(TEMPS(IC)+TEMPF(IC))*0.5D+00
3005      CONTINUE
          TCELL=(TEMPA(1)+TEMPA(2))*0.5D+00
C
          CALL DENSL(TCELL)
          CONC=10.D+00*WT*DENS/119.17D+00
          CALL CELLP(TCELL,PCELL,XW,PGAS)
          CALL HENRY(IGAS,TCELL,HCOEFF)
          CALL AKG(IRES,IGAS,TCELL,PCELL,PGAS,XKG)
          CALL KINVSC(TCELL)
```

```
      CALL DIFF(IGAS,TCELL)
      VISCA=VISCK*DENS*1.D+03
      DDENS=DENS*1.D+03
      GAVG=0.D+00
      DO 3006 IMEAS=1,NMEAS
         G(IMEAS)=(PCELL*SWVOL(IMEAS,IFLOW)*1.D-06)/
     %      (R*(TEMPA(3)+273.15D+00)*SWTIM(IMEAS,IFLOW))
         GAVG=GAVG+G(IMEAS)
3006  CONTINUE
      GAVG=GAVG/DBLE(FLOAT(NMEAS))
      CALL ROTAM(TCELL,FLOW(IFLOW))
      CALL AKL(DNOZ,JETLTH,GAVG,HCOEFF,PGAS,XKG,RESIST)
      PCSAT=GAVG*100.D+00/(QLIQ*CI)
      RES=2.D+00*QLIQ/(PI*RS*VISCK)
      REJ=4.D+00*QLIQ/(PI*DNOZ*VISCK)
C
      CIO=0.D+00
      CO=0.D+00
      KOLD=0.D+00
      ERRORK=0.D+00
      JTERK=0
C
      DELTAP=(3.D+00*QLIQ*VISCK/(2.D+00*PI*RS*GRAVTY))**E3
      ACORR=1.D+00+(2.58712D+00*DELTAP/RS)
      TMAX=(4.D+00*PI*RS*RS/3.D+00)*(2.58712D+00*DELTAP/QLIQ)
      TIMJET=PI*DNOZ*DNOZ*JETLTH/(4.D+00*QLIQ)
      GJET=4.D+00*(CI-CIO)*DSQRT(JETLTH*QLIQ*DGAS)
      GSPH=GAVG-GJET
C
3010  GSPH=GSPH/ACORR
C
      ITERK=0
      KLOW=0.1D+00
      KHI=1000.D+00
      CALL ABSORB(KLOW,GCALC)
      F1=GSPH-GCALC
      CALL ABSORB(KHI,GCALC)
      F2=GSPH-GCALC
3008  CONTINUE
      IF(ITERK.GT.50)THEN
         WRITE(JOUT,6009)
6009     FORMAT(/,' ** More than 50 iterations required',
     %        ' for the inner loop **')
         GO TO 3012
      ENDIF
```

```
      ITERK=ITERK+1
      K1=0.5D+00*(KHI+KLOW)
      DELTAK=KHI-KLOW
      IF((DABS(DELTAK)/K1).LT.1.D-05)GO TO 3009
      CALL ABSORB(K1,GCALC)
      FUNC=GSPH-GCALC
      FSIGN=FUNC*F1
      IF(FSIGN.LT.0.D+00)THEN
          KHI=K1
          F2=FUNC
      ELSE
          KLOW=K1
          F1=FUNC
      ENDIF
      GO TO 3008
3009  GJET=4.D+00*(CI-CIO)*DSQRT(JETLTH*QLIQ*DGAS)*
     %  (1.D+00+K1*TIMJET/3.D+00)
      GSPH=GAVG-GJET
      JTERK=JTERK+1
C
      IF(JTERK.EQ.1)GO TO 3010
      IF(JTERK.GT.25)THEN
          WRITE(JOUT,6010)
6010      FORMAT(/,' ** More than 25 iterations required',
     %           ' for the outer loop **')
          GO TO 3012
      ENDIF
      ERRORK=DABS(K1-KOLD)/K1
      IF(ERRORK.LT.1.D-04)GO TO 3012
      KOLD=K1
      GO TO 3010
C
3012  CONTINUE
      RATIO=(1.D+00+CONC/CI)/DSQRT(KTMAX)
      ALFO=0.03D+00
      CO2IN=ALFO*CONC*QLIQ
      CO2ADD=GAVG/2.D+00
      ALF=(CO2IN+CO2ADD)/(CONC*QLIQ)
      FREEAM=CONC*(1.D+00-ALF)
      TKCELL=TCELL+273.15D+00
      KW=10.D+00**(31286.D+00/TKCELL+94.9734D+00*DLOG(TKCELL)
     %  -0.097611D+00*TKCELL-2170870.D+00/(TKCELL**2)-606.522D+00)
      KP=10.D+00**(-14.01D+00+0.0184D+00*TKCELL)
      KOH=10.D+00**(13.635D+00-2895.D+00/TKCELL)
      OH=KW*(1.D+00-ALF)/(KP*ALF)
```

```
      ZKOH=KOH*OH
      KAPP=K1-ZKOH
      K2=KAPP/FREEAM
      WRITE(JOUT,6004)PCELL,GAS(IGAS),PGAS,TCELL,QLIQ
6004  FORMAT(/,5X,'------Absorber Conditions------',/,
     %  ' Total P',T15,F15.2,
     %  ' kPa',T40,'P',A8,T54,F15.2,' kPa',/,' Temperature',T15,
     %  F15.2,' deg C',T40,'Liquid Flow',T54,D15.5,' m3/s')
      WRITE(JOUT,6005)WT,CONC,VISCA,VISCK,DDENS
6005  FORMAT(5X,'------Fluid Properties------',/,
     %  ' Wt % Amine',T15,F15.2,
     %  T40,'Amine Conc.',T54,F15.3,' kmol/m3',/,' Viscosity',
     %  T15,E15.5,' kg/m-s',T40,'Viscosity',T54,E15.5,' m2/s',/,
     %  ' Density',T15,F15.3,' kg/m3')
      WRITE(JOUT,6006)DIAM,DELTAP,RES,REJ,DNOZ,JETLTH,TAKOFF
6006  FORMAT(5X,'------Sphere Data------',/,
     %  ' Diameter',T15,F15.5,' m',T40,'Film Thick.',T54,D15.5,' m',
     %  /,' Sphere Re',T15,F15.2,T40,'Jet Re',T54,F15.2,/,
     %  ' Jet Diameter',T15,D15.4,' m',T40,'Jet Length',
     %  T54,D15.5,' m',/,' Take-off',T15,F15.5,' m')
      WRITE(JOUT,6007)JTERK,GSPH,GJET,GAVG,K1,ERRORK,
     %  CI,HCOEFF,PCSAT,CIO,CO,DGAS,KTMAX,RATIO,XKG,RESIST
6007  FORMAT(5X,'------Absorption Data------',/,
     %  ' After ',I4,' iterations :',/,' Sphere Rate',T15,
     %  D15.5,' kmol/s',T40,'Jet Rate',T54,D15.5,' kmol/s',/,
     %  ' Measured Rate',T15,D15.5,' kmol/s',/,
     %  ' Predicted k',T15,F15.7,' s-1',T40,'Error',T54,F15.5,' %',
     %  /,' Int. Conc.',T15,F15.7,' kmol/m3',T40,'Henry''s Const.',
     %  T54,F15.3,' kPa-m3/kmol',/,
     %  ' Saturation',T15,F15.3,' %',/,' Jet Inlet',T15,F15.7,
     %  ' kmol/m3',T40,'Sphere Inlet',T54,F15.7,' kmol/m3',/,
     %  ' D',T15,D15.5,' m2/s',/,' k-tmax',T15,F15.7,T40,
     %  'Ratio',T54,F15.7,/,
     %  ' kg',T15,D15.5,' kmol/s...',T40,'% Vap. Resist.',
     %  T54,F15.3,' %')
      WRITE(JOUT,6013)ALF,FREEAM,OH,ZKOH,KAPP,K2
6013  FORMAT(' Avg. Loading',T15,F15.5,' mol/mol',T40,
     %  'Free Amine',T54,F15.3,' kmol/m3',/,
     %  ' OH- Conc.',T15,D15.5,' kmol/m3',T40,'kOH(OH-)',
     %  T54,F15.7,' s-1',/,' kapp',T15,F15.7,' s-1',
     %  T40,'k2',T54,F15.7,' m3/kmol-s')
      WRITE(JOUT,6008)
6008  FORMAT(/,' Ratio = (1+bo/Ci)/SQRT(k-tmax)')
      WRITE(LOUT,6011)(MONTH(J,IMONTH),J=1,2),IDAY,IYEAR,IFLOW,
     %  GAS(IGAS)
```

```
6011      FORMAT(' ',2A8,I3,', ',I5,' Flowrate : ',I3,' Gas : ',A8)
          WRITE(LOUT,6012)PCELL,PGAS,TCELL,QLIQ
6012      FORMAT(5D15.7)
          WRITE(LOUT,6012)TEEP,PIPER
          WRITE(LOUT,6012)WT,CONC,VISCA,VISCK,DDENS
          WRITE(LOUT,6012)RS,DELTAP,DNOZ,JETLTH,TAKOFF
          WRITE(LOUT,6012)GAVG,GSPH,DGAS,K1,KTMAX
          WRITE(LOUT,6012)CI,CIO,HCOEFF,XKG,RESIST
          WRITE(LOUT,6012)ALF,FREEAM,OH,ZKOH,KAPP
          WRITE(LOUT,6012)K2
3004  CONTINUE
      IF(IEND.EQ.-9)GO TO 999
      GO TO 9000
C
C
999   CONTINUE
      WRITE(IOUT,2005)
2005  FORMAT(' Analysis Finished.')
      STOP
      END
C
C
C
      SUBROUTINE NEWPGE
      IMPLICIT REAL*8(A-H,O-Z)
      CHARACTER*4 TOD(2),DATE(3)
      CHARACTER*8 MONTH,FILE
      DIMENSION MONTH(2,12),FILE(3)
      COMMON/IO/IIN,IOUT,JIN,JOUT,LOUT
      COMMON/FNAME/FILE
      COMMON/DATES1/MONTH,TOD,DATE
      COMMON/DATES2/IYEAR,IMONTH,IDAY
      WRITE(JOUT,1000)
1000  FORMAT('1SPHERE ABSORBER DATA ANALYSIS PROGRAM II. ',44('-'),
     %' DETERMINATION OF KINETIC RATE CONSTANT ')
      WRITE(JOUT,1001)TOD(1),TOD(2),(DATE(I),I=1,3),
     %(MONTH(J,IMONTH),J=1,2),IDAY,IYEAR,(FILE(K),K=1,3)
1001  FORMAT(' Analysis at ',2A4,' on ',3A4,10X,'Experiment on ',
     %2A8,I3,',',I5,10X,'Data File ',3A8,/)
      RETURN
      END
```

```
C
C
C
      REAL FUNCTION TCOUPL(ITC,EMF)
      IMPLICIT REAL*8(A-H,O-Z)
      DIMENSION ALPHA(7),BETA(7),GAMMA(7),DELTA(7)
      DATA ALPHA/-7.053D+00,-6.0775D+00,-5.346D+00,-7.6516D+00,
     %-6.7735D+00,-5.422D+00,-7.4650D+00/
      DATA BETA/-12.877D+00,-20.939D+00,-17.175D+00,
     %-14.987D+00,-18.078D+00,-15.800D+00,-15.3803D+00/
      DATA GAMMA/-2.039D+00,3.8254D+00,0.33D+00,-0.3151D+00,
     %1.685D+00,-0.768D+00,-0.4767D+00/
      DATA DELTA/0.7763D+00,-0.0603D+00,0.4408D+00,0.54015D+00,
     %0.2497D+00,0.6216D+00,0.53053D+00/
      EACTUL=EMF+0.0061D+00
      GCORR=ALPHA(ITC)+(BETA(ITC)+(GAMMA(ITC)+(DELTA(ITC)
     %*EACTUL))*EACTUL)*EACTUL
      GCORR=GCORR*1.D-03
      ESTD=EACTUL+GCORR
      ARG=-0.2902502066D+00+(17.31101383D+00+(0.74005336790-01
     %-0.4800534311D-02*ESTD)*ESTD)*ESTD
      ARG=ARG+2.572484D+00/ESTD+4.377872676D+00*DLOG(ESTD)
      TCOUPL=ARG
      RETURN
      END
C
C
C
      SUBROUTINE ROTAM(TC,SCALE)
      IMPLICIT REAL*8(A-H,O-Z)
      COMMON/FLUID/QLIQ,DENS,VISCK,WT
      QLIQ=0.D+00
      IF(WT.LT.10.D+00)THEN
          ICORR=1
      ELSEIF(WT.LT.30.D+00)THEN
          ICORR=2
      ELSEIF(WT.LT.50.D+00)THEN
          ICORR=3
      ELSE
          RETURN
      ENDIF
C
      GO TO (4100,4200,4300),ICORR
C
```

```
C     Water at 25 deg C
C
4100  QLIQ=2.6342815D+00+(-2.7265972D-01+(1.2523934D-02
     %+(-2.6158035D-04+(2.6717540D-06+(-1.0727432D-08*SCALE))
     %*SCALE)*SCALE)*SCALE)*SCALE
      GO TO 5000
C
4200  CONTINUE
C
C     20 wt% MDEA
C
          Q25=1.0783276D-02+(9.4276038D-03+(3.1171087D-04
     %    +(-4.4149080D-06+(2.1782946D-08+(-2.5725522D-11*SCALE))
     %    *SCALE)*SCALE)*SCALE)*SCALE
C
          Q50=-5.3111207D-01+(5.9959681D-02+(-1.3958166D-03
     %    +(2.4778085D-05+(-2.2415571D-07+(7.8993462D-10*SCALE))
     %    *SCALE)*SCALE)*SCALE)*SCALE
C
          Q75=2.3821535D+00+(-2.4500919D-01+(1.1340119D-02
     %    +(-2.3437403D-04+(2.3589534D-06+(-9.3236513D-09*SCALE))
     %    *SCALE)*SCALE)*SCALE)*SCALE
C
      IF(TC.LE.25.D+00)THEN
          SLOPE=(Q50-Q25)/25.D+00
          QLIQ=Q25+SLOPE*(TC-25.D+00)
      ELSEIF(TC.LE.50.D+00)THEN
          SLOPE=(Q50-Q25)/25.D+00
          QLIQ=Q25+SLOPE*(TC-25.D+00)
      ELSEIF(TC.LE.75.D+00)THEN
          SLOPE=(Q75-Q50)/25.D+00
          QLIQ=Q50+SLOPE*(TC-50.D+00)
      ELSE
          SLOPE=(Q75-Q50)/25.D+00
          QLIQ=Q75+SLOPE*(TC-75.D+00)
      ENDIF
      GO TO 5000
C
4300  CONTINUE
C
C     40 wt% MDEA
C
          Q25=-0.44847841D+00+(1.9519216D-02+(1.6611137D-05
     %    +(-2.8227395D-06+(4.1090646D-08+(-1.8990185D-10*SCALE))
     %    *SCALE)*SCALE)*SCALE)*SCALE
```

```
C
      Q50=-0.38829569D+00+(1.9652628D-02+(3.014301800D-04
     %    +(-8.1713716D-06+(7.4494260D-08+(-2.3936380D-10*SCALE))
     %    *SCALE)*SCALE)*SCALE)*SCALE
C
      Q75=-0.49254667D+00+(3.7362110D-02+(-2.4709480D-04
     %    +(-7.1322431D-09+(1.7711812D-08+(-9.0328190D-11*SCALE))
     %    *SCALE)*SCALE)*SCALE)*SCALE
C
      IF(TC.LE.25.D+00)THEN
          SLOPE=(Q50-Q25)/25.D+00
          QLIQ=Q25+SLOPE*(TC-25.D+00)
      ELSEIF(TC.LE.50.D+00)THEN
          SLOPE=(Q50-Q25)/25.D+00
          QLIQ=Q25+SLOPE*(TC-25.D+00)
      ELSEIF(TC.LE.75.D+00)THEN
          SLOPE=(Q75-Q50)/25.D+00
          QLIQ=Q50+SLOPE*(TC-50.D+00)
      ELSE
          SLOPE=(Q75-Q50)/25.D+00
          QLIQ=Q75+SLOPE*(TC-75.D+00)
      ENDIF
      GO TO 5000
C
5000  QLIQ=QLIQ*1.D-06/DENS
      RETURN
      END
C
C
C
      SUBROUTINE DENSL(TC)
      IMPLICIT REAL*8(A-H,O-Z)
      DIMENSION A0(6),A1(6),A2(6),A3(6),A4(6),A5(6),PCT(6)
      COMMON/FLUID/QLIQ,DENS,VISCK,WT
      DATA A0/1.000244355D+00,1.0142473D+00,1.0256906D+00,
     %    1.0322227D+00,1.0459222D+00,1.0654460D+00/
      DATA A1/1.941636116D-05,-0.45772313D-03,-0.49424711D-03,
     %    -0.87288832D-04,-0.48270445D-03,-0.14362347D-02/
      DATA A2/-6.543792186D-06,0.11991943D-04,0.12315728D-04,
     %    -0.35201506D-05,0.117230100-04,0.38224393D-04/
      DATA A3/2.984752134D-08,-0.25297787D-06,-0.32490784D-06,
     %    -0.10930976D-06,-0.49096279D-06,-0.83590104D-06/
      DATA A4/-8.223252092D-11,0.12746992D-08,0.27845152D-08,
     %    0.17230108D-08,0.64039493D-08,0.83860837D-08/
      DATA A5/0.D+00,0.20084018D-12,-0.83167968D-11,
```

```
     %    -0.74705420D-11,-0.28690296D-10,-0.32315523D-10/
      DATA PCT/0.D+00,10.D+00,20.D+00,30.D+00,40.D+00,50.D+00/
C
      DO 10 I=2,6
          IHI=I
          IF(WT.LE.PCT(I))THEN
              ILO=IHI-1
              GO TO 30
          ENDIF
10    CONTINUE
      IHI=6
      ILO=5
C
30    CONTINUE
      XHI=AO(IHI)+(A1(IHI)+(A2(IHI)+(A3(IHI)+(A4(IHI)+A5(IHI)*TC)*
     %    TC)*TC)*TC)*TC
      XLO=AO(ILO)+(A1(ILO)+(A2(ILO)+(A3(ILO)+(A4(ILO)+A5(ILO)*TC)*
     %    TC)*TC)*TC)*TC
      DENS=XLO+((XHI-XLO)/(PCT(IHI)-PCT(ILO)))*(WT-PCT(ILO))
C
      RETURN
      END
C
C
C
      SUBROUTINE KINVSC(TC)
      IMPLICIT REAL*8(A-H,O-Z)
      DIMENSION AK(6),BK(6),CK(6),PCT(6)
      COMMON/FLUID/DLIQ,DENS,VISCK,WT
      DATA AK/0.6641D+00,1.6001D+00,2.6484D+00,2.217D+00,
     %1.5084D+00,2.7418D+00/
      DATA BK/-2549.5D+00,-3183.1D+00,-3920.3D+00,-3762.1D+00,
     %-3404.2D+00,-4344.8D+00/
      DATA CK/691053.D+00,828076.D+00,990917.D+00,
     %1024841.D+00,1026178.D+00,1247827.D+00/
      DATA PCT/0.D+00,10.D+00,19.994D+00,29.993D+00,40.01D+00,
     %49.998D+00/
C
      DO 10 I=2,6
          IHI=I
          IF(WT.LE.PCT(I))THEN
              ILO=IHI-1
              GO TO 30
          ENDIF
10    CONTINUE
```

```
      IHI=6
      ILO=5
C
30    CONTINUE
      T=TC+273.15D+00
      XHI=AK(IHI)+(BK(IHI)/T)+(CK(IHI)/(T*T))
      XLO=AK(ILO)+(BK(ILO)/T)+(CK(ILO)/(T*T))
      XMID=XLO+((XHI-XLO)/(PCT(IHI)-PCT(ILO)))*(WT-PCT(ILO))
      VISCK=DEXP(XMID)*1.0-06
C
      RETURN
      END
C
C
C
      SUBROUTINE HENRY(IGAS,TC,HCOEFF)
      IMPLICIT REAL*8(A-H,O-Z)
      DIMENSION AH(3),BH(3),CH(3),PCT(3)
      COMMON/FLUID/QLIQ,DENS,VISCK,WT
      DATA AH/31.6847D+00,28.747D+00,27.8522D+00/
      DATA BH/-0.301286D-01,-0.27413D-01,-0.27812D-01/
      DATA CH/-5149.67D+00,-4535.4D+00,-4263.8D+00/
      DATA PCT/0.D+00,20.D+00,40.D+00/
C
      TK=TC+273.15D+00
      DUMD=DENS
      DUMWT=WT
      WT=0.D+00
      CALL DENSL(TC)
      DENSO=DENS
      WT=20.D+00
      CALL DENSL(TC)
      DENS20=DENS
      WT=40.D+00
      CALL DENSL(TC)
      DENS40=DENS
      HON20=18.018D+00*DEXP(AH(1)+BH(1)*TK+CH(1)/TK)/DENSO
C
      IF(DUMWT.LE.20.D+00)THEN
          H2ON20=21.70218053D+00*DEXP(AH(2)+BH(2)*TK+CH(2)/TK)/DENS20
          SLOPE=(DLOG(H2ON20)-DLOG(HON20))/(20.D+00-0.D+00)
          HN20=DEXP(DLOG(HON20)+SLOPE*(DUMWT-0.D+00))
      ELSEIF(DUMWT.LE.40.D+00)THEN
          H2ON20=21.70218053D+00*DEXP(AH(2)+BH(2)*TK+CH(2)/TK)/DENS20
          H4ON20=27.28022976D+00*DEXP(AH(3)+BH(3)*TK+CH(3)/TK)/DENS40
```

```
          SLOPE=(DLOG(H4ON20)-DLOG(H2ON20))/(40.D+00-20.D+00)
          HN20=DEXP(DLOG(H2ON20)+SLOPE*(DUMWT-20.D+00))
        ELSE
          H2ON20=21.70218053D+00*DEXP(AH(2)+BH(2)*TK+CH(2)/TK)/DENS20
          H4ON20=27.28022976D+00*DEXP(AH(3)+BH(3)*TK+CH(3)/TK)/DENS40
          SLOPE=(DLOG(H4ON20)-DLOG(H2ON20))/(40.D+00-20.D+00)
          HN20=DEXP(DLOG(H2ON20)+SLOPE*(DUMWT-20.D+00))
        ENDIF
C
        IF(IGAS.EQ.1)THEN
          HCOEFF=HN20
          WT=DUMWT
          DENS=DUMD
          RETURN
        ELSE
C
C       Henry's constant correlation from Mason and Kao (1980)
C       Units are atm/molality
C
          TRED=TK/100.D+00
          TRED2=TRED*TRED
          HOCO2=3.822D+00-7.8665D-04*DEXP(TRED)
     %          -0.04145D+00*TRED2-17.457D+00/TRED2
          HOCO2=101.325D+00*(10.D+00**HOCO2)/DENSO
          HCO2=HOCO2*(HN20/HON20)
          HCOEFF=HCO2
          WT=DUMWT
          DENS=DUMD
          RETURN
        ENDIF
        RETURN
        END
C
C
C
        SUBROUTINE ABSORB(K1,GCALC)
        IMPLICIT REAL*8(A-H,O-Z)
        REAL*8 K1,M,KTMAX
        COMMON/NUMB/PI,GRAVTY,E1,E2,E3,E4,E5,R
        COMMON/EQUIP/RS
        COMMON/FLUID/QLIQ,DENS,VISCK,WT
        COMMON/CONC/CI,CO,CIO
        COMMON/HYDRO/DELTAP,KTMAX,TMAX
        COMMON/VAPOR/DGAS
C
```

```
      M=K1*DELTAP*DELTAP/DGAS
      KTMAX=K1*TMAX
      PSI2=0.6628D+00*KTMAX/M
C
      GSPHO=QLIQ*(CI-CIO)*DSQRT(PSI2)
      SQKT=DSQRT(KTMAX)
      FACT=1.D+00
C
      IF(KTMAX.GE.25.D+00)THEN
          FACT=1.428D+00*SQKT
      ELSEIF(KTMAX.GE.5.D+00)THEN
          FACT=(1.428D+00*SQKT)+(0.54D+00/SQKT)
      ELSEIF(KTMAX.GE.1.D+00)THEN
          FACT=(1.428D+00*SQKT)+(0.689D+00/SQKT)
      ELSE
          FACT=(0.455D+00*KTMAX)+1.693D+00
      ENDIF
      GCALC=GSPHO*FACT
  RETURN
  END
C
C
C
  SUBROUTINE CELLP(TCELL,PCELL,XW,PGAS)
  IMPLICIT REAL*8(A-H,O-Z)
      TK=TCELL+273.16D+00
      TR=647.27D+00-TK
      SAVE1=(TR*TR*1.1702379D-08+5.86826D-03)*TR+3.2437814D+00
      SAVE1=SAVE1*TR/(TK*(1.D+00+2.1878462D-03*TR))
      PWATER=10.D+00**SAVE1
      PWATER=(218.167D+00/PWATER)*101.325D+00
  PWATER=XW*PWATER
  PGAS=PCELL-PWATER
  RETURN
  END
C
C
C
  SUBROUTINE MOLEFC(XWATER)
  IMPLICIT REAL*8(A-H,O-Z)
  COMMON/FLUID/QLIQ,DENS,VISCK,WT
  XA=WT/119.17D+00
  XW=(100.D+00-WT)/18.018D+00
  XWATER=XW/(XA+XW)
  RETURN
  END
```

```
C
C
C
      SUBROUTINE DIFF(IGAS,TC)
      IMPLICIT REAL*8(A-H,O-Z)
      DIMENSION AD(3),BD(3),PCT(3)
      COMMON/FLUID/QLIQ,DENS,VISCK,WT
      COMMON/VAPOR/DGAS
      DATA AD/-13.0090196D+00,-14.49599811D+00,-14.49599811D+00/
      DATA BD/-2103.102033D+00,-1813.375424D+00,-1813.375424D+00/
      DATA PCT/0.D+00,20.D+00,40.D+00/
C
      TK=TC+273.15D+00
      CON20=1.526368D-14
      ALPH20=0.85581D+00
      CON40=3.648227D-14
      ALPH40=0.77845D+00
      DUMD=DENS
      DUMWT=WT
      DUMV=VISCK
      WT=0.D+00
      CALL DENSL(TC)
      CALL KINVSC(TC)
      VISC0=VISCK*DENS*1.D+03
      WT=20.D+00
      CALL DENSL(TC)
      CALL KINVSC(TC)
      VISC20=VISCK*DENS*1.D+03
      WT=40.D+00
      CALL DENSL(TC)
      CALL KINVSC(TC)
      VISC40=VISCK*DENS*1.D+03
      DON20=DEXP(AD(1)+BD(1)/TK)
C
      IF(DUMWT.LE.20.D+00)THEN
          D20N20=CON20*TK/(VISC20**ALPH20)
          SLOPE=(DLOG(D20N20)-DLOG(DON20))/(20.D+00-0.D+00)
          DN20=DEXP(DLOG(DON20)+SLOPE*(DUMWT-0.D+00))
      ELSEIF(DUMWT.LE.40.D+00)THEN
          D20N20=CON20*TK/(VISC20**ALPH20)
          D40N20=CON40*TK/(VISC40**ALPH40)
          SLOPE=(DLOG(D40N20)-DLOG(D20N20))/(40.D+00-20.D+00)
          DN20=DEXP(DLOG(D20N20)+SLOPE*(DUMWT-20.D+00))
      ELSE
          D20N20=CON20*TK/(VISC20**ALPH20)
```

```
          D4ON20=CON40*TK/(VISC40**ALPH40)
          SLOPE=(DLOG(D4ON20)-DLOG(D2ON20))/(40.D+00-20.D+00)
          DN20=DEXP(DLOG(D2ON20)+SLOPE*(DUMWT-20.D+00))
        ENDIF
C
        IF(IGAS.EQ.1)THEN
          DGAS=DN20
          WT=DUMWT
          DENS=DUMD
          VISCK=DUMV
          RETURN
        ELSE
C
C
C
          DOCO2=DEXP(AD(1)+BD(1)/TK)
          DCO2=DOCO2*(DN20/DON20)
          DGAS=DCO2
          WT=DUMWT
          DENS=DUMD
          VISCK=DUMV
          RETURN
        ENDIF
        RETURN
        END
C
C
C
        SUBROUTINE AKG(IRES,IGAS,TCELL,PCELL,PGAS,XKG)
        IMPLICIT REAL*8(A-H,O-Z)
        DIMENSION SIG(3),EOK(3),XM(3)
        COMMON/NUMB/PI,GRAVTY,E1,E2,E3,E4,E5,R
        COMMON/EQUIP/RS
        DATA SIG/3.828D+00,3.941D+00,2.641D+00/
        DATA EOK/232.4D+00,195.2D+00,809.1D+00/
        DATA XM/44.013D+00,44.01D+00,18.018D+00/
C
        IF(IRES.EQ.1)THEN
          SIGMA=(SIG(IGAS)+SIG(3))*0.5D+00
          EK=DSQRT(EOK(IGAS)*EOK(3))
          TK=TCELL+273.15D+00
          TSTAR=TK/EK
          OMEGAD=(1.06036D+00/(TSTAR**0.1561D+00)) +
     %        (0.19300D+00/DEXP(0.47635D+00*TSTAR)) +
     %        (1.03587D+00/DEXP(1.52996D+00*TSTAR)) +
```

```
%       (1.76474D+00/DEXP(3.89411D+00*TSTAR))
      FACTOR=DSQRT((XM(IGAS)+XM(3))/(XM(IGAS)*XM(3)))
      FACT2=0.00217D+00-0.00050D+00*FACTOR
      DAB=FACT2*(TK**1.5D+00)*FACTOR*1.D-04
      DAB=DAB*101.325D+00/(PCELL*SIGMA*SIGMA*OMEGAD)
C
      TSTAR=TK/EOK(IGAS)
      OMEGAV=(1.16145D+00/(TSTAR**0.14874D+00)) +
%       (0.52487D+00/DEXP(0.77320D+00*TSTAR)) +
%       (2.16178D+00/DEXP(2.43787D+00*TSTAR))
      VISC1=26.69D-07*DSQRT(XM(IGAS)*TK)
      VISC1=VISC1/(SIG(IGAS)*SIG(IGAS)*OMEGAV)
      TSTAR=TK/EOK(3)
      OMEGAV=(1.16145D+00/(TSTAR**0.14874D+00)) +
%       (0.52487D+00/DEXP(0.77320D+00*TSTAR)) +
%       (2.16178D+00/DEXP(2.43787D+00*TSTAR))
      VISC2=26.69D-07*DSQRT(XM(3)*TK)
      VISC2=VISC2/(SIG(3)*SIG(3)*OMEGAV)
      Y1=PGAS/PCELL
      Y2=1.D+00-Y1
      PAR1=VISC1/VISC2
      PAR2=XM(IGAS)/XM(3)
      PHI12=(1.D+00+(PAR1**0.5D+00)/(PAR2**0.25D+00))**2
      PHI12=PHI12/DSQRT(8.D+00*(1.D+00+PAR2))
      PHI21=PHI12*PAR2/PAR1
      VISC=Y1*VISC1/(Y1+Y2*PHI12)+Y2*VISC2/(Y2+Y1*PHI21)
      VELG=8.7D-03
      WT=Y1*XM(IGAS)+Y2*XM(3)
      RHOG=WT*PCELL/(R*TK)
      SCG=VISC/(RHOG*DAB)
      REG=2.D+00*RHOG*VELG*RS/VISC
      SHG=2.D+00+0.556D+00*DSQRT(REG)*(SCG**0.3333333333D+00)
C
      XKG=SHG*DAB/(2.D+00*R*TK*RS)
      RETURN
    ELSE
      XKG=1.D+20
      RETURN
    ENDIF
    RETURN
    END
```

```
C
C
C
      SUBROUTINE AKL(DNOZ,JETLTH,GAVG,HCOEFF,PGAS,XKG,RESIST)
      IMPLICIT REAL*8(A-H,O-Z)
      REAL*8 JETLTH
      COMMON/NUMB/PI,GRAVTY,E1,E2,E3,E4,E5,R
      COMMON/EQUIP/RS
      COMMON/FLUID/QLIQ,DENS,VISCK,WT
      COMMON/CONC/CI,CO,CIO
      DELTAP=(3.D+00*QLIQ*VISCK/(2.D+00*PI*RS*GRAVTY))**E3
      ACORR=1.D+00+(2.58712D+00*DELTAP/RS)
      AREA=PI*(DNOZ*JETLTH+4.D+00*RS*RS*ACORR)
      CAPKL=GAVG/(AREA*(PGAS/HCOEFF))
      XKL=1.D+00/((1.D+00/CAPKL)-(1.D+00/(HCOEFF*XKG)))
      RESIST=100.D+00*CAPKL/(HCOEFF*XKG)
      CI=(XKG*PGAS+XKL*CO)/(XKL+HCOEFF*XKG)
      RETURN
      END
C
C
C
      BLOCK DATA
      IMPLICIT REAL*8(A-H,O-Z)
      REAL*8 KTMAX
      CHARACTER*4 TOD(2),DATE(3)
      CHARACTER*8 MONTH,FILE
      DIMENSION MONTH(2,12),FILE(3)
      COMMON/IO/IIN,IOUT,JIN,JOUT,LOUT
      COMMON/FNAME/FILE
      COMMON/DATES1/MONTH,TOD,DATE
      COMMON/DATES2/IYEAR,IMONTH,IDAY
      COMMON/NUMB/PI,GRAVTY,E1,E2,E3,E4,E5,R
      COMMON/EQUIP/RS
      COMMON/FLUID/QLIQ,DENS,VISCK,WT
      COMMON/CONC/CI,CO,CIO
      COMMON/HYDRO/DELTAP,KTMAX,TMAX
      COMMON/VAPOR/DGAS
      DATA MONTH/'January ','        ','February','        ',
     %     'March   ','        ','April   ','        ',
     %     'May     ','        ','June    ','        ',
     %     'July    ','        ','August  ','        ',
     %     'Septembe','r       ','October ','        ',
     %     'November','        ','December','        '/
      DATA IIN,IOUT,JIN,JOUT,LOUT/5,6,7,8,10/
```

```
DATA GRAVTY/9.80665D+00/,PI/3.141592653589793D+00/
DATA R/8.31434D+00/,RS/0.0254D+00/
END
```

APPENDIX 7

Sample Calculations

Calculation of Molecular Diffusion Coefficient

The following procedure was adopted to calculate the value of the molecular diffusion coefficient from the absorption rate data collected with the sphere absorber. The data of May 2, 1986 for the absorption of N_2O into 20 wt% MDEA solution at 50°C are used to illustrate the calculation sequence. The raw data are contained in Appendix 1.

Length of Laminar Jet

The laminar jet length is the difference between the elevation of the jet nozzle and the north pole of the sphere.

87.540 - 87.320 = 0.220 cm = 2.20 mm

Liquid Take-off Length

The liquid take-off length is the difference between the south pole of the sphere and the liquid level in the take-off tube.

82.200 - 79.770 = 2.430 cm = 24.30 mm

This was very close to the optimum value, therefore the absorption rate on the support rod was considered to be negligible.

Barometric Pressure

The barometric pressure was read from the mercury manometer

in the laboratory.

PBARO = 705.3 mm Hg = 94.03 kPa

Manometer Pressure

The manometer pressure is the difference between the right leg and the left-leg readings.

PMANO = 6.4 + 5.6 = 12.0 in H_2O = 2.98 kPa

Absorption Chamber Pressure

The absolute cell pressure is the sum of the atmospheric and gauge pressures.

PCELL = PBARO + PMANO = 97.01 kPa

Consider the run using the first liquid flow rate.

Absorption Chamber Temperature

Using the thermocouple (T/C) calibration described in Appendix 3, the following temperatures were calculated from the mV readings

Start of Run

T/C #1 (liquid entering chamber) : 49.39°C

T/C #2 (liquid leaving chamber) : 49.58°C

End of Run

T/C #1 (liquid entering chamber) : 49.37°C

T/C #2 (liquid leaving chamber) : 49.56°C

The temperature of the absorption chamber was taken to be the time-averaged liquid temperature.

T = (49.39 + 49.58 + 49.37 + 49.56)/4 = 49.47°C

Density of Liquid

The density of the 20 wt% MDEA solution at 49.47°C may be

estimated using the method described in Appendix 4.

ρ = 1006.26 kg/m³

Amine Concentration

Using this density, the concentration of amine in the solution may be determined. Assume 1 m³ of 20 wt% solution

Moles MDEA : 0.20(1006.26)/119.17 = 1.689 kmol/m³

Mole Fraction Water in Liquid

Assume 100 kg of 20 wt% MDEA solution

Moles MDEA = (20 kg)/(119.17 kg/kmol) = 0.1678 kmol MDEA

Moles H_2O = (80 kg)/(18.018 kg/kmol)

= 4.4400 kmol H_2O

Mole fraction water = 4.4400/(0.1678+4.440) = 0.96357

The molecular weight of the liquid may then be calculated

MW = 0.96357(18.018) + 0.03642(119.17) = 21.7022 kg/kmol

Vapor Pressure of Water

The vapor pressure of water at 49.47°C was estimated using steam tables

PWATER = 12.01 kPa

By Raoult's law, the partial pressure of water is reduced according to the mole fraction of water in the liquid solution.

PWATER = 12.014(0.96357) = 11.58 kPa

Partial Pressure of N_2O in Absorption Chamber

The partial pressure of N_2O in the absorption chamber is the difference between the total pressure and the partial pressure of water in the chamber. Vaporization of amine was assumed to be negligible.

PN2O = PCELL - PWATER

= 97.014 - 11.577 = 85.44 kPa

Henry's Constant for N_2O

Using the correlation developed in Appendix 4, the Henry's constant may be determined

TK = 273.15 + 49.47 = 322.67 K

H = exp(28.747 - 0.027413(322.62) - 4535.4/(322.62))

= 345.5 MPa/mole fraction

To convert to the proper units, the molecular weight and the solution density are required.

H = 345500 kPa(21.7022 kg/kmol)/(1006.26 kg/m³)

= 7451.94 kPa·m³/kmol

Kinematic Viscosity of Liquid

The kinematic viscosity of the 20 wt% MDEA solution at 49.47°C was established using the correlation described in Appendix 4.

$$\nu = 10^{-6} \exp(2.6484 - 3920.3/322.62 + 990917/(322.62)^2)$$

$$= 1.017 \times 10^{-6} \text{ m}^2/\text{s}$$

Gas-Phase Mass-Transfer Coefficient

The gas-phase mass-transfer coefficient was estimated using Equation (70). Using the appropriate data, the following values were calculated for the 50.8 mm diameter sphere

$Re_g = 41.74$

$Sc_g = 0.540$

$Sh_g = 4.925$

$k_g = 7.087 \times 10^{-7}$ kmol/s·m²·kPa

Average Overall N_2O Absorption Rate

The average overall absorption rate was calculated from the soap film meter measurements of the rate of gas uptake. The average sweep time for the 17 measurements was determined to be

SWTIM = 100.664 s

The average temperature of the gas in the soap film meter over the duration of the run was calculated to be 22.219°C. For all measurements in this run, the sweep volume was

SWVOL = 10.0 mL

The gas absorption rate can be calculated from

$$GAVG = (PCELL \cdot SWVOL)/(R^* \cdot T \cdot SWTIM)$$
$$= 3.925 \times 10^{-9} \text{ kmol/s}$$

Liquid Volumetric Flow Rate

The rotameter correlation in Appendix 3 was used to determine the flow of liquid to the absorption chamber. The average temperature of the liquid flowing through the rotameter was calculated to be 43.34°C. At a rotameter float reading of 30mm, the flow rate was calculated to be

$$QLIQ = 0.5171 \times 10^{-3} \text{ kg/s}$$

Using the density of the liquid at the conditions of the absorption chamber, the liquid volumetric flow rate was estimated to be

$$L = 0.5171 \times 10^{-3} / 1006.26 = 0.5139 \times 10^{-6} \text{ m}^3/\text{s}$$

Liquid Film Thickness

The thickness of the liquid film at the equator of the sphere was estimated using Equation (22)

$$\Delta_o = \left[\frac{3\nu L}{2\pi Rg}\right]^{1/3}$$

$$= 1.0008 \times 10^{-4} \text{ m}$$

Interfacial Surface Area of Spherical Film

Using Equation (52)

$$A_a = 4\pi R^2(1 + 2.58712\Delta_o/R)$$

$$= 8.190 \times 10^{-3} \text{ m}^2$$

Interfacial Surface Area of Laminar Jet

The dimensions of the jet can be used to calculate the surface area available for mass transfer.

$$A_j = \pi d_j h_j$$

$$= 4.15 \times 10^{-6} \text{ m}^2$$

Gas-Phase Resistance to Mass Transfer

From Equation (93)

$$K_L = 4.177 \times 10^{-5} \text{ m/s}$$

and from Equation (69)

$$k_L = 4.211 \times 10^{-5} \text{ m/s}$$

The gas-phase resistance to mass transfer can be calculated by

$$\text{RESIST} = 100\ K_L/(Hk_g)$$

$$= 0.791\ \%$$

Interfacial N_2O Concentration

Using the above coefficients in Equation (95) gives

$$C_i = 0.01137 \text{ kmol/m}^3$$

Percent Saturation

The liquid leaving the absorption chamber was partially saturated with N_2O. The percent saturation may be calculated by

$$\% \text{ sat.} = 100\ GAVG/(L\ C_i)$$

$$= 67.1\ \%$$

This was within the limits that have been established for the use of Equation (50).

Estimation of Molecular Diffusion Coefficient

The iterative solution procedure to calculate the value of D requires an initial estimate for D. The equation of Davidson and Cullen (1957) was used to provide a starting value. The fraction of the total absorption rate that occurs on the sphere was estimated using

$$FSPH = ZSPH/(ZSPH + ZJET)$$

where

$$ZSPH = 4.49\left(\frac{2\pi g}{3\nu}\right)^{1/6} R^{7/6}\ L^{1/3}$$

$$= 8.172 \times 10^{-3}$$

and

$$ZJET = 4(h_j\ L)^{1/2}$$

$$= 1.345 \times 10^{-4}$$

Therefore

$$FSPH = 0.9838$$

$$GSPH = GAVG(FSPH) = 3.861 \times 10^{-9}\ \text{kmol/s}$$

$$GJET = GAVG - GSPH = 6.345 \times 10^{-11}\ \text{kmol/s}$$

The N_2O concentration entering the spherical film can then be estimated as

$$C_o = GJET/L = 1.236 \times 10^{-4}\ \text{kmol/m}^3$$

The initial estimate for D can then be obtained using

$$D_o = (GSPH/ZSPH(C_i - C_o))^2$$

$= 1.76 \times 10^{-9}$ m²/s

The equations for gas absorption into a spherical liquid film are based on the dry-sphere radius, therefore the value of GSPH must be scaled by the area correction factor

$$GSPH = GSPH/(1 + 2.58712\Delta_o/R)$$

$= 3.822 \times 10^{-9}$ kmol/s

A bisection method was used to calculate the diffusion coefficient. For a given set of parameters, the correct value of D was assumed to lie within the range

$$0.5\ D_o < D < 2.0\ D_o$$

or in this case

$$8.82 \times 10^{-10}\ m^2/s < D < 3.53 \times 10^{-9}\ m^2/s$$

Using a value of $D=8.82 \times 10^{-10}$ m²/s in Equation (50) results in a predicted absorption rate of

$GSPH = 2.69 \times 10^{-9}$ kmol/s

Similarly, a value of $D=3.53 \times 10^{-9}$ m²/s gives a predicted value of

$GSPH = 4.85 \times 10^{-9}$ kmol/s

Using an average value of $D=2.20 \times 10^{-9}$ m²/s results in a predicted value of

$GSPH = 4.09 \times 10^{-9}$ kmol/s

This is still above the target value of 3.822×10^{-9} m²/s. For the next iteration, the domain of D is reduced to

$$8.82 \times 10^{-10}\ m^2/s < D < 2.20 \times 10^{-9}\ m^2/s$$

An average value of $D=1.54 \times 10^{-9}$ m²/s results in a predicted value of

$GSPH = 3.51 \times 10^{-9}$ kmol/s

which is too low. The bisection procedure is continued until

$$\left| \frac{\Delta D}{D} \right| < 10^{-5}$$

In this case, when $D=1.869\times10^{-9}$ m^2/s the predicted N_2O absorption rate on the sphere is exactly 3.822×10^{-9} kmol/s. Using this value of D, a new estimate of the absorption rate on the laminar jet is given by Equation (53)

$$GJET = 6.613\times10^{-11} \text{ kmol/s}$$

and therefore

$$C_o = 1.287\times10^{-4} \text{ kmol/m}^3$$

$$GSPH = 3.858\times10^{-9} \text{ kmol/s}$$

The value of GSPH is scaled by the area factor and the procedure is continued. This iteration results in

$$D = 1.868\times10^{-9} \text{ m}^2/\text{s}$$

The outer loop is continued until values of D do not change by more than 0.01 %. The final converged results gives

$$D = 1.8679\times10^{-9} \text{ m}^2/\text{s}$$

A similar calculation is performed for each liquid flow rate.

Calculation of Reaction Rate Constant

The following procedure was adopted to calculate the value of the second-order reaction rate constant from the absorption rate data collected with the sphere absorber. The data of June 11, 1986 for the absorption of CO_2 into 40 wt% MDEA solution at 75°C are used to illustrate the calculation sequence. The raw data are contained in Appendix 1.

The calculation procedure is essentially the same as the case of pure physical absorption, except that a different system of governing rate expressions are used. Using the same techniques as described earlier, the following values are obtained

Jet Length = 2.15 mm

[illegible]ff Length = 23.95 mm

[illegible] = 93.34 kPa

[illegible]ANO = 2.98 kPa

PCELL = 96.32 kPa

Consider the run using the fourth liquid flow rate.

Chamber Temperature = 74.83°C

ρ = 1003.20 kg/m³

Amine Concentration = 3.367 kmol/m³

Mole fraction water = 0.90843

Molecular weight of liquid = 27.2802 kg/kmol

Vapor Pressure of water = 38.28 kPa

Partial Pressure of water = 34.77 kPa

Partial Pressure of CO_2 = 61.55 kPa

Henry's Constant for N_2O in water = 11142.89 kPa·m³/kmol

Henry's Constant for CO_2 in water = 7406.96 kPa·m³/kmol

Henry's Constant for N_2O in 40 wt% MDEA = 10139.30 kPa·m³/kmol

Using Equation (86), Henry's Constant for CO_2 in 40 wt% MDEA = 6739.85 kPa·m³/kmol

Kinematic Viscosity of liquid = 1.221×10^{-6} m²/s

Re_g = 31.55

Sc_g = 0.602

Sh_g = 4.638

$k_g = 7.338 \times 10^{-7}$ kmol/s·m²·kPa

CO_2 Diffusion Coefficient = 2.346×10^{-9} m²/s

Average Overall CO_2 Absorption Rate = 4.984×10^{-8} kmol/s

Liquid Volumetric Flow Rate = 0.8359×10^{-6} m³/s

$\Delta_o = 1.2507 \times 10^{-4}$ m

$A_a = 8.211 \times 10^{-3}$ m²

$A_j = 4.05 \times 10^{-6}$ m²

$K_L = 6.644 \times 10^{-4}$ m/s

$k_L = 7.675 \times 10^{-4}$ m/s

RESIST = 13.434 %

C_i = 0.007905 kmol/m³

Estimation of Second-Order Rate Constant

The iterative solution procedure to calculate k_2 involves solving for k_{ov} using Equations (63) through (67) along with

Equation (97). The value of k_{ov} was believed to lie within the range of 0.1 to 1000 s^{-1} for all conditions encountered in the experiment, therefore these bounds were used as the high and low limits to the bisection method.

$$0.1 < k_{ov} < 1000$$

The initial rate of absorption of CO_2 into the laminar jet was assumed to involve only physical absorption. Using Equation (53)

$$GJET = 6.49 \times 10^{-11} \text{ kmol/s}$$

Therefore

$$GSPH = 4.9775 \times 10^{-8} \text{ kmol/s}$$

Scaling the value of GSPH using the area correction factor results in

$$GSPH = 4.9148 \times 10^{-8} \text{ kmol/s}$$

Using the same bisection search technique as for the case of physical absorption, values of k_{ov} were used to predict the rate of CO_2 absorption into the spherical liquid film. If the predicted absorption rate was too high, the next trial value of k_{ov} was somewhat lower. For each trial value of k_{ov}, the product of the diffusion time and k_{ov} were calculated to select which rate expression, Equations (63) to (67) would be used. The diffusion time may be calculated using Equation (23)

$$t_D = 1.0461 \text{ s}$$

The bisection procedure is continued until

$$|\Delta k_{ov} / k_{ov}| < 10^{-5}$$

In this case, when $k_{ov} = 249.34\ s^{-1}$, the predicted CO_2

absorption rate on the sphere is 4.9148×10^{-8} kmol/s. Using this value of k_{ov}, a new estimate of the absorption rate on the laminar jet is

GJET = 6.886×10^{-11} kmol/s

and therefore

GSPH = 4.9771×10^{-8} kmol/s

The value of GSPH is scaled by the area factor and the procedure is continued. The final converged results give

$k_{ov} = 249.30\ s^{-1}$

The average CO_2 loading in the liquid may be calculated as follows

CO_2 in with liquid : (0.03 mol/mol)·CONC·L

Average amount of CO_2 absorbed : GAVG/2

Therefore

α = 0.03885 mol CO_2/mol MDEA

The free amine concentration may then be estimated using Equation (98)

FREEAM = 3.236 kmol/m³

The concentration of OH^- ion in the liquid may be estimated using Equation (13)

$[OH^-] = 1.949 \times 10^{-4}$ kmol/m³

Using these values, the second-order rate constant can be calculated as

k_2 = 64.58 m³/kmol·s

A similar calculation is performed for each liquid flow rate.

APPENDIX 8

Integral Heat of Solution

Consider a mixing process where n_1 moles of amine solution with an enthalpy of h_1° are mixed with n_2 moles of a pure acid gas, say CO_2, with an enthalpy of h_2°. The amine solution consists of n_A moles of amine and n_W moles of water. An energy balance may be written as

$$\Delta H = H_{soln} - n_1 h_1^\circ - n_2 h_2^\circ \qquad (A8.1)$$

Using partial molar enthalpies, Equation (A8.1) may be written as

$$\Delta H = n_1(\underline{h}_1 - h_1^\circ) + n_2(\underline{h}_2 - h_2^\circ) \qquad (A8.2)$$

Dividing Equation (A8.2) by n_2 gives

$$\Delta H_i = \frac{\Delta H}{n_2} = \frac{n_1}{n_2}(\underline{h}_1 - h_1^\circ) + (\underline{h}_2 - h_2^\circ) \qquad (A8.3)$$

$$= \frac{n_1}{n_2}\Delta H_1 + \Delta H_d \qquad (A8.4)$$

The form of this expression is illustrated in Figure A8.1. The value of ΔH_d is the differential heat of solution and ΔH_i is the integral heat of solution. Hence

$$\Delta H_i = \frac{n_1}{n_2}\left[\frac{\partial \Delta H_i}{\partial (n_1/n_2)}\right]_{P,T} + \Delta H_d \qquad (A8.5)$$

but

Figure A8.1.

Integral Heat of Solution as a Function of Molar Mixing Ratio

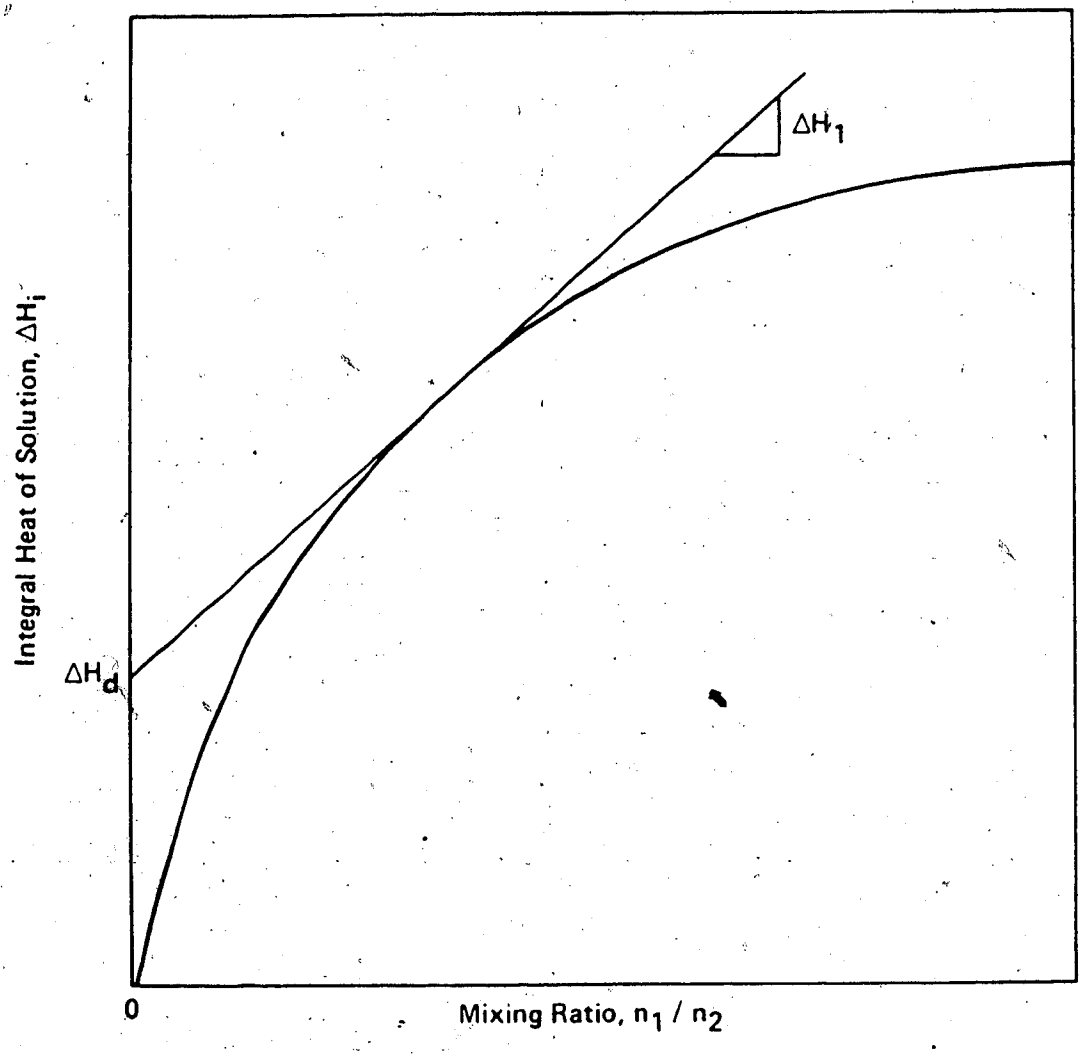

$$n_1/n_2 = (n_A + n_W)/n_2 \qquad \text{(A8.6)}$$

and

$$n_A/(n_A + n_W) = n_o = \text{Constant} \qquad \text{(A8.7)}$$

Therefore

$$n_2/(n_1 n_o) = \alpha \qquad \text{(A8.8)}$$

where α is the acid gas loading in moles acid gas per mole amine. Substituting Equation (A8.8) into Equation (A8.5) gives

$$\Delta H_i = \frac{1}{\alpha}\left[\frac{\partial \Delta H_i}{\partial(1/\alpha)}\right]_{P,T} + \Delta H_d \qquad \text{(A8.9)}$$

Equation (A8.9) can be integrated to give

$$\Delta H_i = \frac{1}{\alpha}\int \Delta H_d \, d\alpha \qquad \text{(A8.10)}$$

Equation (A8.10) may be used to calculate the integral heat of solution from data for the differential heat of solution.

APPENDIX 9

Sample Simulator Output

Example AMSIM V3.0 Output for MDEA Contactor

Stream 3 Gas Feed to Absorber A

Component	lbmol/h	mol frc.
H2S	26.896	0.005581
CO2	37.699	0.007823
MDEA	0.0	0.0
Water	0.0	0.0
Methane	4278.732	0.887832
Ethane	254.413	0.052790
Propane	114.199	0.023696
n-Butane	39.463	0.008188
i-Butane	16.976	0.003522
nPentane	26.896	0.005581
n-Hexane	7.275	0.001510
nHeptane	8.157	0.001693
Nitrogen	8.598	0.001784
Total	4819.306	

Temperature	82.400	F
Pressure	859.061	psia
Enthalpy	29.780	MMBTU/h
Mol. Wt.	18.843	
Liquid Fraction	0.0	
Std. Vol. Flow Rate	43.893	MMSCFD
Actual Vol. Flow Rate	0.783	MMACFD
Std. Density	2.783	lb/ft3
Heating value	1135.222	BTU/SCF
Mol % H2S	0.558	
Mol % CO2	0.782	
Std. Residual H2S	350.797	gr/100 SCF
Std. Residual CO2	635.031	gr/100 SCF
ppmv H2S	5580.970	
ppmv CO2	7822.507	
Viscosity	0.011	cP
Heat Capacity	0.525	BTU/lb-F
Thermal Conductivity	0.018	BTU/h-ft-F

Example AMSIM V3.0 Output for MDEA Contactor

Stream 5 Primary Lean Amine Feed to Absorber A

Component	lbmol/h	mol frc.
H2S	0.066	0.000123
CO2	1.190	0.002216
MDEA	64.044	0.119191
Water	472.023	0.878470
Methane	0.0	0.0
Ethane	0.0	0.0
Propane	0.0	0.0
n-Butane	0.0	0.0
i-Butane	0.0	0.0
nPentane	0.0	0.0
n-Hexane	0.0	0.0
nHeptane	0.0	0.0
Nitrogen	0.0	0.0
Total	537.324	

Temperature	99.500	F
Pressure	855.725	psia
Enthalpy	2.512	MMBTU/h
Mol. Wt.	30.134	
Liquid Fraction	1.000	
Std. Vol. Flow Rate	30.966	US gal/min
Actual Vol. Flow Rate	31.262	US gal/min
Weight % amine	47.296	
Std. Density	65.192	lb/ft3
mol H2S/mol amine	0.001	
mol CO2/mol amine	0.019	
Std. Residual H2S	8.491	gr/US gal
Std. Residual CO2	197.400	gr/US gal
Viscosity	4.874	cP
Heat Capacity	0.811	BTU/lb-F
Thermal Conductivity	0.204	BTU/h-ft-F

AMSIM V3.0
Example AMSIM V3.0 Output for MDEA Contactor

Stream 12 Absorber A Treated Gas

Component	lbmol/h	mol frc.
H2S	1.536	0.000320
CO2	32.019	0.006680
MDEA	0.000	0.000000
Water	5.663	0.001182
Methane	4278.097	0.892530
Ethane	254.364	0.053067
Propane	114.182	0.023822
n-Butane	39.463	0.008233
i-Butane	16.976	0.003542
nPentane	26.896	0.005611
n-Hexane	7.275	0.001518
nHeptane	8.157	0.001702
Nitrogen	8.597	0.001794
Total	4793.225	

Temperature	97.376	F
Pressure	855.725	psia
Enthalpy	30.471	MMBTU/h
Mol. Wt.	18.732	
Liquid Fraction	0.0	
Std. Vol. Flow Rate	43.656	MMSCFD
Actual Vol. Flow Rate	0.804	MMACFD
Std. Density	2.681	lb/ft3
Heating value	1137.681	BTU/SCF
Mol % H2S	0.032	
Mol % CO2	0.668	
Std. Residual H2S	20.137	gr/100 SCF
Std. Residual CO2	542.283	gr/100 SCF
ppmv H2S	320.370	
ppmv CO2	6680.011	
Viscosity	0.011	cP
Heat Capacity	0.536	BTU/lb-F
Thermal Conductivity	0.019	BTU/h-ft-F

Example AMSIM V3.0 Output for MDEA Contactor

Stream 8 Rich Amine from Absorber A

Component	lbmol/h	mol frc.
H2S	25.427	0.045131
CO2	6.871	0.012195
MDEA	64.044	0.113673
Water	466.360	0.827753
Methane	0.635	0.001128
Ethane	0.049	0.000087
Propane	0.018	0.000031
n-Butane	0.000	0.000000
i-Butane	0.000	0.000000
nPentane	0.000	0.000000
n-Hexane	0.000	0.000000
nHeptane	0.000	0.000000
Nitrogen	0.001	0.000001
Total	563.404	

Temperature	82.169	F
Pressure	858.481	psia
Enthalpy	1.821	MMBTU/h
Mol. Wt.	30.558	
Liquid Fraction	1.000	
Std. Vol. Flow Rate	31.290	US gal/min
Actual Vol. Flow Rate	31.434	US gal/min
Weight % amine	47.597	
Std. Density	68.598	lb/ft3
mol H2S/mol amine	0.397	
mol CO2/mol amine	0.107	
Std. Residual H2S	3230.588	gr/US gal
Std. Residual CO2	1127.443	gr/US gal
Viscosity	7.655	cP
Heat Capacity	0.763	BTU/lb-F
Thermal Conductivity	0.197	BTU/h-ft-F

Stream 30 Rich Amine Flash Liquid

Component	lbmol/h	mol frc.
H2S	25.427	0.045131
CO2	6.871	0.012195
MDEA	64.044	0.113673
Water	466.360	0.827753
Methane	0.635	0.001128
Ethane	0.049	0.000087
Propane	0.018	0.000031
n-Butane	0.000	0.000000
i-Butane	0.000	0.000000
nPentane	0.000	0.000000
n-Hexane	0.000	0.000000
nHeptane	0.000	0.000000
Nitrogen	0.001	0.000001
Total	563.404	

Temperature	82.169	F
Pressure	858.481	psia
Enthalpy	1.821	MMBTU/h
Mol. Wt.	30.558	
Liquid Fraction	1.000	
Std. Vol. Flow Rate	31.290	US gal/min
Actual Vol. Flow Rate	31.434	US gal/min
Weight % amine	47.597	
Std. Density	68.598	lb/ft3
mol H2S/mol amine	0.397	
mol CO2/mol amine	0.107	
Std. Residual H2S	3230.588	gr/US gal
Std. Residual CO2	1127.443	gr/US gal
Viscosity	7.655	cP
Heat Capacity	0.763	BTU/lb-F
Thermal Conductivity	0.197	BTU/h-ft-F

** Absorber A **

4793.23 lbmol/h <---------- Treated Gas
855.72 psia
97.38 deg F

<---------- Lean Amine
537.32 lbmol/h
855.72 psia
99.50 deg F

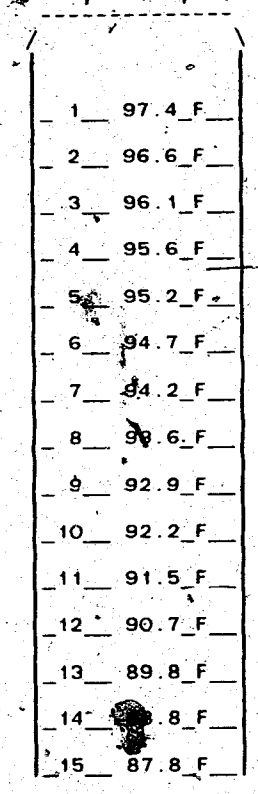

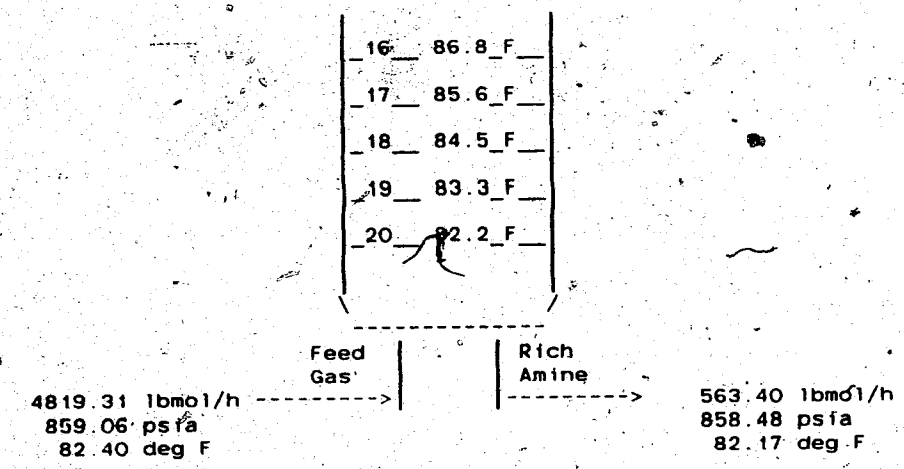
16 86.8 F
17 85.6 F
18 84.5 F
19 83.3 F
20 82.2 F
Feed Gas
Rich Amine
4819.31 lbmol/h
859.06 psia
82.40 deg F
563.40 lbmol/h
858.48 psia
82.17 deg F

***** General Column Information *****

Net H2S pickup = 0.39599 mol/mol or 5.1029 SCF/US gal

Net CO2 pickup = 0.08869 mol/mol or 1.1429 SCF/US gal

** Minimum Lean Amine Circulation Rate Estimation **

At Minimum Lean Amine Circulation :

	H2S	CO2
Equil. Vapor Comp. (ppmv)	1.222	15.639
Rich Amine (mole acid gas/mole amine)	0.224	0.33
Lean Amine (lbmol/h)	1010.067	
(US gal/min)	58.766	
Rich Amine (deg F)	119.1	

** This circulation rate is only an estimate and should not be used for final design purposes.

At Actual Lean Amine Circulation :

	H2S	CO2
Composition of Treated Gas (ppmv)	320.370	6680.011
Rich Amine (mole acid gas/mole amine)	0.397	0.107
Lean Amine (lbmol/h)	537.324	
(US gal/min)	31.262	
Rich Amine (deg F)	82.2	

*** Stage Efficiencies ***

Stage No.	Tomcej		Murphree	
	H2S	CO2	H2S	CO2
1	0.1807	0.0093	0.1805	0.0090
2	0.1807	0.0092	0.1806	0.0090
3	0.1807	0.0091	0.1806	0.0089
4	0.1808	0.0090	0.1806	0.0089
5	0.1808	0.0090	0.1806	0.0088
6	0.1808	0.0089	0.1806	0.0087
7	0.1808	0.0088	0.1806	0.0086
8	0.1808	0.0087	0.1805	0.0085
9	0.1808	0.0087	0.1805	0.0084
10	0.1808	0.0086	0.1805	0.0083
11	0.1808	0.0085	0.1804	0.0081
12	0.1807	0.0083	0.1803	0.0080
13	0.1807	0.0082	0.1803	0.0078
14	0.1807	0.0081	0.1802	0.0077
15	0.1807	0.0080	0.1801	0.0075
16	0.1806	0.0078	0.1800	0.0074
17	0.1806	0.0077	0.1799	0.0072
18	0.1806	0.0075	0.1798	0.0070
19	0.1805	0.0074	0.1797	0.0069
20	0.1806	0.0072	0.1811	0.0075

Royalty : 2662 AMSIM Units